NEW HYPERVALENT IODINE REAGENTS FOR OXIDATIVE COUPLING

EDITED BY: Toshifumi Dohi, Jian-Wei Han and Ravi Kumar
PUBLISHED IN: Frontiers in Chemistry

frontiers Research Topics

ISSN 1664-8714
ISBN 978-2-88966-650-8
DOI 10.3389/978-2-88966-650-8

About Frontiers

Frontiers is more than just an open-access publisher of scholarly articles: it is a pioneering approach to the world of academia, radically improving the way scholarly research is managed. The grand vision of Frontiers is a world where all people have an equal opportunity to seek, share and generate knowledge. Frontiers provides immediate and permanent online open access to all its publications, but this alone is not enough to realize our grand goals.

Frontiers Journal Series

The Frontiers Journal Series is a multi-tier and interdisciplinary set of open-access, online journals, promising a paradigm shift from the current review, selection and dissemination processes in academic publishing. All Frontiers journals are driven by researchers for researchers; therefore, they constitute a service to the scholarly community. At the same time, the Frontiers Journal Series operates on a revolutionary invention, the tiered publishing system, initially addressing specific communities of scholars, and gradually climbing up to broader public understanding, thus serving the interests of the lay society, too.

Dedication to Quality

Each Frontiers article is a landmark of the highest quality, thanks to genuinely collaborative interactions between authors and review editors, who include some of the world's best academicians. Research must be certified by peers before entering a stream of knowledge that may eventually reach the public - and shape society; therefore, Frontiers only applies the most rigorous and unbiased reviews.
Frontiers revolutionizes research publishing by freely delivering the most outstanding research, evaluated with no bias from both the academic and social point of view. By applying the most advanced information technologies, Frontiers is catapulting scholarly publishing into a new generation.

What are Frontiers Research Topics?

Frontiers Research Topics are very popular trademarks of the Frontiers Journals Series: they are collections of at least ten articles, all centered on a particular subject. With their unique mix of varied contributions from Original Research to Review Articles, Frontiers Research Topics unify the most influential researchers, the latest key findings and historical advances in a hot research area! Find out more on how to host your own Frontiers Research Topic or contribute to one as an author by contacting the Frontiers Editorial Office: frontiersin.org/about/contact

NEW HYPERVALENT IODINE REAGENTS FOR OXIDATIVE COUPLING

Topic Editors:
Toshifumi Dohi, Ritsumeikan University, Japan
Jian-Wei Han, East China University of Science and Technology, China
Ravi Kumar, J C Bose University of Science and Technology, YMCA, India

Citation: Dohi, T., Han, J.-W., Kumar, R., eds. (2021). New Hypervalent Iodine Reagents for Oxidative Coupling. Lausanne: Frontiers Media SA.
doi: 10.3389/978-2-88966-650-8

Table of Contents

frontiers in Chemistry

EDITORIAL
published: 22 February 2021
doi: 10.3389/fchem.2021.642889

Editorial: New Hypervalent Iodine Reagents for Oxidative Coupling

Toshifumi Dohi[1]*, *Jian-Wei Han*[2]* and *Ravi Kumar*[3]*

[1]College of Pharmaceutical Sciences, Ritsumeikan University, Shiga, Japan, [2]School of Chemistry and Molecular Engineering, East China University of Science and Technology, Shanghai, China, [3]Department of Chemistry, J. C. Bose University of Science and Technology, YMCA, Faridabad, India

Keywords: hypervalent compounds, iodine, reagent, oxidative coupling, synthetic application

Editorial on the Research Topic

New Hypervalent Iodine Reagents for Oxidative Coupling

In theory, oxidative coupling is a straightforward method for reducing the number of synthetic steps, avoiding the preparation of pre-activated substrates and less waste co-product generation by using metal salts. However, attempts at oxidative cross-coupling are challenging due to its limited synthetic applications and chemoselective issues. In recent years new oxidative coupling methods have emerged, using the C–H bond of the two substrates, and enabling the selective formation of cross-coupling products (Stuart and Fagnou, 2007).

One of the innovative research fronts in this area to have emerged in the past decade is the advance of oxidative coupling chemistry that uses hypervalent iodine reagents (Kita and Dohi, 2015; Yoshimura and Zhdankin, 2016), especially catalytic utilizations (Dohi and Kita, 2009; Dohi et al., 2013; Ito et al., 2013). This Research Topic discusses recent advancements of oxidative couplings and related reactions using hypervalent iodine compounds, highlighting the versatility of these reagents and their continuous development. Contributing to the recent advances in this area, the Research Topic includes contributions by experts exploring designs, preparations, reactions, mechanistic studies of hypervalent iodine compounds, and cooperative reaction systems with transition metals and photoredox catalysts, outlining how these synthetic applications can obtain useful organic molecules, such as pharmaceutical compounds.

In recent years there have been a number of successes in the participation of hypervalent iodine compounds in transition metal chemistry, which serve as strong electrophiles and powerful oxidizing agents, especially for the palladium-catalyzed couplings. The review by Shetgaonkar and Singh narrates recent advancements in this area, summarizing extensive work in the field of Pd-catalyzed C–H functionalizations, arylations, and other miscellaneous transformations with hypervalent iodine reagents and diaryliodonium(III) salts.

The synergistic combination of photoredox catalysis with hypervalent iodine reagents is one of many useful areas of organic synthesis. Chen et al. describe recent synthetic applications with visible-light-induced photoredox catalysis, focusing on the photochemical roles of hypervalent iodine reagents. However, a wide range of hypervalent iodine compounds still need to be explored under these conditions to bring out more synthetically useful transformations. We anticipate an expansion of this hot research area in the next few years.

In 2009, a novel cross-coupling method of heteroaromatic compounds was developed by exploiting the unique reactivities of diaryliodonium(III) salts (Kita et al., 2009). Since then, the chemistry of heteroaryliodonium(III) salts has undergone significant developments. They have

OPEN ACCESS

Edited and reviewed by:
Iwao Ojima,
Stony Brook University, United States

***Correspondence:**
Toshifumi Dohi
td1203@ph.ritsumei.ac.jp
Jian-Wei Han
jianweihan@ecust.edu.cn
Ravi Kumar
ravi.dhamija@rediffmail.com

Specialty section:
This article was submitted to Organic Chemistry, a section of the journal Frontiers in Chemistry

Received: *17 December 2020*
Accepted: *13 January 2021*
Published: *22 February 2021*

Citation:
Dohi T, Han J-W and Kumar R (2021) Editorial: New Hypervalent Iodine Reagents for Oxidative Coupling. Front. Chem. 9:642889. doi: 10.3389/fchem.2021.642889

proved to be useful reagents, acting as highly reactive electrophiles to bring about various transformations, such as NHC-catalyzed C-H bond arylation, Cu-catalyzed tandem arylation of indoles, and vicinal functionalization, etc. Another review by Takenaga et al. discusses the synthetic transformations mediated by heteroaryliodonium(III) salts with two classifications: 1) reactions utilizing the high reactivity of the hypervalent iodine(III) species; and 2) reactions based on unique and new reactivities not observed in other types of conventional diaryliodonium salts.

The Satkar et al. at Universidad de Guanajuato and Universidad Michoacana de San Nicolás de Hidalgo (Mexico) have contributed original research on diaryliodonium(III) salts, exploring their reaction with free-radical mechanisms for one-pot double arylation of naphthols. In this study, the new chemoselectivity pattern of the *C*- and *O*-centered naphthyl radicals toward the more electron-deficient hypervalent bond of the diaryliodonium(III) salts was observed for the first time. The naphthyl radicals were generated in the tetramethylpiperidinyl radical (TMP radical) reaction, resulting from the homolytic fragmentation of the precursor TMP_2O. The generation of these radicals is supported by other spectroscopic, theoretical, experimental, and mechanistic studies.

Another promising study by Hashishin and Miyamoto et al. from Tokyo University presents research on the practical synthesis of useful alkynyliodonium(III) salt using calcium carbide as an ethynyl source. This study illustrates that the stannylation of calcium carbide followed by Sn–hypervalent iodine(III) exchange reaction cleanly affords the electrophilic ethynylating agent, ethynyl(phenyl)-λ^3-iodane, in high yield. The use of inexpensive materials under easily operable reaction conditions and involving no special precautions, makes this protocol an effective, economical route to access unstable ethylnyl iodonium(III) salts.

As a part of the synthetic application of hypervalent iodine-mediated oxidative coupling in bioactive compounds, the Tan et al. research group summarizes efficient methodologies for the C3-H functionalization of quinoxalin-2(1*H*)-ones using hypervalent iodine reagents. Quinoxalin-2(1*H*)-one derivatives are known to show various biological activities and pharmaceutical properties. The review highlights the accomplishments of arylation, trifluoromethylation, alkylation, and alkoxylation of quinoxalin-2(1*H*)-ones with hypervalent iodine reagents by comparing reaction conditions and mechanisms.

Tan et al. report the diastereoselective α-acetoxylation of cyclic ketones by a binary hybrid system comprising a hypervalent iodine reagent and $BF_3{\bullet}OEt_2$ Lewis acid. As they explain, this reaction involves an S_N2 substitution mechanism *via* α-iodonium(III) ketone intermediate, and the diastereoselectivity mainly originates from thermodynamic control.

Iodine is an excellent promoter for several oxidative coupling reactions. Another contribution to this Research Topic by Li et al. demonstrates the I_2-catalyzed oxidative coupling of *N*-tosylhydrazones with elemental sulfur to give 4-aryl-1,2,3-thiadiazoles. During the reaction, the DMSO oxidation of HI was used to generate the I_2 exploiting dual properties of DMSO as oxidant as well solvent, an essential step in this reaction. Interestingly, this practical approach was extended to the synthesis of a neuroprotective compound.

Finally, a study by Qiu et al. suggests 1-benzoyloxy-1,2-benziodoxol-3-(1*H*)-one (IBA-OBz) as a new efficient peptide coupling agent. The developed reaction system was successfully applied even to the solid-phase peptide synthesis and a pentapeptide leu-enkephalin in unprotected form. Density functional theory calculations have revealed that the rate-limiting step is nucleophilic attack of 4-dimethylaminopyridine (DMAP) onto IBA-OBz.

This Research Topic collection highlighs recent contributions on hypervalent iodine chemistry, providing informative research and presenting inspiring research in this area. Although there have been tremendous developments in hypervalent iodine chemistry in recent years, various areas still need to be investigated in detail.

AUTHOR CONTRIBUTIONS

TD conceived and wrote the manuscript. All authors provided comments and discussed the contents, and approved this Editorial for publication.

ACKNOWLEDGMENTS

The guest editors wish to thank the authors for their generous contributions to this Research Topic collection, all while under pressure from the ongoing COVID-19 pandemic. We thank the reviewers for their voluntary work in evaluating the submitted articles. Special thanks are also extended to the staff at *Frontiers in Chemistry*, the Specialty Chief Editor Iwao Ojima, and other editorial board members of the journal's organic chemistry section for their support.

REFERENCES

Dohi, T., and Kita, Y. (2009). Hypervalent iodine reagents as a new entrance to organocatalysts. *Chem. Commun.* 16, 2073–2085. doi:10.1039/b821747e

Dohi, T., Takenaga, N., Nakae, T., Toyoda, Y., Yamasaki, M., Shiro, M., et al. (2013). Asymmetric dearomatizing spirolactonization of naphthols catalyzed by spirobiindane-based chiral hypervalent iodine species. *J. Am. Chem. Soc.* 135, 4558–4566. doi:10.1021/ja401074u

Ito, M., Kubo, H., Itani, I., Morimoto, K., Dohi, T., and Kita, Y. (2013). Organocatalytic C-H/C-H' cross-biaryl coupling: *C*-Selective arylation of sulfonanilides with aromatic hydrocarbons. *J. Am. Chem. Soc.* 135, 14078–14081. doi:10.1021/ja407944p

Kita, Y., and Dohi, T. (2015). Pioneering metal-free oxidative coupling strategy of aromatic compounds using hypervalent iodine reagents. *Chem. Rec.* 15, 886–906. doi:10.1002/tcr.201500020

Kita, Y., Morimoto, K., Ito, M., Ogawa, C., Goto, A., and Dohi, T. (2009). Metal-free oxidative cross-coupling of unfunctionalized aromatic compounds. *J. Am. Chem. Soc.* 131, 1668–1669. doi:10.1021/ja808940n

Stuart, D. A., and Fagnou, K. (2007). The catalytic cross-coupling of unactivated arenes. *Science* 316, 1172–1175. doi:10.1126/science.1141956

Yoshimura, A., and Zhdankin, V. V. (2016). Advances in synthetic applications of hypervalent iodine compounds. *Chem. Rev.* 116, 3328–3435. doi:10.1021/acs.chemrev.5b0054710.1039/c6ob00773b

Conflict of Interest: The authors declare that the research was conducted in the absence of any commercial or financial relationships that could be construed as a potential conflict of interest.

frontiers in Chemistry

ORIGINAL RESEARCH
published: 04 February 2020
doi: 10.3389/fchem.2020.00012

Practical Synthesis of Ethynyl(phenyl)-λ^3-Iodane Using Calcium Carbide as an Ethynyl Group Source

Takahiro Hashishin[1], *Taisei Osawa*[1], *Kazunori Miyamoto*[1]* *and Masanobu Uchiyama*[1,2,3]

[1] Graduate School of Pharmaceutical Sciences, The University of Tokyo, Tokyo, Japan, [2] Research Initiative for Supra-Materials (RISM), Shinshu University, Ueda, Japan, [3] Cluster of Pioneering Research (CPR), Advanced Elements Chemistry Laboratory, RIKEN, Saitama, Japan

Stannylation of calcium carbide followed by Sn–hypervalent iodine(III) exchange reaction cleanly afforded the electrophilic ethynylating agent ethynyl(phenyl)-λ^3-iodane in high yield. This two-step method uses very inexpensive materials and is readily operable without any special precautions.

Keywords: hypervalent, iodine, stannane, calcium carbide, ethynyl

OPEN ACCESS

Edited by:
Toshifumi Dohi,
Ritsumeikan University, Japan

Reviewed by:
Akira Yoshimura,
University of Minnesota Duluth, United States
Sylvain Canesi,
Université du Québec à Montréal, Canada

***Correspondence:**
Kazunori Miyamoto
kmiya@mol.f.u-tokyo.ac.jp

Specialty section:
This article was submitted to Organic Chemistry, a section of the journal Frontiers in Chemistry

Received: *27 November 2019*
Accepted: *07 January 2020*
Published: *04 February 2020*

Citation:
Hashishin T, Osawa T, Miyamoto K and Uchiyama M (2020) Practical Synthesis of Ethynyl(phenyl)-λ^3-Iodane Using Calcium Carbide as an Ethynyl Group Source. Front. Chem. 8:12. doi: 10.3389/fchem.2020.00012

INTRODUCTION

Hypervalent ethynyl(phenyl)-λ^3-iodane **1** is an efficient electrophilic ethynylating agent for a variety of nucleophiles (*C*, *N*, *O*, *P*, *As*, *S*, *Se*, and halides) in the presence or absence of transition metal catalysts (**Figure 1A**; Ochiai et al., 1990; Stang et al., 1990; Varvoglis, 1992; Ochiai, 2003; Waser, 2016; Yoshimura and Zhdankin, 2016). However, its synthetic utility is restricted by its high cost and heat/moisture-sensitive character: it gradually decomposes at room temperature in air (Ochiai et al., 2003; Yudasaka et al., 2019). Therefore, an inexpensive, rapid, and facile preparation method of **1** has long been highly desired. The current approach to the synthesis of **1** relies on electrophilic Si/Sn–I(III) exchange reaction on acetylenic carbon atoms, and has remained essentially unchanged since the early days. In 1990, Stang and Ochiai independently reported pioneering approaches for the synthesis of **1**. Stang et al. prepared ethynyl(phenyl)(triflato)-λ^3-iodane (**1b**) from ethynyl(tributyl)stannane (**3**) and Tf_2O-activated iodosylbenzene (**2**) (**Figure 1B**; Stang et al., 1990). On the other hand, a two-step procedure for the synthesis of **1a** via [β-(trimethylsilyl)ethynyl](phenyl)-λ^3-iodane **5a** was developed by Ochiai and co-workers (**Figure 1C**; Ochiai et al., 1990). Then, in 2011, Kitamura reported another practical stepwise approach using $PhI(OAc)_2$ (**6**) and bis(*tert*-butyldimethylsilyl)acetylene (**4b**) (**Figure 1D**; Kitamura et al., 2011). Although these methods provide short-step approaches to **1**, they have several disadvantages from the viewpoint of cost/safety of reagents. In particular, **3** is still expensive and concentrated aqueous HF is notoriously toxic (Mckee et al., 2014). We report here a safe, low-cost, two-step method for the synthesis of **1a** using calcium carbide CaC_2 (**7**) as an ethynyl group source.

Calcium carbide CaC_2 (**7**) is a widely utilized industrial material that is very inexpensive (0.05 \$/g; 3.2 \$/mol) (Sigma-Aldrich Co., LLC.). However, its synthetic use has been limited by its poor solubility: it is not soluble in non-reactive common organic solvents (Barber and Sloan, 1961). In recent decades, several approaches using strongly coordinating solvents (DMSO, DMF, etc.) and/or coordinating additives (F^-, CO_3^{2-}, HO^-, water, etc.) have been reported, for which **7** served as a practical C_2^{2-} source (Rodygin et al., 2016). It occurred to us that the treatment of **7** with

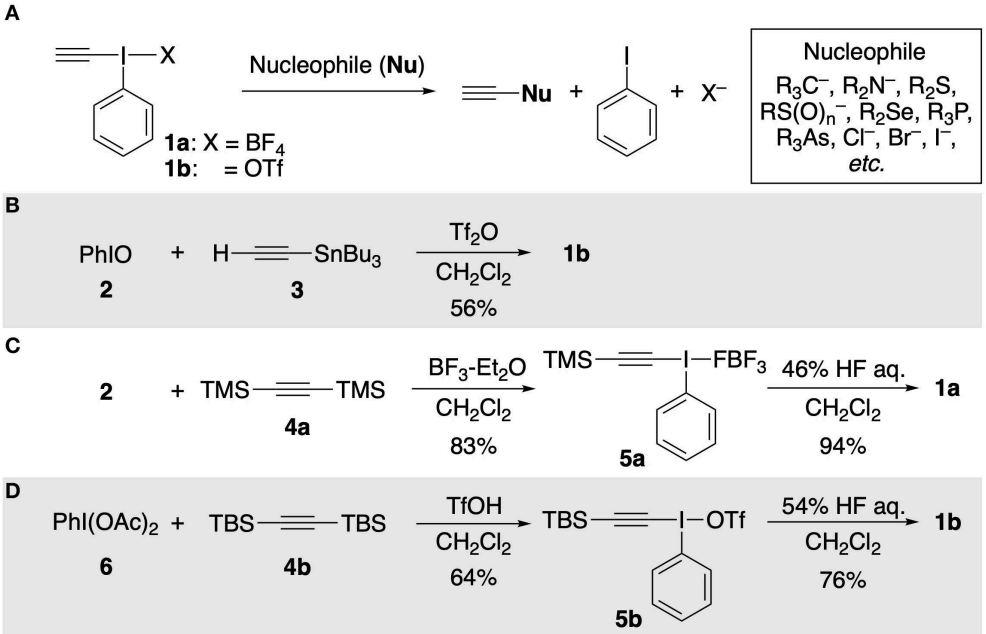

FIGURE 1 | (A) Electrophilic ethynylation of nucleophile with **1**. **(B)** Stang's approach. **(C)** Ochiai's approach. **(D)** Kitamura's approach.

inexpensive chloro(tributyl)stannane (**8**) (0.3 $/g; 98 $/mol) (Sigma-Aldrich Co., LLC.), followed by Sn–I(III) exchange reaction, might provide more convenient and straightforward access to **1**.

MATERIALS AND METHODS

Calcium carbide (∼80%), ethynyl(tributyl)stannane (95%), bis(tributylstannyl)acetylene (95%) were purchased from Sigma Aldrich and used as received. Chloro(tributyl)stannane (>97%), and boron trifluoride etherate (>98%) were purchased from TCI Japan and used as received. (Diacetoxyiodo)benzene (98+%) was purchased from FUJIFILM Wako Pure Chemical or prepared according to the literature (Watanabe et al., 2018). Potassium carbonate (>99.5%) was purchased from FUJIFILM Wako Pure Chemical and used as received. Iodosylbenzene was prepared from (diacetoxyiodo)benzene according to the literature (Sharefkin and Saltzman, 1963). Anhydrous grade of dimethyl sulfoxide, tetrahydrofuran, and *N*, *N*-dimethylformamide was purchased from Kanto Chemical and degassed by purging with argon and/or dried with a solvent purification system containing a one-meter column of activated alumina.

Characterization

NMR spectra were obtained on a Bruker AVANCE 500 spectrometer. Chemical shifts are expressed in δ (ppm) values. ^{1}H NMR, ^{13}C NMR, and ^{19}F NMR spectra were referenced to tetramethylsilane (0 ppm), $CHCl_3$ (7.26, 77.2 ppm), CHD_2CN (1.94 ppm), and CD_3CN (118.3 ppm), $CFCl_3$ (0 ppm) as internal standards. IR spectra were obtained on a JASCO FT/IR-4700 spectrometer. Kieselgel 60 (Merck, 230-400 mesh) was used for column chromatography.

Synthesis of Ethynyl(Tributyl)Stannanes

These reactions were carried out in a two-necked round bottom flask. In a typical reaction: To a stirred suspension of well-ground calcium carbide (**7**) (2.48 g, 38.7 mmol) in DMSO (20 mL) were added chloro(tributyl)stannane (**8**) (3.26 g, 10.0 mmol) and water (0.40 mL, 22.2 mmol) at room temperature under argon. The resulting grayish suspension was warmed to 80°C for 1 h (the disappearance of **8** was monitored by GCMS analysis), then allowed to cool to room temperature. Hexane was added to it, and the organic phase was filtered under reduced pressure through a K_2CO_3-silica gel (1:9) mixture and transferred to a separating funnel. The combined organic phase was washed with water several times, then filtered, and the filtrate was concentrated under reduced pressure to give an oil, which was further purified by chromatography (ø5 mm) on a column packed with K_2CO_3-silica gel (1:9). Elution with hexane gave a pale yellow oil (2.51 g). ^{1}H NMR analysis (mesitylene as an internal standard) showed the formation of a mixture of ethynyl(tributyl)stannane (**3**) (3.4 mmol, 34%) and bis(tributylstannyl)acetylene (**9**) (2.3 mmol, 45%). Capillary GC analysis (n-dodecane as an internal standard; Bruker BR-5ms column 0.25 mm × 30 m, 100°C) showed different yields of **3** (3.6 mmol, 36%) and **9** (1.60 mmol, 32%), probably reflecting partial decomposition of **9** during the GC analysis. This product mixture was used directly for the synthesis of **1a**. Spectroscopic data of **3** and **9** were compared to the authentic samples synthesized according to the literatures (**Supplementary Material**).

Ethynyl(tributyl)stannane (**3**) (Stille and Simpson, 1987): a colorless oil; ^{1}H NMR ($CDCl_3$, 500 MHz) δ 2.20 (s, lH), 1.61–1.54 (m, 6H), 1.40–1.29 (m, 6H), 1.02 (t, $J = 8.2$ Hz, 6H), 0.91 (t, $J = 7.3$ Hz, 9H). ^{13}C NMR ($CDCl_3$, 125 MHz) δ 96.9, 89.1, 29.0, 27.1, 13.8, 11.2.

Bis(tributylstannyl)acetylene (**9**) (Brown and Eichler, 2011): a colorless oil; ^{1}H NMR ($CDCl_3$, 500 MHz) δ 1.69–1.48 (m, 12H), 1.40–1.29 (m, 12H), 1.13–0.94 (m, 12H), 0.90 (t, $J = 7.3$ Hz, 18H). ^{13}C NMR ($CDCl_3$, 125 MHz) δ 116.6, 29.1, 27.1, 13.8, 11.4.

The same procedure was adopted for other conditions shown in **Table 1**.

General Procedure for Synthesis of Ethynyl-λ^3-Iodane 1a From PhI(OAc)$_2$ 6

To a stirred solution of (diacetoxyiodo)benzene (**6**) (159 mg, 0.49 mmol) in dichloromethane (1 mL) was added BF_3-Et_2O (130 μL, 1.04 mmol) at −78°C, and then a 60:40 mixture of stannanes **3** and **9** (301 mg, 0.70 mmol) was slowly added. The reaction mixture was stirred at the same temperature for 1 h, then allowed to warm to room temperature, and the solvent was removed under reduced pressure. The resulting pale yellow solid was washed several times with hexane and Et_2O at 0°C to give **1a** (114 mg, 73%).

Ethynyl(phenyl)(tetrafluoroborato)-λ^3-iodane (**1a**) (Ochiai et al., 1990): a white solid; IR (ATR-FTIR) ν 3,241, 3,080, 2,056, 1,480, 1,442, 1,170–840, 735, 672 cm^{-1}; ^{1}H NMR (CD_3CN, 500 MHz) δ 8.18 (d, $J = 8.5$ Hz, 2H), 7.82 (t, $J = 7.6$ Hz, 1H), 7.64 (dd, $J = 8.5$, 7.6 Hz, 2H), 3.89 (s, 1H). ^{19}F NMR (CD_3CN, 470 MHz) δ −151.8 (s, 4F). ^{13}C NMR ($CDCl_3$, 125 MHz) δ 136.1, 134.6, 133.8, 116.5, 99.0, 26.7 (see also **Supplementary Material**).

General Procedure for Synthesis of Ethynyl-λ^3-Iodane 1a From PhIO 2

To a stirred solution of iodosylbenzene (**2**) (77.6 mg, 0.35 mmol) in dichloromethane (0.7 mL) was added BF_3-Et_2O (100 μL, 0.77 mmol) at −78°C, and then a 38:62 mixture of stannanes **3** and **9** (218 mg, 0.46 mmol) was slowly added. The reaction mixture was stirred at the same temperature for 1 h, then allowed to warm to room temperature, and the solvent was removed under reduced pressure. The resulting pale brown solid was washed several times with hexane and Et_2O at 0°C to give **1a** (90.4 mg, 81%); ^{1}H NMR analysis shows this product contained a small amount of impurities. ^{1}H NMR yield: 67% (mesitylene as an internal standard).

TABLE 1 | Stannylation of CaC_2 **7** with Bu_3SnCl **8**.

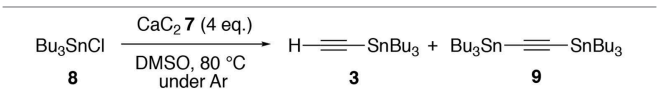

Entry	H_2O (equiv)	Time (h)	Yield (%)[a]	
			3	**9**
1	2	1	(20)	(43)
2[b]	2	1	(34) [36][c]	(45) [32][c]
3	2	6	(10)	(67)
4	2	28	0	72
5	0	28	0	65
6	12	3	[1][c]	[50][c]

Reactions were carried out on 0.3–1 mmol scale.
[a] *Isolated yields based on* ***8****, numbers in parentheses are* ^{1}*H NMR yields.*
[b] *10 mmol scale.*
[c] *GC yields.*

RESULTS AND DISCUSSION

We commenced our study by trapping CaC_2 **7** with **8**. Exposure of well-ground **7** (4 equiv) to **8** in DMSO at room temperature did not give any alkynylstannanes. Addition of small amount of water (2 equiv), which has been reported to be effective for the electrophilic trapping of **7**, was fruitless (Rodygin et al., 2016). On the other hand, heating at 80°C resulted in smooth consumption of **8** and after 1 h, a 6:4 mixture of **3** and bis(tributylstannyl)acetylene (**9**) was obtained in 79% yield (**Table 1**, entry 2). The ratio of **3** and **9** has changed in a range of ca. 3:7–6:4 through several runs, partly due to the reaction scale and the surface area of **7** (entries 1 and 2). Use of longer reaction time increased the ratio of **9** (entries 3 and 4). Under the conditions, the addition of water did not significantly change the yield of **9**, but it accelerated the bis-stannylation (entries 4–6). Interestingly, this stannylation did not occur in other aprotic solvents such as THF and DMF, even at elevated temperatures (≤110°C) (Cochran et al., 1990). It should be noted that these alkynylstannanes **3** and **9** could be separated from other organostannane impurities on a short column packed with K_2CO_3-silica gel (1:9) mixture (Harrowven et al., 2010). Other crystallogen analog, trimethylsilyl chloride did not afford corresponding ethynyl(trimethyl)silanes under optimized conditions, partly because of the more moisture sensitive character of silyl chloride.

Next, we focused on the synthesis of ethynyl-λ^3-iodane **1a** using a mixture of alkynylstannanes **3** and **9**. After screening various reaction conditions, we found an efficient method. Exposure of a 6:4 mixture of **3** and **9** (obtained from the reaction shown in entry 1 in **Table 1**) to a combination of PhI(OAc)$_2$ **6** and BF_3-Et_2O in dichloromethane at −78°C resulted in smooth Sn–I(III) exchange, and after 1 h, **1a** was selectively obtained in 73% yield (**Figure 2A**). The standard PhIO **2**–BF_3-Et_2O system also afforded **1a** in high yield. It should be emphasized that these methods do not require time-consuming work-up. Simple washing of the reaction mixture with hexane and Et_2O by decantation gave pure **1a** and a mixture of Bu_3SnX-type organostannanes thus formed by I(III)–Sn exchange was recovered quantitatively in the supernatant. As we expected, these optimized conditions could also be applied to authentic **3** and **9** individually to provide **1a** in moderate to high yields (**Figure 2B**). In these cases, the combination of I(III)–organostannane pairs (**6**–**3** and **2**–**9**) gave better yields of **1a** than opposite pairs (**6**–**9** and **2**–**3**), although the reason remains unclear. From a mechanistic point of view, our results using **9** is somewhat surprising since the Sn–I(III) exchange of **9** with cyano(trifluoromethylsulfonyloxy)iodobenzene (**10**) selectively affords bis[phenyl(triflato)-λ^3-iodanyl]acetylene (**11**)

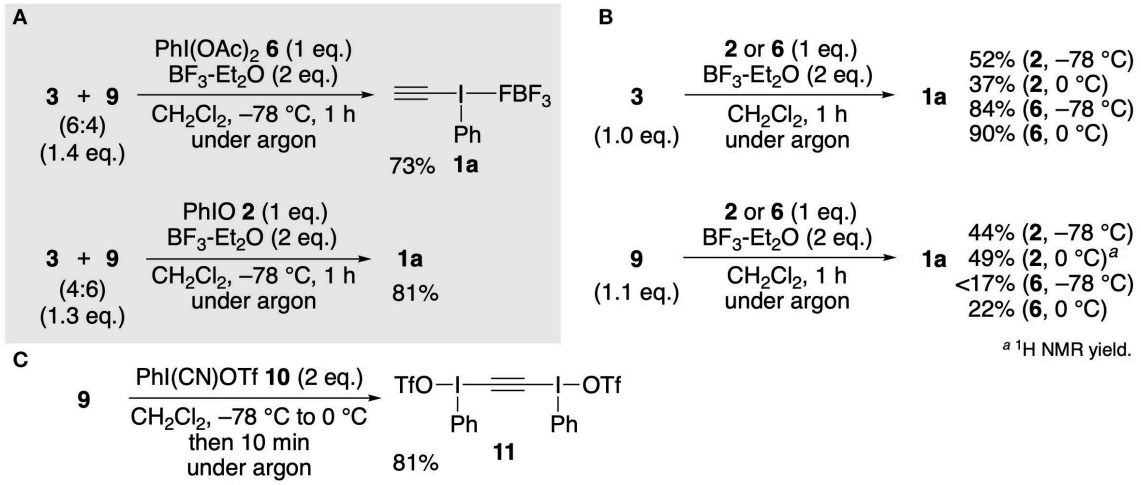

FIGURE 2 | Synthesis of ethynyl(phenyl)-λ^3-iodane **1a**. **(A)** Reaction of a mixture of alkynylstannanes **3** and **9** obtained from CaC_2 **7**. **(B)** Individual reactions of authentic **3** and **9**. **(C)** Stang and Zhdankin's approach.

(**Figure 2C**; Stang and Zhdankin, 1990, 1991). The moderately electrophilic nature of iodine center of the intermediates such as $PhI(OAc)_2$-BF_3 (Izquierdo et al., 2016) or PhIO-BF_3 (Ochiai, 2007) might be partly responsible for the selective formation of **1a**.

CONCLUSION

In summary, we have developed a safe and inexpensive two-step method for the synthesis of **1a** using readily available CaC_2 **7** as an ethynyl group source. This method not only provides time-/cost-/labor-saving methodology to prepare unstable ethynyl-λ^3-iodane **1**, but also serves as an effective approach for synthetically useful but costly bis(stannyl)acetylene **9** (Brend'amour et al., 2018).

DATA AVAILABILITY STATEMENT

All datasets generated for this study are included in the article/**Supplementary Material**.

AUTHOR CONTRIBUTIONS

KM and MU conceived and designed the experiments and wrote the manuscript. TH and TO conducted the experiments. All authors participated in data analyses and discussions.

FUNDING

This work was supported by grants from JSPS KAKENHI (S) (17H06173), KAKENHI (B) (17H03017), NAGASE Science & Technology Development Foundation, and Sumitomo Foundation.

SUPPLEMENTARY MATERIAL

The Supplementary Material for this article can be found online at: https://www.frontiersin.org/articles/10.3389/fchem.2020.00012/full#supplementary-material

REFERENCES

Barber, W. A., and Sloan, C. L. (1961). Solubility of calcium carbide in fused salt system. *J. Phys. Chem.* 65, 2026–2028. doi: 10.1021/j100828a025

Brend'amour, S., Gilmer, J., Bolte, M., Lerner, H. W., and Wagner, M. (2018). *C*-halogenated 9,10-diboraanthracenes: how the halogen load and distribution influences key optoelectronic properties. *Chem. Eur. J.* 24, 16910–16915. doi: 10.1002/chem.201804288

Brown, A. E., and Eichler, B. E. (2011). Symmetric diarylacetylenes: one-pot syntheses and solution photoluminescence. *Tetrahedron Lett.* 52, 1960–1963. doi: 10.1016/j.tetlet.2011.02.062

Cochran, J. C., Lemieux, R. P., Giacobbe, R. C., and Roitstein, A. (1990). Synthesis of bis-stannylacetylenes from calcium carbide; assisted by ultrasound. *Synth. React. Inorg. Met. Org. Chem.* 20, 251–261. doi: 10.1080/00945719008048132

Harrowven, D. C., Curran, D. P., Kostiuk, S. L., Wallis-Guy, I. L., Whiting, S., Stenning, K. J., et al. (2010). Potassium carbonate–silica: a highly effective stationary phase for the chromatographic removal of organotin impurities. *Chem. Commun.* 46, 6335–6337. doi: 10.1039/C0CC01328E

Izquierdo, S., Essafi, S., del Rosal, I., Vidossich, P., Pleixats, R., Vallribera, A., et al. (2016). Acid activation in phenyliodine dicarboxylates: direct observation, structures, and implications. *J. Am. Chem. Soc.* 138, 12747–12750. doi: 10.1021/jacs.6b07999

Kitamura, T., Morshed, M. H., Tsukada, S., Miyazaki, Y., Iguchi, N., and Inoue, D. (2011). Alkynylation of benzotriazole with silylethynyliodonium triflates. Regioselective synthesis of 2-ethynyl-2*H*-benzotriazole derivatives. *J. Org. Chem.* 76, 8117–8120. doi: 10.1021/jo2015467

Mckee, D., Thoma, A., Bailey, K., and Fish, J. (2014). A review of hydrofluoric acid burn management. *Plast. Surg.* 22, 95–98.

Ochiai, M. (2003). "Reactivities, properties and structures," *Topic in Current Chemistry*, *Vol. 224*, ed T. Wirth (Cham: Springer), 5–68.

Ochiai, M. (2007). Stoichiometric and catalytic oxidations with hypervalent organo-λ^3-iodanes. *Chem. Rec.* 7, 12–23. doi: 10.1002/tcr.20104

Ochiai, M., Ito, T., Takaoka, Y., Masaki, Y., Kunishima, M., Tani, S., et al. (1990). Synthesis of ethynyl(phenyl)iodonium tetrafluoroborate. A new reagent for ethynylation of 1,3-dicarbonyl compounds. *J. Chem. Soc. Chem. Commun.* 1990, 118–119. doi: 10.1039/C39900000118

Ochiai, M., Miyamoto, K., Suefuji, T., Sakamoto, S., Yamaguchi, K., and Shiro, M. (2003). Synthesis, characterization, and reaction of ethynyl(phenyl)-λ^3-iodane complex with [18]crown-6. *Angew. Chem. Int. Ed.* 42, 2191–2194. doi: 10.1002/anie.200250866

Rodygin, K. S., Werner, G., Kucherov, F. A., and Ananikov, V. P. (2016). Calcium carbide: a unique reagent for organic synthesis and nanotechnology. *Chem. Asian J.* 11, 965–976. doi: 10.1002/asia.201501323

Sharefkin, J. G., and Saltzman, H. (1963). Iodosobenzene. *Org. Synth.* 43:60. doi: 10.15227/orgsyn.043.0060

Stang, P. J., Arif, A. M., and Crittell, C. M. (1990). Ethynyl(phenyl)iodonium triflate, [HCCIPh][OSO_2CF_3]: preparation, spectral properties, mechanism of formation and X-ray molecular structure. *Angew. Chem. Int. Ed. Engl.* 29, 287–288. doi: 10.1002/anie.199002871

Stang, P. J., and Zhdankin, V. V. (1990). Bis[phenyl[(perfluoroalkanesulfonyl)oxy]iodo]acetylene, $PhI^+CCI^+Ph\bullet 2R_FSO_3^-$, and 1,4-bis[phenyl[(perfluoroalkanesulfonyl)oxy]iodo]-1,3-butadiyne, $PhI^+CC\text{-}CCI^+Ph\bullet 2\ R_FSO_3^-$. *J. Am. Chem. Soc.* 112, 6437–6438. doi: 10.1021/ja00173a064

Stang, P. J., and Zhdankin, V. V. (1991). Preparation and chemistry of $PhI^+CCI^+Ph\bullet 2^-OTf$, bis[phenyl[[(trifluoromethyl) sulfonyl]oxy]iodo]acetylene, a novel difunctional acetylene, bis(iodonium) species and a stable C_2-transfer agent. *J. Am. Chem. Soc.* 113, 4571–4576. doi: 10.1021/ja00012a028

Stille, J. K., and Simpson, J. H. (1987). Stereospecific palladium-catalyzed coupling reactions of vinyl iodides with acetylenic tin reagents. *J. Am. Chem. Soc.* 109, 2138–2152. doi: 10.1021/ja00241a035

Varvoglis, A. (1992). *The Organic Chemistry of Polycoordinated Iodine*. New York, NY: VCH.

Waser, J. (2016). "Alkynylation with hypervalent iodine reagents," *Topic in Current Chemistry*, *Vol. 373,* ed T. Wirth (Cham: Springer), 187–222.

Watanabe, A., Miyamoto, K., Okada, T., Asawa, T., and Uchiyama, M. (2018). Safer synthesis of (diacetoxyiodo)arenes using sodium hypochlorite pentahydrate. *J. Org. Chem.* 83, 14262–14268. doi: 10.1021/acs.joc.8b02541

Yoshimura, A., and Zhdankin, V. V. (2016). Advances in synthetic applications of hypervalent iodine compounds. *Chem. Rev.* 116, 3328–3435.

Yudasaka, M., Shimbo, D., Maruyama, T., Tada, N., and Itoh, A. (2019). Synthesis, characterization, and reactivity of an ethynyl benziodoxolone (EBX)–acetonitrile complex. *Org. Lett.* 21, 1098–1102. doi: 10.1021/acs.orglett.9b00005

Conflict of Interest: The authors declare that the research was conducted in the absence of any commercial or financial relationships that could be construed as a potential conflict of interest.

frontiers in Chemistry

ORIGINAL RESEARCH
published: 18 March 2020
doi: 10.3389/fchem.2020.00183

A Benziodoxole-Based Hypervalent Iodine(III) Compound Functioning as a Peptide Coupling Reagent

Li-Jun Qiu[1†], *Dan Liu*[1†], *Ke Zheng*[1†], *Ming-Tao Zhang*[2*] *and Chi Zhang*[1*]

[1] State Key Laboratory of Elemento-Organic Chemistry, Collaborative Innovation Center of Chemical Science and Engineering (Tianjin), College of Chemistry, Nankai University, Tianjin, China, [2] Computational Center for Molecular Science, Nankai University, Tianjin, China

1-Benzoyloxy-1,2-benziodoxol-3-(1H)-one (IBA-OBz), a readily available and bench stable benziodoxole-based iodine(III) reagent, can be employed for the synthesis of dipeptides from various standard and sterically hindered amino acids in the presence of $(4\text{-}MeOC_6H_4)_3P$. The combined system of IBA-OBz/$(4\text{-}MeOC_6H_4)_3P$ is also successfully applied to the solid-phase peptide synthesis and a pentapeptide leu-enkephalin in unprotected form has been synthesized. Density functional theory calculations reveal that the rate-limiting step is nucleophilic attack of 4-dimethylaminopyridine (DMAP) onto IBA-OBz.

Keywords: peptide, IBA-OBz, hypervalent iodine(III) reagent, solid-phase peptide synthesis (SPPS), DFT calculations

OPEN ACCESS

Edited by:
Toshifumi Dohi,
Ritsumeikan University, Japan

Reviewed by:
Kensuke Kiyokawa,
Osaka University, Japan
Ayman Ahmed El-Faham,
King Saud University, Saudi Arabia

***Correspondence:**
Ming-Tao Zhang
zhangmt@nankai.edu.cn
Chi Zhang
zhangchi@nankai.edu.cn

[†] *These authors have contributed equally to this work*

Specialty section:
This article was submitted to Organic Chemistry, a section of the journal Frontiers in Chemistry

Received: *11 January 2020*
Accepted: *27 February 2020*
Published: *18 March 2020*

Citation:
Qiu L-J, Liu D, Zheng K, Zhang M-T and Zhang C (2020) A Benziodoxole-Based Hypervalent Iodine(III) Compound Functioning as a Peptide Coupling Reagent. Front. Chem. 8:183. doi: 10.3389/fchem.2020.00183

INTRODUCTION

Hypervalent iodine reagents have attracted considerable attention of synthetic chemists due to their rich reactivities, low toxicity, ready, availability, and recyclability (Varvoglis, 1997; Zhdankin and Stang, 2002, 2008; Wirth, 2005; Brown et al., 2013; Singh and Wirth, 2014; Zhdankin, 2014; Duan et al., 2016; Li et al., 2016; Yoshimura and Zhdankin, 2016; Han and Zhang, 2018; Liu et al., 2019). In 2012, we first reported that iodosodilactone, a bicyclic benziodoxole compound, could function as a coupling reagent to promote the efficient syntheses of esters, macrocyclic lactones, amides, and peptides in the presence of PPh_3 at 60°C (**Scheme 1**) (Tian et al., 2012). We subsequently designed and synthesized a new powerful analog of iodosodilactone, FPID, which could mediate the peptide coupling reactions of standard amino acids and sterically hindered amino acids in good to high yields within 30 min in the presence of $(4\text{-}MeOC_6H_4)_3P$ at room temperature (**Scheme 1B**) (Zhang et al., 2015). Recently, we successfully applied this system to the solid-phase peptide synthesis and cyclic peptide synthesis (Liu et al., 2018). Notably, FPID can be readily regenerated after reaction, and iodosodilactone shares the same feature, which is not provided in the existing peptide coupling reagents (Constable et al., 2007; EI-Faham and Albericio, 2011). Although FPID has the advantages of high efficiency, wide range of substrates ranging from standard amino acids to sterically hindered amino acids, and recyclability in peptide synthesis reactions, it should be prepared after four steps reaction of Suzuki coupling, diazotization/iodination, oxidation by potassium permanganate, and oxidation by aqueous sodium hypochlorite solution using commercially available 4-bromo-2,6-dimethylaniline and 3,5-bis(trifluoromethyl)-phenyl boronic acid as starting materials. Apparently, FPID is not readily available, which would have an adverse effect on its practical use. Thus, it is necessary to develop readily available and efficient iodine(III)-based peptide coupling reagents to promote their practical application in oligopeptide

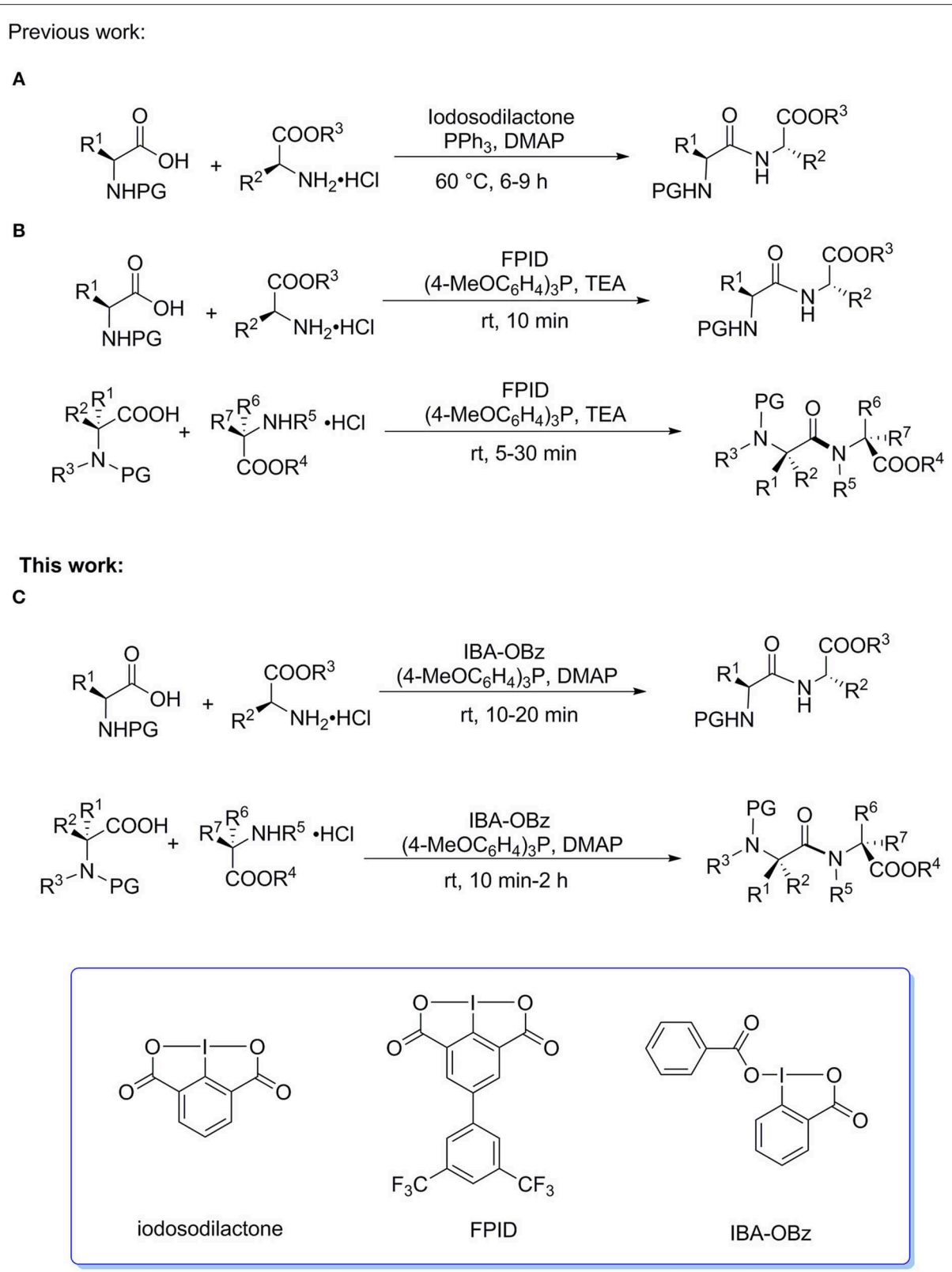

SCHEME 1 | Peptide Synthesis Mediated by Hypervalent Iodine(III) Reagents. **(A)** Peptide coupling of standard amino acids mediated by iodosodilactone. **(B)** Peptide coupling of standard and sterically hindered amino acids mediated by FPID. **(C)** Peptide coupling of standard and sterically hindered amino acids mediated by IBA-OBz.

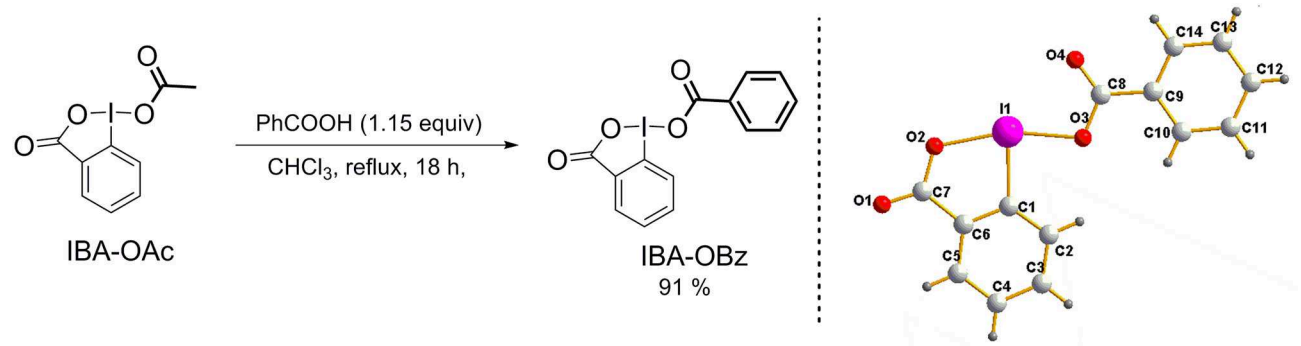

SCHEME 2 | Synthesis and X-ray crystal structure of IBA-OBz.

synthesis. IBA-OBz is a benziodoxole-based iodine(III) compound which can be prepared by one-step reaction from a commercial available I(III) compound IBA-OAc. We speculated that the structure of IBA-OBz would have similarity to FPID when taking account of two benzoyloxy ligands attached to central iodine(III) atom, furthermore, we assumed that it would exhibit a similar reactivity to FPID in peptide coupling reaction. Herein, we reported that an efficient preparation of IBA-OBz and its synthetic utility as an efficient coupling reagent to promote the synthesis of dipeptides and the solid-phase peptide synthesis of a pentapeptide leu-enkephalin. (**Scheme 1C**).

RESULTS AND DISCUSSION

IBA-OBz was readily prepared via a single-step process (**Scheme 2**). On the basis of the previous method (Mocci et al., 2007), a ligand exchange reaction between commercially available IBA-OAc and benzoic acid (1.15 equiv) in anhydrous $CHCl_3$ [0.5 M of IBA-OAc] furnished IBA-OBz in 91% yield as a colorless solid. Notably, IBA-OBz could be prepared on a large scale (20 mmol, 5.9 g) in 81% yield and stored for 1 year at room temperature without detectable decomposition.

The structure of IBA-OBz was elucidated by means of NMR spectroscopy and X-ray crystallography (for details, see **Figure S1** and **Table S1**). The ^{13}C NMR signal for the carbon atom connected to the iodine(III) central atom was found at 118.8 ppm, which was in the typical region for hypervalent iodine(III) compounds. Moreover, the single crystal structure of IBA-OBz was firstly obtained from chloroform/diethyl ether. The X-ray crystallography revealed that the O2-I1-O3 bond angles (163.95°) was <180° and the O3-I1-C1 and O2-I1-C1 bond angles (84.40° and 79.68°, respectively) deviated from 90°, which demonstrated IBA-OBz had the distorted T-shaped structure.

We firstly chose Boc-$_L$-Phe-OH and H-$_L$-Leu-OMe·HCl as two model substrates to test whether IBA-OBz can mediate peptide synthesis (**Table 1**). To our delight, the desired dipeptide Boc-Phe-Leu-OMe was obtained in 66% yield within 10 min upon treatment with 1.2 equiv of IBA-OBz, 1.0 equiv of (4-$MeOC_6H_4)_3P$, and 3.0 equiv of TEA in DCE at room temperature (**Table 1**, entry 1). Subsequently various organic solvents including DCM, $CHCl_3$, THF, EtOAc, acetone, CH_3CN, toluene, and DMF were screened. However, none of these solvents gave better yields than that in DCE (entries 2–9). Thereafter, DCE was selected as the solvent of choice, and other organic bases were accordingly screened in DCE. The results showed that 1,8-diazabicyclo[5.4.0]undec-7-ene (DBU), DMAP, *N,N*-diisopropylethylamine (DIPEA), 4-methylmorpholine (NMM), *N*-methylimidazole (NMI), and 4-pyrrolidinopyridine gave the product in 30–80% yields, in which DMAP was the best one (entries 10–15). When 1.5 equiv of both IBA-OBz and (4-$MeOC_6H_4)_3P$ were used, the yield could be improved to 86% (entry 16). Therefore, we obtained the optimal reaction conditions in which 1.5 equiv of both IBA-OBz and (4-$MeOC_6H_4)_3P$ and 3.0 equiv of DMAP were used in DCE (0.04 M) at room temperature.

With the optimal conditions in hand, we first evaluated the performance of IBA-OBz for the synthesis of dipeptides from various standard amino acids (**Table 2**). All dipeptides were obtained in moderate to excellent yields within 10–20 min. This protocol was successfully applied to different amino protecting groups including Boc and Cbz, without detriment to yields (**Table 2**, entries 4, 5). Nevertheless, TEA was used instead of DMAP to avoid deprotection when amino protecting group was Fmoc (entry 6). When Cbz-Ala-OH was used as the carboxylic acid partner, moderate to high yields were obtained (entries 8–10). It is unnecessary to protect the indole ring of tryptophan in the peptide coupling reaction mediated by IBA-OBz (entry 13). Notably, for amino acids containing unprotected hydroxyl groups, such as serine (entry 17), threonine (entry 18) and tyrosine (entry 19), the use of TEA instead of DMAP could improve the coupling efficiency. Remarkably, reactions of sterically hindered amino acids such as valine (entries 20–22) and proline (entries 10, 22–26) also worked well, providing the corresponding dipeptides in yields up to 93%. Compared to peptide coupling reaction mediated by FPID, the reaction yields of Cbz-$_L$-Phe-$_L$-Thr-OMe (entry 18) and Boc-$_L$-Val-$_L$-Pro-OMe (entry 22) still needed to be improved.

Sterically hindered amino acids such as *N*-methylamino acids and α,α-disubstituted amino acids are widely present in a variety of naturally occurring peptides and pharmaceuticals (the antihypertension drug lisinopril) (Slomczynska et al., 1992; Wenschuh et al., 1995; Humphrey and Chamberlin, 1997).

TABLE 1 | Optimization of reaction conditions for Boc-Phe-Leu-OMe synthesis[a].

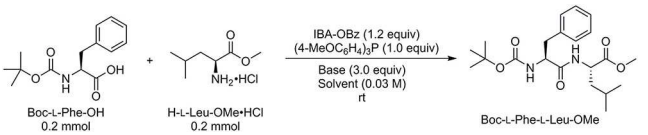

Entry	Solvent	Base	Time (min)	Yield (%)[b]
1	DCE	TEA	10	66
2	$CHCl_3$	TEA	10	48
3	DCM	TEA	10	48
4	THF	TEA	10	31
5	EtOAc	TEA	10	61
6	Acetone	TEA	10	27
7	CH3CN	TEA	10	39
8	Toluene	TEA	300	43
9	DMF	TEA	10	56
10	DCE	DBU	10	30
11	DCE	DMAP	10	80
12	DCE	DIPEA	10	62
13	DCE	NMM	20	60
14	DCE	NMI	10	47
15	DCE	4-Pyrrolidinopyridine	10	68
16[c]	DCE	DMAP	10	86

[a]*Reaction conditions: Boc-$_L$-Phe-OH (0.2 mmol), H-$_L$-Leu-OMe·HCl (0.2 mmol), IBA-OBz (0.24 mmol), (4-MeOC$_6$H$_4$)$_3$P (0.2 mmol), Base (0.6 mmol), Solvent (5 mL).* [b]*Isolated yield.* [c]*The optimal reaction conditions: Boc-$_L$-Phe-OH (0.2 mmol), H-$_L$-Leu-OMe·HCl (0.2 mmol), IBA-OBz (0.3 mmol), (4-MeOC$_6$H$_4$)$_3$P (0.3 mmol), DMAP (0.6 mmol), DCE (5 mL).*

TABLE 2 | IBA-OBz mediated synthesis of dipeptides from standard amino acids[a].

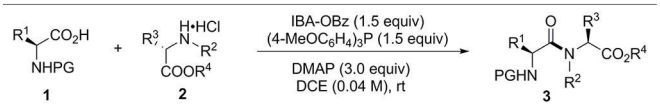

Entry	Dipeptide	Time (min)	Yield (%)[b]
1	Boc-$_L$-Phe-$_L$-Leu-OMe (**3-1**)	10	86
2	Boc-Gly-Gly-OMe (**3-2**)	10	81
3	Boc-$_L$-Leu-$_L$-Lys(Z)-OMe (**3-3**)	10	84
4	Boc-$_L$-Leu-$_L$-Ala-OMe (**3-4**)	10	85
5	Cbz-$_L$-Leu-$_L$-Ala-OMe (**3-5**)	10	78
6[c]	Fmoc-$_L$-Leu-$_L$-Ala-OMe (**3-6**)	10	84
7	Cbz-$_L$-Leu-$_L$-Lys(Z)-OMe (**3-7**)	10	91
8	Cbz-$_L$-Ala-$_L$-His(Trt)-OMe (**3-8**)	10	88
9	Cbz-$_L$-Ala-$_L$-Cys(Trt)-OMe (**3-9**)	20	75
10	Cbz-$_L$-Ala-$_L$-Pro-OMe (**3-10**)	10	59
11	Cbz-$_L$-Met-Gly-OMe (**3-11**)	10	77
12	Cbz-$_L$-Met-Gly-OEt (**3-12**)	10	89
13	Cbz-$_L$-Trp-$_L$-Leu-OMe (**3-13**)	10	80
14	Cbz-$_L$-Asn(Trt)-$_L$-Leu-OMe (**3-14**)	10	75
15	Cbz-$_L$-Phe-$_L$-Ile-OMe (**3-15**)	10	84
16	Cbz-$_L$-Phe-$_L$-Tyr(Bzl)-OMe (**3-16**)	10	73
17[c]	Cbz-$_L$-Phe-$_L$-Ser-OMe (**3-17**)	10	60
18[c]	Cbz-$_L$-Phe-$_L$-Thr-OMe (**3-18**)	10	42
19[c]	Cbz-$_L$-Phe-$_L$-Tyr-OMe (**3-19**)	10	84
20	Boc-$_L$-Val-$_L$-Val-OMe (**3-20**)	10	75
21	Cbz-$_L$-Val-$_L$-Glu(OEt)-OEt (**3-21**)	20	70
22	Boc-$_L$-Val-$_L$-Pro-OMe (**3-22**)	10	46
23	Boc-$_L$-Pro-$_L$-Ala-OMe (**3-23**)	10	84
24	Boc-$_L$-Pro-$_L$-Leu-OMe **(3-24)**	10	93
25	Boc-$_L$-Leu-$_L$-Pro-OMe (**3-25**)	10	63
26	Cbz-Gly-$_L$-Pro-OMe (**3-26**)	10	83

[a]*Conditions: N-PG-AA$_1$-OH (0.2 mmol), H-AA$_2$-OMe·HCl (0.2 mmol), IBA-OBz (0.3 mmol), (4-MeOC$_6$H$_4$)$_3$P (0.3 mmol), DMAP (0.6 mmol), DCE (5 mL).* [b]*Isolated yield.* [c]*TEA was used instead of DMAP.*

However, the synthesis of peptides containing sterically hindered amino acids has limitation due to poor yields using conventional coupling reagents (i.e., DCC/HOBT) (Balasubramanian et al., 1981; Leibfritz et al., 1982). The existing processes generally require the preparation of activated amino acid derivatives to achieve the desired results (Katritzky et al., 2007; Brown and Schafmeister, 2008). Hence, we evaluated the IBA-OBz/(4-MeOC$_6$H$_4$)$_3$P system with several sterically hindered amino acids (**Table 3**). Most dipeptides were obtained in moderate to high yields within 10–60 min. It was worth noting that widely used amino protecting group Boc, which decomposed readily using BOP system, was compatible with the present reaction system (**Table 3**, entries 1–5). Coupling reactions between α,α-disubstituted amino acid (H-Aib-OMe) and a series of standard amino acids provided the corresponding dipeptides in 59–77% yields (entries 6–10). Notably, the coupling reaction proceeded smoothly even when both amino acids were sterically hindered, affording dipeptides in moderate to good yields (entries 11–13). Reactions of *N*-methylamino acids (Cbz-*N*(Me)-Phe-OH) with various standard amino acids produced the corresponding dipeptides in yields up to 91% (entries 14–22). Furthermore, coupling efficiency was improved by using TEA instead of DMAP when tyrosine was a component of dipeptides (entries 4, 22).

In order to verify the application of IBA-OBz/(4-MeOC$_6$H$_4$)$_3$P system in the solid-phase peptide synthesis (SPPS), we chose unprotected Leu-enkephalin as the target short peptide, which was isolated from pig brains and had the effect of modifying neurotransmitters (Hughes et al., 1975; Coste et al., 1991). A commercially available 2-chlorotriphenylmethyl chloride resin (2-Cl-Trt-Cl Resin) was used as a carrier for the solid-phase peptide synthesis under standard conditions of Fmoc-solid-phase peptide synthesis (Fmoc-SPPS). The unprotected Leu-enkephalin was synthesized following the route (**Scheme 3**). The carboxylic group of Fmoc-Leu-OH was connected to 2-Cl-Trt-Cl resins to obtain the 2-chlorotrityl resin-bound Leu(Fmoc) (**7a**) in the presence of 3.0 equiv of *N,N*-diisopropylethylamine in DCM/*N,N*-dimethylformamide (DMF) (v/v = 1:1) within 4 h. The protecting group Fmoc was then removed from **7a** upon the treatment of 20% piperidine/DMF within 30 min. Subsequently the peptide coupling reaction of Fmoc-Phe-OH with the 2-chlorotrityl resin-bound Leu produced 2-chlorotrityl resin-bound Leu-Phe dipeptide **7b** using 3.0 equiv of IBA-OBz, 3.0 equiv of (4-MeOC$_6$H$_4$)$_3$P, and 3.0 equiv of TEA in DMF at room temperature within 2 h. The N-terminus of **7b** was then

TABLE 3 | IBA-OBz mediated synthesis of dipeptides from sterically hindered amino acids[a].

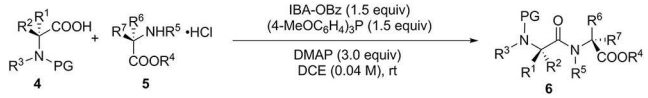

Entry	Dipeptide	Time (min)	Yield (%)[b]
1	Boc-$_L$-Ala-Aib-OMe (**6-1**)	40	79
2	Boc-Gly-Aib-OMe (**6-2**)	10	72
3	Boc-$_L$-Leu-Aib-OMe (**6-3**)	10	67
4[c]	Boc-$_L$-Tyr-Aib-OMe (**6-4**)	10	70
5	Boc-$_L$-Pro-Aib-OMe (**6-5**)	120	81
6	Cbz-$_L$-Trp-Aib-OMe (**6-6**)	20	77
7	Cbz-$_L$-Phe-Aib-OMe (**6-7**)	20	59
8	Cbz-$_L$-Ala-Aib-OMe (**6-8**)	40	62
9	Cbz-$_L$-Met-Aib-OMe (**6-9**)	40	63
10	Cbz-$_L$-Ser(tBu)-Aib-OMe (**6-10**)	10	68
11	Cbz-$_L$-Val-Aib-OMe (**6-11**)	50	46
12	Cbz-$_L$-NMePhe-Aib-OMe (**6-12**)	20	72
13	Cbz-$_L$-NMePhe-$_L$-Val-OMe (**6-13**)	10	83
14	Cbz-$_L$-NMePhe-Gly-OMe (**6-14**)	30	90
15	Cbz-$_L$-NMePhe-$_L$-Ala-OMe (**6-15**)	10	81
16	Cbz-$_L$-NMePhe-$_L$-Ile-OMe (**6-16**)	10	86
17	Cbz-$_L$-NMePhe-$_L$-His(Trt)-OMe (**6-17**)	10	81
18	Cbz-$_L$-NMePhe-$_L$-Tyr(Bzl)-OMe (**6-18**)	10	90
19	Cbz-$_L$-NMePhe-$_L$-Cys(Trt)-OMe (**6-19**)	10	80
20	Cbz-$_L$-NMePhe-$_L$-Lys(Z)-OMe (**6-20**)	10	88
21	Cbz-$_L$-NMePhe-$_L$-Glu(OEt)-OEt (**6-21**)	10	82
22[c]	Cbz-$_L$-NMePhe-$_L$-Tyr-OMe (**6-22**)	10	91

[a]*Conditions: N-PG-AA$_1$-OH (0.2 mmol), H-AA$_2$-OMe·HCl (0.2 mmol), IBA-OBz (0.3 mmol), (4-MeOC$_6$H$_4$)$_3$P (0.3 mmol), DMAP (0.6 mmol), DCE (5 mL).* [b]*Isolated yield.* [c]*TEA was used instead of DMAP.*

sequentially extended with the Fmoc-Gly-OH, Fmoc-Gly-OH, Fmoc-Tyr-OH units using the standard Fmoc solid-phase peptide synthesis (SPPS) procedure to give **7c**. After Fmoc group was removed from **7c**, the pentapeptide chain was then cleaved from the resin upon the treatment of 0.5% trifluoroacetic acid/DCM to give the desired pentapeptide Leu-enkephalin. The Leu-enkephalin was purified by reversed-phase HPLC and it was finally obtained in moderate yield (44% over 10 steps). This successful synthesis of the N-,C-unprotected Leu-enkephalin demonstrated that the IBA-OBz/(4-MeOC$_6$H$_4$)$_3$P system was suitable not only in solution phase peptide synthesis but also in solid-phase peptide synthesis.

To shed light on the reaction mechanism of this peptide bond formation reaction mediated by IBA-OBz, we performed DFT computations (Liu et al., 2009; Schoenebeck and Houk, 2010; Zhou and Li, 2015) to characterize the pathways for the reaction of Boc-Gly-OH and H-Gly-OMe·HCl with IBA-OBz (for details, see **Supporting Information**). As illustrated in **Figure 1**, the reaction would proceed through substitution of the OBz group of IBA-OBz with DMAP, generating zwitterion **IM1** via **TS1**by crossing a barrier of 27.4 kcal/mol (**TS1**). ESI-mass analysis of a reaction mixture containing IBA-OBz, DMAP, and (4-MeOC$_6$H$_4$)$_3$P in DCE under room temperature would yield a peak at m/z = 491.2082, which was assigned to be [**IM1**+H]$^+$ (for details, see the **Figure S2**). Subsequently, the nucleophilic attack of (4-MeOC$_6$H$_4$)$_3$P to zwitterion **IM1** resulted in zwitterion **IM2** by crossing a barrier of 25.3 kcal/mol (**TS2**). The carboxylic group of Boc-Gly-OH would attack **IM2** at the phosphorus center to give **IM3**, following with the leaving of benzoic acid anion via **TS3** to produce **IM4**, which was predicted to require an activation free energy of 3.9 kcal/mol. Then, the **IM4** was attacked by amino group of H-Gly-OMe to afford **IM5**, which had a barrier of only 4.6 kcal/mol. Subsequent (4-MeOC$_6$H$_4$)$_3$P=O dissociation through **TS4** to generate dipeptide product **II**, which was calculated to have a barrier of only 0.8 kcal/mol. Reviewing all of the calculated energy profile, the overall reaction was exergonic by 80.8 kcal/mol and thus highly thermodynamically favorable. The formation of **IM1** via **TS1** constituted to be a rate-limiting step of the reaction with an energy barrier of 27.4 kcal/mol.

On the basis of experimental and computational studies, we proposed a reaction mechanism (**Scheme 4**). IBA-OBz was initially activated by DMAP to form the zwitterion **IM1**. Zwitterion **IM1** then would undergo the ligand exchange with (4-MeOC$_6$H$_4$)$_3$P to give the zwitterion **IM2**, which reacted with the carboxylic group of Boc-Gly-OH to form a key intermediate acyloxyphosphonium intermediate **IM4**. Subsequently intermediate **IM4** was attacked by the amino group of H-Gly-OMe to afford a dipeptide **II** and by-product tris(4-methoxyphenyl)phosphine oxide.

CONCLUSION

In conclusion, we reported a peptide coupling reaction mediated by a readily available, bench stable benziodoxole-based iodine(III) reagent IBA-OBz. In combination with tris(4-methoxyphenyl)phosphine and an organic base (DMAP or TEA), the reagent system not only effectively mediated the peptide coupling reaction of standard amino acids and sterically hindered amino acids in the solution-phase peptide synthesis, but also could be used in the solid-phase peptide synthesis. DFT calculations revealed that the formation of **IM1** was a rate-limiting step of the peptide coupling reaction and the presence of **IM1** was supported by its ESI mass spectrum.

MATERIALS AND METHODS

Experimental and Computational Details

The ^{1}H NMR spectra were recorded at 400 MHz and ^{13}C NMR spectra were measured at 100 MHz using a Bruker AV400 instrument with CDCl3 as the solvent. The chemical shifts (δ) were measured in ppm and with the solvents as references (For CDCl3, ^{1}H: δ = 7.26 ppm, ^{13}C: δ = 77.00 ppm). The multiplicities of the signals are described using the following abbreviations: s = singlet, d = doublet, t = triplet, q = quartet, m = multiplet, dd = doublet of doublets, br = broad. High resolution mass spectral analyses (HRMS) were performed on a high resolution ESI-FTICR mass spectrometer (Varian 7.0 T).

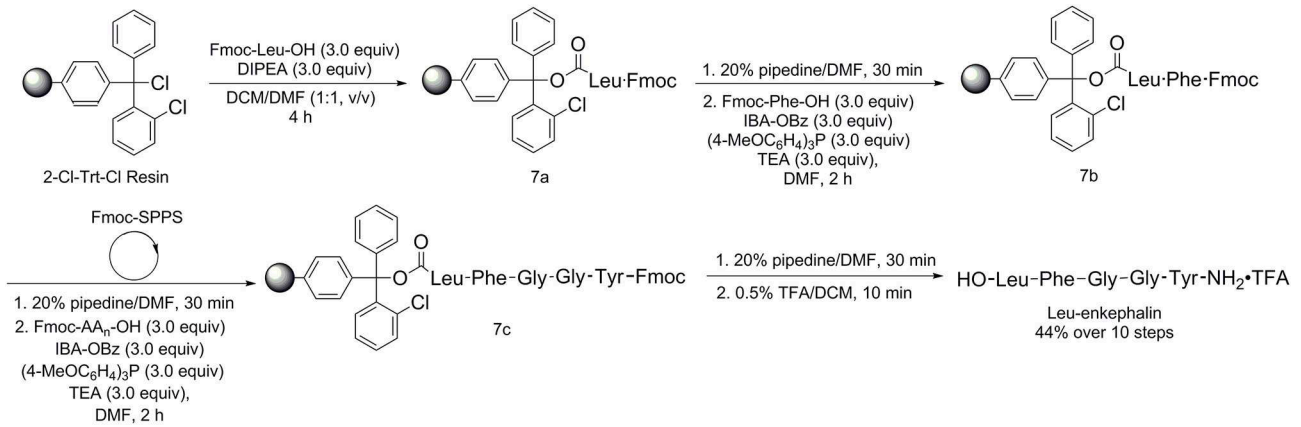

SCHEME 3 | Synthesis of unprotected Leu-enkephalin by solid-phase peptide synthesis.

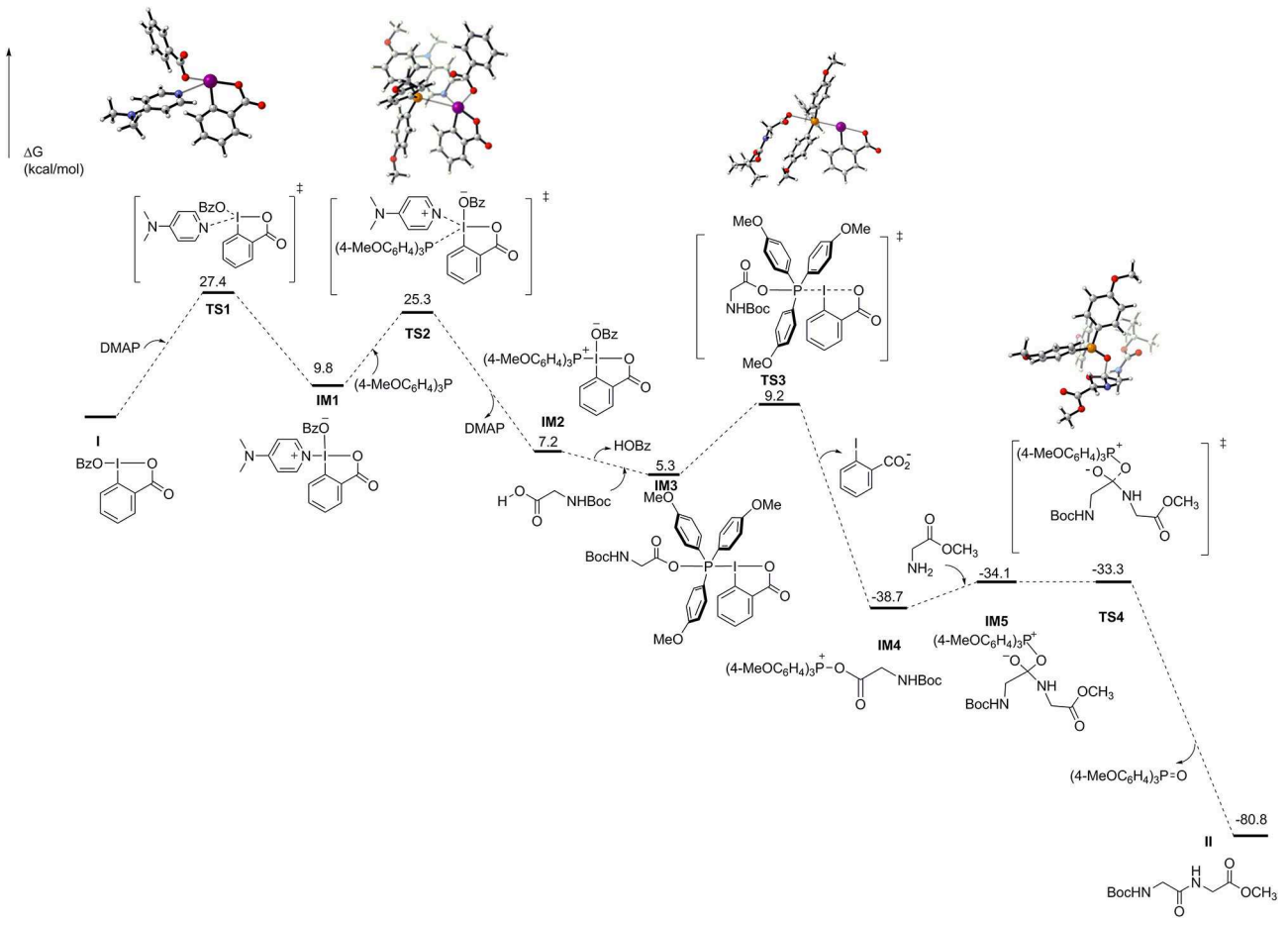

FIGURE 1 | Energy diagram for IBA-OBz-mediated peptide formation calculated at the M06-2X/[6-311++G(2df,2p) + SDD(I)] (SMD)//M06-2X/[6-31+G(d) + Lanl2dz(I)] (SMD) level. Free energies are in kilocalories per mole, and bond lengths are in angstroms.

High performance liquid chromatography (HPLC) analysis was conducted using Shimadzu LC-10 AD coupled diode array-detector SPD-MA-10A-VP and chiral column of Daicel CHIRALCEL OD-H (4.6 mm−25 cm), AD-H (4.6 mm−25 cm), or AS-H (4.6 mm−25 cm). Melting points were recorded on a RY-1 type apparatus. All solvents were obtained from commercial

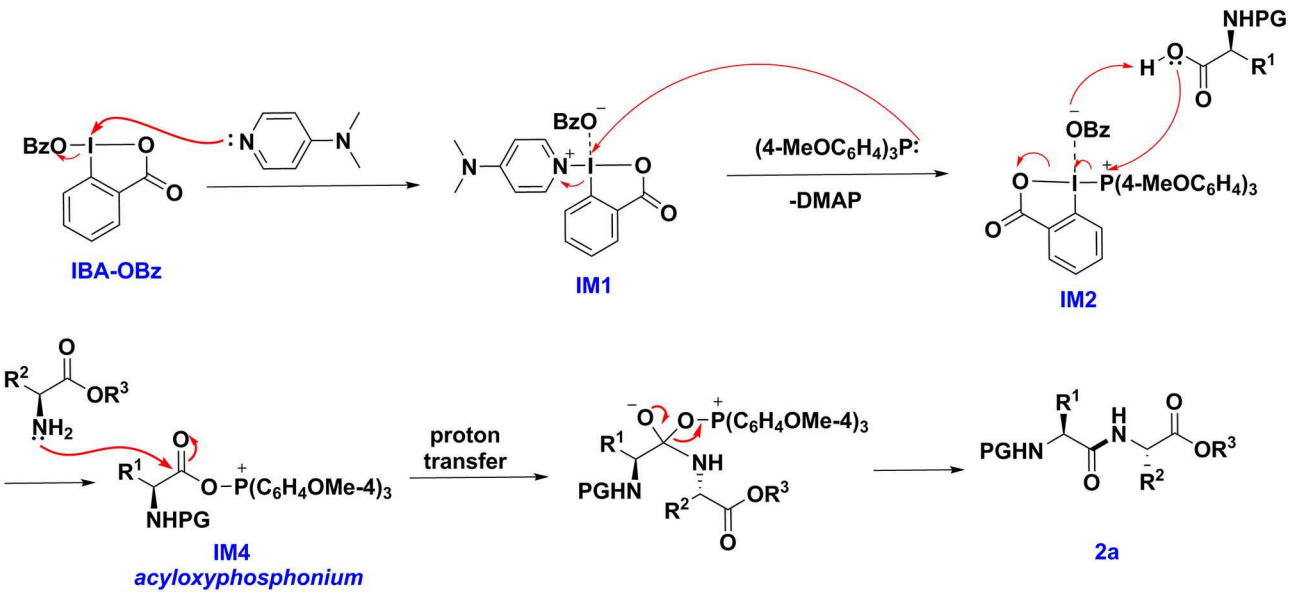

SCHEME 4 | Proposed mechanism for IBA-OBz/(4-MeOC6H4)3P mediated peptide-coupling reaction.

sources and were purified according to standard procedures. Petroleum ether (PE), where used, had the boiling point range 60–90° C.

The M06-2X functional in conjugation with a mixed basis set of the Lanl2dz (Hay and Wadt, 1985) pseudopotential for iodine and 6-31G(d) for all other atoms was used for optimizing the geometry of all the minima and transition states in solution. The universal solvation model (SMD) was employed to account for the effects of DCE solution (Marenich et al., 2009). All the optimized structures were confirmed by frequency calculations to be either minima or transition states at the same level of theory. To obtain more accurate electronic energies, single point energy calculations were performed at the M06-2X/[6-311++G(2df, 2p) + SDD(I)](SMD) level with the M06-2X/[6-31G(d) + Lanl2dz(I)](SMD) structures. Computed structures were illustrated with CYLView (Legault, 2009). All quantum mechanical calculations were performed using Gaussian 16 packages (Frisch et al., 2016).

CHEMICAL SYNTHESIS

Synthesis of IBA-OBz

IBA-OAc (1.53 g, 5 mmol) and benzoic acid (702.1 mg, 5.75 mmol) were added to a 50 mL round-bottom flask, then $CHCl_3$ (15 mL) was added and the mixture was refluxed for 18 h. Then $CHCl_3$ was concentrated in vacuo and 30 mL of petroleum ether was added. The mixture was stirred at 60° C for 1 h, and filtered to give a crude product. The crude product was dissolved in $CHCl_3$, washed sequentially with $NaHCO_3$, H_2O, brine, and dried over anhydrous $MgSO_4$. The solvent was evaporated to give the desired product IBA-OBz (1.68 g, 91%).

Colorless solid; yield: 91%. ^{1}H NMR (400 MHz, $CDCl_3$) δ = 8.30 (dd, J = 7.6, 1.6 Hz, 1H), 8.13–8.08 (m, 3H), 8.01–7.97 (m, 1H), 7.76 (dd, J = 7.4, 0.4 Hz, 1H), 7.66–7.61 (m, 1H), 7.51 (d, J = 7.6 Hz, 2H). ^{13}C NMR (100 MHz, $CDCl_3$) δ = 171.2, 168.1, 136.3, 133.5, 133.3, 131.4, 130.1, 129.2, 129.0, 128.8, 128.6, 118.8. HRMS(ESI): m/z calcd. for $C_{14}H_9IO_4$ $[M+H]^+$: 368.9618, found 368.9604.

Synthesis of 3-1 to 3-26 and 6-1 to 6-22

To a mixture of PG-AA_1-OH (0.2 mmol) and H-AA_2-OMe·HCl (0.2 mmol) in DCE (5 mL) in a 25 mL round-bottom flask was added DMAP (0.6 mmol). The solution was stirred at room temperature for 5 min. Then, IBA-OBz(0.3 mmol) and (4-$MeOC_6H_4)_3P$ (0.3 mmol) was added in sequence. The resulting mixture was stirred at room temperature and monitored by TLC. After 10 min, the reaction was quenched with saturated aq. sodium bicarbonate solution (10 mL) and extracted with EtOAc (50 mL×3). The combined organic layer was washed with brine, dried over anhydrous $MgSO_4$, and concentrated in vacuo to afford the crude product, which was then purified by silica gel flash chromatography to give the pure dipeptide product PG-AA_1-AA_2-OMe.

Boc-$_L$-Phe-$_L$-Leu-OMe (3-1)

Colorless solid; yield: 86%. ^{1}H NMR (400 MHz, $CDCl_3$) δ = 7.31–7.21 (m, 5H), 6.24 (d, J = 7.6 Hz, 1H), 4.99 (s, 1H), 4.58–4.54 (m, 1H), 4.35 (d, J = 6.8 Hz, 1H), 3.69 (s, 3H), 3.07 (d, J = 6.5 Hz, 2H), 1.63–1.41 (m, 12H), 0.92–0.88 (m, 6H); ^{13}C NMR (100 MHz, $CDCl_3$) δ = 172.8, 170.9, 155.4, 136.6, 129.3, 128.6, 126.9, 80.2, 55.6, 52.2, 50.7, 41.5, 38.0, 28.2, 24.6, 22.7, 21.8.

Boc-Gly-Gly-OMe (3-2)

Light yellow solid, yield: 81%. ^{1}H NMR (400 MHz, $CDCl_3$) δ = 6.59 (s, 1H), 5.12 (s, 1H), 4.07 (d, J = 5.6 Hz, 2H), 3.85 (d, J

= 6.0 Hz, 2H), 3.76 (s, 3H), 1.46 (s, 9H); ^{13}C NMR (100 MHz, $CDCl_3$) δ = 170.2, 169.8, 156.1, 80.4, 52.4, 44.2, 41.0, 28.2.

Boc-$_L$-Leu-$_L$-Lys(Z)-OMe (3-3)

Colorless oily liquid; yield: 84%. ^{1}H NMR (400 MHz, $CDCl_3$) δ = 7.36–7.26 (m, 5H), 6.84 (s, 1H), 5.32 (d, J = 13.6 Hz, 1H), 5.12–5.03 (m, 3H), 4.56–4.53 (m, 1H), 4.16 (s, 1H), 3.71 (s, 3H), 3.23–3.11 (m, 2H), 1.80–1.26 (m, 18H), 0.90–0.89 (m, 6H); ^{13}C NMR (100 MHz, $CDCl_3$) δ = 173.1, 172.5, 156.5, 155.9, 136.5, 128.4, 128.2, 128.0, 80.0, 66.6, 52.8, 52.3, 51.9, 41.0, 40.4, 31.7, 29.0, 28.3, 24.6, 22.9, 22.4, 21.6.

Boc-$_L$-Leu-$_L$-Ala-OMe (3-4)

Colorless solid; yield: 85%. ^{1}H NMR (400 MHz, $CDCl_3$): δ = 6.63 (s, 1H), 4.91 (s, 1H), 4.60–4.52 (m, 1H), 4.11 (br s, 1H), 3.74 (s, 3H), 1.72–1.59 (m, 3H), 1.43 (s, 9H), 1.39 (d, J = 7.2 Hz, 3H), 0.93 (dd, J_1 = 6.2 Hz, J_2 = 4.2 Hz, 6H); ^{13}C NMR (100 MHz, $CDCl_3$): δ = 173.1, 172.2, 155.6, 79.9, 52.4, 47.8, 41.3, 28.2, 24.6, 22.9, 21.9, 18.1.

Cbz-$_L$-Leu-$_L$-Ala-OMe (3-5)

Colorless solid; yield: 78%. ^{1}H NMR (400 MHz, $CDCl_3$) δ = 7.36–7.30 (m, 5H), 6.45 (d, J = 7.2 Hz, 1H), 5.18–5.11 (m, 3H), 4.58–4.54 (m, 1H), 4.20–4.19 (m, 1H), 3.75 (s, 3H), 1.72–1.50 (m, 6H), 1.40 (d, J = 7.2 Hz, 3H), 0.94 (d, J = 6.0 Hz, 6H); ^{13}C NMR (100 MHz, $CDCl_3$) δ = 173.1, 171.8, 156.2, 136.2, 128.5, 128.1, 128.0, 67.0, 53.4, 52.4, 48.0, 41.5, 24.6, 22.9, 21.9, 18.1.

Fmoc-$_L$-Leu-$_L$-Ala-OMe (3-6)

Colorless solid; yield: 84%. ^{1}H NMR (400 MHz, $CDCl_3$) δ = 7.75 (d, J = 7.6 Hz, 2H), 7.58 (d, J = 5.6 Hz, 2H), 7.39 (d, J = 7.4 Hz, 2H), 7.30–7.26 (m, 2H), 6.62 (s, 1H), 5.36 (s, 1H), 4.59–4.53 (m, 1H), 4.44–4.34 (m, 2H), 4.25–4.19 (m, 2H), 3.73 (s, 3H), 1.67–1.55 (m, 3H), 1.39 (d, J = 7.2 Hz, 3H), 0.95–0.94 (m, 6H); ^{13}C NMR (100 MHz, $CDCl_3$) δ = 173.1, 171.7, 156.2, 143.8, 143.7, 141.3, 127.7, 127.1, 125.0, 120.0, 120.0, 67.0, 53.4, 52.5, 48.1, 47.2, 41.6, 24.6, 22.9, 22.0, 18.3.

Cbz-$_L$-Leu-$_L$-Lys(Z)-OMe (3-7)

Colorless solid; yield: 91%. ^{1}H NMR (400 MHz, $CDCl_3$) δ = 7.31–7.26 (m, 10H), 6.82 (d, J = 7.6 Hz, 1H), 5.38 (d, J = 7.6 Hz, 2H), 5.10–5.02 (m, 4H), 4.55–4.50 (m, 1H), 4.27–4.26 (m, 1H), 3.72 (s, 3H), 3.20–3.06 (m, 2H), 1.81–1.79 (m, 2H), 1.61–1.60 (m, 3H), 1.49–1.43 (m, 3H), 1.28–1.27 (m, 2H), 0.91–0.90 (m, 6H); ^{13}C NMR (101 MHz, $CDCl_3$) δ = 172.5, 172.5, 156.6, 156.3, 136.5, 136.1, 128.5, 128.5, 128.2, 128.1, 128.0, 67.0, 66.6, 53.3, 52.4, 51.9, 41.3, 40.3, 31.6, 29.0, 24.5, 22.9, 22.1, 21.8.

Cbz-$_L$-Ala-$_L$-His(Trt)-OMe (3-8)

Colorless solid; yield: 88%. ^{1}H NMR (400 MHz, $CDCl_3$) δ = 7.67 (d, J = 7.6 Hz, 1H), 7.36–7.26 (m, 16H), 7.11–7.08 (m, 6H), 6.54 (s, 1H), 5.63 (d, J = 6.8 Hz, 1H), 5.11–5.02 (m, 2H), 4.80–4.75 (m, 1H), 4.33–4.30 (m, 1H), 3.59 (s, 3H), 3.07–2.97 (m, 2H), 1.43–1.39 (m, 3H); ^{13}C NMR (100 MHz, $CDCl_3$) δ = 172.0, 171.3, 155.6, 142.1, 138.6, 136.4, 136.2, 129.6, 128.4, 128.0, 128.0, 127.9, 127.8, 119.6, 75.3, 66.6, 52.5, 52.1, 50.4, 29.4, 19.1.

Cbz-$_L$-Ala-$_L$-Cys(Trt)-OMe (3-9)

Colorless oily liquid; yield: 75%. ^{1}H NMR (400 MHz, $CDCl_3$) δ = 7.39–7.19 (m, 20H), 6.22 (d, J = 6.8 Hz, 1H), 5.29 (d, J = 8.8 Hz, 1H), 5.15–5.06 (m, 2H), 4.54–4.50 (m, 1H), 4.20 (s, 1H), 3.70 (s, 3H), 2.72–2.61 (m, 2H), 1.36 (d, J = 7.2 Hz, 3H); ^{13}C NMR (100 MHz, $CDCl_3$) δ = 171.8, 170.5, 155.7, 144.2, 136.2, 129.4, 128.5, 128.1, 128.0, 126.9, 66.9, 52.6, 51.2, 50.2, 33.5, 18.8.

Cbz-$_L$-Ala-$_L$-Pro-OMe (3-10)

Colorless oily liquid; yield: 59%. ^{1}H NMR (400 MHz, $CDCl_3$) δ = 7.34–7.26 (m, 5H), 5.64 (d, J = 7.6 Hz, 1H), 5.08 (s, 2H), 4.55–4.51 (m, 2H), 3.72–3.61 (m, 5H), 2.24–2.17 (m, 1H), 2.10–1.96 (m, 3H), 1.39 (d, J = 6.8 Hz, 3H); ^{13}C NMR (100 MHz, $CDCl_3$) δ = 172.3, 171.2, 155.6, 136.4, 128.4, 128.0, 127.9, 66.6, 58.6, 52.2, 48.2, 46.7, 28.8, 24.8, 18.2.

Cbz-$_L$-Met-Gly-OMe (3-11)

Colorless solid; yield: 77%. ^{1}H NMR (400 MHz, $CDCl_3$) δ = 7.36–7.26 (m, 5H), 6.70 (s, 1H), 5.55 (d, J = 7.2 Hz, 1H), 5.11 (s, 2H), 4.45–4.43 (m, 1H), 4.13–3.96 (m, 2H), 3.75 (s, 3H), 2.62–2.58 (m, 2H), 2.15–1.95 (m, 5H); ^{13}C NMR (100 MHz, $CDCl_3$) δ = 171.5, 170.0, 156.1, 136.0, 128.5 128.2, 128.0, 67.1, 53.7, 52.3, 41.1, 31.6, 29.9, 15.1.

Cbz-$_L$-Met-Gly-OEt (3-12)

Colorless solid; yield: 81%. ^{1}H NMR (400 MHz, $CDCl_3$) δ = 7.36–7.26 (m, 5H), 6.65 (s, 1H), 5.52 (s, 1H), 5.12 (s, 2H), 4.44–4.42 (m, 1H), 4.21 (d, J = 7.2 Hz, 2H), 4.10–4.06 (m, 1H), 4.00–3.94 (m, 1H), 2.60 (t, J = 7.0 Hz, 2H), 2.14–1.97 (m, 5H), 1.30–1.25 (m, 5H); ^{13}C NMR (100 MHz, $CDCl_3$) δ = 171.5, 169.5, 156.1, 136.0, 128.5, 128.1, 128.0, 67.0, 61.5, 53.6, 41.2, 31.6, 29.9, 15.1, 14.0.

Cbz-$_L$-Trp-$_L$-Leu-OMe (3-13)

Colorless oily liquid; yield: 80%. ^{1}H NMR (400 MHz, $CDCl_3$) δ = 8.07 (s, 1H), 7.71 (d, J = 7.6 Hz, 1H), 7.37–7.28 (m, 6H), 7.20 (t, J = 7.6 Hz, 1H), 7.14–7.10 (m, 2H), 6.00 (s, 1H), 5.50 (s, 1H), 5.13 (s, 2H), 4.53–4.47 (m, 2H), 3.65 (s, 3H), 3.37–3.34 (m, 1H), 3.19–3.14 (m, 1H), 1.69–1.35 (m, 7H), 0.84–0.81 (m, 6H); ^{13}C NMR (100 MHz, $CDCl_3$) δ = 172.8, 171.0, 155.9, 136.2, 128.5, 128.1, 128.0, 127.3, 123.5, 122.2, 119.7, 118.8, 111.2, 110.2, 66.9, 55.3, 52.2, 50.8, 41.4, 28.5, 24.6, 22.6, 21.9.

Cbz-$_L$-Asn(Trt)-$_L$-Leu-OMe (3-14)

Colorless solid; yield: 75%. ^{1}H NMR (400 MHz, $CDCl_3$) δ = 7.37–7.17 (m, 20H), 6.93 (s, 1H), 6.41 (d, J = 7.2 Hz, 1H), 5.14–5.07 (m, 2H), 4.57–4.53 (m, 1H), 4.47–4.42 (m, 1H), 3.70 (s, 3H), 3.07–3.03 (m, 1H), 2.69–2.64 (m, 1H), 1.58–1.48 (m, 2H), 1.43–1.38 (m, 1H), 0.87–0.84 (m, 6H); ^{13}C NMR (100 MHz, $CDCl_3$) δ = 172.8, 170.9, 170.4, 156.3, 144.2, 136.1, 128.6, 128.5, 128.1, 127.9, 127.0, 70.8, 66.9, 52.1, 51.1, 50.9, 40.6, 38.2, 24.7, 22.6, 21.7.

Cbz-$_L$-Phe-$_L$-Leu-OMe (3-15)

Colorless solid; yield: 84%. ^{1}H NMR (400 MHz, $CDCl_3$) δ = 7.38–7.19 (m, 11H), 6.25 (d, J = 7.6 Hz, 1H), 5.33 (d, J = 7.2 Hz, 1H), 5.13–5.06 (m, 2H), 4.50–4.43 (m, 2H), 3.69 (s, 3H), 3.15–3.02 (m, 2H), 1.80 (s, 1H), 1.39–1.25 (m, 1H), 1.11–1.00 (m, 1H), 0.87 (t, J = 7.4 Hz, 3H), 0.79 (d, J = 6.8 Hz, 3H); ^{13}C NMR (100

MHz, $CDCl_3$) δ = 171.7, 170.6, 155.9, 136.2, 136.1, 129.3, 128.6, 128.5, 128.1, 127.9, 126.9, 67.0, 56.5, 56.1, 52.0, 38.3, 37.7, 25.0, 15.2, 11.4.

Cbz-$_L$-Phe-$_L$-Tyr(Bzl)-OMe (3-16)

Colorless solid; yield: 73%. ^{1}H NMR (400 MHz, $CDCl_3$) δ = 7.42–7.16 (m, 19H), 6.88–6.81 (m, 4H), 6.17 (d, J = 7.2 Hz, 1H), 5.23 (d, J = 8.8 Hz, 1H), 5.08 (s, 2H), 4.99 (s, 2H), 4.75–4.71 (m, 1H), 4.40 (d, J = 6.4 Hz, 1H), 3.67 (s, 3H), 3.05–2.92 (m, 4H); ^{13}C NMR (101 MHz, $CDCl_3$) δ = 171.4, 170.3, 157.9, 155.8, 136.9, 136.2, 136.1, 130.2, 129.3, 128.6, 128.5, 128.5, 128.1, 127.9, 127.9, 127.7, 127.4, 127.0, 114.8, 69.9, 67.0, 55.9, 53.4, 52.2, 38.3, 37.0; HRMS(ESI): m/z calcd. for $C_{34}H_{34}N_2O_6$ $[M+H]^+$: 567.2490, found 567.2486.

Cbz-$_L$-Phe-$_L$-Ser-OMe (3-17)

Colorless solid; yield: 60%. ^{1}H NMR (400 MHz, $CDCl_3$) δ = 7.34–7.25 (m, 10H), 7.20–7.18 (m, 2H), 6.68 (s, 1H), 5.25 (s, 1H), 5.08 (s, 2H), 4.57–4.55 (m, 1H), 4.43–4.38 (m, 1H), 3.91–3.88 (m, 2H), 3.75 (s, 3H), 3.10 (d, J = 6.8 Hz, 2H), 2.52 (s, 1H); ^{13}C NMR (100 MHz, $CDCl_3$) δ = 171.6, 170.5, 156.3, 136.2, 136.0, 129.3, 128.5, 128.4, 128.1, 127.9, 126.9, 67.0, 62.6, 56.1, 54.7, 52.6, 38.4.

Cbz-$_L$-Phe-$_L$-Thr-OMe (3-18)

Colorless solid; yield: 42%. ^{1}H NMR (400 MHz, $CDCl_3$) δ = 7.34–7.18 (m, 10H), 6.74 (d, J = 8.4 Hz, 1H), 5.40 (d, J = 8.0 Hz, 1H), 5.06 (s, 2H), 4.57–4.48 (m, 2H), 4.29–4.25 (m, 1H), 3.71 (s, 3H), 3.15–3.04 (m, 2H), 2.56 (d, J = 4.8 Hz, 1H), 1.12 (d, J = 6.4 Hz, 3H); ^{13}C NMR (100 MHz, $CDCl_3$) δ = 171.7, 171.1, 156.1, 136.2, 136.0, 129.3, 128.5, 128.4, 128.1, 127.9, 126.9, 68.1, 67.0, 57.4, 56.1, 52.5, 38.2, 19.7.

Cbz-$_L$-Phe-$_L$-Tyr-OMe (3-19)

Colorless solid; yield: 84%. ^{1}H NMR (400 MHz, $CDCl_3$) δ = 7.34–7.23 (m, 8H), 7.14 (d, J = 6.8 Hz, 2H), 6.81 (d, J = 8.0 Hz, 2H), 6.64 (d, J = 8.4 Hz, 2H), 6.36 (s, 1H), 5.88 (s, 1H), 5.32 (d, J = 7.2 Hz, 1H), 5.06 (s, 2H), 4.77–4.73 (m, 1H), 4.42 (d, J = 6.8 Hz, 1H), 3.67 (s, 3H), 3.03–2.89 (m, 4H); ^{13}C NMR (100 MHz, $CDCl_3$) δ = 171.5, 170.8, 156.0, 155.3, 136.1, 130.3, 129.3, 128.6, 128.5, 128.2, 128.0, 127.0, 126.8, 115.5, 67.1, 55.9, 53.5, 52.3, 38.3, 37.0.

Boc-$_L$-Val-$_L$-Val-OMe (3-20)

Colorless solid; yield: 75%. ^{1}H NMR (400 MHz, $CDCl_3$) δ = 6.36 (d, J = 6.8 Hz, 1H), 5.04 (d, J = 8.4 Hz, 1H), 4.54 (dd, J = 8.8, 4.8 Hz, 1H), 3.92–3.88 (m, 1H), 3.73 (s, 3H), 2.22–2.12 (m, 2H), 1.44 (s, 9H), 0.97–0.90 (m, 12H); ^{13}C NMR (100 MHz, $CDCl_3$) δ = 172.1, 171.7, 155.8, 79.6, 59.9, 57.0, 51.9, 31.0, 30.6, 28.2, 19.1, 18.8, 17.9, 17.7.

Cbz-$_L$-Val-$_L$-Glu(OEt)-OEt (3-21)

Colorless solid; yield: 70%. ^{1}H NMR (400 MHz, $CDCl_3$) δ = 7.36–7.30 (m, 5H), 6.64 (d, J = 7.2 Hz, 1H), 5.38 (d, J = 7.6 Hz, 1H), 5.14–5.07 (m, 2H), 4.60–4.54 (m, 1H), 4.22–4.10 (m, 4H), 4.05–4.01 (m, 1H), 2.46–2.31 (m, 2H), 2.24–1.96 (m, 3H), 1.29–1.22 (m, 6H), 0.95 (dd, J = 16.4, 6.8 Hz, 6H); ^{13}C NMR (101 MHz, $CDCl_3$) δ = 172.9, 171.4, 171.2, 156.3, 136.2, 128.5, 128.1, 128.0, 66.9, 61.6, 60.8, 60.2, 51.8, 31.2, 30.2, 26.9, 19.0, 17.7, 14.1, 14.0.

Boc-$_L$-Val-$_L$-Pro-OMe (3-22)

Colorless oily liquid; yield: 46%. ^{1}H NMR (400 MHz, $CDCl_3$) δ = 5.19 (d, J = 9.2 Hz, 1H), 4.52–4.49 (m, 1H), 4.28–4.24 (m, 1H), 3.78–3.61 (m, 5H), 2.25–2.17 (m, 1H), 2.06–1.91 (m, 4H), 1.40 (s, 9H), 1.01 (d, J = 6.8 Hz, 3H), 0.92 (d, J = 6.8 Hz, 3H); ^{13}C NMR (100 MHz, $CDCl_3$) δ = 172.4, 171.2, 155.8, 79.4, 58.7, 56.8, 52.1, 47.1, 31.3, 29.0, 28.3, 24.9, 19.2, 17.3.

Boc-$_L$- Pro-$_L$-Ala-OMe (3-23)

Colorless solid; yield: 84%. ^{1}H NMR (400 MHz, $CDCl_3$) δ = 7.31 (s, 0.64H), 6.56 (s, 0.35H), 4.54 (s, 1H), 4.29–4.20 (m, 1H), 3.72 (s, 3H), 3.54–3.32 (m, 2H), 2.30–2.12 (m, 2H), 1.86 (s, 2H), 1.45 (s, 9H), 1.37 (d, J = 7.2 Hz, 3H); ^{13}C NMR (100 MHz, $CDCl_3$) δ = 173.1, 172.1, 171.6, 155.6, 154.5, 80.6, 80.3, 60.9, 59.7, 52.3, 47.9, 47.0, 30.8, 28.2, 24.5, 23.6, 18.5, 18.1.

Boc-$_L$- Pro-$_L$-Leu-OMe (3-24)

Colorless solid; yield: 93%. ^{1}H NMR (400 MHz, $CDCl_3$) δ = 7.36 (s, 0.43H), 6.39 (s, 0.36H), 4.60–4.51 (m, 1H), 4.31–4.23 (m, 1H), 3.70 (s, 3H), 3.46–3.31 (m, 2H), 2.35–2.12 (m, 2H), 1.86 (s, 2H), 1.63–1.45 (m, 12H), 0.90 (s, 6H); ^{13}C NMR (100 MHz, $CDCl_3$) δ = 173.0, 172.3, 171.6, 155.8, 154.6, 130.8, 128.8, 80.3, 61.0, 59.5, 52.1, 50.7, 46.9, 41.3, 31.8, 31.4, 30.8, 30.1, 29.6, 29.6, 29.3, 28.2, 27.5, 24.8, 23.9, 22.8, 22.6, 21.7, 19.1, 14.0.

Boc-$_L$- Leu-$_L$-Pro-OMe (3-25)

Colorless oily liquid; yield: 63%. ^{1}H NMR (400 MHz, $CDCl_3$) δ = 5.11 (d, J = 8.8 Hz, 1H), 4.53–4.44 (m, 2H), 3.79–3.71 (m, 4H), 3.62–3.55 (m, 1H), 2.24–2.17 (m, 1H), 2.07–1.94 (m, 3H), 1.50–1.41 (m, 12H), 1.00–0.94 (m, 7H); ^{13}C NMR (100 MHz, $CDCl_3$) δ = 172.4, 171.8, 155.6, 79.4, 58.6, 52.1, 50.2, 46.6, 41.9, 28.9, 28.3, 24.8, 24.5, 23.3, 21.7.

Cbz-Gly-$_L$-Pro-OMe (3-26)

Colorless oily liquid; yield: 83%. ^{1}H NMR (400 MHz, $CDCl_3$) δ = 7.36–7.26 (m, 5H), 5.68 (s, 1H), 5.11 (s, 2H), 4.54–4.51 (m, 1H), 4.08–3.97 (m, 2H), 3.73 (s, 3H), 3.64–3.57 (m, 1H), 3.49–3.44 (m, 1H), 2.24–2.00 (m, 4H); ^{13}C NMR (100 MHz, $CDCl_3$) δ = 172.2, 166.9, 156.1, 136.4, 128.4, 127.9, 127.8, 66.7, 58.8, 52.2, 45.8, 43.2, 28.9, 24.5, 22.1.

Cbz-$_L$-Ala-Aib-OMe (6-1)

Colorless oily liquid; yield: 62%. ^{1}H NMR (400 MHz, $CDCl_3$) δ = 7.35–7.31 (m, 5H), 6.71 (s, 1H), 5.43 (d, J = 5.2 Hz, 1H), 5.10 (s, 2H), 4.25–4.21 (m, 1H), 3.71 (s, 3H), 1.57–1.51 (m, 6H), 1.36 (d, J = 7.2 Hz, 3H); ^{13}C NMR (100 MHz, $CDCl_3$) δ = 174.7, 171.5, 156.0, 136.2, 128.5, 128.1, 127.9, 66.9, 56.4, 52.6, 50.4, 24.7, 24.6, 18.4.

Boc-Gly-Aib-OMe (6-2)

Colorless solid; yield: 72%. ^{1}H NMR (400 MHz, $CDCl_3$) δ = 6.70 (s, 1H), 5.20 (s, 1H), 3.76–3.73 (m, 5H), 1.55 (s, 6H), 1.45 (s, 9H); ^{13}C NMR (100 MHz, $CDCl_3$) δ = 174.8, 168.8, 156.1, 80.0, 56.4, 52.6, 44.4, 28.2, 24.7.

Boc-$_L$-Leu-Aib-OMe (6-3)

Colorless solid; yield: 67%. ^{1}H NMR (400 MHz, $CDCl_3$) δ = 6.65 (s, 1H), 4.84 (s, 1H), 4.05 (s, 1H), 3.72 (s, 3H), 1.69–1.64

(m, 3H), 1.57–1.50 (m, 6H), 1.45 (s, 9H), 0.95–0.92 (m, 6H); ^{13}C NMR (100 MHz, $CDCl_3$) δ = 174.7, 171.8, 155.8, 79.9, 56.2, 52.9, 52.4, 40.8, 28.2, 24.7, 24.6, 22.8, 22.0; HRMS(ESI): *m*/*z* calcd. for $C_{16}H_{30}N_2O_5$ $[M+H]^+$: 331.2227, found 331.2227.

Boc-$_L$-Tyr-Aib-OMe (6-4)

Light yellow oily liquid; yield:70%. ^{1}H NMR (400 MHz, $CDCl_3$) δ = 7.07 (d, J = 8.0 Hz, 2H), 6.75 (d, J = 8.4 Hz, 2H), 6.30 (s, 1H), 5.65 (s, 1H), 5.10 (s, 1H), 4.22 (s, 1H), 3.72 (s, 3H), 3.04–2.88 (m, 2H), 1.46–1.43 (m, 15H); ^{13}C NMR (100 MHz, $CDCl_3$) δ = 174.6, 170.7, 155.6, 155.3, 130.5, 127.9, 115.5, 80.3, 56.4, 55.9, 52.6, 37.5, 28.2, 24.7, 24.5.

Boc-$_L$-Pro-Aib-OMe (6-5)

Colorless solid; yield: 81%. ^{1}H NMR (400 MHz, $CDCl_3$) δ = 7.47 (s, 0.44H), 6.48 (s, 0.45H), 4.26–4.14 (m, 1H), 3.71 (s, 3H), 3.47–3.32 (m, 2H), 2.33–1.85 (m, 4H), 1.53–1.46 (m, 15H); ^{13}C NMR (100 MHz, $CDCl_3$) δ = 174.6, 171.7, 171.1, 155.7, 154.4, 80.2, 61.0, 59.7, 56.0, 52.3, 46.8, 30.7, 28.2, 24.9, 24.6, 23.6.

Cbz-$_L$-Trp-Aib-OMe (6-6)

Colorless solid; yield: 77%. ^{1}H NMR (400 MHz, $CDCl_3$) δ = 8.28 (s, 1H), 7.71 (d, J = 6.0 Hz, 1H), 7.37–7.30 (m, 6H), 7.22–7.10 (m, 3H), 6.20 (s, 1H), 5.56 (d, J = 6.0 Hz, 1H), 5.12 (s, 2H), 4.51 (s, 1H), 3.67 (s, 3H), 3.36–3.33 (m, 1H), 3.17–3.11 (m, 1H), 1.35 (d, J = 5.6 Hz, 6H); ^{13}C NMR (100 MHz, $CDCl_3$) δ = 174.5, 170.3, 156.0, 136.2, 128.5, 128.1, 128.0, 127.3, 123.5, 122.3, 119.8, 118.9, 111.2, 110.4, 66.9, 56.3, 55.3, 52.5, 28.4, 24.7.

Cbz-$_L$-Phe-Aib-OMe (6-7)

Colorless solid; yield: 59%. ^{1}H NMR (400 MHz, $CDCl_3$) δ = 7.37–7.22 (m, 10H), 6.21 (s, 1H), 5.43 (d, J = 4.8 Hz, 1H), 5.09 (s, 2H), 4.37 (d, J = 6.4 Hz, 1H), 3.69 (s, 3H), 3.15–3.10 (m, 1H), 3.02–2.96 (m, 1H), 1.41 (d, J = 10.4 Hz, 6H); ^{13}C NMR (100 MHz, $CDCl_3$) δ = 174.4, 169.8, 155.9, 136.5, 136.2, 129.4, 128.6, 128.5, 128.1, 127.9, 127.0, 66.9, 56.4, 56.2, 52.6, 38.6, 24.5, 24.4.

Boc-$_L$-Ala-Aib-OMe (6-8)

Colorless oily liquid; yield: 79%. ^{1}H NMR (400 MHz, $CDCl_3$) δ = 6.77 (s, 1H), 5.04 (s, 1H), 4.12 (s, 1H), 3.71 (s, 3H), 1.52 (d, J = 6.0 Hz, 6H), 1.44 (s, 9H), 1.32 (d, J = 6.8 Hz, 3H); ^{13}C NMR (100 MHz, $CDCl_3$) δ = 174.8, 171.8, 155.7, 80.0, 56.3, 52.6, 49.9, 28.3, 24.8, 24.7, 17.8; HRMS(ESI): *m*/*z* calcd. for $C_{13}H_{24}N_2O_5$ $[M+H]^+$: 289.1758, found 289.1759.

Cbz-$_L$-Met-Aib-OMe (6-9)

Light yellow oily liquid; yield: 63%. ^{1}H NMR (400 MHz, $CDCl_3$) δ = 7.35–7.29 (m, 5H), 6.75 (s, 1H), 5.58 (d, J = 7.6 Hz, 1H), 5.10 (s, 2H), 4.36–4.31 (m, 1H), 3.71 (s, 3H), 2.64–2.52 (m, 2H), 2.10–1.93 (m, 5H), 1.51 (d, J = 5.2 Hz, 6H); ^{13}C NMR (100 MHz, $CDCl_3$) δ = 174.4, 170.2, 156.0, 136.1, 128.5, 128.1, 128.0, 67.0, 56.4, 53.6, 52.6, 31.5, 29.8, 24.9, 24.5, 15.0.

Cbz-$_L$-Ser(*t*Bu)-Aib-OMe (6-10)

Colorless oily liquid; yield: 68%. ^{1}H NMR (400 MHz, $CDCl_3$) δ = 7.36–7.26 (m, 6H), 5.73 (s, 1H), 5.15–5.08 (m, 2H), 4.18 (s, 1H), 3.80–3.72 (m, 4H), 3.34 (d, J = 8.4 Hz, 1H), 1.54 (d, J = 8.0 Hz, 6H), 1.21 (s, 9H); ^{13}C NMR (100 MHz, $CDCl_3$) δ = 174.6, 169.4, 155.9, 136.2, 128.4, 128.1, 128.0, 74.1, 66.8, 61.6, 56.4, 54.1, 52.5, 27.3, 24.8, 24.5; HRMS(ESI): *m*/*z* calcd. for $C_{20}H_{30}N_2O_6$ $[M+H]^+$: 395.2177, found 395.2182.

Cbz-$_L$-Val-Aib-OMe (6-11)

Colorless solid; yield: 46%. ^{1}H NMR (400 MHz, $CDCl_3$) δ = 7.35–7.28 (m, 5H), 6.50 (s, 1H), 5.39 (d, J = 7.2 Hz, 1H), 5.11 (s, 2H), 3.98–3.94 (m, 1H), 3.71 (s, 3H), 2.14–2.09 (m, 1H), 1.53 (s, 6H), 0.94 (dd, J = 16.8, 6.8 Hz, 6H); ^{13}C NMR (100 MHz, $CDCl_3$) δ = 174.7, 170.3, 156.4, 136.2, 128.5, 128.1, 128.0, 67.0, 60.2, 56.5, 52.6, 31.1, 24.8, 24.5, 19.0, 17.7.

Cbz-$_L$-NMePhe-Aib-OMe (6-12)

Colorless oily liquid; yield: 72%. ^{1}H NMR (400 MHz, $CDCl_3$) δ = 7.36–7.11 (m, 10H), 6.50 (s, 0.6H), 6.22 (s, 0.3H), 5.15–5.07 (m, 1.7H), 4.94–4.78 (m, 1.5H), 3.72–3.67 (m, 3H), 3.32–3.27 (m, 1H), 2.97–2.86 (m, 4H), 1.48–1.42 (m, 6H); ^{13}C NMR (100 MHz, $CDCl_3$) δ = 174.4, 169.3, 169.0, 157.2, 155.9, 137.4, 137.2, 136.5, 136.0, 128.9, 128.4, 128.1, 127.9, 127.5, 126.5, 67.6, 67.3, 61.0, 59.9, 56.4, 56.2, 52.5, 52.4, 33.9, 33.7, 30.8, 30.2, 25.0, 24.7, 24.4.

Cbz-$_L$-NMePhe-$_L$-Val-OMe (6-13)

Colorless oily liquid; yield: 83%. ^{1}H NMR (400 MHz, $CDCl_3$) δ = 7.35–7.12 (m, 10H), 6.53 (d, J = 8.8 Hz, 0.6H), 6.23 (s, 0.3H), 5.16–5.07 (m, 1.8H), 4.98–4.95 (m, 1H), 4.86 (s, 0.3H), 4.52–4.49 (m, 1H), 3.71 (s, 3H), 3.36–3.27 (m, 1H), 3.07–2.50 (m, 4H), 2.16–2.07 (m, 1H), 0.86–0.79 (m, 6H); ^{13}C NMR (100 MHz, $CDCl_3$) δ = 171.8, 170.0, 169.7, 157.1, 155.9, 137.3, 137.1, 136.3, 135.9, 128.8, 128.4, 128.1, 127.9, 127.6, 126.5, 67.7, 67.4, 61.0, 60.1, 56.9, 52.0, 34.1, 33.8, 31.3, 31.0, 30.6, 18.8, 17.6, 17.4; HRMS(ESI): *m*/*z* calcd. for $C_{24}H_{30}N_2O_5$ $[M+H]^+$: 427.2227 found 427.2228.

Cbz-$_L$-NMePhe-Gly-OMe (6-14)

Colorless oily liquid; yield: 90%. ^{1}H NMR (400 MHz, $CDCl_3$) δ = 7.34–7.13 (m, 10H), 6.58 (s, 0.7H), 6.27 (s, 0.3H), 5.14–4.87 (m, 3H), 4.15–4.04 (m, 1H), 3.92–3.87 (m, 1H), 3.73 (s, 3H), 3.38–3.33 (m, 1H), 3.03–2.87 (m, 4H); ^{13}C NMR (100 MHz, $CDCl_3$) δ = 170.5, 169.9, 157.2, 137.1, 136.3, 128.8, 128.4, 128.0, 127.9, 127.4, 126.5, 67.6, 67.3, 61.0, 59.9, 52.1, 41.0, 34.0, 33.8, 31.1, 30.4.

Cbz-$_L$-NMePhe-$_L$-Ala-OMe (6-15)

Colorless oily liquid; yield: 81%. ^{1}H NMR (400 MHz, $CDCl_3$) δ = 7.35–7.12 (m, 10H), 6.53 (s, 0.6H), 6.26 (s, 0.4H), 5.10–5.05 (m, 1.8H), 4.95–4.93 (m, 1H), 4.80 (s, 0.4H), 4.56–4.51 (m, 1H), 3.72 (s, 3H), 3.34–3.31 (m, 1H), 3.05–2.84 (m, 4H), 1.35–1.33 (m, 3H); ^{13}C NMR (100 MHz, $CDCl_3$) δ = 172.8, 169.7, 169.3, 156.9, 155.9, 137.3, 137.1, 136.4, 135.9, 128.8, 128.4, 128.0, 127.9, 127.5, 126.5, 67.6, 67.3, 61.0, 60.1, 52.3, 48.0, 34.0, 31.3, 30.6, 18.0; HRMS(ESI): *m*/*z* calcd. for $C_{22}H_{26}N_2O_5$ $[M+H]^+$: 399.1914 found 399.1914.

Cbz-$_L$-NMePhe-$_L$-Ile-OMe (6-16)

Colorless oily liquid; yield: 86%. ^{1}H NMR (400 MHz, $CDCl_3$) δ = 7.36–7.10 (m, 10H), 6.55 (d, J = 8.0 Hz, 0.6H), 6.24 (d, J = 9.2 Hz, 0.3H), 5.15–5.07 (m, 1.7H), 4.98–4.94 (m, 1H), 4.84 (s, 0.3H), 4.56–4.53 (m, 1H), 3.70 (s, 3H), 3.62–3.28 (m, 1H), 3.07–2.85 (m, 4H), 1.86 (s, 1H), 1.40–1.29 (m, 1H), 1.10–1.01 (m, 1H), 0.89–0.82 (m, 6H); ^{13}C NMR (100 MHz, $CDCl_3$) δ = 171.7, 169.9, 169.6, 157.1, 155.9, 137.3, 137.1, 136.3, 135.9, 128.8, 128.4, 128.0,

127.9, 127.6, 126.5, 67.7, 67.4, 61.1, 60.2, 56.3, 51.9, 37.6, 34.1, 33.8, 31.3, 30.6, 24.9, 15.3, 11.4.

Cbz-$_L$-NMePhe-$_L$-His(Trt)-OMe (6-17)

Colorless oily liquid; yield: 87%. ^{1}H NMR (400 MHz, $CDCl_3$) δ = 7.32–7.07 (m, 27H), 6.53 (d, J = 4.0 Hz, 1H), 5.11–4.87 (m, 3H), 4.75 (d, J = 3.6 Hz, 1H), 3.59 (s, 3H), 3.44–3.39 (m, 1H), 3.15–2.88 (m, 3H), 2.81 (d, J = 14.0 Hz, 3H); ^{13}C NMR (100 MHz, $CDCl_3$) δ = 171.3, 170.1, 169.9, 156.6, 155.8, 142.1, 138.6, 138.4, 137.6, 137.5, 136.5, 136.2, 129.5, 128.8, 128.7, 128.3, 128.2, 128.2, 127.9, 127.6, 127.6, 127.5, 127.2, 126.3, 126.2, 119.3, 119.2, 75.1, 67.1, 66.9, 61.0, 60.4, 52.6, 51.9, 33.9, 31.2, 30.9, 29.5, 29.1.

Cbz-$_L$-NMePhe-$_L$-Tyr(Bzl)-OMe (6-18)

Colorless oily liquid; yield: 90%. ^{1}H NMR (400 MHz, $CDCl_3$) δ = 7.40–7.07 (m, 15H), 6.96–6.80 (m, 4H), 6.45 (d, J = 7.6 Hz, 0.6H), 6.14 (d, J = 6.0 Hz, 0.3H), 5.12–4.89 (m, 5H), 4.78–4.77 (m, 1H), 3.71 (s, 3H), 3.28–3.23 (m, 1H), 3.14–3.04 (m, 1H), 2.96–2.86 (m, 2H), 2.64–2.59 (m, 3H); ^{13}C NMR (100 MHz, $CDCl_3$) δ = 171.5, 169.6, 169.3, 157.8, 157.6, 156.9, 155.6, 137.1, 137.0, 136.8, 136.2, 135.9, 130.0, 128.7, 128.4, 128.3, 128.0, 127.9, 127.8, 127.5, 127.2, 126.4, 115.0, 114.7, 69.7, 67.5, 67.3, 60.5, 59.6, 53.0, 52.2, 36.9, 36.7, 33.8, 33.6, 30.6, 30.0; HRMS(ESI): m/z calcd. for $C_{35}H_{36}N_2O_6$ $[M+H]^+$: 581.2646 found 581.2642.

Cbz-$_L$-NMePhe-$_L$-Cys(Trt)-OMe (6-19)

Colorless oily liquid; yield: 80%. 1H NMR (400 MHz, CDCl3) δ = 7.33–7.01 (m, 25H), 6.52 (d, J = 6.8 Hz, 0.6H), 6.22 (d, J = 6.8 Hz, 0.4H), 5.05–4.73 (m, 3H), 4.38–4.34 (m, 1H), 3.59 (s, 3H), 3.23–3.18 (m, 1H), 2.92–2.67 (m, 4H), 2.60–2.56 (m, 1H), 2.47–2.42 (m, 1H); 13C NMR (100 MHz, CDCl3) δ = 170.3, 169.7, 169.5, 157.1, 155.8, 144.1, 137.2, 137.0, 136.2, 135.9, 129.3, 128.8, 128.4, 128.3, 127.9, 127.4, 127.1, 126.7, 126.5, 67.6, 67.4, 66.7, 66.6, 60.7, 59.6, 52.6, 52.4, 51.3, 34.0, 33.6, 33.5, 33.5, 31.1, 30.3; HRMS(ESI): m/z calcd. for C41H40N2O5S [M+H]+: 695.2550 found 695.2538.

Cbz-$_L$-NMePhe-$_L$-Lys(Z)-OMe (6-20)

Colorless oily liquid; yield: 88%. ^{1}H NMR (400 MHz, $CDCl_3$) δ = 7.33–7.10 (m, 16H), 6.56 (d, J = 7.2 Hz, 0.6H), 6.30 (d, 0.3H), 5.08–4.80 (m, 6H), 4.56–4.51 (m, 1H), 3.71 (s, 3H), 3.32–2.81 (m, 7H), 1.82–1.24 (m, 6H); ^{13}C NMR (100 MHz, $CDCl_3$) δ = 172.2, 170.1, 169.7, 156.9, 156.4, 137.2, 137.0, 136.5, 136.3, 128.8, 128.4, 127.9, 127.5, 127.1, 126.5, 67.3, 66.4, 60.9, 60.5, 52.4, 52.3, 51.9, 51.8, 40.4, 40.3, 34.0, 31.7, 31.1, 29.3, 29.0, 22.3, 22.1; HRMS(ESI): m/z calcd. for $C_{33}H_{39}N_3O_7$ $[M+H]^+$: 590.2861 found 590.2862.

Cbz-$_L$-NMePhe-$_L$-Glu(OEt)-OEt (6-21)

Colorless oily liquid; yield: 82%. ^{1}H NMR (400 MHz, $CDCl_3$) δ = 7.33–7.08 (m, 10H), 6.71–6.61 (m, 1H), 5.08–5.02 (m, 1.6H), 4.95–4.89 (m, 1H), 4.78 (s, 0.4H), 4.52–4.51 (m, 1H), 4.19–4.06 (m, 4H), 3.33–3.28 (m, 1H), 3.08–2.82 (m, 4H), 2.31–2.21 (m, 3H), 1.96–1.90 (m, 1H), 1.26–1.19 (m, 6H); ^{13}C NMR (100 MHz, $CDCl_3$) δ = 172.6, 172.5, 171.2, 170.1, 169.9, 156.8, 155.8, 137.3, 137.0, 136.3, 135.9, 128.8, 128.4, 128.0, 127.9, 127.5, 126.5, 67.5, 67.3, 61.4, 61.2, 60.7, 60.5, 60.4, 51.9, 51.6, 34.1, 33.9, 31.5, 30.9, 30.1, 30.0, 27.0, 26.7, 14.0, 14.0; HRMS(ESI): m/z calcd. for $C_{27}H_{34}N_2O_7$ $[M+H]^+$: 499.2439 found 499.2439.

Cbz-$_L$-NMePhe-$_L$-Tyr-OMe (6-22)

Colorless oily liquid; yield: 91%. ^{1}H NMR (400 MHz, $CDCl_3$) δ = 7.34–7.06 (m, 10H), 6.88–6.59 (m, 5H), 6.40 (s, 0.4H), 6.22–6.14 (m, 1H), 5.13–4.78 (m, 4H), 3.73–3.71 (m, 3H), 3.28–2.83 (m, 4H), 2.64–2.63 (m, 3H); ^{13}C NMR (100 MHz, $CDCl_3$) δ = 171.9, 171.7, 170.0, 169.6, 157.1, 155.3, 137.0, 136.7, 136.2, 135.7, 130.1, 128.8, 128.6, 128.5, 128.1, 128.0, 127.6, 127.0, 126.6, 67.8, 67.5, 60.7, 59.9, 53.2, 52.4, 37.1, 36.8, 33.8, 30.9, 30.3; HRMS(ESI): m/z calcd. for $C_{28}H_{30}N_2O6$ $[M+H]^+$: 491.2177 found 491.2180.

General Procedure for Fmoc-SPPS Mediated by IBA-OBz

All Fmoc-protected amino acids and 2-chlorotrityl chloride resin (2-Cl-Trt-Cl resin, 0.98 mmol/g) were purchased and used without further purification. All peptides were synthesized using 200 mg resin in solid-phase peptide synthesis vessel. The synthetic route included immobilized the C terminal amino acid onto resin, deprotection, coupling, cleavage from resin, and purification of peptides.

Immobilized the C-Terminal Amino Acid Onto Resin

To a 5 mL round-bottom flask was added 2-Cl-Trt-Cl resin (0.196 mmol, 200 mg) and C-terminal Fmoc-amino acid (Fmoc-AA_1-OH, 0.6 mmol), then DCM and DMF (2 mL, v:v = 1:1) were added and the mixture was stirred at room temperature. Then DIPEA (0.1 mL) was added and the mixture was stirred at room temperature for 4 h. Afterward, the mixture was filtered and washed with MeOH (3 × 5 mL) and DCM (3 × 5 mL) in sequence. The resin was used for next step without any purification.

Blocked the Reaction Sites

To a 5 mL round-bottom flask was added the resin from last step and MeOH/DIPEA/DCM (2 mL, v:v:v = 1:2:7), the mixture was stirred at room temperature for 4 h. Afterward, the mixture was filtered and washed with MeOH (3 × 5 mL) and DCM (3 × 5 mL) in sequence. The resin was used for next step without any purification.

Deprotection of Fmoc

To a solid-phase peptide synthesis vessel was added the resin from last step and 20% piperidine/DMF (2 mL), the tube was capped and the mixture was shaken with air bubbling from the bottom of the reaction vessel by using air-pump at room temperature for 30 min. The mixture was filtered and washed with MeOH (3 × 5 mL) and DCM (3 × 5 mL) in sequence. The resin was used for next step without any purification.

Coupling

To a solid phase peptide synthesis vessel was added the resin from last step, Fmoc-AA_2-OH (0.6 mmol) and DMF (2 mL), then the mixture was shaken with air bubbling from the bottom of the reaction vessel by using air-pump. Afterward, TEA (0.6 mmol, 84 μL) was added. After 5 min, IBA-OBz (221 mg, 0.6 mmol) and $(4\text{-}MeOC_6H_4)_3P$ (216 mg, 0.6 mmol) was added. After 2 h, the mixture was filtered and washed with MeOH (3 ×

5 mL) and DCM (3 × 5 mL) in sequence. The resin was used for next step without any purification. The peptide chain elongation was completed by repeating deprotection of Fmoc and peptide coupling reaction.

Cleavage

The resin was treated with a solution of 0.5% TFA/DCM (2 mL) for 10 min. Then the mixture was filtered and washed with MeOH (3 × 5 mL) and DCM (3 × 5 mL) in sequence. The filtrate was evaporated under vacuum to afford the crude peptide as a oily liquid.

Purification of Peptides

The crude peptide was purified via RP-HPLC. Analytical HPLC was performed using a J&K C18 (5 μm, 4.6 mm × 250 mm) analytical column. Linear gradients using A: H_2O (0.1% TFA) and B: MeCN (0.1% TFA) were run at a flow rate of 0.8 mL·min^{-1}. Preparative HPLC was performed using a Shimpack Prep-ODS C18 (15 μm, 20 mm × 250 mm) preparative column. Linear gradients using A: H_2O (0.1% TFA) and B: MeCN (0.1% TFA) were run at a flow rate of 8.0 mL·min^{-1}.

H_2N-Tyr-Gly-Gly-Phe-Leu-OH

Colorless solid, yield: 44%. QFT/ESI: m/z calcd. for $C_{28}H_{37}N_5O_7$ $[M+H]^+$: 556.2693, found: 556.2768; for $C_{28}H_{37}N_5O_7$. $[M+Na]^+$: 578.2585, found: 578.2549.

DATA AVAILABILITY STATEMENT

All datasets generated for this study are included in the article/**Supplementary Material**.

AUTHOR CONTRIBUTIONS

L-JQ completed SPPS and completed the draft. DL synthesized iodine(III) compounds and dipeptides. KZ completed computational studies. M-TZ guided computational studies. CZ directed the project and finalized the manuscript.

FUNDING

This work was financially supported by the National Key R&D Program of China (2017YFD020030202), the National Natural Science Foundation of China (21472094 and 21772096), and The Tianjin Natural Science Foundation (17JCYBJC20300).

SUPPLEMENTARY MATERIAL

The Supplementary Material for this article can be found online at: https://www.frontiersin.org/articles/10.3389/fchem.2020.00183/full#supplementary-material

REFERENCES

Balasubramanian, T. M., Kendrick, N. C. E., Taylor, M., Marshall, G. R., Hall, J. E., Vodyanov, I., et al. (1981). Synthesis and characterization of the major component of alamethicin. *J. Am. Chem. Soc.* 103, 6127–6132. doi: 10.1021/ja00410a024

Brown, M., Farid, U., and Wirth, T. (2013). Hypervalent iodine reagents as powerful electrophiles. *Synlett* 24, 424–431. doi: 10.1055/s-0032-1318103

Brown, Z. Z., and Schafmeister, C. E. (2008). Exploiting an inherent neighboring group effect of α-amino acids to synthesize extremely hindered dipeptides. *J. Am. Chem. Soc.* 130, 14382–14383. doi: 10.1021/ja806063k

Constable, D. J. C., Dunn, P. J., Hayler, J. D., Humphrey, G. R., Leazer, J. L. Jr., Linderman, R. J., et al. (2007). Key green chemistry research areas—a perspective from pharmaceutical manufacturers. *Green Chem.* 9, 411–420. doi: 10.1039/B.703488C

Coste, J., Frerot, E., Jouin, P., and Castro, B. (1991). Oxybenzotriazole free peptide coupling reagents for N-methylated amino acids. *Tetrahedron Lett.* 32, 1967–1970. doi: 10.1016/0040-4039(91)85015-W

Duan, Y. N., Jiang, S., Han, Y., Sun, B., and Zhang, C. (2016). Recent advances in hypervalent iodine chemistry. *Chin. J. Org. Chem.* 36, 1973–1984. doi: 10.6023/cjoc201605007

EI-Faham, A., and Albericio, F. (2011). Peptide coupling reagents, more than a letter soup. *Chem. Rev.* 111, 6557–6602. doi: 10.1021/cr100048w

Frisch, M. J., Trucks, G. W., Schlegel, H. B., Scuseria, G. E., Robb, M. A., Cheeseman, J. R., et al. (2016). Gaussian 16, revision A.03. Wallingford, CT: Gaussian Inc.

Han, Y. C., and Zhang, C. (2018). Synthetic application of water-soluble hypervalent iodine reagents in aqueous media. *Tetrahedron Lett.* 59, 3052–3057. doi: 10.1016/j.tetlet.2018.06.059

Hay, P. J., and Wadt, W. R. (1985). Ab initio effective core potentials for molecular calculations. Potentials for K to Au including the outermost core orbitals. *J. Chem. Phys.* 82, 299–310. doi: 10.1063/1.448975

Hughes, J., Smith, T. W., Kosterlitz, H. W., Fothergill, L. A., Morgan, B. A., and Morris, H. R. (1975). Identification of two related pentapeptides from the brain with potent opiate agonist activity. *Nature* 258, 577–579. doi: 10.1038/258577a0

Humphrey, J. M., and Chamberlin, A. R. (1997). Chemical synthesis of natural product peptides: coupling methods for the incorporation of noncoded amino acids into peptides. *Chem. Rev.* 97, 2243–2266. doi: 10.1021/cr950005s

Katritzky, A. R., Todadze, E., Angrish, P., and Draghici, B. (2007). Efficient peptide coupling involving sterically hindered amino acids. *J. Org. Chem.* 72, 5794–5801. doi: 10.1021/jo0704255

Legault, C. Y. (2009). *CYLview, 1.0b; Université de Sherbrooke.* Sherbrooke, QC: http://www.cylview.org.

Leibfritz, D., Haupt, E., Dubischar, N., Lachmann, H., Oekonomopoulos, R., and Jung, G. (1982). Synthese von 2-methylalanin-peptiden, die pH-Abhängiggkeit ihrer ^{13}C-NMR-spektren und eine neue methode zurauswertung über CS-diagramme. *Tetrahedron* 38, 2165–2181. doi: 10.1016/0040-4020(82)85164-8

Li, Y. F., Hari, D. P., Vita, M. V., and Waser, J. (2016). Cyclic hypervalent iodine reagents for atom-transfer reactions: beyond trifluoromethylation. *Angew. Chem. Int. Ed.* 55, 4436–4454. doi: 10.1002/anie.201509073

Liu, D., Guo, Y. L., Qu, J., and Zhang, C. (2018). Recyclable hypervalent-iodine-mediated solid-phase peptide synthesis and cyclic peptide synthesis. *Beilstein J. Org. Chem.* 14, 1112–1119. doi: 10.3762/bjoc.14.97

Liu, Q., Lan, Y., Liu, J., Li, G., Wu, Y. D., and Lei, A. W. (2009). Revealing a second transmetalation step in the Negishi coupling and its competition with reductive elimination: improvement in the interpretation of the mechanism of biaryl syntheses. *J. Am. Chem. Soc.* 131, 10201–10210. doi: 10.1021/ja903277d

Liu,D., He, J. H., and Zhang, C. (2019). Introduction of Hypervalent Iodine Chemistry and Its Application. *Univ. Chem*, 34, 1–16. doi: 10.3866/PKU.DXHX201806019

Marenich, A. V., Cramer, C. J., and Truhlar, D. G. (2009). Universal solvation model based on solute electron density and on a continuum model of the solvent defined by the bulk dielectric constant and atomic surface tensions. *J. Phys. Chem. B* 113, 6378–6396. doi: 10.1021/jp810292n

Mocci, F., Uccheddu, G., Frongia, A., and Cerioni, G. (2007). Solution Structure of Some λ^3 Iodanes: an ^{17}O NMR and DFT study. *J. Org. Chem.* 72, 4163–4168. doi: 10.1021/jo070111h

Schoenebeck, F., and Houk, K. N. (2010). Ligand-controlled regioselectivity in palladium-catalyzed cross coupling reactions. *J. Am. Chem. Soc*. 132, 2496–2497. doi: 10.1021/ja9077528

Singh, F. V., and Wirth, T. (2014). Hypervalent iodine-catalyzed oxidative functionalizations including stereoselective reactions. *Chem. Asian J.* 9, 950–971. doi: 10.1002/asia.201301582

Slomczynska, U., Beusen, D. D., Zabrocki, J., Kociolek, K., Redlinski, A., Reusser, F., et al. (1992). Emerimicins III and IV and their Ethylalanine12 epimers. Facilitated chemical-enzymatic synthesis and a qualitative evaluation of their solution structures. *J. Am. Chem. Soc.* 114, 4095–4106. doi: 10.1021/ja00037a010

Tian, J., Gao, W. C., Zhou, D. M., and Zhang, C. (2012). Recyclable hypervalent iodine(III) reagent iodosodilactone as an efficient coupling reagent for direct esterification, amidation, and peptide coupling. *Org. Lett*. 14, 3020–3023. doi: 10.1021/ol301085v

Varvoglis, A. (1997). *Hypervalent Iodine in Organic Synthesis.* London: Academic Press.

Wenschuh, H., Beyermann, M., Haber, H., Seydel, J. K., Krause, E., Bienert, M., et al. (1995). Stepwise automated solid phase synthesis of naturally occurring peptaibols using FMOC amino acid fluorides. *J. Org. Chem*. 60, 405–410. doi: 10.1021/jo00107a020

Wirth, T. (2005). Hypervalent iodine chemistry in synthesis: scope and new directions. *Angew. Chem. Int. Ed.* 44, 3656–3665. doi: 10.1002/anie.200500115

Yoshimura, A., and Zhdankin, V. V. (2016). Advances in synthetic applications of hypervalent iodine compounds. *Chem. Rev.* 116, 3328–3435. doi: 10.1021/acs.chemrev.5b00547

Zhang, C., Liu, S. S., Sun, B., and Tian, J. (2015). Practical peptide synthesis mediated by a recyclable hypervalent iodine reagent and tris(4-methoxyphenyl)phosphine. *Org. Lett*. 17, 4106–4109. doi: 10.1021/acs.orglett.5b02045

Zhdankin, V. V. (2014). *Hypervalent Iodine Chemistry: Preparation, Structure, and Synthetic Applications of Polyvalent Iodine Compounds*. New York, NY: Wiley.

Zhdankin, V. V., and Stang, P. J. (2002). Recent developments in the chemistry of polyvalent iodine compounds. *Chem. Rev.* 102, 2523–2584. doi: 10.1021/cr010003+

Zhdankin, V. V., and Stang, P. J. (2008). Chemistry of polyvalent iodine. *Chem.Rev*. 108, 5299–5358. doi: 10.1021/cr800332c

Zhou, Q. H., and Li, Y. X. (2015). The real role of n-heterocyclic carbene in reductive functionalization of CO_2: an alternative understanding from density functional theory study. *J. Am. Chem. Soc*. 137, 10182–10189. doi: 10.1021/jacs.5b03651

Conflict of Interest: The authors declare that the research was conducted in the absence of any commercial or financial relationships that could be construed as a potential conflict of interest.

frontiers in Chemistry

ORIGINAL RESEARCH
published: 12 June 2020
doi: 10.3389/fchem.2020.00466

I_2/DMSO-Catalyzed Transformation of *N*-tosylhydrazones to 1,2,3-thiadiazoles

Weiwei Li[1], *Jun Zhang*[1], *Jing He*[1], *Liang Xu*[1], *Luigi Vaccaro*[3], *Ping Liu*[1]* *and Yanlong Gu*[2]*

[1] *The Key Laboratory for Green Processing of Chemical Engineering of Xinjiang Bingtuan, School of Chemistry and Chemical Engineering, Shihezi University, Shihezi, China,* [2] *Key Laboratory of Material Chemistry for Energy Conversion and Storage, Ministry of Education, Hubei Key Laboratory of Material Chemistry and Service Failure, School of Chemistry and Chemical Engineering, Huazhong University of Science and Technology, Wuhan, China,* [3] *Laboratory of Green S.O.C., Dipartimento di Chimica, Biologia e Biotecnologie, Università degli Studi di Perugia, Perugia, Italy*

An iodine/DMSO catalyzed selective cyclization of *N*-tosylhydrazones with sulfur without adding external oxidant was developed for the synthesis of 4-aryl-1,2,3-thiadiazoles. In this reaction, oxidation of HI by using DMSO as dual oxidant and solvent is the key, which allowed the regeneration of I_2, ensuring thus the success of the synthesis. This protocol features by simple operation, high step-economy (one-pot fashion), broad substrate scope as well as scale-up ability.

Keywords: *N*-tosylhydrazone, 1,2,3-thiadiazoles, iodine, DMSO, sulfur

OPEN ACCESS

Edited by:
Jian-Wei Han,
East China University of Science and Technology, China

Reviewed by:
Jamal Rafique,
Federal University of Mato Grosso do Sul, Brazil
Feng-Cheng Jia,
Wuhan Institute of Technology, China

***Correspondence:**
Ping Liu
liuping1979112@aliyun.com
Yanlong Gu
klgyl@hust.edu.cn

Specialty section:
This article was submitted to Organic Chemistry, a section of the journal Frontiers in Chemistry

Received: *16 January 2020*
Accepted: *04 May 2020*
Published: *12 June 2020*

Citation:
Li W, Zhang J, He J, Xu L, Vaccaro L, Liu P and Gu Y (2020) I_2/DMSO-Catalyzed Transformation of N-tosylhydrazones to 1,2,3-thiadiazoles. Front. Chem. 8:466. doi: 10.3389/fchem.2020.00466

INTRODUCTION

1,2,3-Thiadiazole, as an important 2N1S-heterocyclic structural unit, is ubiquitous in natural products and drug molecules (**Figure 1**; Bakulev and Dehaen, 2004; Shafran et al., 2018). Because of their unique biological activity and intrinsic reactivity, 1,2,3-thiadiazoles were widely used in medicine (Mloston and Huisgen, 1985, 1989; Thomas et al., 1985; Huisgen and Mloston, 1999; Wu et al., 2007; Cikotiene et al., 2009; Atta et al., 2010; Dong et al., 2010; Amirhamzeh et al., 2013), pesticides (Jalilian et al., 2003; Li et al., 2005; Fan et al., 2009; Wang et al., 2009; Zheng et al., 2010) and organic synthesis (Förster et al., 1997; Takimiya et al., 1997; Androsov and Neckers, 2007; Androsov, 2008; Teplyakov et al., 2013). In the past two decades, many efforts have been made to construct the 1,2,3-thiadiazole skeleton. The reported methods can be cataloged as the followings: (a) the 1,3-dipolar cycloaddition of diazoalkanes to thiocarbonyl compounds (Pechmann and Nold, 1896; Sheehan and Izzo, 1949; Martin and Mucke, 1965; Capuano et al., 1983; Aoyama et al., 1986); (b) Hurd-Mori synthesis and the analogous processes (Hurd and Mori, 1955; Kumar et al., 2012; Mo et al., 2019; Zhang et al., 2019); (c) the cyclization of Lawesson reagent with diazotized α-aminoketone (Caron, 1986); and (d) the [3 + 2] cycloaddition of α-enolic dithioester with tosyl azide (Singh et al., 2013). Although these methods provided some promising routes to access 1,2,3-thiadiazoles, the reported protocols also plagued by some drawbacks, such as the use of highly reactive reagents or pre-functionalized substrates, harsh reaction conditions, and a limited scope of substrate. Therefore, an effective route to construct 1,2,3-thiadiazole skeleton by using readily available chemicals is appealingly needed.

Recently, *N*-tosylhydrazones, which are readily accessible and inexpensive chemicals, have attracted much attention in the construction of heterocyclic compounds (Xia and Wang, 2017). In particular, iodine-catalyzed cyclization of *N*-tosylhydrazone with elemental sulfur has become one of the most efficient methods to synthesize 4-aryl-1,2,3-thiadiazoles (Chen et al., 2015; Ishikawa et al., 2017; Liu et al., 2018; Li et al., 2019). This transformation was triggered by α-iodation of

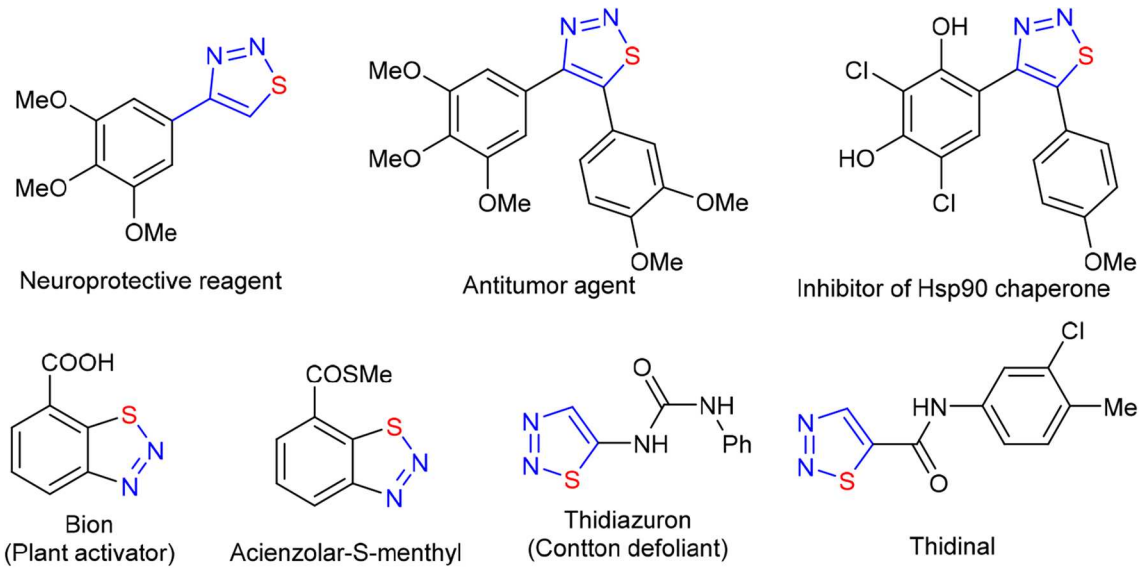

FIGURE 1 | Bioactive molecules with a 1,2,3-thiadiazole moiety.

acetophenone tosylhydrazone, which was generated *in situ* from the corresponding precursors (**Scheme 1**). One molecule of hydrogen iodide (HI) was also formed at the same time. To avoid the detrimental effect of acidic HI, and also to facilitate progress of a catalytic reaction, in the previous reports, an oxidizing reagent was adopted to convert HI to I_2. With this strategy, some effective systems, such as $K_2S_2O_8$/TBAI (**Scheme 1**, method a; Chen et al., 2015), TBHP/NH_4I (method b; Li et al., 2019), and flavin-catalyzed O_2 oxidation/NH_4I (method c; Liu et al., 2018), have been developed successfully. Electrochemical oxidation in the combination of using NH_4I as additive was also proved to be effective (method d; Ishikawa et al., 2017). Although the reported synthesis of 4-aryl-1,2,3-thiadiazoles through cyclization of *N*-tosylhydrazones is promising, owing to the addition of a large amount of oxidizing reagent or the use of special equipment, the effectiveness and the greenness of the synthesis were negatively affected by a time-consuming product separation procedure and the generation of waste.

Very recently, Wu et al. reported an efficient I_2/$CuCl_2$-promoted one-pot three-component strategy for the construction of 1,2,3-thiadiazoles from aliphatic- or aromatic-substituted methyl ketones, *p*-toluenesulfonyl hydrazide, and potassium thiocyanate in the presence of DMSO as solvent (Wang et al., 2019). However, excess stoichiometric amounts of I_2 and $CuCl_2$ are required. On the other hand, the combination of I_2 and DMSO emerged recently as an effective and eco-friendly oxidative system for organic synthesis (Saba et al., 2015, 2016; Rafique et al., 2016; Silva et al., 2017; Monga et al., 2018). The past decade already witnessed the powerful productivity of this unique system to strengthen atom- and step-economic organic synthesis. Particularly, under appropriate conditions, regeneration of I_2 from HI with the aid of DMSO proven to be practically feasible (Kalmode et al., 2014; Wu et al., 2014; Deshidi et al., 2015; Mohammed et al., 2015; Huang et al., 2019; Li et al., 2019). This not only minimized the dosage of I_2 but also enabled us to establish some new reactions without adding external auxiliary reagent, simplifying thus the reaction system. Based on this observation, we envisaged that the I_2/DMSO system may be applicable in the cyclization of *N*-tosylhydrazone with elemental sulfur. The dual role of DMSO as both solvent and oxidant, if it works, will allow us to synthesize 1,2,3-thiadiazoles in a simple system. Our preliminary results show that our speculation is indeed reasonable. Herein, we wish to report a facile synthesis of 4-aryl-1,2,3-thiadiazoles via an I_2-catalyzed reaction between *N*-tosylhydrazones and element sulfur in DMSO solvent (**Scheme 1**, method e).

RESULTS AND DISCUSSION

Our study commenced from a reaction of *N*-tosylhydrazone **1a** and sulfur (S_8). Initially, 0.30 mmol of **1a** was mixed with 0.90 mmol of S_8. The reaction was performed in DMSO, and the obtained results are listed in **Table 1**. No reaction occurred after 5 h of heating under air at 100°C (entry 1). Addition of 20 mol% of KI or tetrabutylammonium iodide (TBAI) cannot initiate the reaction either (entries 2 and 3). This is quite reasonable because, under non-acidic conditions, it is difficult to oxidize the iodide anion to elemental iodine by DMSO. Ammonium iodide (NH_4I) has stronger acidity compared with that of TBAI. By using NH_4I as a catalyst, the reaction proceeded slowly. And after 5 h, the desired product, 4-phenyl-1,2,3-thiadiazole **3a**, was obtained in 11% of yield (entry 4). Intriguingly, I_2 can catalyze the cyclization reaction effectively in conjunction with using DMSO as solvent, and the reaction yield reached 79% (entry 5). The choice of

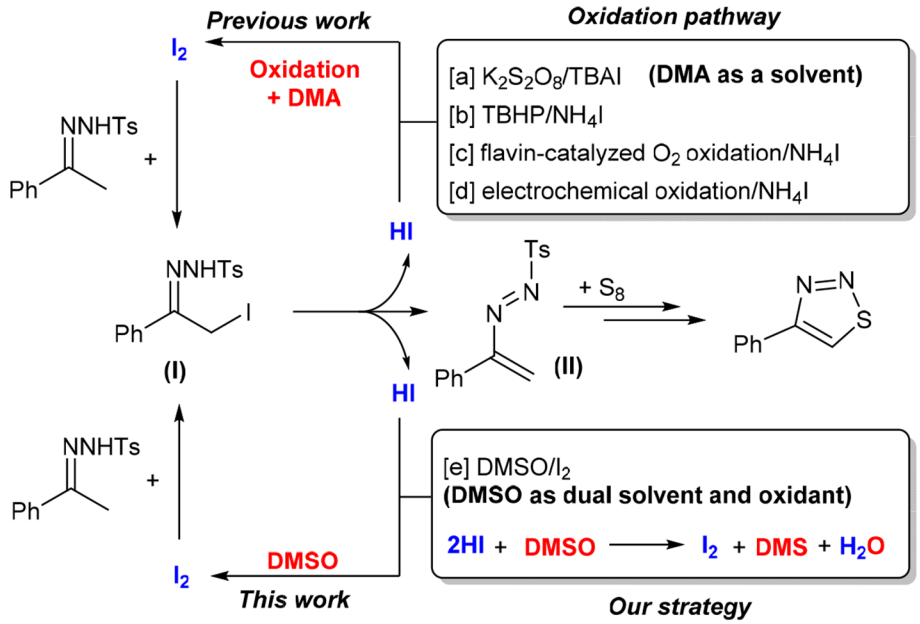

SCHEME 1 | Iodine-catalyzed cyclization of *N*-tosylhydrazone with S_8.

solvent is crucial. When DMSO was replaced by the other organic solvents, such as toluene, DMF, and 1,4-dioxane, the reaction proceeded hardly (entries 6–8). In an alcoholic solvent, isopropanol (IPA), the reaction can be initiated, but it proceeded very slowly. As a result, the yield stopped only at 15% (entry 9). To further improve the reaction yield, the effect of the dosage of I_2 was scrutinized. Interestingly, it was found that the reaction yield could be improved to 86% by decreasing the amount of I_2 to 10 mol% (entry 10). However, a further decrease of the I_2 loading resulted in a drastic loss of the reaction yield (entry 11). With 2.5 mol% of I_2, **3a** can be isolated only in 10% yield (entry 12). We also tested the model reaction under argon. In this case, the reaction proceeded smoothly, and **3a** can be isolated in 90% yield (entry 13). The yield can be slightly improved by decreasing the amount of S_8 to 2.0 equivalents (92%, entry 14). From the viewpoint of green chemistry, the best system should allow also the use of an equal amount of precursors. Unfortunately, when **1a** and **2a** were charged equally, the reaction proceeded sluggishly (entry 15). Also, adjustment of the reaction temperature, reaction time, and the amount of DMSO did not significantly promote the reaction (entries 16–21). And finally, to reach a compromise of all of the reaction parameters, the optimal conditions were confirmed to be I_2 catalyst (10 mol%), DMSO solvent, the ratio of **1a**/**2a** is 1/2. The performance of NBS or NIS, which has also been used as an oxidizing reagent (Huang et al., 2017; Gu et al., 2018a,b; Xu et al., 2019), was also examined under the optimal conditions. However, only a trace amount of **3a** can be detected (entries 22 and 23). This result demonstrated that to take the oxidizing ability of DMSO as a means to implement the synthesis, the use of I_2 is mandatory.

With the optimized reaction conditions in hand, we then explored the effect of the arylsulfonyl group in the sulfonylhydrazone component on the reaction. As shown in **Scheme 2**, all the examined *N*-arylsulfonylhydrazones reacted with sulfur readily. Electron-rich *N*-arylsulfonylhydrazones seemingly like favorable for producing **3a**. For example, while 81% of yield was obtained with an *N*-phenylsulfonylhydrazone formed from $PhSO_2NHNH_2$, the electron-deficient congener from 4-F-$C_6H_4SO_2NHNH_2$ gave **3a** in 73% yield. Similarly, the reactions with electron-rich *N*-arylsulfonylhydrazones, like *N*-tosylhydrazone or its analogous with a methoxy group formed from 4-OMe-$C_6H_4SO_2NHNH_2$, provided a slightly higher yield of **3a** than the former two (92 and 84%).

The effect of the imine part in the *N*-tosylhydrazone component on the reaction was also investigated, and the results are shown in **Scheme 3**. *N*-tosylhydrazones with different functional groups on the arene ring of the imine part all worked well under the standard conditions, efficiently providing the corresponding 4-aryl-1,2,3-thiadiazoles **3b**−**3i** with yields ranging from 82 to 92%. The electronic nature of the substituents on the arene ring of the imine part, involving electron-donating (4-Me, 4-nBu, and 4-MeO) and electron-withdrawing (4-F, 4-Cl, 4-Br, 4-I, and 4-CF_3) groups, had no obvious effect on the yields. Further, substituents in the *meta* position of the arene ring also showed good compatibility, giving cyclization products **3j** and **3k** in 91 and 92% yield, respectively. The *N*-tosylhydrazones with an *ortho*-substituted arene in their imine parts were also applicable in this reaction. For example, **3l** and **3m** can be synthesized in 90 and 72% yield, respectively. More sterically demanding *N*-tosylhydrazones derived from substituted acetylnaphthalenes participated also successfully in the reaction, furnishing the desired products **3n**−**3q** in 83–98% yields. Similarly, biaryl substituted *N*-tosylhydrazones could also be used in this transformation, delivering the desired products

3r—3t in 83–97% yields. The *N*-tosylhydrazone synthesized from trans-4-phenyl-3-buten-2-one participated readily into this reaction as well. And the double bond in the substrate **1** was delivered into the structure of the expected product **3u**, without any damage. While good yield was obtained with acetophenone-derived *N*-tosylhydrazones, the introduction of a functional group on the carbon of the imine group significantly decreased the reactivity of substrate **1**. As a result, the *N*-tosylhydrazones came from 2-phenylacetophenone, 1*H*-indene-1,3(2*H*)-dione, and propiophenone, reluctantly engaged in the reaction, giving **3v—3x** in <50% yield. The usefulness of this method was demonstrated by a very efficient synthesis of the neuroprotective reagent **3y**. Through a reaction of 1-(3,4,5-trimethoxyphenyl)ethan-1-one *N*-tosylhydrazone with sulfur, **3y** was obtained in 85% yield. It should be noted that, although the reported method for synthesizing **3y** started also from the same *N*-tosylhydrazone derivative (Thomas et al., 1985), owing to the use of highly toxic reagent, thionyl chloride, our method can be considered as a green protocol for implementing the synthesis of **3y**. Furthermore, the transformations of aliphatic and heterocyclic *N*-tosylhydrazones with sulfur were also investigated, but the desired products **3z** and **4a** were not obtained. We also tried to use selenium or tellurium instead of sulfur to perform this reaction, but unfortunately, none of them succeeded.

TABLE 1 | Optimization of reaction conditions[a].

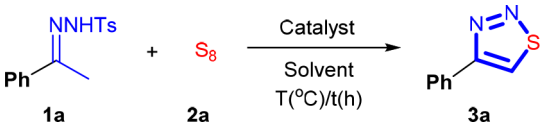

Entry	Catalyst	Solvent	T/°C	t/h	Yield(%)[b]
1	—	DMSO	100	5	0
2	KI (20 mol%)	DMSO	100	5	Trace
3	TBAI (20 mol%)	DMSO	100	5	Trace
4	NH_4I (20 mol%)	DMSO	100	5	11
5	I_2 (20 mol%)	DMSO	100	5	79
6	I_2 (20 mol%)	Toluene	100	5	Trace
7	I_2 (20 mol%)	DMF	100	5	Trace
8	I_2 (20 mol%)	1,4-Dioxane	100	5	Trace
9	I_2 (20 mol%)	IPA	100	5	15
10	I_2 (10 mol%)	DMSO	100	5	86
11	I_2 (5.0 mol%)	DMSO	100	5	52
12	I_2 (2.5 mol%)	DMSO	100	5	10
13	I_2 (10 mol%)	DMSO	100	5	90
14[c]	I_2 (10 mol%)	DMSO	100	5	92
15[d]	I_2 (10 mol%)	DMSO	100	5	58
16	I_2 (10 mol%)	DMSO	80	5	86
17	I_2 (10 mol%)	DMSO	120	5	59
18	I_2 (10 mol%)	DMSO	100	2	78
19	I_2 (10 mol%)	DMSO	100	10	75
20	I_2 (10 mol%)	DMSO(1 mL)	100	5	72
21	I_2 (10 mol%)	DMSO(0.5 mL) + DMA(2.0 mL)	100	5	68
22	NBS (10 mol%)	DMSO	100	10	Trace
23	NIS (10 mol%)	DMSO	100	10	Trace

[a]*Reaction conditions:* ***1a*** *(0.30 mmol),* ***2a*** *(0.90 mmol), solvent (3 mL), under air (entries 1–12); under argon (entries 13–23).*
[b]*Isolated yield.*
[c]*0.60 mmol of* ***2a*** *was added.*
[d]*0.30 mmol of* ***2a*** *was added.*

Since *N*-tosylhydrazone **1** can be easily formed from *p*-toluenesulfonhydrazide and a ketone (Sun et al., 2018; El-Harairy et al., 2019a,b; Li et al., 2019; Liu et al., 2019), we then investigated whether or not the cyclization reaction could be carried out in one-pot fashion directly using a ketone and the hydrazide as the precursors. If it was established, the isolation and purification of the *N*-tosylhydrazone component can be avoided, thus significantly strengthening the synthetic efficiency. The results showed that this idea was indeed feasible, and the cyclization products were obtained with 70–97% yields (**Scheme 4**). To ensure a good yield of the reaction, all the three-component reactions were performed under argon atmosphere. It should be noted that 2-hydroxyacetophone that contains a reactive arene ring toward electrophilic iodination can tolerate the I_2-based conditions. The corresponding product **3m** can be formed in 70% yield.

The neuroprotective reagent **3y** can also be synthesized in this way, but the yield obtained is slightly inferior compared with the method in **Scheme 3**. Despite this fact, this three-component protocol is quite promising as it saved one step while minimized the generation of waste. The reaction can also be carried out on a gram-scale synthesis. For instance, the reaction performed well using 7.5 mmol of 4-bromoacetophenone, 8.25 mmol of $TsNHNH_2$, and 15 mmol of sulfur, leading to isolation of 1.57 g of the product **3a** with 87% of yield (**Scheme 5**).

To shed light on the mechanism, some control experiments were conducted. As shown in **Scheme 6**, although **1a** was completely consumed, **3a** can be hardly detected when 2.0 equivalents of 2,2,6,6-tetramethylpiperidinooxy (TEMPO) were added. The addition of benzoquinone (BQ) was found to be detrimental for the reaction either. But in this case, the reaction was not quenched, and it proceeded slowly, and **3a**

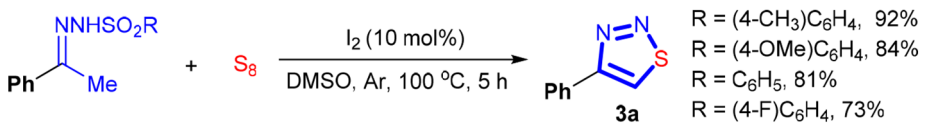

SCHEME 2 | Effect of arylsulfonyl groups on yield of **3a**.

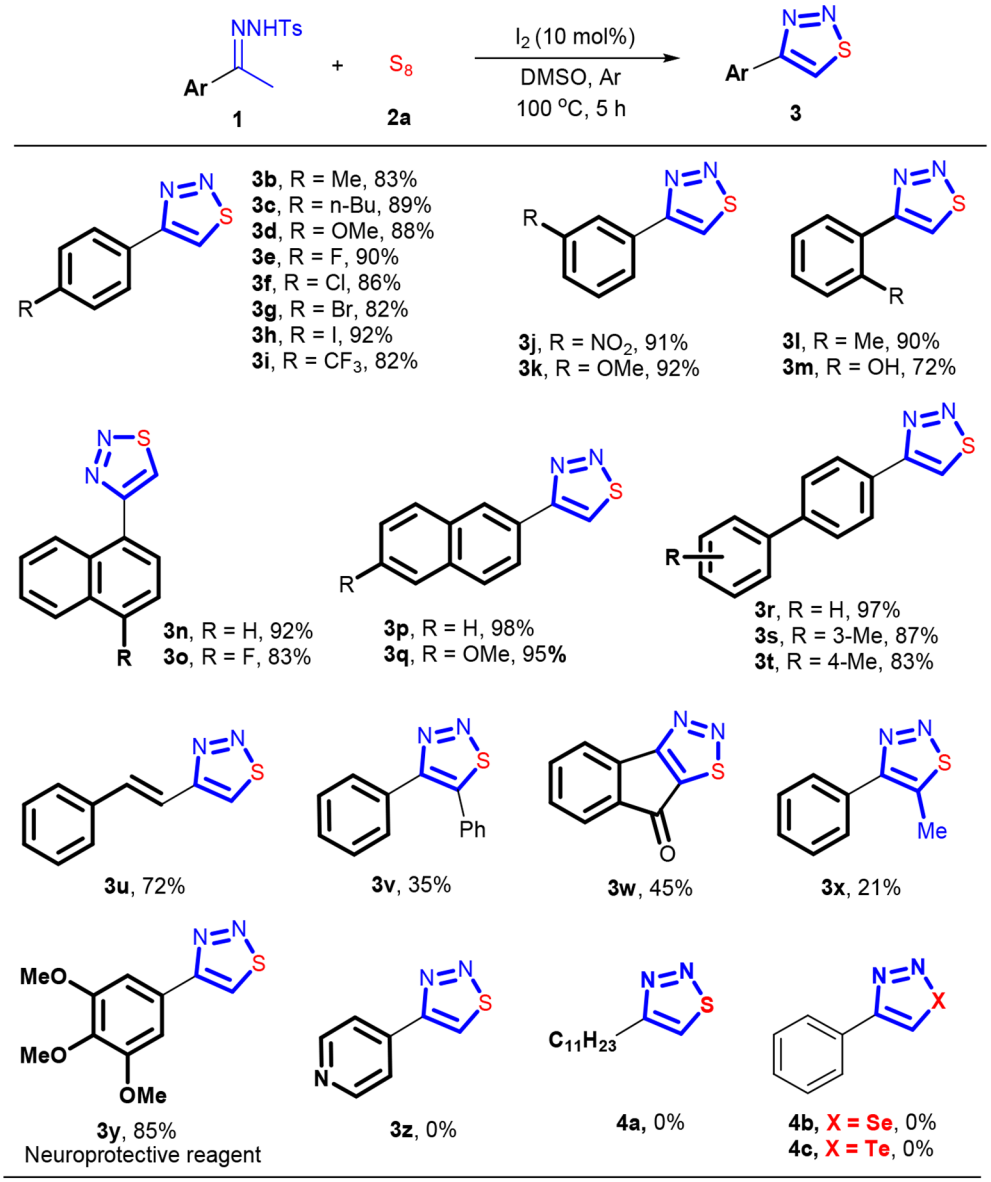

SCHEME 3 | The substrate scope of *N*-tosylhydrazones. Reaction conditions: 0.3 mmol **1**, 0.6 mmol S_8, I_2 (10 mol%), DMSO (3 mL), 5 h, under argon. Isolated yield.

can be isolated in 32% yield under the identical conditions. The effects of 9,10-dihydroanthracene and 1,1-diphenylethylene, which are acid-compatible radical scavengers, on the model reaction were also investigated. And **3a** can be isolated in 93 and 90% yields, respectively. The reaction proceeded uneventfully in the presence of 2,6-di-tert-butyl-4-methylphenol (BHT). In the absence of sulfur, decomposition of **1a** occurred, providing II′ as the main product (Pramanik et al., 2019). In this case, the isolated II′ is not pure, and the ^{1}H and ^{13}C NMR spectra led us to have speculation on the formation of II. HRMS also supported our speculation as a peak at 287.0575 ($M + H^+$) can be observed. The treatment of the mixture of 2-iodo-1-phenylethan-1-one and $TsNHNH_2$ with sulfur resulted in the formation of **3a**. It should be noted that, when DMSO was used as solvent, the transformation was always successful either in the presence or in the absence of I_2. However, replacing DMSO with the other solvents, such as DMF and toluene, resulted in a dramatic loss of the reaction yield. These results indicated that the choice of solvent is the key to ensure a good yield of this cyclization.

Based on all these observations, a plausible mechanism was proposed. We conjectured that the reaction followed a polar reaction mechanism rather than a free-radical mechanism. As shown in **Scheme 7**, the initial event should be α-iodation of **1a**, which gives I as an intermediate. Then, an elimination of one molecule of HI of I occurred, providing an intermediate

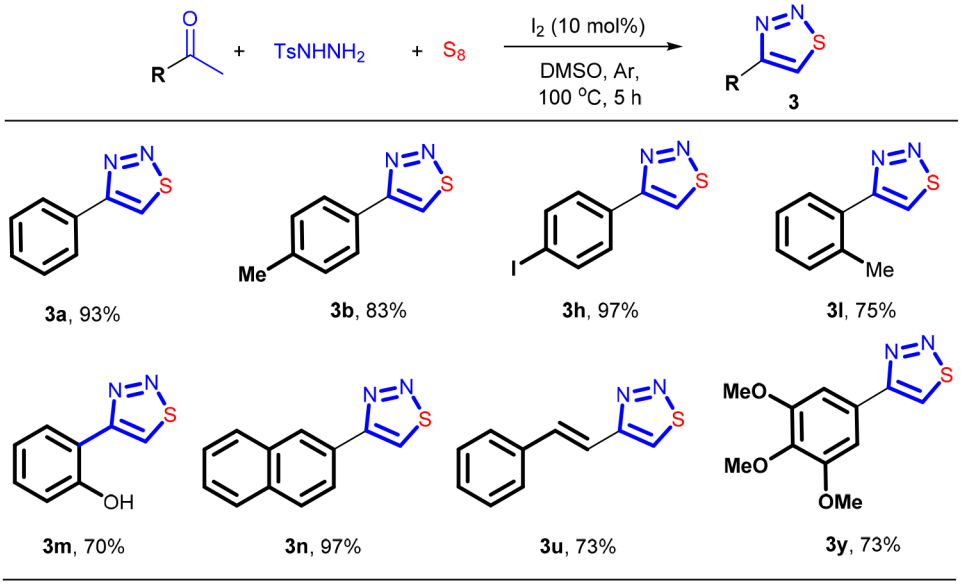

SCHEME 4 | The synthesis of 4-aryl-1,2,3-thiadiazoles via one-pot fashion. Reaction conditions: 0.3 mmol of aryl ketone, 0.33 mmol of $TsNHNH_2$, 0.6 mmol of S_8, I_2 (10 mol%), DMSO (3 mL), 5 h, under argon. Isolated yield.

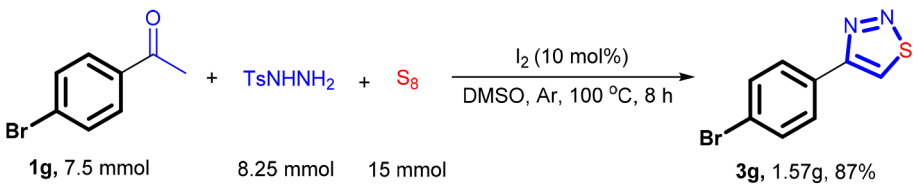

SCHEME 5 | A gram-scale synthesis of **3g**.

II. Because of the presence of an electron-rich vinyl group, this species behaves like a nucleophile, can thus react with sulfur to form an intermediate III (Chen et al., 2015; Ishikawa et al., 2017; Liu et al., 2018; Li et al., 2019). Finally, **3a** was formed through an intramolecular cyclization and the following elimination of TsH and S_7. In the first two steps of the reaction, two molecules of HI were generated. To establish a catalytic cycle, HI must be oxidized to I_2. The unique oxidizing ability of the solvent DMSO played the key role in regenerating I_2 (Steuer et al., 2011; Deshidi et al., 2014, 2015; Kalmode et al., 2014, 2015; Wu et al., 2014; Mohammed et al., 2015; Mupparapu et al., 2015). The combination of I_2 and DMSO ensured the success of this synthetic reaction.

CONCLUSION

In summary, we have developed an iodine-catalyzed cyclization of *N*-tosylhydrazones with sulfur using DMSO a dual solvent and oxidant. This reaction provided an efficient approach to produce diversified 4-aryl-1,2,3-thiadiazoles in good yields. This method can be used in a gram scale synthesis. Furthermore, a one-pot synthesis was also established, which allowed the direct use of ketone as substrate, without isolating the *N*-tosylhydrazone intermediate. This approach was proven also to be applicable in the synthesis of a neuroprotective reagent. An eminent advantage of this strategy is that it avoided the use of external oxidants. Considering expensive photochemical catalyst or electrochemical instruments are required in the previously reported methods, the present method can be considered as a practically applicable and environmentally benign approach for the synthesis of 1,2,3-thiadiazoles.

MATERIALS AND METHODS

Chemicals were obtained commercially and used as received. NMR spectra were recorded on a Bruker DPX−400 spectrometer using TMS as the internal standard. DMSO as solvent was used directly without any treatment. All products were isolated by short chromatography on a silica gel (200–300 mesh) column using petroleum ether (60–90°C), unless otherwise noted. All of reagents were of analytical grade quality, purchased from Adamas-beta Pharmaceuticals, Inc.

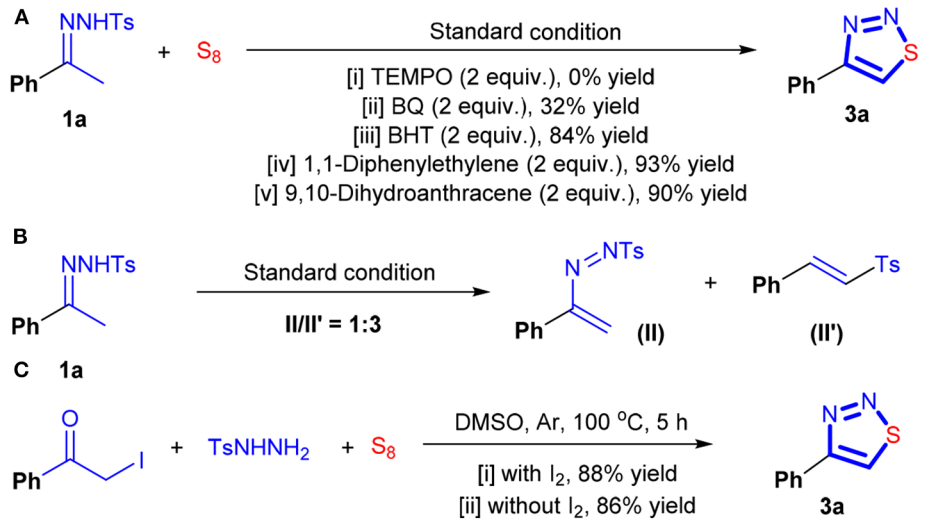

SCHEME 6 | The control experiments.

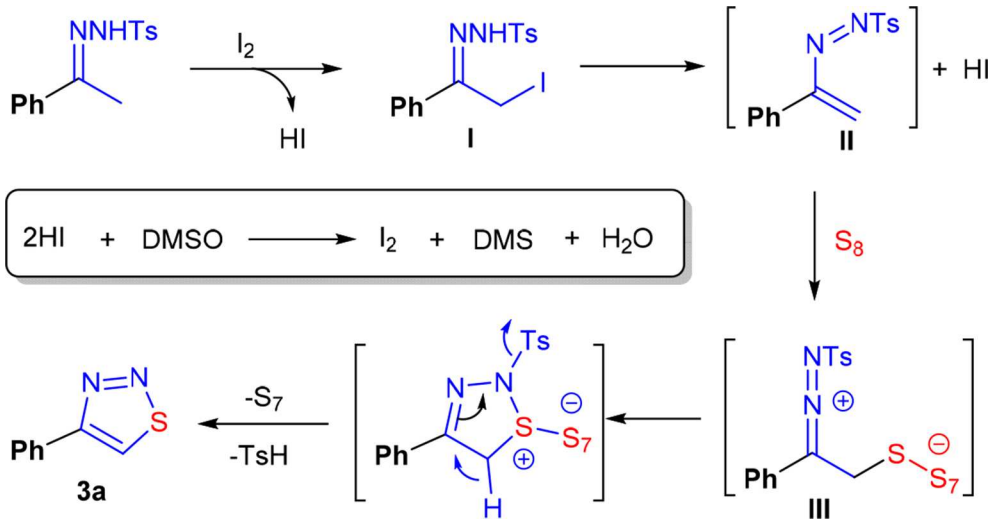

SCHEME 7 | Proposed mechanism.

General Procedure for I_2/DMSO-Catalyzed Transformation From *N*-tosylhydrazones and Sulfur to 4-aryl 1,2,3-thiadiazoles

A mixture of substituted *N*-tosylhydrazones (0.3 mmol), sulfur (0.6 mmol), I_2 (10 mol%) were loaded into a Schlenk tube (25 mL). Then, the tube was degassed for 30 s and filled with Argon. This process was repeated for a total of three times. Afterward, DMSO (3 mL) was added under an argon atmosphere. The resulting reaction mixture was stirred and heated to 100°C for 5 h. After reaction completion, the solution was quenched the saturated solution of sodium thiosulfate (5 mL) and extracted with EtOAc (3 × 10 mL). The combined EtOAc extracts were dried over anhydrous Na_2SO_4, filtered, and concentrated under reduced pressure. The crude residue was purified by flash column chromatography on silica gel using PE/EtOAc as the eluent.

General Procedure for the Synthesis of 4-aryl-1,2,3-thiadiazoles via One-Pot Fashion

A Schlenk tube (25 mL) equipped with a stir bar was charged with $TsNHNH_2$ (0.33 mmol), sulfur (0.6 mmol), I_2 (10 mol%). Then, the tube was degassed for 30 s and filled with Argon. This process was repeated for a total of three times. Afterward, aryl ketone (0.3 mmol) and DMSO (3 mL) was added under an argon atmosphere. The resulting reaction mixture was stirred and heated to 100°C for 5 h. After reaction completion, the solution

was quenched the saturated solution of sodium thiosulfate (5 mL) and extracted with EtOAc (3 × 10 mL). The combined EtOAc extracts were dried over anhydrous Na_2SO_4, filtered, and concentrated under reduced pressure. The crude residue was purified by flash column chromatography on silica gel using PE/EtOAc as the eluent.

DATA AVAILABILITY STATEMENT

The raw data supporting the conclusions of this article will be made available by the authors, without undue reservation, to any qualified researcher.

AUTHOR CONTRIBUTIONS

PL, YG, and LV constructed the workflow. WL, JZ, and JH synthesized and purified the compounds. LX performed the NMR spectrometric analysis. PL and YG completed the paper.

FUNDING

This work was supported by the National Natural Science Foundation of China (Nos. 21563025, 2171101076, and 21872060) and the Shihezi University (No. CXRC201602). MIUR was acknowledged for the support via the project AMIS - Dipartimenti di Eccellenza 2018-2022.

SUPPLEMENTARY MATERIAL

The Supplementary Material for this article can be found online at: https://www.frontiersin.org/articles/10.3389/fchem.2020.00466/full#supplementary-material

REFERENCES

Amirhamzeh, A., Vosoughi, M., Shafiee, A., and Amini, M. (2013). Synthesis and docking study of diaryl-isothiazole and 1,2,3-thiadiazole derivatives as potential neuroprotective agents. *Med. Chem. Res.* 22, 1212–1223. doi: 10.1007/s00044-012-0124-9

Androsov, D. A. (2008). Synthesis of 1, 1-dialkylindolium-2-thiolates via base-induced transformation of 4-(2-chloro-5-nitrophenyl)-1,2,3-thiadiazole in the presence of secondary amines. *J. Org. Chem.* 73, 8612–8614. doi: 10.1021/jo801801y

Androsov, D. A., and Neckers, D. C. (2007). Synthesis and reactivity of 4-(2-chloro-5-nitrophenyl)-1, 2, 3-thiadiazole. A novel one-pot synthesis of N-substituted indole-2-thiols. *J. Org. Chem.* 72, 5368–5373. doi: 10.1021/jo0707784

Aoyama, T., Iwamoto, Y., and Shioiri, T. (1986). New methods and reagents in organic synthesis. 59. Lithium trimethylsilydiazomethane: a new synthon for the preparation of 5-substituted 1,2,3-thiadiazoles. *Heterocycles* 24, 589–592. doi: 10.3987/R-1986-03-0589

Atta, S. M. S., Farrag, D. S., Sweed, A. M., and Abdel-Rahman, A. H. (2010). Preparation of new polycyclic compounds derived from benzofurans and furochromones. An approach to novel 1,2,3-thia-, and selena-diazolofurochromones of anticipated antitumor activities. *Eur. J. Med. Chem.* 45, 4920–4927. doi: 10.1016/j.ejmech.2010.07.065

Bakulev, V. A., and Dehaen, W. (2004). *The Chemistry of 1,2,3-Thiadiazoles*. New York, NY: John Wiley and Sons Press.

Capuano, L., Boschat, P., Müller, I., Zander, R., Schramm, V., and Hädicke, E. (1983). Synthesen mit 2,4-dimethylen-1,3-dithietanen. mercaptopyridine; thiazole; dithiole; mesoionische und nichtmesoionische 1,2,3-thiadiazole. *Chem. Ber.* 116, 2058–2067. doi: 10.1002/cber.19831160603

Caron, M. (1986). Convenient preparation of 5-alkyl-4-carbalkoxy-1,2,3-thiadiazoles. *J. Org. Chem.* 51, 4075–4077. doi: 10.1021/jo00371a033

Chen, J., Jiang, Y., Yu, J. T., and Cheng, J. (2015). TBAI-catalyzed reaction between N-tosylhydrazones and sulfur: a procedure toward 1,2,3-thiadiazole. *J. Org. Chem.* 81, 271–275. doi: 10.1021/acs.joc.5b02280

Cikotiene, I., Kazlauskas, E., Matuliene, J., Michailoviene, V., Torresan, J., Jachno, J., et al. (2009). 5-Aryl-4-(5-substituted-2,4-dihydroxyphenyl)-1,2,3-thiadiazoles as inhibitors of Hsp90 chaperone. *Bioorg. Med. Chem. Lett.* 19, 1089–1092. doi: 10.1016/j.bmcl.2009.01.003

Deshidi, R., Devari, S., and Shah, B. A. (2015). Iodine-promoted oxidative amidation of terminal alkenes–synthesis of α-ketoamides, benzothiazoles, and quinazolines. *Eur. J. Org. Chem.* 1428–1432. doi: 10.1002/ejoc.201403547

Deshidi, R., Kumar, M., Devari, S., and Shah, B. A. (2014). A general metal free approach to α-ketoamides via oxidative amidation-diketonization of terminal alkynes. *Chem. Commun.* 50, 9533–9535. doi: 10.1039/C4CC03783A

Dong, W. L., Liu, Z. X., Liu, X. H., Li, Z. M., and Zhao, W. G. (2010). Synthesis and antiviral activity of new acrylamide derivatives containing 1,2,3-thiadiazole as inhibitors of hepatitis B virus replication. *Eur. J. Med. Chem.* 45, 1919–1926. doi: 10.1016/j.ejmech.2010.01.032

El-Harairy, A., Lai, B., Vaccaro, L., Li, M., and Gu, Y. (2019a). A sulfone-containing imidazolium-based brønsted acid ionic liquid catalyst enables replacing dipolar aprotic solvents with butyl acetate. *Adv. Synth. Catal.* 361, 3342–3350. doi: 10.1002/adsc.201900246

El-Harairy, A., Yue, M., Fan, W., Popowycz, F., Queneau, Y., Li, M., et al. (2019b). Novel non-toxic and non-hazardous solvent systems for the chemistry of indoles: use of a sulfone-containing brønsted acid ionic liquid catalyst in butyl acetate. *ChemCatChem.* 11, 4403–4410. doi: 10.1002/cctc.201900784

Fan, Z., Shi, Z., Zhang, H., Liu, X., Bao, L., Ma, L., et al. (2009). Synthesis and biological activity evaluation of 1,2,3-thiadiazole derivatives as potential elicitors with highly systemic acquired resistance. *J. Agric. Food Chem.* 57, 4279–4286. doi: 10.1021/jf8031364

Förster, W. R., Isecke, R., Spanka, C., and Schaumann, E. (1997). Functionalized β-thiolactams by lewis acid catalyzed addition of alkynyl silyl sulfides to azomethines. *Synthesis* 1997, 942–948. doi: 10.1055/s-1997-1275

Gu, Y., Huang, W., Chen, S., and Wang, X. (2018a). Bismuth (III) triflate catalyzed three-component reactions of indoles, ketones, and α-bromoacetaldehyde acetals enable indole-to-carbazole transformation. *Org. Lett.* 20, 4285–4289. doi: 10.1021/acs.orglett.8b01707

Gu, Y., Wu, F., and Yang, J. (2018b). Oxidative [3+3] annulation of atropaldehyde acetals with 1,3-bisnucleophiles: an efficient method of constructing six-membered aromatic rings, including salicylates and carbazoles. *Adv. Synth. Catal.* 360, 2727–2741. doi: 10.1002/adsc.201800462

Huang, W., Liu, C., and Gu, Y. (2017). Auto-tandem catalysis-induced synthesis of trisubstituted furans through domino acid-acid-catalyzed reaction of aliphatic aldehydes and 1,3-dicarbonyl compounds by using N-bromosuccinimide as oxidant. *Adv. Synth. Catal.* 359, 1811–1818. doi: 10.1002/adsc.201700074

Huang, W., Xu, J., Liu, C., Chen, Z., and Gu, Y. (2019). Lewis acid-catalyzed synthesis of benzofurans and 4,5,6,7-tetrahydrobenzofurans from acrolein dimer and 1,3-dicarbonyl compounds. *J. Org. Chem.* 84, 2941–2950. doi: 10.1021/acs.joc.9b00270

Huisgen, R., and Mloston, G. (1999). Adamantanethione and diazomethane: dual regiochemistry of cycloadditions [1]. *Pol. J. Chem.* 73, 635–644. doi: 10.1002/chin.199928044

Hurd, C. D., and Mori, R. I. (1955). On acylhydrazones and 1,2,3-thiadiazoles. *J. Am. Chem. Soc.* 77, 5359–5364. doi: 10.1021/ja01625a047

Ishikawa, T., Kimura, M., Kumoi, T., and Iida, H. (2017). Coupled flavin-iodine redox organocatalysts: aerobic oxidative transformation from N-tosylhydrazones to 1,2,3-thiadiazoles. *ACS Catal.* 7, 4986–4989. doi: 10.1021/acscatal.7b01535

Jalilian, A. R., Sattari, S., Bineshmarvasti, M., Daneshtalab, M., and Shafiee, A. (2003). Synthesis and *in vitro* antifungal and cytotoxicity evaluation of substituted 4,5-dihydronaphtho [1,2-d] [1,2,3] thia (or selena) diazoles. *Farmaco* 58, 63–68. doi: 10.1016/S0014-827X(02)00029-0

Kalmode, H. P., Vadagaonkar, K. S., and Chaskar, A. C. (2014). Metal-free *in situ* sp3, sp2, and sp C–H functionalization and oxidative cross coupling with benzamidines hydrochloride: a promising approach for the synthesis of α-ketoimides. *RSC Adv.* 4, 60316–60326. doi: 10.1039/C4RA07556K

Kalmode, H. P., Vadagaonkar, K. S., and Chaskar, A. C. (2015). The oxidative cross-coupling of benzonitriles with multiform substrates: a domino strategy inspired easy access to α-ketoimides. *Synthesis* 47, 429–438. doi: 10.1055/s-0034-1379955

Kumar, A., Muthyala, M. K., Choudhary, S., Tiwari, R. K., and Parang, K. (2012). Ionic liquid as soluble support for synthesis of 1,2,3-thiadiazoles and 1,2,3-selenadiazoles. *J. Org. Chem.* 77, 9391–9396. doi: 10.1021/jo301607a

Li, W., He, J., Liu, P., Zhang, J., and Dai, B. (2019). Synthesis of 4-aryl-1,2,3-thiadiazoles via NH_4I-catalyzed cyclization of *N*-tosylhydrazones with sulfur. *Chem. Select* 4, 10587–10590. doi: 10.1002/slct.201902684

Li, Z., Wu, Z., and Luo, F. (2005). Synthesis and antifungal activities of alkyl N-(1,2,3-thiadiazole-4-carbonyl) carbamates and S-alkyl N-(1,2,3-thiadiazole-4-carbonyl) carbamothioates. *J. Agric. Food Chem.* 53, 3872–3876. doi: 10.1021/jf0501746

Liu, B. B., Bai, H. W., Liu, H., Wang, S. Y., and Ji, S. J. (2018). Cascade trisulfur radical anion ($S3^{\bullet-}$) addition/electron detosylation process for the synthesis of 1,2,3-thiadiazoles and isothiazoles. *J. Org. Chem.* 83, 10281–10288. doi: 10.1021/acs.joc.8b01450

Liu, Y., Chen, L., Wang, Z., Liu, P., Liu, Y., and Dai, B. (2019). Cascade reaction of arylboronic acids and 2′-cyano-biaryl-2-aldehyde N-Tosylhydrazones: access to functionalized 9-amino-10-arylphenanthrenes. *J. Org. Chem.* 84, 204–215. doi: 10.1021/acs.joc.8b02605

Martin, D., and Mucke, W. (1965). Cycloaddition von diazoalkanen an isothiocyanate. *Justus Liebigs Ann. Chem.* 682, 90–98. doi: 10.1002/jlac.19656820109

Mloston, G., and Huisgen, R. (1985). Acid-base reactions of 1,3,4-thiadiazolines and thiocarbonyl ylides; 1,3,4-thiadiazoline-2-spiro-2′-adamantane. *Tetrahedron Lett.* 26, 1053–1056. doi: 10.1016/S0040-4039(00)98510-1

Mloston, G., and Huisgen, R. (1989). Open-chain aliphatic thiones and diazomethane; reactions of 1,3,4-thiadiazolines and thiocarbonyl ylides. *Tetrahedron Lett.* 30, 7045–7048. doi: 10.1016/S0040-4039(01)93419-7

Mo, S. K., Teng, Q. H., Pan, Y. M., and Tang, H. T. (2019). Metal- and oxidant- free electrosynthesis of 1,2,3-thiadiazoles from element sulfur and *N*-tosyl Hydrazones. *Adv. Synth. Catal.* 361, 1756–1760. doi: 10.1002/adsc.201801700

Mohammed, S., Vishwakarma, R. A., and Bharate, S. B. (2015). Iodine catalyzed oxidative synthesis of quinazolin-4 (3 H)-ones and pyrazolo [4,3-d] pyrimidin-7(6H)-ones via amination of sp3 C–H bond. *J. Org. Chem.* 80, 6915–6921. doi: 10.1021/acs.joc.5b00989

Monga, A., Bagchi, S., and Sharma, A. (2018). Iodine/DMSO oxidations: a contemporary paradigm in C–N bond chemistry. *New J. Chem.* 42, 1551–1576. doi: 10.1039/C7NJ04513A

Mupparapu, N., Vishwakarma, R. A., and Ahmed, Q. N. (2015). Iodine-DMSO promoted C–H (SP3) functionalization approach to α-ketoamides. *Tetrahedron* 71, 3417–3421. doi: 10.1016/j.tet.2015.03.088

Pechmann, H. V., and Nold, A. (1896). Ueber die einwirkung von diazomethan auf phenylsenföl. *Ber. Dtsch. Chem. Ges.* 29, 2588–2593. doi: 10.1002/cber.18960290336

Pramanik, M., Choudhuri, K., and Mal, P. (2019). N-Iodosuccinimide as bifunctional reagent in (E)-selective C(sp2)–H sulfonylation of styrenes. *Asian J. Org. Chem.* 8, 144–150. doi: 10.1002/ajoc.201800644

Rafique, J., Saba, S., Rosario, A. R., and Braga, A. L. (2016). Regioselective, solvent- and metal-free chalcogenation of imidazo [1,2-*a*] pyridines by employing I_2/DMSO as the catalytic oxidation system. *Chem. Eur. J.* 22, 11854–11862. doi: 10.1002/chem.201600800

Saba, S., Rafique, J., and Braga, A. L. (2015). Synthesis of unsymmetrical diorganyl chalcogenides under greener conditions: use of an Iodine/DMSO system, solvent- and metal-free approach. *Adv. Synth. Catal.* 357, 1446–1452. doi: 10.1002/adsc.201500024

Saba, S., Rafique, J., and Braga, A. L. (2016). DMSO/iodine-catalyzed oxidative C–Se/C–S bond formation: a regioselective synthesis of unsymmetrical chalcogenides with nitrogen-or oxygen-containing arenes. *Catal. Sci. Technol.* 6, 3087–3098. doi: 10.1039/C5CY01503K

Shafran, Y., Glukhareva, T., Dehaen, W., and Bakulev, V. (2018). Recent developments in the chemistry of 1,2,3-thiadiazoles. *Adv. Heterocycl. Chem.* 126, 109–172. doi: 10.1016/bs.aihch.2017.12.001

Sheehan, J. C., and Izzo, P. T. (1949). The reaction of diazomethane with isocyanates and isothiocyanates. *J. Am. Chem. Soc.* 71, 4059–4062. doi: 10.1021/ja01180a054

Silva, L. T., Azeredo, J. B., Saba, S., Rafique, J., Bortoluzzi, A. J., and Braga, A. L. (2017). Solvent- and metal-free chalcogenation of bicyclic arenes using I_2/DMSO as non-metallic catalytic system., *Eur. J. Org. Chem.* 2017, 4740–4748. doi: 10.1002/ejoc.201700744

Singh, M. S., Nagaraju, A., Verma, G. K., Shukla, G., Verma, R. K., and Srivastava, A. (2013). Eco-efficient, regioselective and rapid access to 4,5-disubstituted 1,2,3-thiadiazoles via [3 + 2] cycloaddition of α-enolicdithioesters with tosyl azide under solvent-free conditions. *Green Chem.* 15, 954–962. doi: 10.1039/C3GC37047J

Steuer, C., Gege, C., Fischl, W., Heinonen, K. H., Bartenschlager, R., and Klein, C. D. (2011). Synthesis and biological evaluation of α-ketoamides as inhibitors of the dengue virus protease with antiviral activity in cell-culture. *Bioorg. Med. Chem.* 19, 4067–4074. doi: 10.1016/j.bmc.2011.05.015

Sun, Z., Du, C., Liu, P., Wei, Y., Xu, L., and Dai, B. (2018). Highly selective β-hydride elimination in the Pd-catalyzed cross-coupling of *N*-Tosylhydrazones with benzyl bromides. *Chem. Select* 3, 900–903. doi: 10.1002/slct.201702521

Takimiya, K., Morikami, A., and Otsubo, T. (1997). A convenient preparation of 1,3-dithiole-2-thione and 1,3-diselenole-2-selone derivatives. *Synlett* 1997, 319–321. doi: 10.1055/s-1997-787

Teplyakov, F. S., Vasileva, T. G., Petrov, M. L., and Androsov, D. A. (2013). A new synthesis of benzo [b] thiophene-2-thiolates and their derivatives via base-promoted transformation of 4-(2-mercaptophenyl)-1,2,3-thiadiazoles. *Org. Lett.* 15, 4038–4041. doi: 10.1021/ol401981w

Thomas, E. W., Nishizawa, E. E., Zimmermann, D. C., and Williams, D. J. (1985). Synthesis and platelet aggregation inhibitory activity of 4,5-bis (substituted)-1,2,3-thiadiazoles. *J. Med. Chem.* 28, 442–446. doi: 10.1021/jm00382a009

Wang, C., Geng, X., Zhao, P., Zhou, Y., Wu, Y. D., and Cui, Y. F. (2019). $I_2/CuCl_2$-promoted one-pot three-component synthesis of aliphatic or aromatic substituted 1,2,3-thiadiazoles. *Chem. Commun.* 55, 8134–8137. doi: 10.1039/C9CC04254G

Wang, Z. H., Guo, Y. Z., Zhang, J., Ma, L., Song, H. B., and Fan, Z. J. (2009). Synthesis and biological activity of organotin 4-methyl-1,2,3-thiadiazole-5-carboxylates and Benzo [1,2,3] thiadiazole-7-carboxylates. *J. Agric. Food Chem.* 58, 2715–2719. doi: 10.1021/jf902168d

Wu, M., Sun, Q., Yang, C., Chen, D., Ding, J., Chen, Y., et al. (2007). Synthesis and activity of combretastatin A-4 analogues: 1,2,3-thiadiazoles as potent antitumor agents. *Bioorg. Med. Chem. Lett.* 17, 869–873. doi: 10.1016/j.bmcl.2006.11.060

Wu, X., Gao, Q., Liu, S., and Wu, A. (2014). I_2-catalyzed oxidative cross-coupling of methyl ketones and benzamidines hydrochloride: a facile access to α-ketoimides. *Org. Lett.* 16, 2888–2891. doi: 10.1021/ol501029w

Xia, Y., and Wang, J. (2017). N-Tosylhydrazones: versatile synthons in the construction of cyclic compounds. *Chem. Soc. Rev.* 46, 2306–2362. doi: 10.1039/C6CS00737F

Xu, J., Huang, W., Bai, R., Queneau, Y., Jérôme, F., and Gu, Y. (2019). Utilization of bio-based glycolaldehyde aqueous solution in organic synthesis: application to the synthesis of 2,3-dihydrofurans. *Green Chem*. 21, 2061–2069. doi: 10.1039/C8GC04000A

Zhang, Y., Cao, Y., Lu, L., Zhang, S., Bao, W., Huang, S., et al. (2019). Perylenequinonoid-catalyzed [4+1]-and [4 + 2]-annulations of azoalkenes: photocatalytic access to 1,2,3-thiadiazole/1,4,5,6-tetrahydropyridazine derivatives. *J. Org. Chem*. 84, 7711–7721. doi: 10.1021/acs.joc.9b00545

Zheng, Q., Mi, N., Fan, Z., Zuo, X., Zhang, H., Wang, H., et al. (2010). 5-Methyl-1,2,3-thiadiazoles synthesized via Ugi reaction and their fungicidal and antiviral activities. *Food Chem*. 58, 7846–7855. doi: 10.1021/jf1006193

Conflict of Interest: The authors declare that the research was conducted in the absence of any commercial or financial relationships that could be construed as a potential conflict of interest.

frontiers in Chemistry

ORIGINAL RESEARCH
published: 10 July 2020
doi: 10.3389/fchem.2020.00467

Hypervalent Iodine-Mediated Diastereoselective α-Acetoxylation of Cyclic Ketones

Jiashen Tan[1†], Weiqin Zhu[1†], Weiping Xu[1], Yaru Jing[1,2], Zhuofeng Ke[2], Yan Liu[1] and Keiji Maruoka[1,3*]*

[1] School of Chemical Engineering and Light Industry, Guangdong University of Technology, Guangzhou, China, [2] PCFM Lab, School of Materials Science and Engineering, Sun Yat-sen University, Guangzhou, China, [3] Graduate School of Pharmaceutical Sciences, Kyoto University, Kyoto, Japan

A binary hybrid system comprising a hypervalent iodine(III) reagent and BF_3•OEt_2 Lewis acid was found to be effective for the diastereoselective α-acetoxylation of cyclic ketones. In this hybrid system, BF_3•OEt_2 Lewis acid allowed the activation of the hypervalent iodine(III) reagent and cyclic ketones for smooth α-acetoxylation reaction, achieving high diastereoselectivity. This hypervalent iodine-mediated α-acetoxylation of the cyclic ketone reaction plausibly undergoes an S_N2 substitution mechanism via an α-*C*-bound hypervalent iodine intermediate. The diastereoselectivity of the reaction mainly originates from thermodynamic control.

Keywords: α-acetoxylation, hypervalent iodine (III) reagent, cyclic ketones, diastereoselectivity, density functional theory

OPEN ACCESS

Edited by:
Jian-Wei Han,
East China University of Science and Technology, China

Reviewed by:
Chang-Hua Ding,
Shanghai University, China
Yin Wei,
Shanghai Institute of Organic Chemistry (CAS), China
Chi Zhang,
Nankai University, China

****Correspondence:***
Yan Liu
yanliu@gdut.edu.cn
Keiji Maruoka
maruoka@kuchem.kyoto-u.ac.jp

[†]These authors share first authorship

Specialty section:
This article was submitted to Organic Chemistry, a section of the journal Frontiers in Chemistry

Received: *05 March 2020*
Accepted: *04 May 2020*
Published: *10 July 2020*

Citation:
Tan J, Zhu W, Xu W, Jing Y, Ke Z, Liu Y and Maruoka K (2020) Hypervalent Iodine-Mediated Diastereoselective α-Acetoxylation of Cyclic Ketones. Front. Chem. 8:467. doi: 10.3389/fchem.2020.00467

INTRODUCTION

The direct α-acetoxylation of ketones provides an efficient and synthetically practical method for α-oxygen functionalization of carbonyl compounds, which exhibits various applications as synthetic key precursors and versatile synthons in organic synthesis (Mizukami et al., 1978; Hecker and Werner, 1993; Varma et al., 1998; Kaila et al., 2007; Edwards et al., 2008; Richter et al., 2018; Huang et al., 2019). Therefore, considerable efforts have been made in the development of synthetic protocols for α-acetoxylation of ketones (**Scheme 1**). Traditional methods to prepare α-acetoxy ketones are the acetolysis of α-diazo ketone (Newman and Beal, 1950; Erickson et al., 1951; Corey and Knapp, 1976; Kitamura et al., 2012; Wang et al., 2014; Tan et al., 2016; Yuan et al., 2016; Zhang et al., 2016; Hu et al., 2018), α-bromo ketone (Tanner et al., 1991; Valgimigli et al., 2003; Ahmed and Langer, 2006; Chen et al., 2013, 2016; Nolla-Saltiel et al., 2014; Carneiro et al., 2015; Liu et al., 2016; Yuan et al., 2019), and *in situ* generated α-iodo derivatives (Du et al., 2015; Ren et al., 2016; Chen et al., 2017; Tan et al., 2017; Pogaku et al., 2019), which usually require the pre-functionalization of ketones (**Scheme 1A**). In contrast, umpolung reactions have taken a prominent place for the direct α-oxygenation of carbonyl compounds via oxidation of the enolates or related derivatives with transition metal complexes (Littler, 1962; Heiba and Dessau, 1971; Ng and Henry, 1976; Rubottom et al., 1983; El-Qisairi and Qaseer, 2002; Hamed et al., 2012), or hypervalent iodine reagents (Mizukami et al., 1978; Nicolaou et al., 2002; Bogevig et al., 2004; Sunden et al., 2004; Ochiai et al., 2005; Huang et al., 2007; Yu et al., 2010; Izquierdo et al., 2016; Arava et al., 2017) (**Scheme 1B**). Metal-free hypervalent iodine compounds as classical oxidative functionalization reagents have attracted considerable interest due to a variety of advantages relative to conventional oxidants such as heavy metals (Pb, Tl, or Hg), including low toxicity, ready availability, mild conditions, excellent selectivity, and a comparable reactivity (Du et al., 2015; Ren et al., 2016; Chen et al., 2017). However,

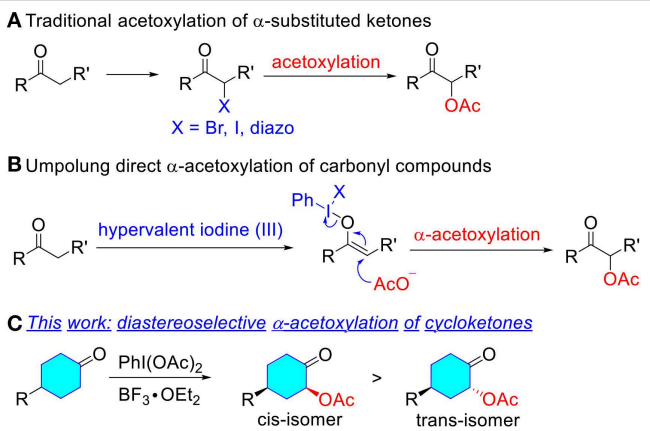

SCHEME 1 | Different methods for the α-acetoxylation reaction of ketones. **(A)** Traditional acetoxylation of α-substituted ketones. **(B)** Umpolung direct α-acetoxylation of carbonyl compounds. **(C)** This work: diastereoselective α-acetoxylation of cycloketones.

efficient and practical methods for the diastereoselective α-acetoxylation of cyclic ketones have not yet been well-developed.

As one of our ongoing interests (Sakamoto et al., 2016, 2017, 2018; Liu et al., 2017; Selvakumar et al., 2017; Shu et al., 2019) to construct selective methods for α-functionalization of carbonyl compounds, we have become keenly interested in the possibility of the diastereoselective α-acetoxylation of cyclic ketones (**Scheme 1C**). In this context, we wish to report our initial study on creating a hybrid system comprised of hypervalent iodine(III) reagent and BF_3•OEt_2.

RESULTS AND DISCUSSION

We began our study on the diastereoselective α-acetoxylation reaction of cyclic ketone with hypervalent iodine(III) reagent and certain acid as an activator. As shown in **Table 1**, the reaction of 4-phenylcyclohexanone with (diacetoxyiodo)benzene in acetic acid solvent at room temperature for 24 h resulted in almost recovery of the starting ketone (**Table 1**, entry 1). In the presence of additives such as CF_3CO_2H, α-acetoxylation product **1** was obtained in low yields (**Table 1**, entry 2), whereas the use of Lewis acids $ZnCl_2$ and $AlCl_3$ as additives resulted in no target product even though 4-phenylcyclohexanone was fully consumed under the applied reaction conditions (**Table 1**, entries 5 and 6). Fortunately, addition of Brønsted acid TfOH (**Table 1**, entry 3), and Lewis acids AgOTf, $Sc(OTf)_3$, $Mg(OTf)_2$, $Cu(OTf)_2$, $Zn(OTf)_2$, and BF_3•OEt_2 (**Table 1**, entries 4, 7–11) improved the yield of the product **1**. BF_3•OEt_2 gave rise to desired *cis*-isomer of α-acetoxylation product, *cis*-**1**, in good yield (**Table 1**, entry 11). Increasing the loading of BF_3•OEt_2 from 1 equiv to 3 equiv resulted in an increased selectivity (**Table 1**, entry 13). However, reducing the reaction time from 24 h to 12 or 6 or 2 h resulted in a gradual decrease in selectivity toward *cis*-**1** (**Table 1**, entries 15–17). Further increasing the BF_3•OEt_2 loading to 5 equiv, or extending the reaction time (48 h), or enhancing the reaction temperature to 50°C, however, did not increase the transformation or selectivity (**Table 1**, entries 14, 18, and 19). Lewis acid BF_3•OEt_2 plays a key role in the α-acetoxylation of cyclohexanone, which should be attributed to the enolization of cyclohexanone to enol that is essential for the reaction to smoothly take place (Ochiai et al., 2005). Changing acetic acid solvent to other organic solvents such as CH_2Cl_2, EtOAc, Et_2O, toluene, CH_3CN, CF_3CH_2OH, and $(CF_3)_2CHOH$ even in the presence of 10 equiv acetic acid resulted in the decrease of both yield and selectivity (**Table 1**, entries 20–32). Therefore, the optimal condition for the synthesis of *cis*-**1** was established as follows: Reaction of 4-phenylcyclohexanone (1 equiv) with $PhI(OAc)_2$ (1.5 equiv) and BF_3•OEt_2 (3 equiv) in acetic acid solvent at room temperature for 24 h. The α-acetoxylation of 4-phenylcyclohexanone proceeded smoothly in ten-gram scale under this optimal reaction condition, without a lose of reactivity and selectivity. The configuration of the major α-acetoxylation product was determined as *cis*-isomer by a single-crystal X-ray diffraction analysis (**Table 1**).

Having established a practical method for the selective α-acetoxylation of 4-phenylcyclohexanone by hybrid catalysis, we became interested in the substrate generality for diastereoselective α-acetoxylation of cyclic ketones with the aforementioned hybrid system: hypervalent iodine (III) reagents and BF_3•OEt_2. The results are summarized (**Table 2**). Firstly, we tested several substituents at C4 position of cyclohexanones to probe the versatility of this hybrid system. Switching phenylcyclohexanone to 4-*tert*-butylcyclohexanone resulted in a slight decrease in the yield to 57% with similar *cis*-selectivity (**Table 2**, entry 2). Further replacing the substituent to the dimethylphenylsilyl group resulted in a further decrease in both yield and selectivity (**Table 2**, entry 3). Extending the reaction time to 24 h, better diastereoselectivity (>9: 1) was observed by lowing the yield to 21%, presumably due to a decomposition of the starting material under the reaction conditions. In the case of 3-substituted cyclohexanones, good to high selectivities were observed (**Table 2**, entries 4 and 5).

Thirdly, we studied the substrates with substituents at both C3 and C4 positions of cyclohexanones. *cis*-3,4-Dimethylcyclohexene as substrate gave 30% yield of the product *cis*-**6** with high diastereoselectivity (>20:1) under standard reaction conditions. Lowering the loading of BF_3•OEt_2 to 1.0 equiv resulted in a full consumption of starting material in 3 h with 41% yield and high diastereoselectivity (>20:1) (**Table 2**, entry 6). To our delight, *trans*-octahydro-naphthalen-2(1*H*)-one as substrate resulted in 51% yield of the product *cis*-**7** with 9.9: 1 diastereoselectivity under the reaction conditions (**Table 2**, entry 7). We tried the application of this hybrid system of PIDA and BF_3•OEt_2 to both cyclopentanone and cycloheptanone. Unfortunately, the yield of the target molecules were quiet low, indicating that this hybrid system was not effective for the α-acetoxylation of cyclopentanones or cycloheptanones.

Having investigated the substrate scope for diastereoselective α-acetoxylation of cyclic ketones, we are interested in the application of the hypervalent iodine(III) reagent–BF_3•OEt_2 hybrid system. Changing AcOH solvent to *i*-$PrCO_2H$, 2-acyloxy-4-phenylcyclohexanone **8** was obtained smoothly in 50% yield with high diastereoselectivity (11.1:1) (**Scheme 2**).

TABLE 1 | Diastereoselective α-acetoxylation of ketone with hypervalent iodine(III) reagents in the presence of additives[a].

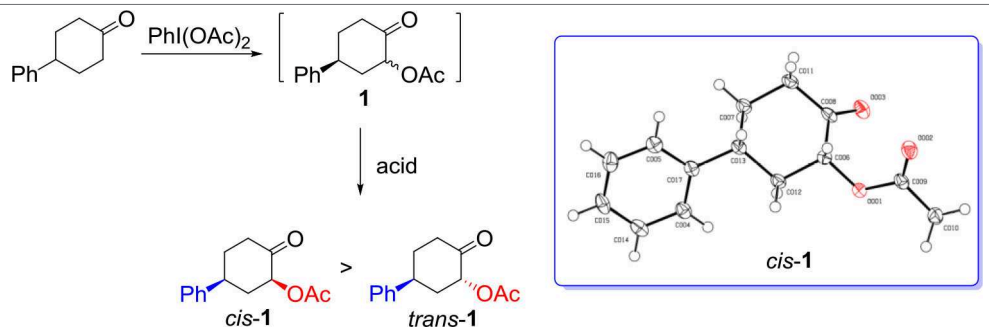

Entry	Solvent	Additive (equiv)	Condition (°C, h)	% yield of 1[b] (*cis*/*trans* ratio)
1	AcOH	—	RT, 24	Trace
2	AcOH	CF_3CO_2H (1)	RT, 24	17 (1.4:1)
3	AcOH	TfOH (1)	RT, 24	54 (12.2:1)
4	AcOH	AgOTf (1)	RT, 24	37 (2.1:1)
5	AcOH	$ZnCl_2$ (1)	RT, 24	0
6	AcOH	$AlCl_3$ (1)	RT, 24	0
7	AcOH	$Sc(OTf)_3$ (1)	RT, 24	42 (7.0:1)
8	AcOH	$Mg(OTf)_2$ (1)	RT, 24	52 (2.1:1)
9	AcOH	$Cu(OTf)_2$ (1)	RT, 24	60 (3.7:1)
10	AcOH	$Zn(OTf)_2$ (1)	RT, 24	68 (3.0:1)
11	AcOH	BF_3•OEt_2 (1)	RT, 24	70 (6.8:1)
12	AcOH	BF_3•OEt_2 (2)	RT, 24	73 (10.5:1)
13	AcOH	BF_3•OEt_2 (3)	RT, 24	67 (11.8:1)
14	AcOH	BF_3•OEt_2 (5)	RT, 24	71 (12.5:1)
15	AcOH	BF_3•OEt_2 (3)	RT, 12	69 (8.1:1)
16	AcOH	BF_3•OEt_2 (3)	RT, 6	71 (4.6:1)
17	AcOH	BF_3•OEt_2 (3)	RT, 2	68 (2.6:1)
18	AcOH	BF_3•OEt_2 (3)	RT, 48	68 (11.2:1)
19	AcOH	BF_3•OEt_2 (3)	50, 24	60 (10.9:1)
20	CH_2Cl_2	—	RT, 24	Trace
21	CH_2Cl_2	BF_3•OEt_2 (3)	RT, 24	23 (5.6:1)
22	CH_2Cl_2	BF_3•OEt_2 (3)/AcOH (10)	RT, 24	63 (9.3:1)
23	AcOEt	BF_3•OEt_2 (3)	RT, 24	48 (6.7:1)
24	AcOEt	BF_3•OEt_2 (3)/AcOH (10)	RT, 24	61 (8.2:1)
25	Et_2O	BF_3•OEt_2 (3)	RT, 24	28 (3.5:1)
26	Et_2O	BF_3•OEt_2 (3)/AcOH (10)	RT, 24	70 (4.7:1)
27	toluene	BF_3•OEt_2 (3)	RT, 24	18 (3.2:1)
28	toluene	BF_3•OEt_2 (3)/AcOH (10)	RT, 24	37 (8.2:1)
29	CH_3CN	BF_3•OEt_2 (3)	RT, 24	Trace
30	CH_3CN	BF_3•OEt_2 (3)/AcOH (10)	RT, 24	12 (>20:1)
31	CF_3CH_2OH	BF_3•OEt_2 (3)/AcOH (10)	RT, 24	37 (2.8:1)
32	$(CF_3)_2CHOH$	BF_3•OEt_2 (3)/AcOH (10)	RT, 24	44 (8.6:1)

[a]Reaction conditions: reaction of 4-phenylcyclohexanone (1 equiv) with $PhI(OAc)_2$ (1.5 equiv) and additives (1∼3 equiv or without) in the acetic acid solvent or other organic solvents at room temperature for 2∼48 h. [b]The yield and the cis/trans ratio were determined by NMR analysis.

It should be fundamentally interesting to understand the origin of the diastereoselectivity of the hypervalent iodine-mediated α-acetoxylation of cyclic ketones. With the assistance of Lewis acid BF_3•OEt, the keto-enol equilibrium would lead to the activated enol to react with hypervalent iodine $PhI(OAc)_2$. Generally, it is believed that an iodonium enolate (*O*-bound intermediate) or an α-iodanyl ketone (α-*C*-bound intermediate) could be formed for the subsequent

TABLE 2 | Substrate scope for diastereoselective α-acetoxylation of cyclic ketones with hypervalent iodine(III) reagents and BF_3•OEt_2[a].

Entry	Substrate	% yield (dr ratio)
	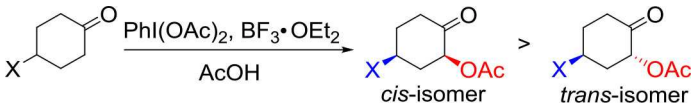	
1	X = Ph	*cis*-**1** 67 (11.8: 1)
2	X = *t*-Bu	*cis*-**2** 57 (11.1: 1)
3	X = –$SiMe_2Ph$	*cis*-**3** 36[b] (6.8: 1)
	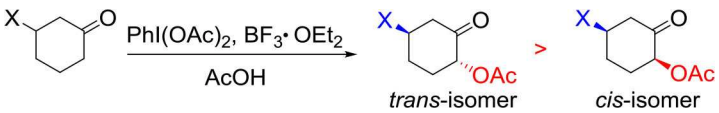	
4	X = Ph	*trans*-**4** 47 (6.1: 1)
5	X = *t*-Bu	*trans*-**5** 36 (12.3: 1)
	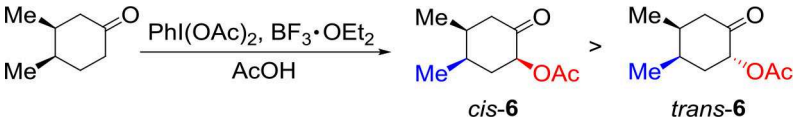	
6		*cis*-**6** 41[c] (> 20: 1)
	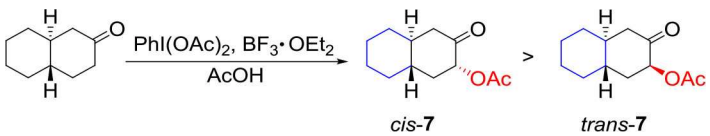	
7		*cis*-**7** 51 (9.9: 1)

[a]*Reaction conditions: reaction of cyclic ketone (1.0 equiv) with PhI(OAc)2 (1.5 equiv) and BF_3•Et_2O (3 equiv) in AcOH (1 mL) at room temperature for 24 h.* [b]*The result was obtained when the reaction time was 0.5 h.* [c]*The result was obtained when the reaction time was 3 h with 1.0 equiv BF_3•Et_2O. Standard reaction conditions provided 30% yield with dr > 20: 1.*

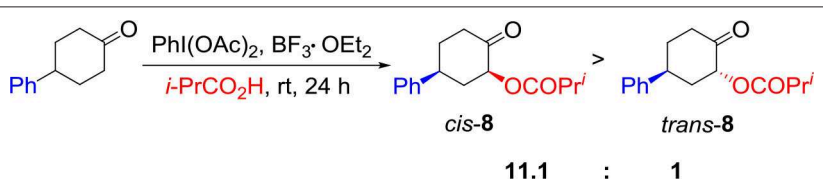

SCHEME 2 | Synthesis of 2-acyloxy-4-phenylcyclohexanone **8** by using the hypervalent iodine (III) reagent–BF_3•OEt_2 hybrid system.

α-acetoxylation. The *O*-bound hypervalent iodine intermediate can be traced back to Mizukami's proposal in their work in tosylation reactions in 1978. (Mizukami et al., 1978) The *C*-bound hypervalent iodine intermediate was first proposed by Moriarty et al. (1981). Accordingly, the possible mechanism for hypervalent iodine-mediated α-acetoxylation of cyclic ketones is proposed (**Scheme 3**). The *O*-bound intermediate would lead to the α-acetoxylation via the sigmatropic rearrangement pathway, while the *C*-bound intermediate will undergo an S_N2 substitution by the acetate in the solution to form α-acetoxylation product.

To further understand the diastereoselectivity α-acetoxylation of cyclic ketones, density functional theory (DFT) calculations were carried out with Gaussian 16 program. Frisch et al. (2016) Geometry optimizations and frequency calculations were carried out using the M06-2X functional (Zhao and Truhlar, 2007; Walker et al., 2013) in solution by the SMD continuum solvent model (solvent = acetic acid) (Marenich et al., 2009), with the basis sets of SDD (Andrae et al., 1991) for iodine atom and 6–311++G** for other atoms.

The calculated free energies of the hypervalent iodine intermediates **I** (*O*-bound) and **II** (*C*-bound) are depicted (**Scheme 4**). In the stable chair-conformer of 4-phenylcyclohexanone, different isomeric intermediates **I** ($\mathbf{I}_{transoidal}$, $\mathbf{I}_{cisoidal}$, and $\mathbf{I}_{vert}$) are calculated to be close in free energy, among which $\mathbf{I}_{cisoidal}$ is predicted to be the most stable one. In contrast, the *C*-bound intermediates **II** ($\mathbf{II}_{cisoidal}$ and

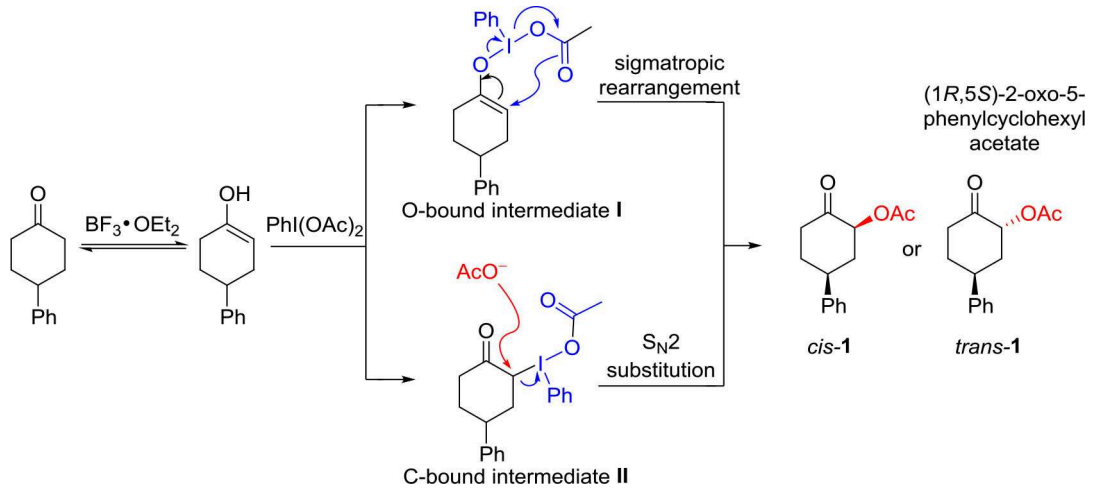

SCHEME 3 | The possible mechanism for the hypervalent iodine-mediated α-acetoxylation of cyclic ketones.

$\mathbf{II}_{vert}$) are much more thermodynamically stable than the *O*-bound ones (by 22.6 (7) kcal/mol) in acetic acid. DFT results interestingly revealed a case of preferred *C*-bound species for the interaction between hypervalent iodine with cyclo-enol, which is complementary to previous suggestions that the enolate-like *O*-bound intermediates were more likely to be formed in the reaction of non-cyclic ketones. Norrby et al. (2010), Beaulieu and Legault (2015), Shneider et al. (2015), Arava et al. (2017) This predicted preference of α-*C*-bound hypervalent iodine species is also interestingly supported by the experimentally observed structures of the isolable iodonium ylides (Ivanov et al., 2014).

Since the *O*-bound intermediate **I** is more than 22 kcal/mol higher than the *C*-bound intermediate **II** in free energy, the sigmatropic rearrangement reaction pathway should be unlikely to operate in this system. The α-acetoxylation of cyclic ketones should prefer the S_N2 substitution mechanism via the α-*C*-bound intermediate. This explains well the importance of acetic acid as solvent to facilitate the S_N2 substitution in our studied system (**Table 1**, entries 20–27).

Although the *C*-bound intermediates IIcisoidal and IIvert are close in free energy, the equatorial iodanyl group (IIcisoidal) is forbidden for S_N2 substitution. The axial iodanyl intermediate IIvert should play a key role in the diastereoselective α-acetoxylation of cyclic ketones. Relative free energies (in kcal/mol) of the isomers of α-*C*-bound intermediates IIvert are depicted (**Scheme 5**). The equatorial phenyl intermediate IIvert corresponds to the *cis* product for the S_N2 substitution, while the axial phenyl intermediate axial-IIvert leads to the *trans* product. IIvert is thermodynamically more stable than axial-IIvert by 2.2 kcal/mol, due to the steric effect of the axial phenyl on the chair conformation of the cyclic ketone. According to the Hammond–Leffler postulate, this implies the kinetic preference of the formation of the *cis* product from intermediate IIvert. Indeed, the calculated free energy of the transition state (*cis*-TS) for the *cis* pathway is lower than that (*trans*-TS) for the *trans* Pathway by 1.0 kcal/mol. The free energy of *cis*-TS is −12.0 kcal/mol and the activation free energy of the S_N2 step is only 10.7 kcal/mol, which further supports that the S_N2 substitution mechanism should be more plausible than the sigmatropic rearrangement mechanism via the *O*-bound intermediate. More importantly, our experimentally observed diastereoselective results strongly supported the influence of the thermodynamic control in selectivity. Extending the reaction time from 2 to 48 h, the *cis/trans* ratio increased from 2.6:1 to 11.2:1, with unchanged yield (**Table 1**, entries 15–18), when we performed a control experiment by subjecting the product 1 with low cis/trans ratio of 3.1:1 to the standard reaction condition for 24 h, a cis/trans ratio of 11.8:1 was observed. The equilibrium between the *cis/trans* products in acetic acid was observed, leading to the most table isomer as the major product. To further verify the thermodynamic control selectivity, we compared the relative free energy difference between *cis* product and *trans* product for representative substrates, i.e., 4-phenylcyclohexanone, 3-phenylcyclohexanone, and *cis*-3,4-dimethylcyclohexene, as shown in **Scheme 6**. The DFT-predicted free energy difference clearly demonstrated the thermodynamic control in selectivity, which is in good agreement with the experimentally observed diastereoselective ratio. The product *cis*-**1** is lower in free energy than *trans*-**1** by 1.9 kcal/mol, consistent with the experimentally observed *cis/trans* ratio of 11.2:1. When the phenyl substituent moves from the β position of the acetoxyl to the further γ position, the free energy difference decreases to 1.6 kcal/mol, in accordance with a slightly lower diastereoselective ratio of 6.1:1, and the inverse ratio of *trans/cis* is well-reproduced. With respect to *cis*-3,4-dimethylcyclohexene, DFT results suggest a free energy difference of 1.0 kcal/mol for the *cis/trans* products, in good agreement with the experimentally observed *cis/trans* ratio of 6.8:1 as well-indicating the β-substituent is predominant compared to the γ-position, probably due to the distance between the substituent and the acetoxyl group.

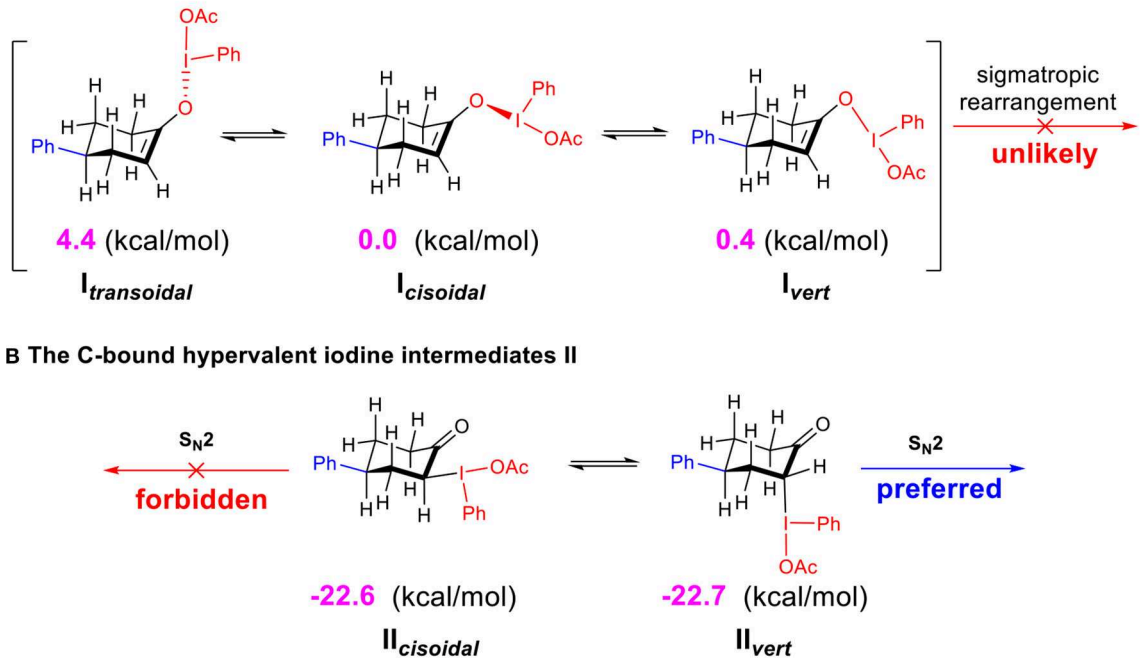

SCHEME 4 | Relative free energies (in kcal/mol) of the *O*-bound intermediates I and *C*-bound intermediates II calculated at the M06-2X/6311++G**&SDD(I)/SMD(solvent = acetic acid) level of theory. **(A)** The *O*-bound hypervalent iodine intermediates I. **(B)** The *C*-bound hypervalent iodine intermediates II.

CONCLUSION

In conclusion, we have developed a practical approach for diastereoselective α-acetoxylation of cyclic ketones by a binary hybrid system comprising a hypervalent iodine(III) reagent and BF_3•OEt_2 Lewis acid. In this hybrid system, BF_3•OEt_2 Lewis acid allowed the activation of the hypervalent iodine(III) reagent for the smooth α-acetoxylation reaction of cyclic ketones and also for achieving high diastereoselectivity. The substrate scoping investigation showed that sterically hindered substituent groups on cyclic ketones are favorable for the diastereoselectivity. Cyclic ketone substrates bearing the mono-substituent group at C3 or C4 position, and substrates bearing *di*-substituent groups at C3 and C4 positions demonstrated good to high diastereoselectivity. This approach was successfully applied to the synthesis of other *cis*-substituted 2-acyloxycyclohexanones in moderate yield with high diastereoselectivity. Computational studies showed that this α-acetoxylation of cyclic ketone reaction plausibly undergoes an S_N2 substitution mechanism, in which the α-*C*-bound hypervalent iodine species is the important intermediate. The diastereoselectivity of the reaction mainly originated from the thermodynamic control. This hypervalent iodine(III) reagent–BF_3•OEt_2 hybrid system can thus be applied to certain selective organic reactions and the efficient diastereoselective synthesis of cyclic ketone derivatives or other related biologically active compounds.

MATERIALS AND METHODS

General

^{1}H NMR and ^{13}C NMR spectra were recorded on a Bruker AVANCE III 400 MHz spectrometer [400 MHz for ^{1}H NMR, 100 MHz for ^{13}C NMR]. Tetramethylsilane (TMS) was used as an internal standard (0 ppm) for the ^{1}H NMR spectra, and $CDCl_3$ was used as the internal standard (77.0 ppm) for the ^{13}C NMR spectra. High-resolution mass spectra (HRMS) were recorded on a Thermo MAT95XP or on an Agilent 6540 UHD Accurate-Mass Q-TOF LC-MS spectrometer. Infrared (IR) spectra were obtained on a Thermo Scientific Nicolet FT/IR-6700 spectrometer. Reactions were monitored by thin-layer chromatography (TLC). Reaction products were purified by column chromatography on silica gel. AcOH was dried before use. Other chemical reagents were purchased from common commercial suppliers and used as received.

General procedures for the α-acetoxylation of cyclic ketones: To a solution of cyclic ketones (0.5 mmol) and $PhI(OAc)_2$ (241.5 mg, 0.75 mmol) in acetic acid (1 mL) was added BF_3•OEt_2 (212.9 mg, 1.5 mmol) dropwise, and the reaction mixture was stirred at room temperature for 24 h. The reaction progress was monitored by TLC. Upon completion, the reaction mixture was quenched with saturated aqueous $Na_2S_2O_3$ and then saturated aqueous $NaHCO_3$, washed with brine, extracted with dichloromethane, and dried over anhydrous Na_2SO_4. After filtration, the solvent was removed under reduced pressure to

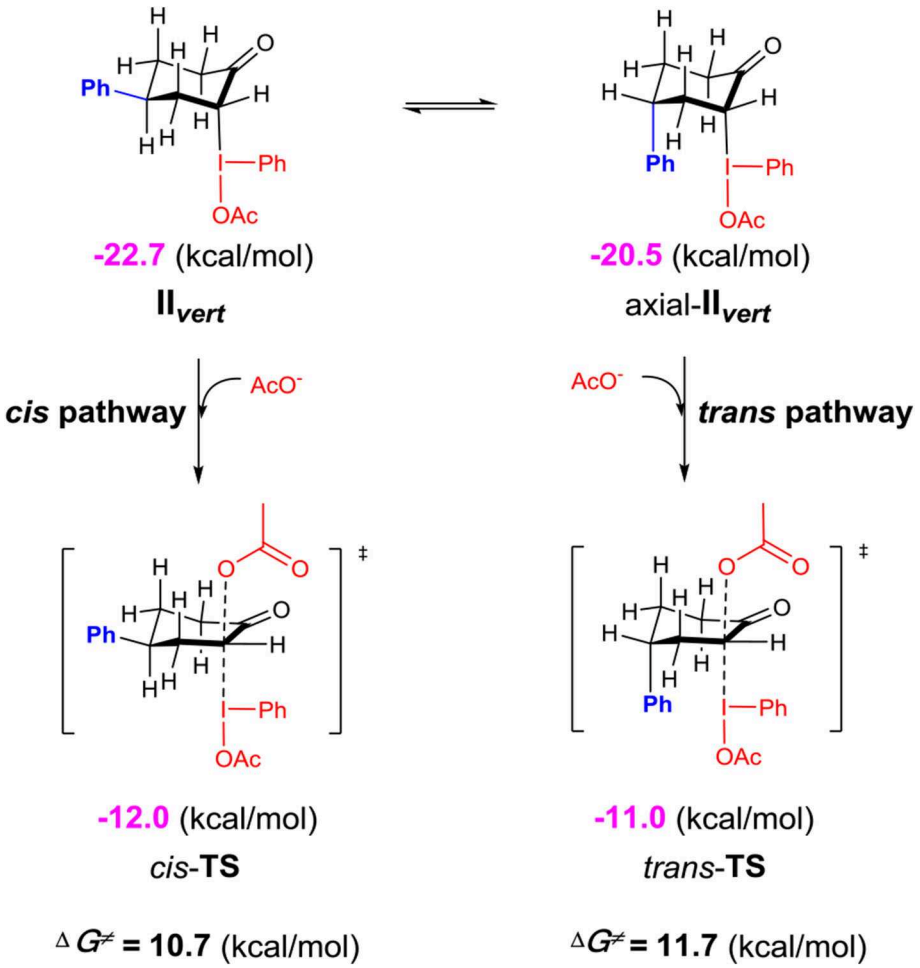

SCHEME 5 | Relative free energies (in kcal/mol) of the isomers of α-*C*-bound intermediates II_{vert} calculated at the M06-2X/6311++G**&SDD(I)/SMD(solvent = acetic acid) level of theory.

afford the crude product, which was purified by silica gel column chromatography using hexane/acetone and analyzed by ^{1}H and ^{13}C NMR spectroscopy.

2-Oxo-5-Phenylcyclohexyl Acetate (1)

The crude product was purified via flash chromatography, eluting with hexane/acetone = 30/1 to give a white solid (77.8 mg, 67%). Characterization of the major product (*cis*-isomer): Mp: 90–92°C; ^{1}H NMR (400 MHz, $CDCl_3$): δ = 7.35–7.23 (m, 5H), 5.38 (dd, J = 12.8, 6.4 Hz, 1H), 3.23 (t, J = 12.4 Hz, 1H), 2.62–2.59 (m, 2H), 2.49–2.44 (m, 1H), 2.27–2.24 (m, 1H), 2.17 (s, 3H), 2.08 (q, J = 12.4 Hz, 1H), 1.96–1.85 (m, 1H); ^{13}C NMR (100 MHz, $CDCl_3$): δ = 204.0, 170.1, 143.2, 128.9, 127.1, 126.8, 75.8, 42.1, 40.0, 39.9, 34.5, 20.8; IR (KBr): 3,081, 3,021, 2,938, 2,875, 2,854, 1,757, 1,718, 1,641, 1,492, 1,445, 1,423, 1,385, 1,370, 1,324, 1,287, 1,263, 1,245, 1,150, 1,120, 1,072, 1,061, 982, 935, 911, 852, 756, 743, 695, 610, 517, 466 cm^{-1}; HRMS (ESI) calcd for $C_{14}H_{17}O_3$ $[M+H]^+$: 233.1178; found: 233.1168; calcd for $C_{14}H_{16}O_3Na$ $[M+Na]^+$: 255.0997; found: 255.0987.

5-(tert-Butyl)-2-Oxocyclohexyl Acetate (2)

The crude product was purified via flash chromatography, eluting with hexane/acetone = 30/1 to give a colorless oil (60.5 mg, 57%). Characterization of the major product (*cis*-isomer): ^{1}H NMR (400 MHz, $CDCl_3$): δ = 5.23–5.18 (m, 1H), 2.52–2.47 (m, 1H), 2.43–2.34 (m, 1H), 2.33–2.27 (m, 1H), 2.15 (s, 3H), 2.13–2.07 (m, 1H), 1.74–1.66 (m, 1H), 1.57 (q, J = 12.4 Hz, 1H), 1.48–1.37 (m, 1H), 0.93 (s, 9H); ^{13}C NMR (100 MHz, $CDCl_3$): δ = 205.0, 170.2, 76.3, 46.0, 39.7, 34.4, 32.6, 28.2, 27.7, 20.9.

5-(Dimethyl(Phenyl)Silyl)-2-Oxocyclohexyl Acetate (3)

The crude product was purified via flash chromatography, eluting with hexane/acetone = 30/1 to give a light yellow solid (52.3 mg, 36%). Characterization of the major product (*cis*-isomer): Mp: 121–123°C; ^{1}H NMR (400 MHz, $CDCl_3$): δ = 7.49–7.37 (m, 5H), 5.15 (dd, J = 12.4, 6.4 Hz, 1 H), 2.53–2.50 (m, 1H), 2.43–2.35 (m, 1H), 2.27–2.23 (m, 1H), 2.13 (s, 3H), 2.09–2.04 (m, 1H), 1.61 (q, J = 12.8 Hz, 1H), 1.53–1.42 (m, 1H), 1.38–1.32 (m, 1H), 0.33 (s, 6H); ^{13}C NMR (100 MHz, $CDCl_3$): δ = 204.9, 170.2, 136.5, 133.9, 129.9, 129.6, 128.1, 77.7, 42.5, 34.7, 28.9, 24.1, 20.9, −4.9, −5.0;

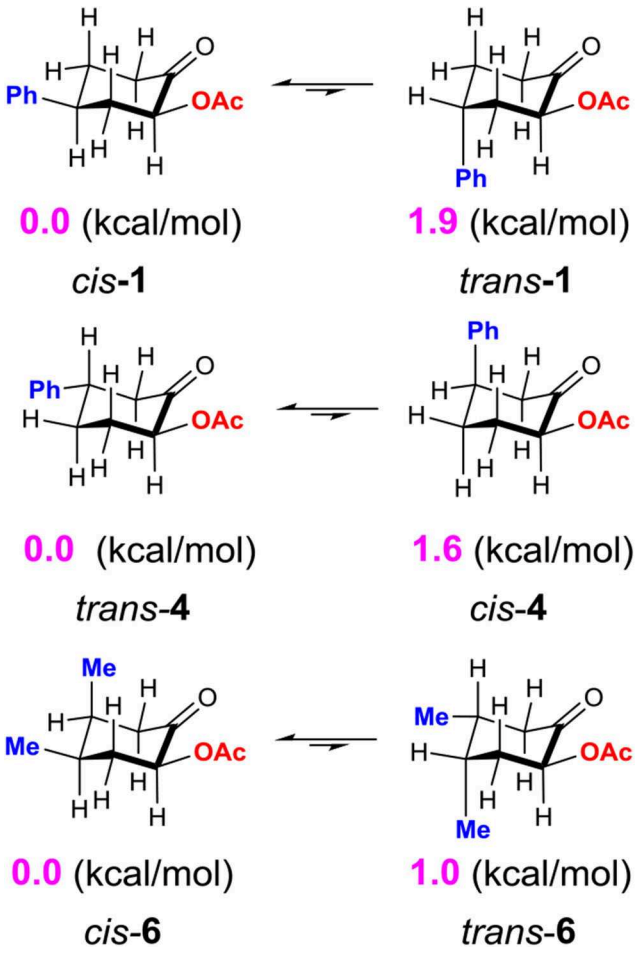

SCHEME 6 | Relative free energy difference (in kcal/mol) between *cis* product and *trans* product for representative cyclic ketones, calculated at the M06-2X/6311++G**/SMD (solvent = acetic acid) level of theory.

IR (KBr): 3,071, 3,012, 2,949, 2,935, 2,865, 2,841, 1,748, 1,721, 1,427, 1,407, 1,376, 1,342, 1,321, 1,257, 1,233, 1,173, 1,143, 1,112, 1,102, 1,082, 1,050, 968, 912, 885, 850, 834, 821, 776, 763, 742, 728, 704, 661, 643, 605, 570, 482, 451, 436 cm^{-1}; HRMS (ESI) calcd for $C_{16}H_{23}O_3Si$ $[M+H]^+$: 291.1416; found: 291.1420; calcd for $C_{16}H_{22}O_3Na$ $[M+Na]^+$: 313.1236; found: 313.1227.

2-Oxo-4-Phenylcyclohexyl Acetate (4)

The crude product was purified via flash chromatography, eluting with hexane/acetone = 30/1 to give a white solid (54.6 mg, 47%). Characterization of the major product (*trans*-isomer): Mp: 72–74°C; ^1H NMR (400 MHz, $CDCl_3$): δ = 7.35–7.31 (m, 2H), 7.25–7.20 (m, 3H), 5.29 (dd, J = 12.8, 6.4 Hz, 1H), 3.02–2.94 (m, 1H), 2.70–2.62 (m, 2H), 2.40–2.35 (m, 1H), 2.18 (s, 3H), 2.14 (m, 1H), 2.09–1.98 (m, 1H), 1.95–1.84 (m, 1H); ^{13}C NMR (100 MHz, $CDCl_3$): δ = 203.4, 170.3, 143.2, 129.0, 127.2, 126.6, 76.3, 47.9, 45.4, 31.8, 31.7, 20.9; IR (KBr): 3,033, 2,959, 2,941, 2,908, 1,745, 1,721, 1,602, 1,501, 1,458, 1,432, 1,376, 1,319, 1,281, 1,233, 1,174, 1,081, 1,046, 897, 763, 703, 665, 599, 531, 501 cm^{-1}; HRMS (ESI) calcd for $C_{14}H_{17}O_3$ $[M+H]^+$: 233.1178; found: 233.1145; calcd for $C_{14}H_{16}O_3Na$ $[M+Na]^+$: 255.0997; found: 255.0986.

4-(Tert-Butyl)-2-Oxocyclohexyl Acetate (5)

The crude product was purified via flash chromatography, eluting with hexane/acetone = 30/1 to give a light yellow oil (38.2 mg, 36%). Characterization of the major product (*trans*-isomer): ^1H NMR (400 MHz, $CDCl_3$): δ = 5.15 (dd, J = 12.8, 6.8 Hz, 1H), 2.56–2.53 (m, 1H), 2.33–2.27 (m, 1H), 2.22–2.13 (m, 1H), 2.16 (s, 3H), 2.03–2.00 (m, 1H), 1.73–1.63 (m, 1H), 1.56–1.51 (m, 2H), 0.91 (s, 9H); ^{13}C NMR (100 MHz, $CDCl_3$): δ = 205.3, 170.3, 76.6, 50.0, 42.4, 32.9, 31.7, 27.4, 25.0, 20.9.

4,5-Dimethyl-2-Oxocyclohexyl Acetate (6)

The crude product was purified via flash chromatography, eluting with hexane/acetone = 30/1 to give a light yellow oil (37.8 mg, 41%). Characterization of the major isomer: ^1H NMR (400 MHz, $CDCl_3$): δ = 5.19 (dd, J = 12.4, 6.8 Hz, 1H), 2.67–2.62 (m, 1H), 2.35–2.21 (m, 3H), 2.14 (s, 3H), 2.07–2.03 (m, 1H), 1.74 (q, J = 12.8 Hz, 1H), 1.01 (d, J = 6.8 Hz, 3H), 0.83 (d, J = 6.8 Hz, 3H); ^{13}C NMR (100 MHz, $CDCl_3$): δ = 204.6, 170.1, 75.6, 47.3, 36.5, 34.9, 33.2, 20.8, 18.5, 12.1; IR (KBr): 2,959, 2,928, 2,891, 2,871, 1,749, 1,721, 1,470, 1,455, 1,431, 1,380, 1,370, 1,243, 1,175, 1,102, 1,087, 1,075, 1,036, 975, 941, 885, 790, 715, 651, 609, 549, 510, 482, 436 cm^{-1}; HRMS (ESI) calcd for $C_{10}H_{16}O_3Na$ $[M+Na]^+$: 207.0997; found: 207.0988.

3-Oxodecahydronaphthalen-2-yl Acetate (7)

The crude product was purified via flash chromatography, eluting with hexane/acetone = 30/1 to give a light yellow solid (53.6 mg, 51%). Characterization of the major isomer: ^1H NMR (400 MHz, $CDCl_3$): δ = 5.19 (dd, J = 12.0, 6.8 Hz, 1H), 2.41–2.37 (m, 1H), 2.20–2.10 (m, 2H), 2.13 (s, 3H), 1.78–1.68 (m, 4H), 1.56–1.46 (m, 2H), 1.36–0.99 (m, 5H); ^{13}C NMR (100 MHz, $CDCl_3$): δ = 204.0, 170.2, 76.1, 47.2, 43.8, 40.5, 39.4, 33.7, 32.5, 25.8, 25.5, 20.8.

2-Oxo-5-Phenylcyclohexyl Isobutyrate (8)

The crude product was purified via flash chromatography, eluting with hexane/acetone = 30/1 to give a white solid (65.1 mg, 50%). Characterization of the major isomer: Mp: 63–65°C; ^1H NMR (400 MHz, $CDCl_3$): δ = 7.38–7.34 (m, 2H), 7.29–7.26 (m, 3H), 5.41(dd, J = 12.8, 6.0 Hz, 1H), 3.26 (t, J = 12.8 Hz, 1H), 2.71–2.62 (m, 3H), 2.51–2.46 (m, 1H), 2.30–2.26 (m, 1H), 2.11 (q, J = 12.8 Hz, 1H), 2.00–1.89 (m, 1H); 1.28 (d, J = 6.8 Hz, 3H), 1.23 (d, J = 6.8 Hz, 3H); ^{13}C NMR (100 MHz, $CDCl_3$): δ = 204.1, 176.4, 143.3, 128.9, 127.1, 126.8, 75.4, 42.1, 40.0, 39.9, 34.5, 34.0, 19.2, 19.1; IR (KBr): 3,030, 2,977, 2,929, 2,866, 1,751, 1,727, 1,632, 1,605, 1,498, 1,462, 1,429, 1,385, 1,349, 1,293, 1,260, 1,200, 1,165, 1,147, 1,117, 1,069, 977, 918, 843, 763, 739, 701, 596, 540, 507 cm^{-1}; HRMS (ESI) calcd for $C_{16}H_{20}O_3Na$ $[M+Na]^+$: 283.1310; found: 283.1299.

DATA AVAILABILITY STATEMENT

The datasets presented in this study can be found in online repositories. The names of the repository/repositories and accession number(s) can be found below: Cambridge Crystallographic Data Centre (CCDC-1997827).

AUTHOR CONTRIBUTIONS

JT, WZ, and WX were responsible for designing and performing the experiments. YJ and ZK were responsible for DPT calculation. YL and KM directed the project and wrote the manuscript.

FUNDING

This research was supported by the NSFC (21977019, 21502023), the Guangdong Provincial Key Research and Development Program (2019B020201005), and the Open Project of Guangdong Provincial Key Laboratory of New Drug Screening (GDKLNDS-2018OF004).

SUPPLEMENTARY MATERIAL

The Supplementary Material for this article can be found online at: https://www.frontiersin.org/articles/10.3389/fchem.2020.00467/full#supplementary-material

REFERENCES

Ahmed, Z., and Langer, P. (2006). Synthesis of functionalized 4-chlorophenols and 1,4-dihydroquinones by 3+3 cyclization of 1,3-bis-silyl enol ethers with 2-chloro- and 2-acyloxy-3-(silyloxy)alk-2-en-1-ones. *Tetrahedron Lett.* 47, 417–419. doi: 10.1016/j.tetlet.2005.11.077

Andrae, D., Häußermann, U., Dolg, M., Stoll, H., and Preu,ß, H. (1991). Energy-adjusted ab initio pseudopotentials for the second- and third-row transition elements. *Theor. Chim. Acta* 1991, 78, 247–266. doi: 10.1007/BF01112848

Arava, S., Kumar, J. N., Maksymenko, S., Iron, M. A., Parida, K. N., Fristrup, P., et al. (2017). Enolonium species-umpoled enolates. *Angew. Chem. Int. Ed.* 56, 2599–2603. doi: 10.1002/anie.201610274

Beaulieu, S., and Legault, C. Y. (2015). Mechanistic insights on the iodine(III)-mediated α-Oxidation of Ketones. *Chem. Eur. J.* 21, 11206–11211. doi: 10.1002/chem.201501177

Bogevig, A., Sunden, H., and Cordova, A. (2004). Direct catalytic enantioselective alpha-aminoxylation of ketones: a stereoselective synthesis of alpha-hydroxy and alpha,alpha'-dihydroxy ketones. *Angew. Chem. Int. Ed.* 43, 1109–1112. doi: 10.1002/anie.200353018

Carneiro, P. F., Gutmann, B., de Souza, R. O. M. A., and Kappe, C. O. (2015). Process intensified flow synthesis of 1H-4-substituted imidazoles: toward the continuous production of daclatasvir. *Acs Sust. Chem. Eng.* 3, 3445–3453. doi: 10.1021/acssuschemeng.5b01191

Chen, C., Liu, W. B., Zhou, P., and Liu, H. L. (2017). I-2/TBHP-mediated oxidative coupling of ketones and toluene derivatives: a facile method for the preparation of alpha-benzoyloxy ketones. *RSC Adv.* 7, 20394–20397. doi: 10.1039/C7RA02298K

Chen, J. Z., Liu, D. L., Butt, N., Li, C., Fan, D. Y., Liu, Y. G., et al. (2013). Palladium-catalyzed asymmetric hydrogenation of alpha-acyloxy-1-arylethanones. *Angew. Chem. Int. Ed.* 52, 11632–11636. doi: 10.1002/anie.201306231

Chen, J. Z., Zhang, Z. F., Liu, D. L., and Zhang, W. B. (2016). Palladium-catalyzed chemo- and enantioselective C-O bond cleavage of alpha-acyloxy ketones by hydrogenolysis. *Angew. Chem. Int. Ed.* 55, 8444–8447. doi: 10.1002/anie.201603590

Corey, E. J., and Knapp, S. (1976). α-functionalization of ketones via N, N-dimethylhydrazones. *Tetrahedron Lett.* 17, 4687–4690. doi: 10.1016/S0040-4039(00)92996-4

Du, J., Zhang, X., Sun, X., and Wang, L. (2015). Copper-catalyzed direct alpha-ketoesterification of propiophenones with acetophenones via C(sp(3))-H oxidative cross-coupling. *Chem Commun.* 51, 4372–4375. doi: 10.1039/C4CC09524C

Edwards, M. G., Kenworthy, M. N., Kitson, R. R. A., Scott, M. S., and Taylor, R. J. K. (2008). The telescoped intramolecular Michael/olefination (TIMO) approach to alpha-alkylidene-gamma-butyrolactones: synthesis of (+)-paeonilactone B. *Angew. Chem. Int. Ed.* 47, 1935–1937. doi: 10.1002/anie.200705329

El-Qisairi, A. K., and Qaseer, H. A. (2002). Oxidation of ketone by palladium(II). α-Hydroxyketone synthesis catalyzed by a bimetallic palladium(II) complex. *J. Organomet. Chem.* 659, 50–55. doi: 10.1016/S0022-328X(02)01691-1

Erickson, J. L. E., Dechary, J. M., and Kesling, M. R. (1951). Diazoketones as reagents for the identification of organic acids. *J. Am. Chem. Soc.* 73, 5301–5302. doi: 10.1021/ja01155a086

Frisch, M. J., Trucks, G. W., Schlegel, H. B., Scuseria, G. E., Robb, M. A., Cheeseman, J. R., et al. (2016). *Gaussian 16 Revision A.03*. Wallingford, CT: Gaussian, Inc.

Hamed, O. A., El-Qisairi, A., Qaseer, H., Hamed, E. M., Henry, P. M., and Becker, D. P. (2012). Asymmetric α-hydroxy ketone synthesis by direct ketone oxidation using a bimetallic palladium(II) complex. *Tetrahedron Lett.* 53, 2699–2701. doi: 10.1016/j.tetlet.2012.03.066

Hecker, S. J., and Werner, K. M. (1993). Total synthesis of (+/-)-leuhistin. *J. Org. Chem.* 58, 1762–1765. doi: 10.1021/jo00059a028

Heiba, E.-A. I., and Dessau, R. M. (1971). Oxidation by metal salts. VII. Syntheses based on the selective oxidation of organic free radicals. *J. Am. Chem. Soc.* 93, 524–527. doi: 10.1021/ja00731a042

Hu, X. W., Chen, X., Shao, Y. X., Xie, H. S., Deng, Y. F., Ke, Z. F., et al. (2018). Co(III)-catalyzed coupling-cyclization of aryl C-H bonds with alpha-diazoketones involving wolff rearrangement. *ACS Catal.* 8, 1308–1312. doi: 10.1021/acscatal.7b03668

Huang, G., Sheng, J., Li, X., Tang, M., and Gao, B. (2007). An efficient method for the α-acetoxylation of ketones. *Synthesis* 2007, 1165–1168. doi: 10.1055/s-2007-965984

Huang, X., Zhang, Y. G., Zhang, C. S., Zhang, L., Xu, Y., Kong, L. C., et al. (2019). The ortho-difluoroalkylation of aryliodanes with enol silyl ethers: rearrangement enabled by a fluorine effect. *Angew. Chem. Int. Ed.* 58, 5956–5961. doi: 10.1002/anie.201900745

Ivanov, A. S., Popov, I. A., Boldyrev, A. I., and Zhdankin, V. V. (2014). The I=X (X=O, N, C) double bond in hypervalent iodine compounds: is it real?. *Angew. Chem. Int. Ed.* 53, 9617–9621. doi: 10.1002/anie.201405142

Izquierdo, S., Essafi, S., Del Rosal, I., Vidossich, P., Pleixats, R., Vallribera, A., et al. (2016). Acid activation in phenyliodine dicarboxylates: direct observation, structures, and implications. *J. Am. Chem. Soc.* 138, 12747–12750. doi: 10.1021/jacs.6b07999

Kaila, N., Janz, K., DeBernardo, S., Bedard, P. W., Camphausen, R. T., Tam, S., et al. (2007). Synthesis and biological evaluation of quinoline salicylic acids as P-selectin antagonists. *J. Med. Chem.* 50, 21–39. doi: 10.1021/jm0602256

Kitamura, M., Kisanuki, M., and Okauchi, T. (2012). Synthesis of 1,2-naphthalenediol diacetates by rhodium(II)-catalyzed reaction of 1,2-diazonaphthoquinones with acetic anhydride. *Eur. J. Org. Chem.* 2012, 905–907. doi: 10.1002/ejoc.201101698

Littler, J. S. (1962). 156. The mechanisms of oxidation of cyclohexanone under acid conditions. Part I. Two-electron oxidants. *J. Chem. Soc.* 827–832. doi: 10.1039/jr9620000827

Liu, L., Feng, S. L., and Li, C. B. (2016). Practical approach for quantitative green esterifications. *ACS Sust. Chem. Eng.* 4, 6754–6762. doi: 10.1021/acssuschemeng.6b01718

Liu, Y., Huang, D., Huang, J., and Maruoka, K. (2017). Hypervalent iodine mediated chemoselective iodination of alkynes. *J. Org. Chem.* 82, 11865–11871. doi: 10.1021/acs.joc.7b01555

Marenich, A. V., Cramer, C. J., and Truhlar, D. G. (2009). Universal solvation model based on solute electron density and on a continuum model of the solvent defined by the bulk dielectric constant and atomic surface tensions. *J. Phys. Chem. B.* 113, 6378–6396. doi: 10.1021/jp810292n

Mizukami, F., Ando, M., Tanaka, T., and Imamura, J. (1978). The acetoxylation ofp-substituted acetophenones and β-diketones with (diacetoxyiodo)benzene. *Bull. Chem. Soc. Jpn.* 51, 335–336. doi: 10.1246/bcsj.51.335

Moriarty, R. M., Hu, H., and Gupta, S. C. (1981). Direct α-hydroxylation of ketones using iodosobenzene. *Tetrahedron Lett.* 22, 1283–1286. doi: 10.1016/S0040-4039(01)90297-7

Newman, M. S., and Beal, P. F. (1950). A new synthesis of α-alkoxy ketones1. *J. Am. Chem. Soc.* 72, 5161–5163. doi: 10.1021/ja01167a100

Ng, F. T. T., and Henry, P. M. (1976). Kinetics and mechanism of the outer-sphere oxidation of cyclohexanone by tris(polypyridyl) complexes of iron(III) and ruthenium(III). *J. Am. Chem. Soc.* 98, 3606–3611. doi: 10.1021/ja00428a036

Nicolaou, K. C., Montagnon, T., Ulven, T., Baran, P. S., Zhong, Y. L., and Sarabia, F. (2002). Novel chemistry of alpha-tosyloxy ketones: applications to the solution- and solid-phase synthesis of privileged heterocycle and enediyne libraries. *J. Am. Chem. Soc.* 124, 5718–5728. doi: 10.1021/ja012146j

Nolla-Saltiel, R., Alonso Carrillo-Arcos, U., and Porcel, S. (2014). Silver acetate mediated acetoxylations of alkyl halides. *Synth. Stuttgart* 46, 165–169. doi: 10.1055/s-0033-1338551

Norrby, P. O., Petersen, T. B., Bielawski, M., and Olofsson, B. (2010). α-arylation by rearrangement: on the reaction of enolates with diaryliodonium salts. *Chem. Eur. J.* 16, 8251–8254. doi: 10.1002/chem.201001110

Ochiai, M., Takeuchi, Y., Katayama, T., Sueda, T., and Miyamoto, K. (2005). Iodobenzene-catalyzed alpha-acetoxylation of ketones. *in situ* generation of hypervalent (diacyloxyiodo)benzenes using m-chloroperbenzoic acid. *J. Am. Chem. Soc.* 127, 12244–12245. doi: 10.1021/ja0542800

Pogaku, N., Krishna, P. R., and Prapurna, Y. L. (2019). Iodine-mediated nucleophilic direct oxidative α-acetoxylation and α-alkoxylation of ketones. *ChemistrySelect* 4, 12333–12336. doi: 10.1002/slct.201903028

Ren, S. C., Song, S. J., Ye, L., Feng, C., and Loh, T. P. (2016). Copper-catalyzed oxyamination of electron-deficient alkenes with N-acyloxyamines. *Chem. Commun.* 52, 10373–10376. doi: 10.1039/C6CC04638J

Richter, M. J. R., Schneider, M., Brandstatter, M., Krautwald, S., and Carreira, E. M. (2018). Total synthesis of (-)-mitrephorone A. *J. Am. Chem. Soc.* 140, 16704–16710. doi: 10.1021/jacs.8b09685

Rubottom, G. M., Gruber, J. M., Marrero, R., Juve, H. D., and Kim, C. W. (1983). Oxidation of alkyl trimethylsilyl ketene acetals with lead(IV) carboxylates. *J. Org. Chem.* 48, 4940–4944. doi: 10.1021/jo00173a031

Sakamoto, R., Hirama, N., and Maruoka, K. (2018). The radical acylarylation of N-arylacrylamides with aliphatic aldehydes using the photolysis of hypervalent iodine(iii) reagents. *Org. Biomol. Chem.* 16, 5412–5415. doi: 10.1039/C8OB01420E

Sakamoto, R., Inada, T., Selvakumar, S., Moteki, S. A., and Maruoka, K. (2016). Efficient photolytic C-H bond functionalization of alkylbenzene with hypervalent iodine(III) reagent. *Chem. Commun.* 52, 3758–3761. doi: 10.1039/C5CC07647A

Sakamoto, R., Kashiwagi, H., and Maruoka, K. (2017). The direct C-H difluoromethylation of heteroarenes based on the photolysis of hypervalent iodine(III) reagents that contain difluoroacetoxy ligands. *Org. Lett.* 19, 5126–5129. doi: 10.1021/acs.orglett.7b02416

Selvakumar, S., Kang, Q. K. Arumugam, N., Almansour, A. I, Kumar, R. S. Maruoka, K. (2017). Hypervalent iodine(III) catalyzed radical hydroacylation of chiral alkylidenemalonates with aliphatic aldehydes under photolysis. *Tetrahedron Lett.* 73, 5841–5846. doi: 10.1016/j.tet.2017.08.018

Shneider, O. S., Pisarevsky, E., Fristrup, P., and Szpilman, A. M. (2015). Oxidative Umpolung α-Alkylation of Ketones. *Org. Lett.* 17, 282–285. doi: 10.1021/ol503384c

Shu, S., Li, Y., Jiang, J., Ke, Z., and Liu, Y. (2019). Mechanism of hypervalent iodine promoted fluorocyclization of unsaturated alcohols: metathesis via double acids activation. *J. Org. Chem.* 84, 458–462. doi: 10.1021/acs.joc.8b02741

Sunden, H., Engqvist, M., Casas, J., Ibrahem, I., and Cordova, A. (2004). Direct amino acid catalyzed asymmetric alpha oxidation of ketones with molecular oxygen. *Angew. Chem. Int. Ed.* 43, 6532–6535. doi: 10.1002/anie.200460295

Tan, F., Liu, X. H., Hao, X. Y., Tang, Y., Lin, L. L., and Feng, X. M. (2016). Asymmetric catalytic insertion of alpha-diazo carbonyl compounds into O-H bonds of carboxylic acids. *ACS Catal.* 6, 6930–6934. doi: 10.1021/acscatal.6b02184

Tan, L., Chen, C., and Liu, W. (2017). alpha-acetoxyarone synthesis via iodine-catalyzed and tert-butyl hydroperoxide-mediateded self-intermolecular oxidative coupling of aryl ketones. *Beilstein J. Org. Chem.* 13, 1079–1084. doi: 10.3762/bjoc.13.107

Tanner, D. D., Chen, J. J., Chen, L., and Luelo, C. (1991). Fragmentation of substituted acetophenones and halobenzophenone ketyls. Calibration of a mechanistic probe. *J. Am. Chem. Soc.* 113, 8074–8081. doi: 10.1021/ja00021a038

Valgimigli, L., Brigati, G., Pedulli, G. F., DiLabio, G. A., Mastragostino, M., Arbizzani, C., et al. (2003). The effect of ring nitrogen atoms on the homolytic reactivity of phenolic compounds: understanding the radical-scavenging ability of 5-pyrimidinols. *Chem.Eur. J.* 9, 4997–5010. doi: 10.1002/chem.200304960

Varma, R. S., Kumar, D., and Liesen, P. J. (1998). Solid state synthesis of 2-aroylbenzo b furans, 1,3-thiazoles and 3-aryl-5,6-dihydroimidazo 2,1-b 1,3 thiazoles from alpha-tosyloxyketones using microwave irradiation. *J. Chem. Soc. Perkin Trans.* 1, 4093–4096. doi: 10.1039/a807563h

Walker, M., Harvey, A. J., Sen, A., and Dessent, C. E. (2013). Performance of M06, M06-2X, and M06-HF density functionals for conformationally flexible anionic clusters: M06 functionals perform better than B3LYP for a model system with dispersion and ionic hydrogen-bonding interactions. *J. Phys. Chem. A.* 117, 12590–12600. doi: 10.1021/jp408166m

Wang, Z. K., Bi, X. H., Liang, Y. J., Liao, P. Q., and Dong, D. W. (2014). A copper-catalyzed formal O-H insertion reaction of alpha-diazo-1,3-dicarbonyl compounds to carboxylic acids with the assistance of isocyanide. *Chem. Commun.* 50, 3976–3978. doi: 10.1039/C4CC00402G

Yu, J., Tian, J., and Zhang, C. (2010). Various α-oxygen functionalizations of β-dicarbonyl compounds mediated by the hypervalent iodine(III) reagentp-iodotoluene difluoride with different oxygen-containing nucleophiles. *Adv. Synth. Catal.* 352, 531–546. doi: 10.1002/adsc.200900737

Yuan, W. K., Zhu, M. H., Geng, R. S., Ren, G. Y., Zhang, L. B., Wen, L. R., et al. (2019). Construction of benzofuran-3(2H)-one scaffolds with a quaternary center via Rh/Co relay catalyzed C-H functionalization/annulation of N-aryloxyacetamides and propiolic acids. *Org. Lett.* 21, 1654–1658. doi: 10.1021/acs.orglett.9b00181

Yuan, W. M., Eriksson, L., and Szabo, K. J. (2016). Rhodium-catalyzed geminal oxyfluorination and oxytrifluoro-methylation of diazocarbonyl compounds. *Angew. Chem. Int. Ed.* 55, 8410–8415. doi: 10.1002/anie.201602137

Zhang, T. S., Hao, W. J., Wang, N. N., Li, G. G., Jiang, D. F., Tu, S. J., et al. (2016). Catalytic oxidative carbene coupling of alpha-diazo carbonyls for the synthesis of beta-amino ketones via C(sp(3))-H functionalization. *Org. Lett.* 18, 3078–3081. doi: 10.1021/acs.orglett.6b01189

Zhao, Y., and Truhlar, D. G. (2007). The M06 suite of density functionals for main group thermochemistry, thermochemical kinetics, noncovalent interactions, excited states, and transition elements: two new functionals and systematic testing of four M06-class functionals and 12 other functionals. *Theor. Chem. Acc.* 120, 215–241. doi: 10.1007/s00214-007-0310-x

Conflict of Interest: The authors declare that the research was conducted in the absence of any commercial or financial relationships that could be construed as a potential conflict of interest.

frontiers in Chemistry

MINI REVIEW
published: 03 August 2020
doi: 10.3389/fchem.2020.00582

The C3-H Bond Functionalization of Quinoxalin-2(1*H*)-Ones With Hypervalent Iodine(III) Reagents

Yushi Tan, Jiabo Wang, Hong-Yu Zhang, Yuecheng Zhang* and Jiquan Zhao**

Tianjin Key Laboratory of Chemical Process Safety, Hebei Provincial Key Laboratory of Green Chemical Technology & High Efficient Energy Saving, School of Chemical Engineering and Technology, Hebei University of Technology, Tianjin, China

The modification of quinoxalin-2(1*H*)-ones *via* direct C-H bond functionalization has begun to receive widespread attention, due to quinoxalin-2(1*H*)-one derivatives' various biological activities and pharmaceutical properties. This mini review concentrates on the accomplishments of arylation, trifluoromethylation, alkylation, and alkoxylation of quinoxalin-2(1*H*)-ones with hypervalent iodine(III) reagents as reaction partners or oxidants. The reaction conditions and mechanisms are compared and discussed in detail.

Keywords: hypervalent Iodine(III) reagent, quinoxalin-2(1*H*)-one, C-H functionalization, arylation, trifluoromethylation, alkylation, alkoxylation

OPEN ACCESS

Edited by:
Jian-Wei Han,
East China University of Science and Technology, China

Reviewed by:
Cheng-Pan Zhang,
Wuhan University of Technology, China
Yunfei Du,
Tianjin University, China
Norio Shibata,
Nagoya Institute of Technology, Japan

****Correspondence:***
Hong-Yu Zhang
zhanghy@hebut.edu.cn
Yuecheng Zhang
yczhang@hebut.edu.cn
Jiquan Zhao
zhaojq@hebut.edu.cn

Specialty section:
This article was submitted to Organic Chemistry, a section of the journal Frontiers in Chemistry

Received: *01 April 2020*
Accepted: *05 June 2020*
Published: *03 August 2020*

Citation:
Tan Y, Wang J, Zhang H-Y, Zhang Y and Zhao J (2020) The C3-H Bond Functionalization of Quinoxalin-2(1H)-Ones With Hypervalent Iodine(III) Reagents. Front. Chem. 8:582. doi: 10.3389/fchem.2020.00582

INTRODUCTION

In recent years, direct C-H functionalization has become one of the most popular topics due to its advantages of having a high bonding efficiency and good atomic economy, and some remarkable achievements having been accomplished in this field (Ackermann et al., 2009; Yang et al., 2017; Yi et al., 2017). Among these significant works, hypervalent iodine reagents have been widely used as ideal and highly efficient oxidants or reaction partners (Kita et al., 1994; Nasrallah et al., 2019) due to their superior bench stability, high reactivity, low toxicity, environmental friendliness, ease of operation, and ready availability (Dohi et al., 2009; Sun and Shi, 2014). For instance, diverse iodine(III) reagents were invented to introduce fluorinated group into organic molecules (Yang et al., 2013; Matsuzaki et al., 2014; Suzuki et al., 2014; Das and Shibata, 2017; Das et al., 2017; Wang et al., 2017). Because of the large size of iodine atoms, a linear three-center, four-electron (3c-4e) bond (L–I–L) which uses a non-hybridized 5p orbital of iodine atom is formed. This 3c-4e bond, termed a "hypervalent bond," is highly polarized, longer, and weaker than normal covalent bonds, so the hypervalent iodine compounds have high electrophilic reactivity (Zhdankin and Stang, 2008). The distinctive reactivities of hypervalent iodine compounds are similar to those of heavy metals such as lead^{IV}, mercury^{II}, cadmium^{IV}, and thallium^{III}. However, compared with heavy metals, iodine is greener and cheaper (Yoshimura and Zhdankin, 2016), and the annual production of iodine reagents is 30,000 tons (Yusubov and Zhdankin, 2015). It is promising that hypervalent iodine compounds can be an environmentally sustainable alternative to heavy metals. The different hypervalent iodine reagents vary in properties. For instances, iodosobenzene and its derivatives have strong oxidability and can replace many toxic oxidants in various oxidation reactions; iodonium salts have no significant oxidative capacity but can react in various ways due to the special leaving ability of the -IAr fragment. Iodonium ylides and imides are excellent carbene and nitrene precursors, respectively, while heterocyclic iodanes have a higher stability than their acyclic analogs, which makes it possible to separate them and makes them a good alternative to several unstable iodine derivatives (Zhdankin and Stang, 2002; Stang, 2003; Wirth, 2005; Küpper et al., 2011).

On the other hand, quinoxalin-2(1*H*)-one is a privileged structural motif found in various natural active products and drug molecules (Liu et al., 2011; Galal et al., 2014; Pereira et al., 2015). 3-substituted quinoxalinone derivatives specifically have attracted much attention because of their distinctive biological and pharmacological activities. For instance, $CFTR_{act}$-J027 is a safe and efficient CFTR (cystic fibrosis transmembrane conductance regulator) activator which increases intestinal fluid secretion (Cil et al., 2016), and ML281 is a nanomolar STK33 inhibitor that selectively kills KRAS cancers (Weïwer et al., 2012). Some bioactive molecules containing quinoxalin-2(1*H*)-one skeleton, such as **Compounds 1**-**3**, also show potential applications in medicinal chemistry fields (Meyer et al., 2006; Khattab et al., 2015; Qin et al., 2015) (**Figure 1A**). Because of their synthetic usefulness and potential biological importance, the introduction of functional groups into the C3-position of the quinoxalin-2(1*H*)-ones has already become a research hotspot, and various protocols for the direct C3-H functionalization of quinoxalin-2(1*H*)-ones have been reported (Ebersol et al., 2019; Gu et al., 2019; Hong et al., 2019; Li et al., 2019; Peng et al., 2019; Rostoll-Berenguer et al., 2019; Teng et al., 2019; Wang et al., 2019a, 2020; Xie et al., 2019b; Zhao et al., 2019; Zheng and Studer, 2019; Tian et al., 2020; Yuan et al., 2020). In particular, the C3-H functionalization of quinoxalin-2(1*H*)-ones involving hypervalent iodine reagents has drawn wide attention for the aforementioned advantages of hypervalent iodine reagents, mainly including arylation (Paul et al., 2017; Yin and Zhang, 2017), trifluoromethylation (Wang et al., 2018; Xue et al., 2019a), alkylation (Wang et al., 2019b; Xie et al., 2019a; Xue et al., 2019b; Shen et al., 2020), and alkoxylation (Xu et al., 2019; Yang et al., 2019) of quinoxalin-2(1*H*)-ones, which provide convenient and environmentally friendly means for the synthesis of 3-substituted quinoxalinone derivatives. In this mini review, we will focus on the progress being made in the direct C3-H functionalization of quinoxalin-2(1*H*)-ones involving the hypervalent iodine reagents and discuss their mechanisms, in order to inspire more applications of hypervalent iodine reagents in related reactions.

C–H ARYLATION OF QUINOXALIN-2(1*H*)-ONES INVOLVING HYPERVALENT IODINE REAGENTS

Due to the distinctive pharmaceutical and electrical activities of 3-arylquinoxalin-2(1*H*)-ones, various methods for the direct C3-H arylation of quinoxalin-2(1*H*)-ones have been reported, involving two ones taking advantage of hypervalent iodine reagents.

In March 2017, Paul et al. reported on iodosobenzene-promoted oxidative C3-arylation of quinoxalin-2(1*H*)-ones with arylhydrazines, which is a widely used aryl radical source (Ravi et al., 2015; Rossi et al., 2015) (**Figure 1B**, Equation a) (Paul et al., 2017). The transformation afforded a variety of 3-arylquinoxalin-2(*H*)-one derivatives in moderate to good yields with a broad substrate scope, and the reaction conditions were mild, using only iodosobenzene as the oxidant. This protocol developed a new system for the synthesis of 3-arylquinoxalin-2(1*H*)-one derivatives. The aryl-TEMPO adduct was detected in the presence of the radical trapping reagent (2,2,6,6-tetramethylpiperidin-1-yl)oxyl (TEMPO) under the standard conditions, indicating that an aryl radical was involved in the reaction. Based on the experimental results, a plausible mechanism was proposed by the authors (**Figure 2A**). First, arylhydrazine adds to PhIO to form the iodine(III) active species **2**, which then eliminates the H_2O and PhI to give aryldiazene **3**. Subsequently, the intermediate **3** is oxidized by oxygen to afford the diazenyl radical **4**. The radical **4** releases molecular nitrogen to generate aryl radical **5**, which reacts with quinoxalin-2(*H*)-one **1** to form the intermediate **6**. Eventually, the intermediate **6** is oxidized by the hydroperoxyl radicals generated in the process of the formation of **4** to provide the final product **7**.

In the same year, Zhang group reported a method for C3-H arylation of quinoxalin-2(1*H*)-ones to give 3-arylquinoxalin-2(1*H*)-ones with diaryliodonium salts (**Figure 1B**, Equation b) (Yin and Zhang, 2017). Diaryliodonium salts are generally used in organic synthesis as aryl radical sources due to their easy availability (Yamaoka et al., 2013; Wang D. et al., 2014). This protocol could tolerate a series of readily available diaryliodonium salts and quinoxalin-2(1*H*)-ones, indicating its broad substrate scope. A possible mechanism was proposed for the coupling reaction based on the results of radical trapping with TEMPO (**Figure 2B**). Initially, aryl radical **8** is generated *via* the decomposition of diaryliodonium salt, and then immediately adds to quinoxalin-2(1*H*)-one to form the nitrogen radical **10**. The nitrogen radical **10** is then oxidized by high-valence iodonium salt **9** to produce the intermediate **11**, which eliminates the H^+ and BF_4^- in the presence of Cs_2CO_3 to give the final product **12**.

C–H TRIFLUOROMETHYLATION OF QUINOXALIN-2(1*H*)-ONES INVOLVING HYPERVALENT IODINE REAGENTS

Because of the special biological and drug activities of 3-trifluoromethylquinoxalin-2(1*H*)-one derivatives (Patel et al., 2000; Carta et al., 2006), it is necessary to explore efficient, simple, and mild methods to synthesize the 3-trifluoromethylquinoxalin-2(*H*)-ones. In 2018, we employed sodium trifluoromethanesulfinate (Langlois reagent) as a trifluoromethyl source and successfully realized the C3-H trifluoromethylation of quinoxalin-2(*H*)-ones under mild and transition metal-free conditions (**Figure 1B**, Equation c) (Wang et al., 2018). Due to the low-cost of sodium trifluoromethanesulfinate and easy availability of hypervalent iodine reagents, this protocol offers simple, efficient, and cheap access to 3-trifluoromethylquinoxalin-2(*H*)-ones. When the reaction was performed in the presence of the radical trapping reagent 1,1-diphenylethylene (DPE), the target product (3-trifluoromethylquinoxalin-2(*H*)-one) was isolated only in a 46% yield, and a DPE-CF_3 coupled byproduct (3,3,3-trifluoroprop-1-ene-1,1-diyl)dibenzene was observed, which suggested that the reaction followed a radical mechanism (**Figure 2C**). First,

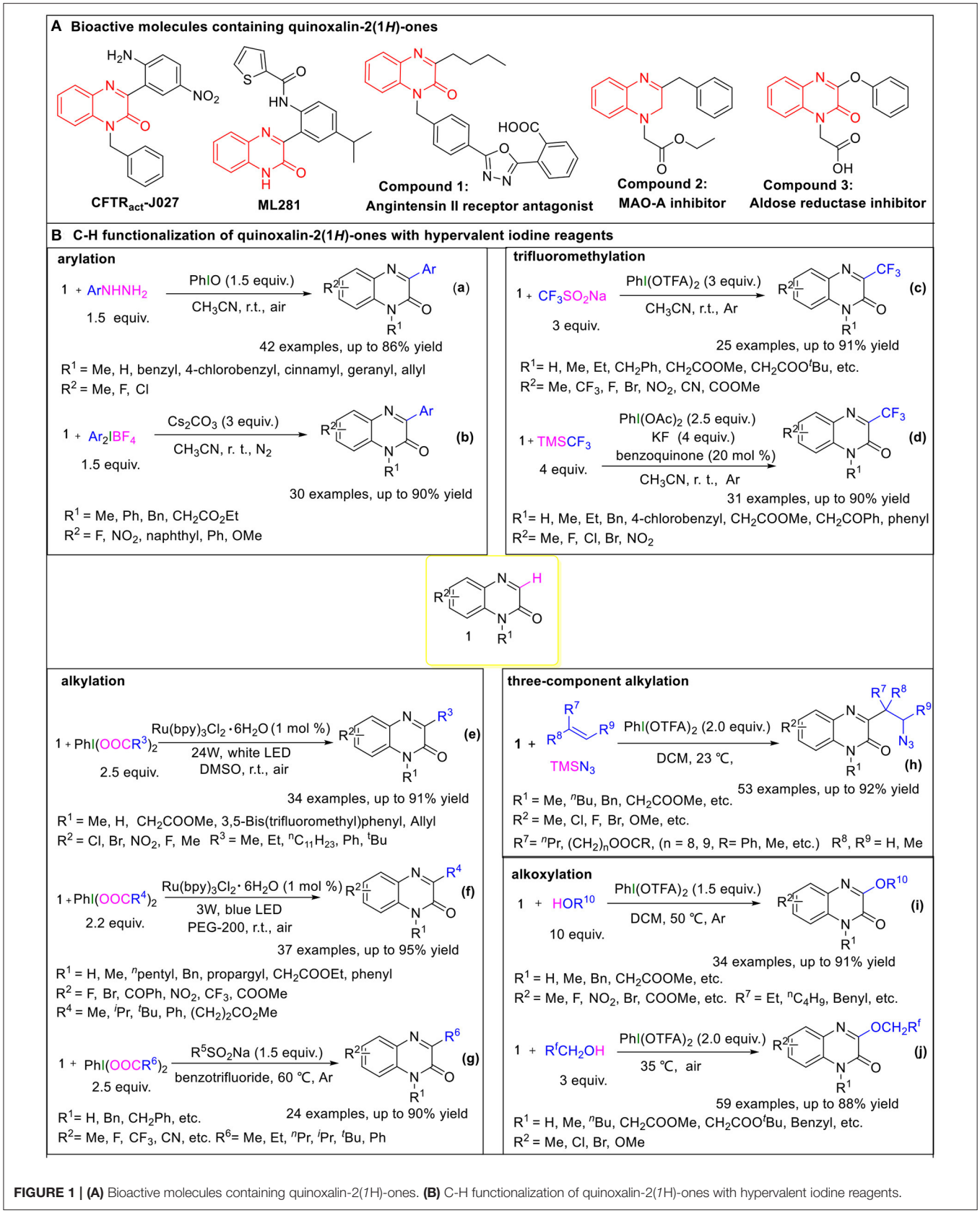

FIGURE 1 | (A) Bioactive molecules containing quinoxalin-2(1H)-ones. **(B)** C-H functionalization of quinoxalin-2(1H)-ones with hypervalent iodine reagents.

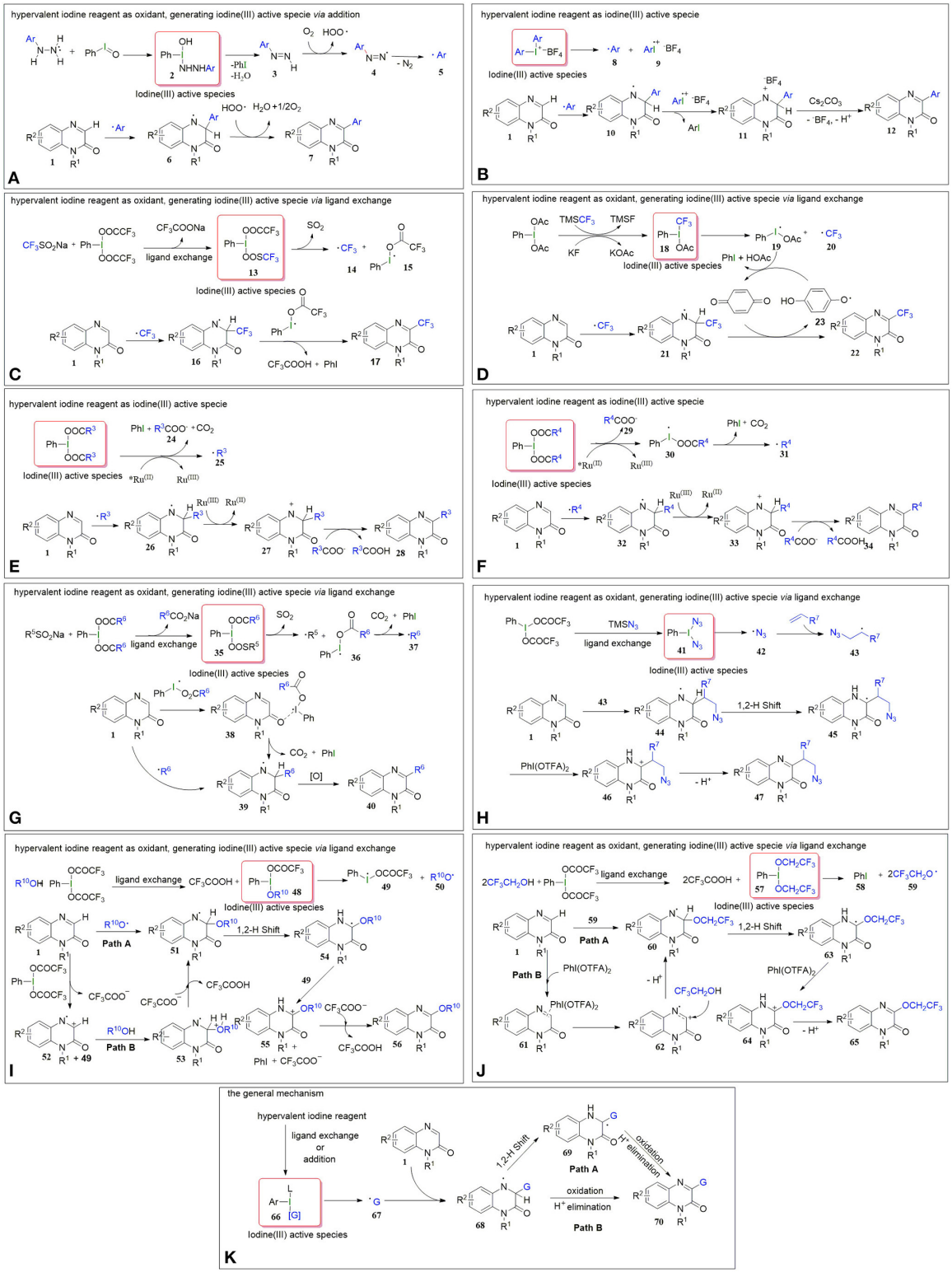

FIGURE 2 | (A) The possible mechanism of C-H arylation (a) of Quinoxalin-2(1*H*)-ones. **(B)** The possible mechanism of C-H arylation (b) of Quinoxalin-2(1*H*)-ones. **(C)** The possible mechanism of C-H trifluoromethylationn (c) of Quinoxalin-2(1*H*)-one. **(D)** The possible mechanism of C-H trifluoromethylationn. (d) of Quinoxalin-2(1*H*)-ones. **(E)** The possible mechanism of C-H alkylation (e) of Quinoxalin-2(1*H*)-ones. **(F)** The possible mechanism of C-H alkylation (f) of Quinoxalin-2(1*H*)-ones. **(G)** The possible mechanism of C-H alkylation (g) of Quinoxalin-2(1*H*)-ones. **(H)** The possible mechanism of C-H alkylation (h) of Quinoxalin-2(1*H*)-ones. **(I)** The possible mechanism of C-H alkoxylation (i) of Quinoxalin-2(1*H*)-ones. **(J)** The possible mechanism of C-H alkoxylation (j) of Quinoxalin-2(1*H*)-ones. **(K)** A general mechanism for these reactions.

[bis(trifluoroacetoxy)iodo]benzene ($PhI(OTFA)_2$) undergoes anion exchange with sodium trifluoromethanesulfinate to afford iodine(III) active species **13**, which then releases sulfur dioxide to generate trifluoromethyl radical **14** and I-radical **15**. Thereafter, trifluoromethyl radical **14** reacts with quinoxalin-2(1*H*)-ones to afford the intermediate **16,** which eventually goes through oxidization and H-elimination to form the final product **17**.

Soon afterwards, in March 2019, Xue et al. reported a method to synthesize 3-trifluoromethylquinoxalin-2(1*H*)-ones with (trifluoromethyl)trimethylsilane (Ruppert-Prakash reagent) as a trifluoromethyl source under transition metal-free conditions (**Figure 1B**, Equation d) (Xue et al., 2019a). This protocol has the advantages of using cheaper (diacetoxyiodo)benzene($PhI(OAc)_2$)compared with $PhI(OTFA)_2$ as an oxidant and stable (trifluoromethyl)trimethylsilane as the trifluoromethyl source. When TEMPO was added into the model reaction as a radical scavenger, the desired transformation was completely suppressed, while the TEMPO-CF_3 adduct was obtained in a 70% yield. Based on this experiment's results, the following possible mechanism was proposed (**Figure 2D**). Initially, the $PhI(OAc)_2$ reacts with KF and $TMSCF_3$ to generate the iodine(III) active species **18**, which then decomposes to I-radical **19** and trifluoromethyl radical **20**. Subsequently, trifluoromethyl radical **20** attacks quinoxalin-2(1*H*)-one to form intermediate **21**, which then oxidizes by 1,4-benzoquinone to form the final product **22**, with the 1,4-benzoquinone converting to phenoxy radical **23**. Finally, the phenoxy radical **23** recovers to 1,4-benzoquinone *via* oxidation of the I-radical **19**.

C–H ALKYLATION OF QUINOXALIN-2(1*H*)-ONES INVOLVING HYPERVALENT IODINE REAGENTS

As we know, phenyliodine(III) dicarboxylates have been regarded as effective reagents for the introduction of alkyl groups into organic molecules through a radical decarboxylation procedure (Togo and Katohgi, 2001; Lu et al., 2018). Besides, phenyliodine(III) dicarboxylate reagents could be easily prepared and stored (Stang et al., 1988; Mocci et al., 2007). So, several strategies for the synthesis of 3-alkylquinoxalin-2(1*H*)-ones with phenyliodine(III) dicarboxylates as the alkyl sources have been developed.

Very recently, Xue et al. developed a method to synthesize 3-alkylquinoxalin-2(1*H*)-ones with phenyliodine(III) dicarboxylates under visible-light conditions (**Figure 1B**, Equation e) (Xue et al., 2019b). The use of cheap and readily available phenyliodine(III) dicarboxylates as the alkylation reagents and mild reaction conditions make this protocol convenient and efficient in the synthesis of 3-alkylquinoxalin-2(1*H*)-ones. Two control experiments were carried out to probe into the mechanism. One was to use DMSO-*d*6 instead of DMSO as solvent. In this case the product was 3-methylquinoxalin-2(1*H*)-one but not the deuterated methyl substituted quinoxalin-2(1*H*)-one, which illustrated that the methyl group came from $PhI(OAc)_2$ rather than solvent DMSO. The other one was to run the reaction in the presence of TEMPO under the standard conditions. The TEMPO-CH_3 adduct was detected, indicating that the reaction was a radical process. Based on these control experiments, a plausible mechanism for this alkylation was proposed, as shown in **Figure 2E**. First, the catalyst Ru(II) is irradiated by visible light to produce the excited state $^*Ru(II)$, which promotes the decarboxylation of $PhI(OOCR^3)_2$ to generate alkyl radical **25**. Subsequently, the alkyl radical **25** regio-selectively attacks the quinoxalin-2(1*H*)-ones to provide intermediate **26**, which oxidizes by Ru(III) to transform into cation **27**, regenerating catalyst Ru(II). Eventually, the cation **27** undergoes dehydrogenation with the assistance of carboxylate anion **24** to furnish the final product **28**.

In the same year, He and coworkers also reported a method for the synthesis of 3-alkylquinoxalin-2(1*H*)-ones utilizing phenyliodine(III) dicarboxylates as the alkyl sources under visible-light conditions (**Figure 1B**, Equation f) (Xie et al., 2019a). And, more remarkable, this protocol uses eco-friendly PEG-200 as a reaction solvent. Based on the radical trapping results with dibutylhydroxytoluene (BHT) or TEMPO, a probable mechanism similar to the former was proposed (**Figure 2F**).

Alternatively, we accomplished the synthesis of 3-alkylquinoxalin-2(1*H*)-ones with phenyliodine(III) dicarboxylates as alkyl agents mediated by sodium alkylsulfinates under mild conditions (**Figure 1B**, Equation g) (Wang et al., 2019b). This protocol does not need any expensive metal catalysts, endowing it with an efficient process for the synthesis of 3-alkylquinoxalin-2(1*H*)-ones without metallic residues. Based on radical trapping experimental results with TEMPO and previous studies, a plausible mechanism was proposed, as given in **Figure 2G**. Initially, the anion exchange of $PhI(O_2CR^6)_2$ with R^5SO_2Na generates the iodine(III) active species **35**, which then turns into radical R^5 and I-radical **36,** excluding SO_2 at the same time. Then I-radical **36** decomposes into alkyl radical **37** and PhI, along with the release of CO_2. Next, in the presence of I-radical **36**, quinoxalin-2(1*H*)-one transforms into intermediate **38**, which undergoes decarboxylation to generate intermediate **39**. Meanwhile, the attack of alkyl radical **37** on the quinoxalin-2(1*H*)-one can also produce intermediate **39**, which is another path to producing intermediate **39**. Finally, intermediate **39** transforms to final product **40** *via* oxidization and dehydrogenation.

In short, the above three protocols for the alkylation of quinoxalin-2(1*H*)-ones showed superiority in functional group tolerance under mild reaction conditions. And yet the first two featured the efficient and sustainable visible-light-induced reaction systems, while the third one displayed the character of transition metal-free conditions.

THREE-COMPONENT C–H ALKYLATION OF QUINOXALIN-2(1*H*)-ONES INVOLVING HYPERVALENT IODINE REAGENTS

In 2020, Zhang's group developed a hypervalent iodine(III)-promoted three-component alkylation of quinoxalin-2(1*H*)-ones

with unactivated alkenes and $TMSN_3$ (**Figure 1B**, Equation h) (Shen et al., 2020). This method provides a step-economical solution for the introduction of β-azido alkyl groups into the quinoxalin-2(1*H*)-ones to rapidly synthesize bioactive organoazides. The various substituted quinoxalin-2(1*H*)-ones bearing electron-rich or electron-deficient groups, and olefins with functional groups including ester or hydroxyl substituents, were well-compatible in this transformation. A radical mechanism is proposed in **Figure 2H**. A double ligand exchange between $PhI(OTFA)_2$ and $TMSN_3$ furnishes iodine(III) active species, which provides an azide radical (**42**) *via* the homolytic cleavage of I-N bond (Matcha et al., 2013). Then, **42** chemoselectively attacks olefins to generate alkyl radical intermediate **43**, which is trapped by substrate **1** to afford nitrogen radical intermediate **44**. Afterwards, **44** undergoes a 1,2-H shift process to afford carbon radical **45**. Finally, the target product **47** was obtained *via* the sequential procedures of oxidation and deprotonation from **45**.

C–H ALKOXYLATION OF QUINOXALIN-2(1*H*)-ONES INVOLVING HYPERVALENT IODINE REAGENTS

Alkoxy groups are widely present in various natural active products and drug molecules (Han et al., 2018; Zhang et al., 2019), but the methods for the introduction of alkoxy groups in quinoxalin-2(1*H*)-ones have been rarely reported. In 2019, we disclosed a method to synthesize 3-alkoxyquinoxalin-2(1*H*)-ones with alcohols and $PhI(OTFA)_2$ under mild conditions (**Figure 1B**, Equation i) (Yang et al., 2019). This protocol provides easy access to 3-alkoxyquinoxalin-2(1*H*)-ones by using readily available and low cost alcohols as the alkoxy sources, and cheap $PhI(OTFA)_2$ as the oxidant, and shows good functional-group tolerance. Similarly, either BHT or TEMPO was employed as the radical trapping agent to explore information on the reaction mechanism. The results indicated that a radical mechanism could be involved in this alkoxylation process (**Figure 2I**). First, the ligand exchange of $PhI(OTFA)_2$ with alcohol takes place to afford the iodine(III) active species **48**, which then decomposes into I-radical **49** and alkoxy radical **50**. Subsequently, alkoxy radical **50** adds to quinoxalin-2(1*H*)-ones to generate the nitrogen radical **51**. There is also another way to form the intermediate **51**, namely, quinoxalin-2(1*H*)-one reacts with $PhI(OTFA)_2$ to generate radical cation **52**, and radical cation **52** is captured by nucleophilic alcohols to form oxonium intermediate **53** which undergoes deprotonation to afford the intermediate **51** with the assistance of trifluoroacetate. The nitrogen radical **51** converts to carbon radical **54** *via* 1,2-H shift process, which goes through oxidation and deprotonation successively to transform into final product **56**.

In addition, fluorine-containing units have been found in various drugs and nature products and are widely used in the pharmaceutical industry and in material science (Liang et al., 2013; Wang J. et al., 2014). Fluoroalkoxyl aryl ethers have also become a research hotspot because of their special pharmaceutical and biological activities. In June 2019, Zhang group reported a method to synthesize 3-fluoroalkoxylquinoxalin-2(1*H*)-ones with fluoroalkyl-alcohols and $PhI(OTFA)_2$ under catalyst-free and solvent-free conditions (**Figure 1B**, Equation j) (Xu et al., 2019). The use of commercially available fluoroalkyl alcohols as the fluoroalkoxyl sources, and convenient $PhI(OTFA)_2$ as the oxidant in the absence of a catalyst and solvent, endows this novel strategy with environmental friendliness and efficiency for the direct C3-H fluoroalkoxylation of quinoxalin-2(1*H*)-ones. The observation of TEMPO-OCH_2CF_3 or DPE-OCH_2CF_3 adducts in the radical trapping experiments revealed that a radical pathway may be involved in the reaction. The probable mechanism of the fluoroalkoxylation is similar to the aforementioned alkoxylation of quinoxalin-2(1*H*)-ones (**Figure 2J**).

CONCLUSION

In this mini review, we summarized recent efforts on direct C3-H functionalization of quinoxalin-2(1*H*)-ones with the commercially available and environmentally benign hypervalent iodine reagents, mainly including arylation, trifluoromethylation, alkylation, and alkoxylation. The accomplishments have provided us with simple, mild, efficient, and eco-friendly methods for the synthesis of various C3-substituted quinoxalin-2(1*H*)-ones. Herein, the hypervalent iodine reagents play two different roles, reaction partners (**equations b**, **e**, **f,** and **g**), and oxidants (**equations a**, **c**, **d**, **h, Io,** and **j**). A general mechanism for these reactions could be given (**Figure 2K**). For all the reactions, iodine(III) active species are initial key intermediates. In the case of hypervalent iodine reagents as oxidants, they must initially transform to the iodine(III) active species **66** *via* ligand exchange (**equations c**, **d**, **h**, **i,** and **j**) or addition (**equation a**); in the case of hypervalent iodine reagents as reaction partners, they are the iodine(III) active species **66** themselves (**equations b**, **e**, **f,** and **g**). Once the formation or introduction of iodine(III) active species occurs, they decompose to afford the radical **67** (G = aryl, trifluoromethyl, alkyl, azide and alkoxyl radical), which regio-selectively adds on to the N=C bond of quinoxalin-2(1*H*)-one to provide the carbon radical intermediate **68** (not including the azide radical). In some situations, the intermediate **68** transforms into nitrogen radical intermediate **69** *via* a 1,2-*H* shift process. Finally, the target product **70** is obtained *via* the successive oxidation and H^+-elimination of the carbon radical intermediate **68** or nitrogen radical intermediate **69**.

There are still some limitations in the reactions involving hypervalent iodine reagents. For instance, superstoichiometric hypervalent iodine reagents or noble transition-metal-catalysts are required in some cases. Also, the application scope of hypervalent iodine reagents is slightly narrow; they have only been successful in the arylation, trifluoromethylation, alkylation, and alkoxylation of quinoxalin-2(1*H*)-ones up till now. It is desirable to develop efficient reaction systems and expand on more reaction models such as the acylation, alkoxycarbonylation, amination, sulfonation, and phosphonation of quinoxalin-2(1*H*)-ones involving hypervalent iodine reagents.

AUTHOR CONTRIBUTIONS

YT, JW, and H-YZ collected the related references and prepared the manuscript. YZ and JZ directed the preparation of this manuscript. All authors critically reviewed the text and figures prior to submission.

ACKNOWLEDGMENTS

We acknowledge the financial support from the National Natural Science Foundation of China (Grant No. 21776056) and the Natural Science Foundation of Hebei Province (CN) (Grant No. B2018202253).

REFERENCES

Ackermann, L., Vicente, R., and Kapdi, A. R. (2009). Transition-metal-catalyzed direct arylation of (hetero)arenes by C-H bond cleavage. *Angew. Chem. Int. Ed.* 48, 9792–9826. doi: 10.1002/anie.200902996

Carta, A., Piras, S., Loriga, G., and Paglietti, G. (2006). Chemistry, biological properties and SAR analysis of quinoxalinones. *Mini-Rev. Med. Chem.* 6, 1179–1200. doi: 10.2174/138955706778742713

Cil, O., Phuan, P.-W., Lee, S., Tan, J., Haggie, P. M., Levin, M. H., et al. (2016). CFTR activator increases intestinal fluid secretion and normalizes stool output in a mouse model of constipation. *Cell. Mol. Gastroenterol. Hepatol.* 2, 317–327. doi: 10.1016/j.jcmgh.2015.12.010

Das, P., and Shibata, N. (2017). Electrophilic triflyl-arylation and triflyl-pyridylation by unsymmetrical aryl/pyridyl-λ3-iodonium salts: synthesis of aryl and pyridyl triflones. *J. Org. Chem.* 82, 11915–11924. doi: 10.1021/acs.joc.7b01690

Das, P., Takada, M., Matsuzaki, K., Saitob. N., and Shibata, N. (2017). SF5-pyridylaryl-λ3-iodonium salts and their utility as electrophilic reagents to access SF5?pyridine derivatives in the late-stage of synthesis. *Chem. Commun.* 53, 3850–3853. doi: 10.1039/C7CC01043E

Dohi, T., Ito, M., Yamaoka, N., Morimoto, K., Fujioka, H., and Kita, Y. (2009). Hypervalent iodine(III), selective and efficient single-electron-transfer (SET) oxidizing agent. *Tetrahedron* 65, 10797–10815. doi: 10.1016/j.tet.2009.10.040

Ebersol, C., Rocha, N., Penteado, F., Silva, M. S., Hartwig, D., Lenardão, E. J., et al. (2019). A niobium-catalyzed coupling reaction of α-keto acids with ortho-phenylenediamines: synthesis of 3-arylquinoxalin-2(1*H*)-ones. *Green Chem.* 21, 6154–6160. doi: 10.1039/C9GC02662B

Galal, S. A., Khairat, S. H. M., Ragab, F. A. F., Abdelsamie, A. S., Ali, M. M., Soliman, S. M., et al. (2014). Design, synthesis and molecular docking study of novel quinoxalin-2(1*H*)-ones as anti-tumor active agents with inhibition of tyrosine kinase receptor and studying their cyclooxygenase-2 activity. *Eur. J. Med. Chem.* 86, 122–132. doi: 10.1016/j.ejmech.2014.08.048

Gu, Y.-R., Duan, X.-H., Chen, L., Ma, Z.-Y., Gao, P., and Guo, L.-N. (2019). Iminyl radical-triggered intermolecular distal C(sp^3)–H heteroarylation *via* 1,5-hydrogen-atom transfer (HAT) cascade. *Org. Lett.* 21, 917–920. doi: 10.1021/acs.orglett.8b03865

Han, B., Li, K., Wang, Q., Zhang, L., Shi, J., Wang, Z., et al. (2018). Effect of anlotinib as a third-line or further treatment on overall survival of patients with advanced non-small cell lung cancer: The ALTER 0303 phase 3 randomized clinical trial. *JAMA Oncol.* 4, 1569–1575. doi: 10.1001/jamaoncol.2018.3039

Hong, G., Yuan, J., Fu, J., Pan, G., Wang, Z., Yang, L., et al. (2019). Transition-metal-free decarboxylative C3-difluoroarylmethylation of quinoxalin-2(1*H*)-ones with α,α-difluoroarylacetic acids. *Org. Chem. Front.* 6, 1173–1182. doi: 10.1039/C9QO00105K

Khattab, S. N., Abdel Moneim, S. A. H., Bekhit, A. A., El Massry, A. M., Hassan, S. Y., El-Faham, A., et al. (2015). Exploring new selective 3-benzylquinoxaline-based MAO-A inhibitors: design, synthesis, biological evaluation and docking studies. *Eur. J. Med. Chem.* 93, 308–320. doi: 10.1016/j.ejmech.2015.02.020

Kita, Y., Tohma, H., Hatanaka, K., Takada, T., Fujita, S., Mitoh, S., et al. (1994). Hypervalent iodine-induced nucleophilic substitution of *para*-substituted phenol ethers. Generation of cation radicals as reactive intermediates. *J. Am. Chem. Soc.* 116, 3684–3691. doi: 10.1021/ja00088a003

Küpper, F. C., Feiters, M. C., Olofsson, B., Kaiho, T., Yanagida, S., Zimmermann, M. B., et al. (2011). Commemorating two centuries of iodine research: An interdisciplinary overview of current research. *Angew. Chem. Int. Ed.* 50, 11598–11620. doi: 10.1002/anie.201100028

Li, K.-J., Jiang, Y.-Y., Xu, K., Zeng, C.-C., and Sun, B.-G. (2019). Electrochemically dehydrogenative C–H/P–H cross-coupling: effective synthesis of phosphonated quinoxalin-2(1*H*)-ones and xanthenes. *Green Chem.* 21, 4412–4421. doi: 10.1039/C9GC01474H

Liang, T., Neumann, C. N., and Ritter, T. (2013). Introduction of fluorine and fuorine-containing functional groups. *Angew. Chem. Int. Ed.* 52, 8214–8264. doi: 10.1002/anie.201206566

Liu, R., Huang, Z., Murray, M. G., Guo, X., and Liu, G. (2011). Quinoxalin-2(1*H*)-one derivatives as inhibitors against hepatitis C virus. *J. Med. Chem.* 54, 5747–5768. doi: 10.1021/jm200394x

Lu, S.-C., Li, H.-S., Gong, Y.-L., Zhang, S.-P., Zhang, J.-G., and Xu, S. (2018). Combination of $PhI(OAc)_2$ and 2-nitropropane as the source of methyl radical in room-temperature metal-free oxidative decarboxylation/cyclization, Construction of 6-methyl phenanthridines and 1-methyl isoquinolines. *J. Org. Chem.* 83, 15415–15425. doi: 10.1021/acs.joc.8b02701

Matcha, K., Narayan, R., and Antonchick, A. P. (2013). Metal-free radical azidoarylation of alkenes: rapid access to oxindoles by cascade C-N and C-C bond-forming reactions. *Angew. Chem. Int. Ed.* 52, 7985–7989. doi: 10.1002/anie.201303550

Matsuzaki, K., Okuyama, K., Tokunaga, E., Shiro, M., and Shibata, N. (2014). Sterically demanding unsymmetrical diaryl-λ3-iodanes for electrophilic pentafluorophenylation and an approach to α-pentafluorophenyl carbonyl compounds with an all-carbon stereocenter. *Chem. Open* 3, 233–237. doi: 10.1002/open.201402045

Meyer, E., Joussef, A. C., and de Souza, L. B. P. (2006). Synthesis of new 1,2,4- and 1,3,4-oxadiazole derivatives as potential nonpeptide angiotensin II receptor antagonists. *Synthetic Commun.* 36, 729–741. doi: 10.1080/00397910500447066

Mocci, F., Uccheddu, G., Frongia, A., and Cerioni, G. (2007). Solution structure of some λ^3 iodanes: An ^{17}O NMR and DFT study. *J. Org. Chem.* 72, 4163–4168. doi: 10.1021/jo070111h

Nasrallah, A., Lazib, Y., Boquet, V., Darses, B., and Dauban, P. (2019). Catalytic intermolecular C(sp^3)-H amination with sulfamates for the asymmetric synthesis of amines. *Org. Process Res. Dev.* 24, 724–728. doi: 10.1021/acs.oprd.9b00424

Patel, M., McHugh, R. J., Cordova, B. C., Klabe, R. M., Erickson-Viitanen, S., Trainor, G. L., et al. (2000). Synthesis and evaluation of quinoxalinones as HIV-1 reverse transcriptase inhibitors. *Bioorg. Med. Chem. Lett.* 10, 1729–1731. doi: 10.1016/S0960-894X(00)00321-8

Paul, S., Ha, J. H., Park, G. E., and Lee, Y. R. (2017). Transition metal-free iodosobenzene-promoted direct oxidative 3-arylation of quinoxalin-2(*H*)-ones with arylhydrazines. *Adv. Synth. Catal.* 359, 1515–1521. doi: 10.1002/adsc.201700070

Peng, S., Hu, D., Hu, J.-L., Lin, Y.-W., Tang, S.-S., Tang, H.-S., et al. (2019). Metal-free C3 hydroxylation of quinoxalin-2(1*H*)-ones in water. *Adv. Synth. Catal.* 361, 5721–5726. doi: 10.1002/adsc.201901163

Pereira, J. A., Pessoa, A., M., Cordeiro, M. N. D. S., Fernandes, R., Prudêncio, C., Noronha, J. P., et al. (2015). Quinoxaline, its derivatives and applications: A State of the Art review. *Eur. J. Med. Chem.* 97, 664–672. doi: 10.1016/j.ejmech.2014.06.058

Qin, X., Hao, X., Han, H., Zhu, S., Yang, Y., Wu, B., et al. (2015). Design and synthesis of potent and multifunctional aldose reductase inhibitors based on quinoxalinones. *J. Med. Chem.* 58, 1254–1267. doi: 10.1021/jm501484b

Ravi, M., Chauhan, P., Kant, R., Shukla, S. K., and Yadav, P. P. (2015). Transition-metal-free C-3 arylation of quinoline-4-ones with arylhydrazines. *J. Org. Chem.* 80, 5369–5376. doi: 10.1021/acs.joc.5b00739

Rossi, R., Lessi, M., Manzini, C., Marianetti, G., and Bellina, F. (2015). Transition metal-free direct C-H (hetero)arylation of heteroarenes: A sustainable methodology to access (hetero)aryl-substituted heteroarenes. *Adv. Synth. Catal.* 357, 3777–3814. doi: 10.1002/adsc.201500799

Rostoll-Berenguer, J., Blay, G., Muñoz, M. C., Pedro, J. R., and Vila, C. (2019). A combination of visible-light organophotoredox catalysis and asymmetric organocatalysis for the enantioselective mannich reaction of dihydroquinoxalinones with ketones. *Org. Lett.* 21, 6011–6015. doi: 10.1021/acs.orglett.9b02157

Shen, J., Xu, J., Huang, L., Zhu, Q., and Zhang, P. (2020). Hypervalent iodine(III)-promoted rapid cascade reaction of quinoxalinones with unactivated alkenes and $TMSN_3$. *Adv. Synth. Catal.* 362, 230–241. doi: 10.1002/adsc.201901314

Stang, P. J. (2003). Polyvalent iodine in organic chemistry. *J. Org. Chem.* 68, 2997–3008. doi: 10.1021/jo030022e

Stang, P. J., Boehshar, M., Wingert, H., and Kitamura, T. (1988). Acetylenic esters. Preparation and characterization of alkynyl carboxylates via polyvalent iodonium species. *J. Am. Chem. Soc.* 110, 3272–3278. doi: 10.1021/ja00218a043

Sun, C.-L., and Shi, Z.-J. (2014). Transition-metal-free coupling reactions. *Chem. Rev.* 114, 9219–9280. doi: 10.1021/cr400274j

Suzuki, S., Kamo, T., Fukushi, K., Hiramatsu, T., Tokunaga, E., Dohi, T., et al. (2014). Iodoarene-catalyzed fluorination and aminofluorination by an Ar-I/HF pyridine/mCPBA system. Chem. Sci.5, 2754–2760. doi: 10.1039/c3sc53107d

Teng, Q.-H., Yao, Y., Wei, W.-X., Tang, H.-T., Li, J.-R., and Pan, Y.-M. (2019). Direct C-H sulfenylation of quinoxalinones with thiols under visible-light-induced photocatalyst-free conditions. *Green Chem.* 21, 6241–6245. doi: 10.1039/C9GC03045J

Tian, M., Liu, S., Bu, X., Yu, J., and Yang, X. (2020). Covalent Organic Frameworks: A sustainable photocatalyst toward visible-light-accelerated C3 arylation and alkylation of quinoxalin-2(1*H*)-ones. *Chem. Eur. J.* 26, 369–373. doi: 10.1002/chem.201903523

Togo, H., and Katohgi, M. (2001). Synthetic uses of organohypervalent iodine compounds through radical pathways. *Synlett.* 2001, 0565–0581. doi: 10.1055/s-2001-13349

Wang, D., Ge, B., Li, L., Shan, J., and Ding, Y. (2014). Transition metal-free direct C-H functionalization of quinones and naphthoquinones with diaryliodonium salts, Synthesis of aryl naphthoquinones as β-secretase inhibitors. *J. Org. Chem.* 79, 8607–8613. doi: 10.1021/jo501467v

Wang, J., Jia, S., Okuyama, K., Huang, Z., Tokunaga, E., Sumii, Y., et al. (2017). Synthesis of sulfur perfluorophenyl compounds using a pentafluorobenzenesulfonyl hypervalent iodonium ylide. *J. Org. Chem.* 82, 11939–11945. doi: 10.1021/acs.joc.7b01908

Wang, J., Sánchez-Roselló, M., Aceña, J. L., del, Pozo, C., Sorochinsky, A. E., Fustero, S., et al. (2014). Fluorine in pharmaceutical industry: fluorine-containing drugs introduced to the market in the last decade (2001–2011). *Chem. Rev.* 114, 2432–2506. doi: 10.1021/cr4002879

Wang, J., Sun, B., Zhang, L., Xu, T., Xie, Y., and Jin, C. (2020). Transition-metal-free direct C-3 cyanation of quinoxalin-2(1*H*)-ones with ammonium thiocyanate as the "CN" source. *Org. Chem. Front.* 7, 113–118. doi: 10.1039/C9QO01055F

Wang, L., Liu, H., Li, F., Zhao, J., Zhang, H.-Y., and Zhang, Y. (2019a). Copper-catalyzed C3-H difluoroacetylation of quinoxalinones with ethyl bromodifluoroacetate. *Adv. Synth. Catal.* 361, 2354–2359. doi: 10.1002/adsc.201900066

Wang, L., Zhang, Y., Li, F., Hao, X., Zhang, H.-Y., and Zhao, J. (2018). Direct C-H trifluoromethylation of quinoxalin-2(1*H*)-ones under transition-metal-free conditions. *Adv. Synth. Catal.* 360, 3969–3977. doi: 10.1002/adsc.201800863

Wang, L., Zhao, J., Sun, Y., Zhang, H.-Y., and Zhang, Y. (2019b). A catalyst-free minisci-type reaction: the C-H alkylation of quinoxalinones with sodium alkylsulfinates and phenyliodine(III) dicarboxylates. *Eur. J. Org. Chem.* 2019, 6935–6944. doi: 10.1002/ejoc.201901266

Weïwer, M., Spoonamore, J., Wei, J., Guichard, B., Ross, N. T., Masson, K., et al. (2012). A potent and selective quinoxalinone-based STK33 inhibitor does not show synthetic lethality in KRAS-dependent cells. *ACS Med. Chem. Lett.* 3, 1034–1038. doi: 10.1021/ml300246r

Wirth, T. (2005). Hypervalent iodine chemistry in synthesis: Scope and new directions. *Angew. Chem. Int. Ed.* 44, 3656–3665. doi: 10.1002/anie.200500115

Xie, L.-Y., Jiang, L.-L., Tan, J.-X., Wang, Y., Xu, X.-Q., Zhang, B., et al. (2019a). Visible-light-initiated decarboxylative alkylation of quinoxalin-2(1*H*)-ones with phenyliodine(III) dicarboxylates in recyclable ruthenium(II) catalytic system. *ACS Sustain. Chem. Eng.* 7, 14153–14160. doi: 10.1021/acssuschemeng.9b02822

Xie, L.-Y., Peng, S., Fan, T.-G., Liu, Y.-F., Sun, M., Jiang, L.-L., et al. (2019b). Metal-free C3-alkoxycarbonylation of quinoxalin-2(1*H*)-ones with carbazates as ecofriendly ester sources. *Sci. China Chem.* 62, 460–464. doi: 10.1007/s11426-018-9446-1

Xu, J., Yang, H., Cai, H., Bao, H., Li, W., and Zhang, P. (2019). Transition-metal and solvent-free oxidative C-H fluoroalkoxylation of quinoxalinones with fluoroalkyl alcohols. *Org. Lett.* 21, 4698–4702. doi: 10.1021/acs.orglett.9b01578

Xue, W., Su, Y., Wang, K.-H., Cao, L., Feng, Y., Zhang, W., et al. (2019a). Phenyliodonium diacetate mediated carbotrifluoromethylation of quinoxalin-2(1*H*)-ones. *Asian J. Org. Chem.* 8, 887–892. doi: 10.1002/ajoc.201900118

Xue, W., Su, Y., Wang, K.-H., Zhang, R., Feng, Y., Cao, L., et al. (2019b). Visible-light induced decarboxylative alkylation of quinoxalin-2(1*H*)-ones at the C3-position. *Org. Biomol. Chem.* 17, 6654–6661. doi: 10.1039/C9OB01169B

Yamaoka, N., Sumida, K., Itani, I., Kubo, H., Ohnishi, Y., Sekiguchi, S., et al. (2013). Single-electron-transfer (SET)-induced oxidative biaryl coupling by polyalkoxybenzene-derived diaryliodonium(III) salts. *Chem. Eur. J.* 19, 15004–15011. doi: 10.1002/chem.201301148

Yang, Q., Han, X., Zhao, J., Zhang, H.-Y., and Zhang, Y. (2019). Direct C3 alkoxylation of quinoxalin-2(1*H*)-ones with alcohols *via* cross-dehydrogenative coupling under catalyst-free conditions. *J. Org. Chem.* 84, 11417–11424. doi: 10.1021/acs.joc.9b01181

Yang, Y., Lan, J., and You, J. (2017). Oxidative C-H/C-H coupling reactions between two (hetero)arenes. *Chem. Rev.* 117, 8787–8863. doi: 10.1021/acs.chemrev.6b00567

Yang, Y-D., Azuma, A., Tokunaga, E., Yamasaki, M., Shiro, M., Shibata, N. (2013). Trifluoromethanesulfonyl hypervalent iodonium ylide for copper-catalyzed trifluoromethylthiolation of enamines, indoles, and β-ketoEsters. *J. Am. Chem. Soc.* 135, 8782–8785. doi: 10.1021/ja402455f

Yi, H., Zhang, G., Wang, H., Huang, Z., Wang, J., Singh, A. K., et al. (2017). Recent advances in radical C-H activation/radical cross-coupling. *Chem. Rev.* 117, 9016–9085. doi: 10.1021/acs.chemrev.6b00620

Yin, K., and Zhang, R. (2017). Transition-metal-free direct C-H arylation of quinoxalin-2(1*H*)-ones with diaryliodonium salts at room temperature. *Org. Lett.* 19, 1530–1533. doi: 10.1021/acs.orglett.7b00310

Yoshimura, A., and Zhdankin, V. V. (2016). Advances in synthetic applications of hypervalent iodine compounds. *Chem. Rev.* 116, 3328–3435. doi: 10.1021/acs.chemrev.5b00547

Yuan, J.-W., Zhu, J.-L., Zhu, H.-L., Peng, F., Yang, L.-Y., Mao, P., et al. (2020). Transition-metal free direct C–H functionalization of quinoxalin-2(1*H*)-ones with oxamic acids leading to 3-carbamoyl quinoxalin-2(1*H*)-ones. *Org. Chem. Front.* 7, 273–285. doi: 10.1039/C9QO01322A

Yusubov, M. S., and Zhdankin, V. V. (2015). Iodine catalysis, A green alternative to transition metals in organic chemistry and technology. *Res-Effic Technol.* 1, 49–67. doi: 10.1016/j.reffit.2015.06.001

Zhang, K., Hong, R., Kaping, L., Xu, F., Xia, W., Qin, G., et al. (2019). CDK4/6 inhibitor palbociclib enhances the effect of pyrotinib in HER2-positive breast cancer. *Cancer Lett.* 447, 130–140. doi: 10.1016/j.canlet.2019.01.005

Zhao, L., Wang, L., Gao, Y., Wang, Z., and Li, P. (2019). Visible-light-induced alkoxylation of quinoxalin-2(1*H*)-ones with alcohols for the synthesis of heteroaryl ethers. *Adv. Synth. Catal.* 361, 5363–5370. doi: 10.1002/adsc.201900732

Zhdankin, V. V., and Stang, P. J. (2002). Recent developments in the chemistry of polyvalent iodine compounds. *Chem. Rev.* 102, 2523–2584. doi: 10.1021/cr010003+

Zhdankin, V. V., and Stang, P. J. (2008). Chemistry of polyvalent iodine. *Chem. Rev.* 108, 5299–5358. doi: 10.1021/cr800332c

Zheng, D., and Studer, A. (2019). Photoinitiated three-component α-perfluoroalkyl-β-heteroarylation of unactivated alkenes *via* electron catalysis. *Org. Lett.* 21, 325–329. doi: 10.1021/acs.orglett.8b03849

Conflict of Interest: The authors declare that the research was conducted in the absence of any commercial or financial relationships that could be construed as a potential conflict of interest.

frontiers in Chemistry

REVIEW
published: 23 September 2020
doi: 10.3389/fchem.2020.551159

Recent Synthetic Applications of the Hypervalent Iodine(III) Reagents in Visible-Light-Induced Photoredox Catalysis

Chaoyue Chen[1]*, *Xin Wang*[1] and *Tinghai Yang*[1,2]*

[1] School of Chemistry and Environmental Engineering, Jiangsu University of Technology, Changzhou, China, [2] State Key Laboratory of Coordination Chemistry, School of Chemistry and Chemical Engineering, Nanjing University, Nanjing, China

The synergistic combination of visible-light-induced photoredox catalysis with hypervalent iodine(III) reagents (HIRs) represents a particularly important achievement in the field of hypervalent iodine chemistry, and numerous notable organic transformations were achieved in a mild and environmentally benign fashion. This account intends to summarize recent synthetic applications of HIRs in visible-light-induced photoredox catalysis, and they are organized in terms of the photochemical roles of HIRs played in reactions.

Keywords: hypervalent iodine reagent, photoredox catalysis, photochemistry, radical intermediate, synthetic methods

OPEN ACCESS

Edited by:
Jian-Wei Han,
East China University of Science and Technology, China

Reviewed by:
Andrea Gualandi,
University of Bologna, Italy
Alakananda Hajra,
Visva-Bharati University, India

***Correspondence:**
Chaoyue Chen
njuchaoyuechen@163.com
Tinghai Yang
tinghai_yang@hotmail.com

Specialty section:
This article was submitted to Organic Chemistry, a section of the journal Frontiers in Chemistry

Received: *12 April 2020*
Accepted: *13 August 2020*
Published: *23 September 2020*

Citation:
Chen C, Wang X and Yang T (2020) Recent Synthetic Applications of the Hypervalent Iodine(III) Reagents in Visible-Light-Induced Photoredox Catalysis. Front. Chem. 8:551159. doi: 10.3389/fchem.2020.551159

INTRODUCTION

During the past several decades, the chemistry of hypervalent iodine reagents (HIRs) has gained more and more attention due to their unique electrophilic properties (Brand et al., 2011; Charpentier et al., 2015), valuable oxidizing abilities (Yoshimura and Zhdankin, 2016; Wang and Studer, 2017), and environment friendly features (Zhdankin, 2013; Yoshimura and Zhdankin, 2016). The special structural features and unparalleled reactivities of HIRs lie in their unique 3-center-4-electron (3c-4e) bonds (L—I(III) —X), which are highly polarized and are longer and weaker than classical covalent bonds (Zhdankin, 2013; Yoshimura and Zhdankin, 2016; Jia and Chen, 2018). Generally, HIRs offer multiple advantages for synthetic organic chemistry: (i) mild and highly chemoselective oxidizing properties; (ii) benign environmental character; (iii) commercial availability; and (iiii) convenient structural modification (Brand et al., 2011; Zhdankin, 2013; Li Y. et al., 2016; Yoshimura and Zhdankin, 2016; Hari et al., 2018). These advantages of HIRs give synthetic chemists the opportunities to design and access novel and more challenging reactions. As a result, a wide array of organic transformations ranging from oxidative coupling processes (Wang and Liu, 2016; Jia and Chen, 2018), ligand transfer reactions (Zhdankin, 2013; Yoshimura and Zhdankin, 2016), rearrangements (Zhdankin, 2009; Brand et al., 2011), C–C, C–O or C–N bond formations (Li Y. et al., 2016; Hyatt et al., 2019) to numerous other reactions have recently been developed based on HIRs.

Since 2008, visible-light-induced photoredox catalysis has emerged as one of the most rapidly expanding fields in organic chemistry (Xuan and Xiao, 2012; Koike and Akita, 2014; Romero and Nicewicz, 2016; Shaw et al., 2016; Staveness et al., 2016; Twilton et al., 2017). In photoredox-catalyzed procedures, metal photocatalysts (iridium-, ruthenium-, and copper-based) or organic dyes (rose bengal, eosin Y, BODIPY, 4CzIPN, coumarins, and rhodamine derivatives) can efficiently

convert visible light into chemical energy, thereby allowing the activation of organic substrates *via* single-electron transfer (SET) events, and eventually accessing to a large number of synthetically important reactions under very mild reaction conditions.

Very recently, HIRs have quickly established themselves as efficient and versatile reaction partners for visible-light-induced photoredox catalysis. Many studies related to the elegant merging of photoredox catalysis with HIRs have resulted in significant advancements (Wang and Liu, 2016; Wang and Studer, 2017; Jia and Chen, 2018). By the appropriate choice of HIRs, photocatalysts, light sources and solvents, a wide array of bond-forming reactions were developed in mild and environmentally benign fashion (**Figure 1**).

Mechanistically, a typical photoredox catalytic cycle consists of a sequence of three key steps: a photoexcitation process followed by two SET processes. On account of the smooth occurrence of the SET processes, the redox (oxidation/reduction) potentials of both photocatalysts and HIRs must be taken into consideration in order to find the best-matched partners in a photoredox catalysis/HIR reaction. The oxidative/reductive abilities of commonly used transition metal and organic photocatalysts are relatively well investigated (**Table 1**) (Reckenthaler and Griesbeck, 2013; Koike and Akita, 2014; Romero and Nicewicz, 2016; Roth et al., 2016; Lemos et al., 2019). However, despite the practical significance of HIRs, redox potentials of them has not been sufficiently evaluated until now, only limited of redox potential values of HIRs were reported in literatures (**Figure 2**) (Charpentier et al., 2015; Roth et al., 2016; Vaillant and Waser, 2017). Just in 2020, Radzhabov and coworkers reported new calculated values of the relative redox potentials of [bis(acetoxy)iodo]-arenes (Radzhabov et al., 2020). The influence of various substituents and the effects of various solvents on the reduction potentials of HIRs was both detailed evaluated. This theoretical assessments may provide a useful reference for the design of new photoredox reactions based on $ArI(OAc)_2$.

In line with photoredox catalysis, HIRs play two different kind of photochemical roles such as reagent for functional-group transfer and mild oxidant for substrates activation (Wang and Liu, 2016; Wang and Studer, 2017; Jia and Chen, 2018). HIRs bearing trifluoromethyl, azido, alkynyl, and cyano groups can readily participate in photocatalytic reactions for the transformation of perfluoroalkylation (Koike and Akita, 2016), azidation (Fumagalli et al., 2015), alkynylation (Kaschel and Werz, 2015), and cyanation (Le Vaillant et al., 2017), respectively. In contrast, hydroxyl-, alkoxyl-, and acetoxy- benziodoxoles (BI-OH, BI-OR, and BI-OAc) are usually acted as the oxidant for activation of carboxylic acids (Huang et al., 2016), alcohols (Liu et al., 2018) or alkyl C-H bonds (Li et al., 2017) for the generation of oxygen- or carbon-centered radicals under photoredox catalysis. In certain cases (Jia et al., 2016, 2018), two HIRs were employed in the same photoredox procedure: one of which acts as a reagent and the other serves as mild oxidant.

The review herein intends to summarize recent synthetic applications of HIRs in visible-light-induced photoredox catalysis. The document is organized in terms of the photochemical roles of HIRs played in reactions, with particular emphasis placed on the literature from 2016 until the end of March of 2020. In every section, we arrange the synthetic methods according to their reaction types.

HIRS ACT AS FUNCTIONAL GROUP TRANSFER REAGENTS

Fluoroalkylation

Visible-light photoredox catalytic methods have been proven to be one of the most efficient pathways for the incorporation of a variety of fluoroalkyl groups into organic skeletons (Koike and Akita, 2016). Both cyclic and acyclic HIRs possessing various fluorinated groups can serve as effective fluoroalkyl-transfer reagents in photoredox-catalyzed fluoroalkylation (Li Y. et al., 2016; Wang and Liu, 2016). In these processes, HIRs usually choose the oxidative quenching pathway to furnish the key fluoroalkyl radicals, thus enabling the synthesis of a wide variety of fluoroalkylated compounds.

In 2018, Qing and coworkers reported the decarboxylative trifluoromethylation of (hetero)arenes using $ArI(OCOCF_3)_2$ as CF_3 source by ruthenium photoredox catalysis (Yang et al., 2018) (**Figure 3A**). A series of fluorinated $ArI(OCOCF_3)_2$ were examined and $C_6F_5I(OCOCF_3)_2$ (FPIFA) was proved to be the best option. Notably, FPIFA is easily accessible from C_6F_5I and TFA in the presence of oxone (Harayama et al., 2006; Zagulyaeva et al., 2010), and C_6F_5I could be recycled from the decarboxylation reaction in high yield.

The authors proposed the reaction mechanism depicted in **Figure 3E**. Initially, $Ru(bpy)_3^{2+}$ is excited by visible light to generate the excited specie $^*Ru(bpy)_3^{2+}$, which performs the SET process with FPIFA to afford the iodanyl radical, accompanied by the formation of $Ru(bpy)_3^{3+}$. Then, the resulting iodanyl radical extrudes C_6F_5I to release the trifluoroacetoxy radical, which can undergo further scission, leading to the formation of CF_3 radical. The CF_3 radical thus attack the aromatic ring in arene to give aromatic radical. The aromatic radical might be oxidized either by $Ru(bpy)_3^{3+}$ (path a) or by FPIFA (path b) to yield the corresponding aromatic cation. At last, the aromatic cation is converted into the target product through the deprotonation or nucleophilic attack process.

Later, Xia and coworkers reported a mechanistically similar reaction for the synthesis of perfluoroalkylated aminoquinolines *via* R_f radical intermediates (Han et al., 2019) (**Figure 3B**). The perfluoroalkylation reagents, such as FPIFA, $C_6F_5I(OCOCF_2CF_3)_2$ and $C_6F_5I(OCOCF_2CF_2CF_3)_2$, were all effective in the reaction. Moreover, similar to reported by Qing et al. (Yang et al., 2018), those HIRs can also be easily re-covered by reaction of the by-product pentafluoroiodobenzene with perfluorocarboxylic acids in the presence of oxone.

Xu and coworkers developed a method of hydrotrifluoromethylation of benzyl-protected homoallylic alcohol and amine derivatives employing Togni's reagent as the CF_3 radical source under organic photoredox catalysis (Wang et al., 2019) (**Figure 3C**). Togni's reagent was found to be a more effective trifluoromethylation reagent than CF_3SO_2Cl

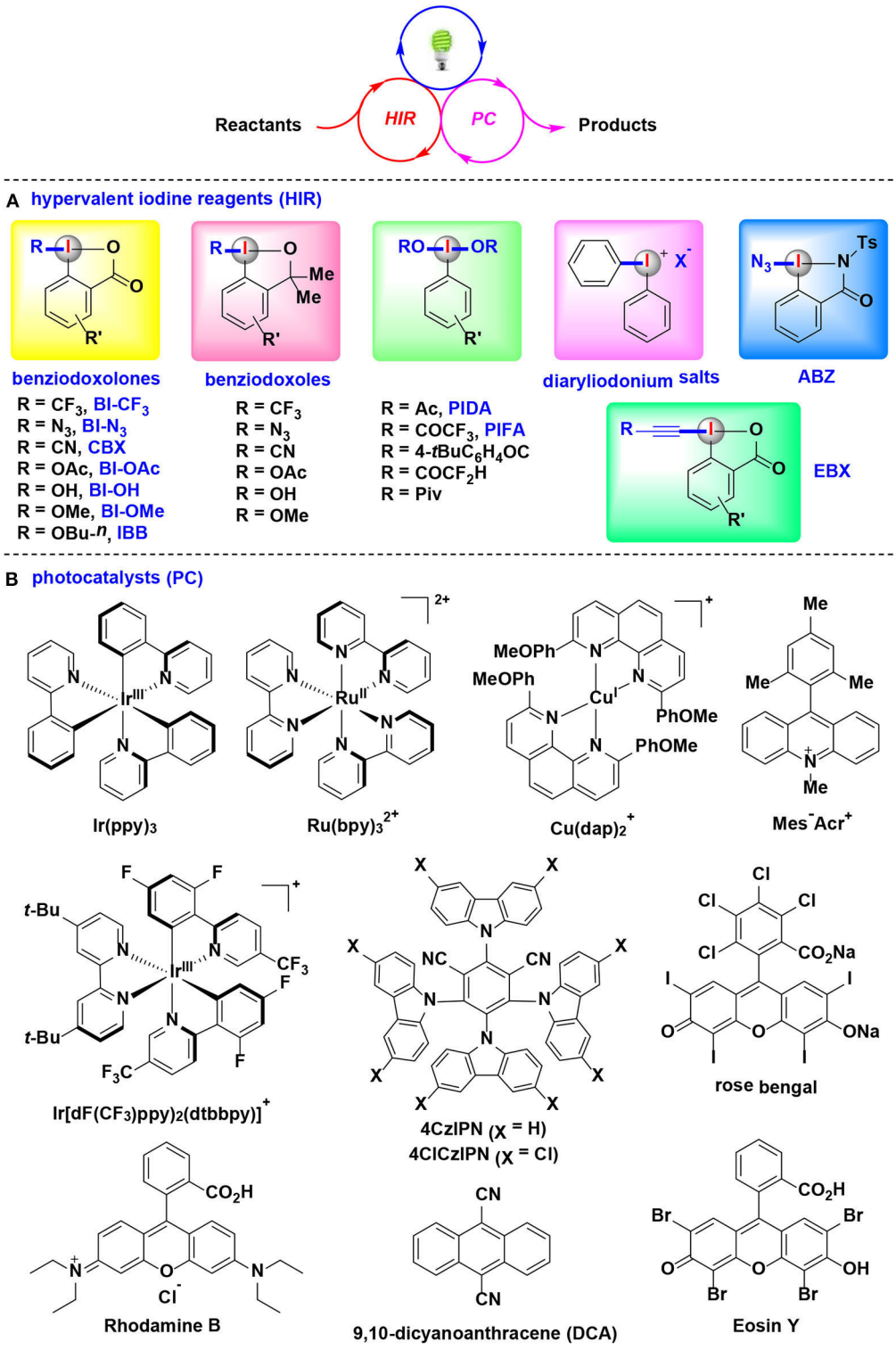

FIGURE 1 | The synergistic combination of visible-light-induced photoredox catalysis with HIRs, and typical photocatalysts and HIRs using in this methodology.

TABLE 1 | Redox potentials of typical photocatalysts that featured in this review.

PC	$E_{1/2}$ (PC^+/PC^*)	$E_{1/2}$ (PC^*/PC^-)	$E_{1/2}$ (PC^+/PC)	$E_{1/2}$ (PC/PC^-)	References
fac-Ir(ppy)$_3$	−1.73	+0.31	+0.77	−2.19	(Lemos et al., 2019)
$[Ru(bpy)_3]^{2+}$	−0.81	+0.77	+1.29	−1.33	(Lemos et al., 2019)
$[Ir(dF(CF_3)ppy)_2(dtbbpy)]^+$	−0.89	+1.21	+1.69	−1.37	(Lemos et al., 2019)
4CzIPN	−1.04	+1.35	+1.52	−1.21	(Lemos et al., 2019)
Eosin Y	−1.60	+1.18	+0.72	−1.14	(Reckenthaler and Griesbeck, 2013)
Rose bengal	−0.68	+0.99	+1.09	−0.78	(Reckenthaler and Griesbeck, 2013)
DCA	−1.01	+2.07	+1.89	−0.83	(Reckenthaler and Griesbeck, 2013)

All potentials are given in volts in CH_3CN vs. the saturated calomel electrode (SCE).

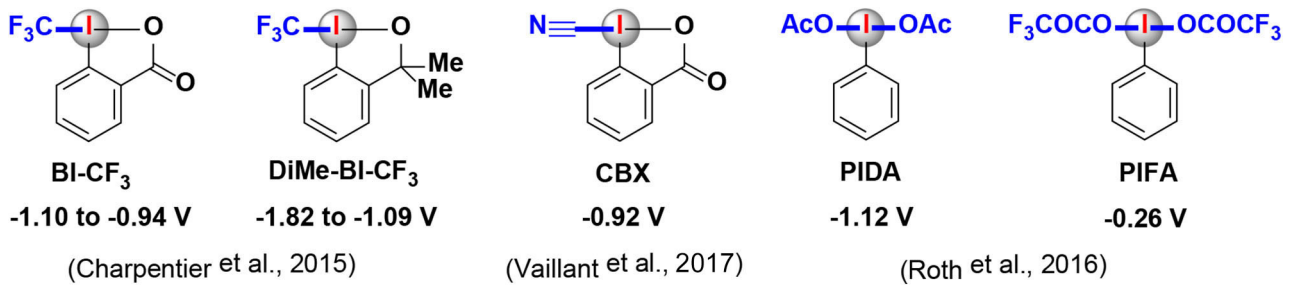

FIGURE 2 | Redox potentials of HIRs that featured in this review.

in the reaction. Dye 4CzIPN (2,4,5,6-tetra(9*H*-carbazol-9-yl)isophthalonitrile) has been demonstrated as a competent organic photoredox catalyst for generation of trifluoromethyl radicals from Togni's reagent. It is noteworthy that the reaction proceeds through an oxidative quenching process to deliver a CF_3· radical followed by a crucial 1,5-hydrogen transfer relay with *in situ* removal of benzyl group.

An efficient photoredox-catalyzed protocol for the introduction of fluorinated groups into the coumarin framework was established by Xiang's group in 2019 (Song et al., 2019) (**Figure 3D**). The reaction takes place efficiently using *fac*-Ir(ppy)$_3$ as the photocatalyst under the irradiation of blue LEDs. When Togni's reagent used as the perfluoroalkylated radical resource in this protocol, *ortho*-hydroxycinnamic esters were converted into 3-trifluoromethylated coumarins *via* a photoredox-catalyzed cascade in moderate to good yields.

Azidation

Since its first report in 1994 by Zhdankin and co-workers, azidobenziodoxol(on)es (ABXs, Zhdankin reagents) have established themself as valuable alternatives to other azide sources due to easy handling (crystalline solid) and the enhanced stability (being stable up to 130°C) (Fumagalli et al., 2015). These cyclic HIRs have recently been popularly utilized as azide-transfer reagents for azidation of a broad range of substrates (Huang and Groves, 2016). Under visible-light irradiation and in the presence of PC, the weak I–N_3 bond in azido I(III) reagent frequently undergoes homolytic cleavage to form an azidyl radical and an iodanyl radical, thus triggering the radical chain process to provide the azidated product.

Chen and coworkers disclosed an impressive protocol for the azidation of 3°C(sp^3)–H bonds of complex substrates using the Zhdankin reagent under Ru photoredox catalysis (Wang et al., 2016) (**Figure 4A**). The azidation reactions demonstrated excellent 3°C–H selectivity and functional group compatibility. Interestingly, when chlorine or bromide donor was added into the reaction system, this protocol can be further modulated to access aliphatic C–H chlorination and bromination, respectively.

Greaney and coworkers have achieved a direct benzylic C–H azidation using the Zhdankin reagent under photoredox catalysis (Rabet et al., 2016) (**Figure 4B**). Reaction optimization showed that common photoredox catalysts such as Ru(bpy)$_3$Cl$_2$ and Ir(ppy)$_3$ are totally ineffective, while Sauvage catalyst Cu(dap)$_2$Cl is found to be unique for this azidation. Moreover, the C–N bond formation is wide applicable to primary, secondary, or tertiary benzylic position. The authors proposed the reaction mechanism depicted in **Figure 4F**. It is believed that the photoexcited state $^*Cu(dap)^{2+}$ firstly reductive cleaves BI-N_3 to generate a source of azide radicals, then the azide radical serves as the H abstractor to convert the benzylic C–H substrate to a benzyl radical. Subsequently, the benzyl radical attacks BI-N_3 to form the azidated product and gives the chain-carrying iodane radical. The iodane radical thus regenerates benzyl radical by abstracting

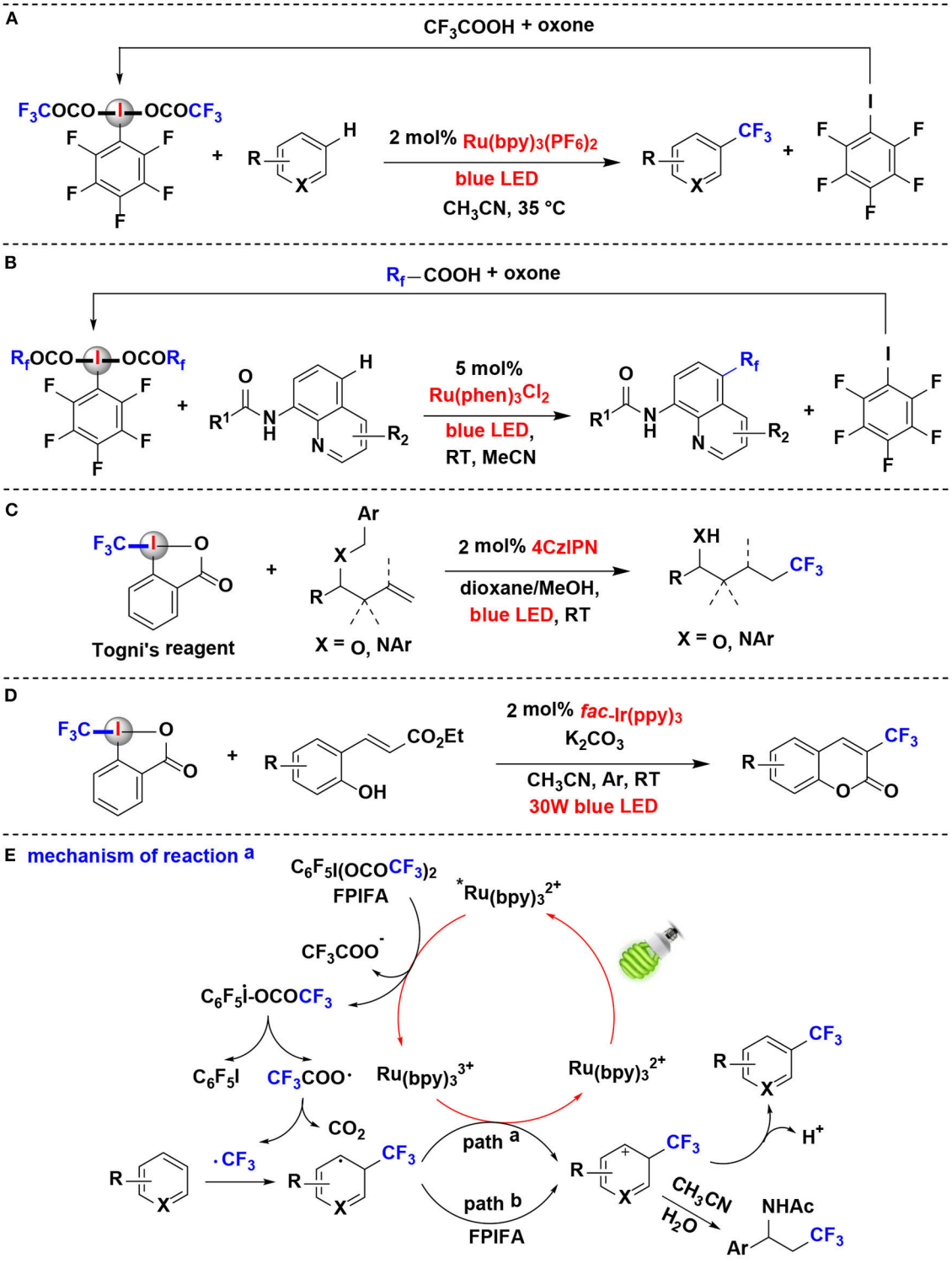

FIGURE 3 | Photoredox-catalyzed fluoroalkylation using HIRs as fluoroalkyl-transfer reagents. **(A)** Trifluoromethylation of (hetero)arenes. **(B)** Perfluoroalkylation of aminoquinolines. **(C)** hydrotrifluoromethylation of benzyl-protected homoallylic alcohol and amine derivatives. **(D)** Trifluoromethylation of ortho-hydroxycinnamic esters. **(E)** Mechanism of reaction **(A)**.

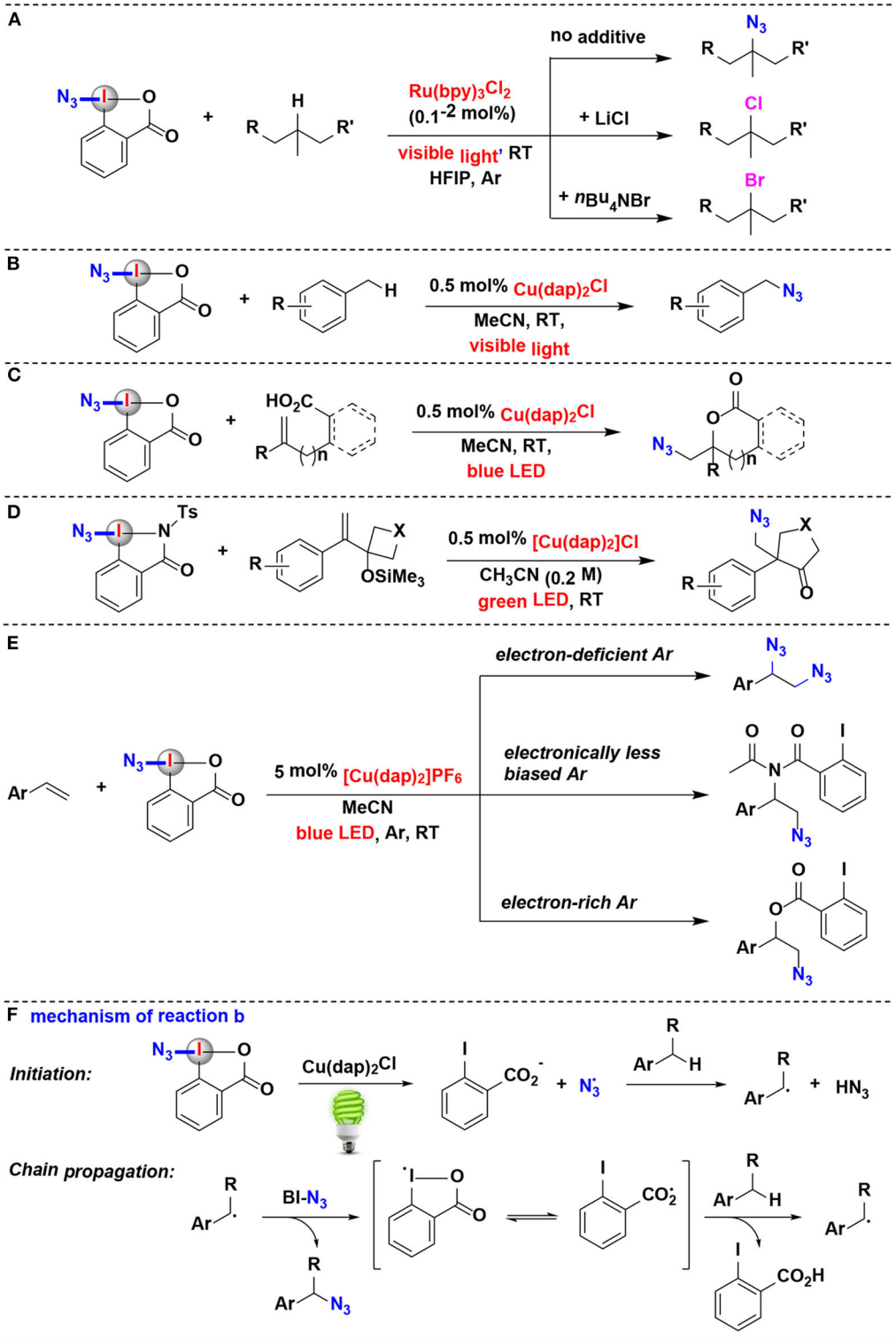

FIGURE 4 | Photoredox-catalyzed azidation using HIRs as azide-transfer reagents. **(A)** Azidation and halogenation of tertiary aliphatic C–H bonds. **(B)** azidation of benzylic C–H bonds. **(C)** Azidation and cyclization of carboxylic acids onto alkenes. **(D)** Azidative ring-expansion of silylated cyclobutanols. **(E)** Azidation/difunctionalization of vinyl arenes. **(F)** Mechanism of reaction **(B)**.

a hydrogen atom from benzylic substrate and then propagates the radical chain reaction.

In 2017, the Waser's group reported a method of synthesis of azidolactones starting from alkene-containing carboxylic acids (Alazet et al., 2017) (**Figure 4C**). Using Zhdankin reagent as the azide-transfer reagent and only 0.5 mol% $Cu(dap)_2Cl$ as photoredox catalyst, (1,2)-azidolactones were achieved under visible light irradiation. Zhdankin reagent and azidodimethylbenziodoxole (ADBX), two typical azide-transfer reagents, exhibited divergent reactivity in the azidolactonization: Zhdankin reagent was ideally suited for 1,2-azidation under photoredox conditions, while Lewis acid activation of ADBX led to 1,1-azidolactonization *via* a 1,2-aryl shift. When ADBX was used instead of Zhdankin reagent under the same photoredox conditions, only traces of (1,2)-azidolactones were observed.

Shortly after its discovery, this visible-light-promoted photoredox-catalyzed azidation methodology was elegantly expanded to alkene-substituted cyclobutanol derivatives by the same group (Alazet et al., 2018) (**Figure 4D**). In 2018, they introduced two new cyclic iodine(III) reagents (CIRs) with higher molecular weight for azidation: *t*Bu-ABX and ABZ (azidobenziodazolone). The two reagents showed a better safety profile than the most commonly used Zhdankin reagent, which was both shock and friction sensitive. Furthermore, either *t*Bu-ABX or ABZ can be used as alternatives to the Zhdankin reagent in a broad range of transformations including photoredox catalysis. They developed an azidative ring-expansion of alkene-substituted cyclobutanol derivatives using ABZ as the safer azido-radical source and $Cu(dap)_2Cl$ as photoredox catalyst.

In 2019, the group of Yu has investigated the visible-light-driven azidation of vinyl arenes with Zhdankin reagent as azidating agent in acetonitrile by using $[Cu(dap)_2]PF_6$ as photocatalyst (Wu et al., 2019) (**Figure 4E**). It was found that the electronic nature of the aryl group attached to the olefin moiety plays a profound effect on the reaction consequence: when the aryl group was less electronically biased, amido-azidation products were obtained as major products through a three-component reaction involving the solvent acetonitrile as well as Zhdankin reagent. The mechanistic investigations suggested that these amido-azidation products were probably formed *via* the photoredox catalysis pathway.

Alkynylation

HIRs, such as alkynyliodonium salts and ethynylbenziodoxol(on)es (EBXs), have been demonstrated as efficient and versatile alkynylating reagents for alkynylation. Very recently, the synergistic merger of photoredox catalysis with HIRs (especially EBXs) paved the way to radical alkynylation of carboxylic acids and alcohols, thus enabling the synthesis of valuable aryl-, alkyl and silyl-substituted acetylenes (Kaschel and Werz, 2015; Waser, 2016; Vaillant and Waser, 2017).

Decarboxylative Alkynylation of Carboxylic Acids

Based on the previous success on visible-light photoredox catalytic decarboxylative alkynylation of carboxylic acids, Li, Cheng, and co-workers developed a metal-free procedure in which 9,10-dicyanoanthracene (DCA) (Romero and Nicewicz, 2016; Neumeier et al., 2018) serve as the photoredox catalyst for the replacement of the classic iridium catalysts (Yang C. et al., 2016) (**Figure 5A**). The results showed that carboxylic acids could be efficiently photo-oxidated by only 5 mol% of cheap organic photocatalyst DCA at room temperature. Moreover, natural sunlight can also be used as a light source. A gram-scale reaction further demonstrates the synthetic utility of this methodology.

Due to its mild conditions to generate radicals, the photoredox catalysis provides a rational basis for developing novel strategies in biomolecule functionalization (Hu and Chen, 2015). Especially, photoredox-catalyzed decarboxylation strategies were successfully applied to selectively functionalize the C-terminal position of native peptides. Following their success on photoredox-catalyzed decarboxylative alkynylation of α-amino acids using EBXs, Waser and coworkers recently extended the methodology for decarboxylative alkynylation on C-terminus of peptides (Garreau et al., 2019) (**Figure 5B**). Using EBXs as alkynylation reagents and 4CzIPN as photoredox catalysts, alkynylated peptides can be efficiently achieved in 30 min at room temperature under blue LEDs irradiation. Moreover, this reaction exhibited superior selectivity for the C-terminus in the presence of carboxylic acid side-chains. The results showed that EBX reagents possess a high potential for biomolecule functionalization under mild photoredox-catalyzed conditions.

In 2018, the same group has shown that EBX reagents allowed the alkynylation of cyclic alkyl ketone oxime ethers through oxidative photoredox cycles, and versatile alkynyl nitriles were synthesized *via* a fragmentation-alkynylation sequence (Franck et al., 2018) (**Figure 5C**). It is worth noting that modified 4XCzIPN dyes were demonstrated as efficient photoredox organocatalysts in this methodology, and their redox properties were determined by both cyclic voltammetry and computation. Among them, 4ClCzIPN dye exhibited highly efficient in the fragmentation-alkynylation process. Various aryl-substituted EBX reagents worked well under the reaction condition. Preliminary investigations showed that other HIRs, such as silyl EBX reagent (TIPS-EBX), cyanobenziodoxolone (CBX) and phenyl vinyl benziodoxolone (PhVBX), can also react with oxime ethers under the same reaction conditions to achieve the corresponding alkynylation, cyanation, and alkenylation products. However, when Togni's reagent was employed, no desired trifluoromethylation product was obtained.

Based on investigations conducted in this study, it is believed that the mechanistic pathway in this process (**Figure 5D**) begins with reductive quenching of the photoexcited state PS* of 4ClCzIPN dye by potassium carboxylate to give carboxyl radical and the reduced state photocatalyst. The resulting carboxyl radical undergoes decarboxylation to furnish the α-oxy radical, which subsequently eliminates the acetone to generate iminyl radical. ^{1}H NMR evidence showed that the carboxyl radical can also be trapped by EBX reagent and then hydrated to give a by-product of the ketone. Ring-opening of the iminyl radical then gives an alkyl nitrile radical. The alkyl nitrile radical reacts with EBX and proceeds through a transition

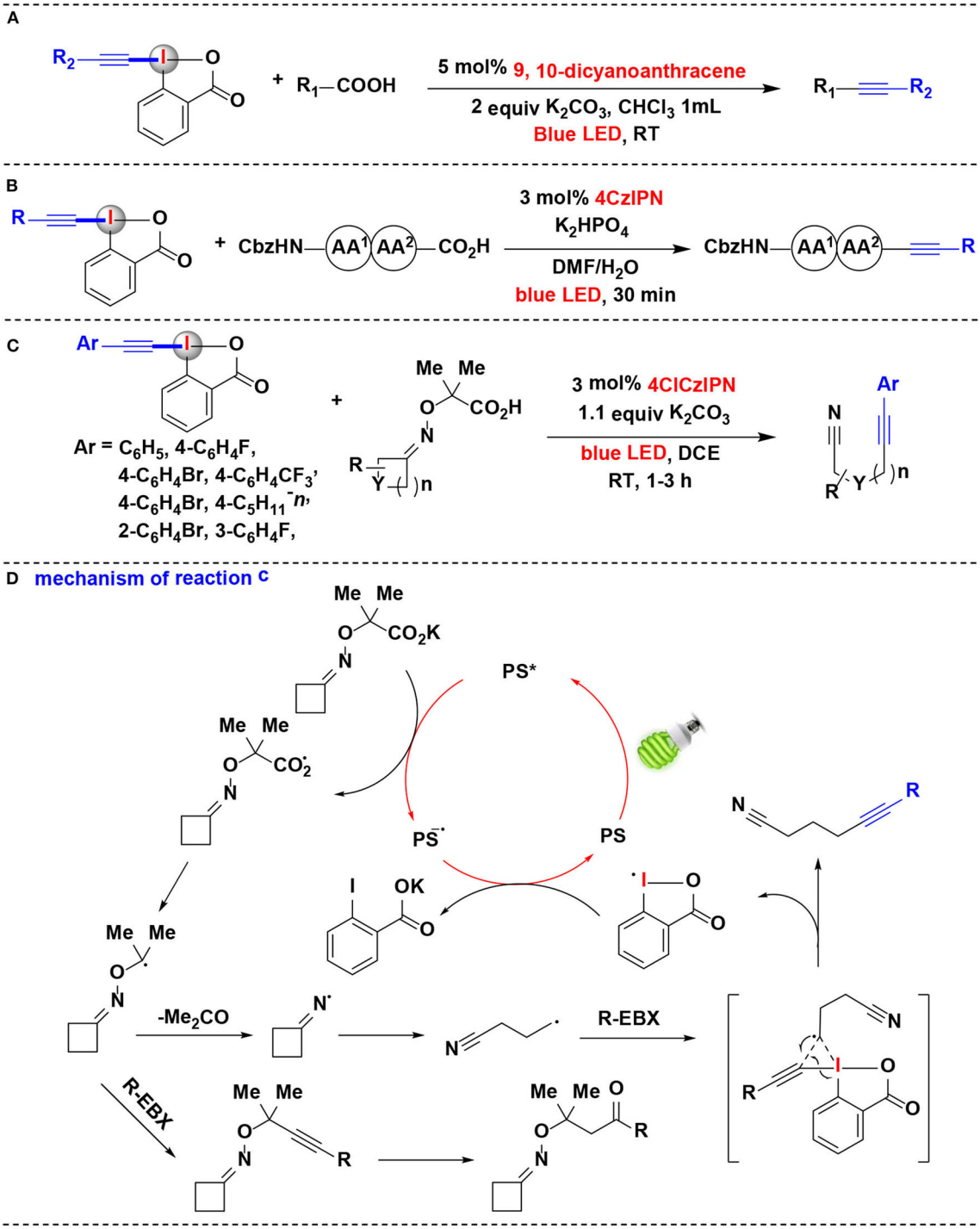

FIGURE 5 | Photoredox-catalyzed decarboxylative alkynylations of carboxylic acids with EBXs. **(A)** Decarboxylative alkynylation of α-amino/α-oxo/α-keto acids. **(B)** Decarboxylative alkynylation of the C-terminus of peptides. **(C)** Fragmentation-alkynylation cascades of cyclic oxime ethers. **(D)** Mechanism of reaction **(C)**.

state to give the final product and cyclic hypervalent iodine radical. The reduction of the hypervalent iodine radical provides carboxylate and regenerates the ground state PS to accomplish the organocatalysis cycle.

Alkynylation of Alcohols

Similar to carboxylic acids, alcohols can also be efficiently alkynylated employing EBXs as alkynylating reagents under photoredox-catalyzed conditions. It should be noted that an HIR

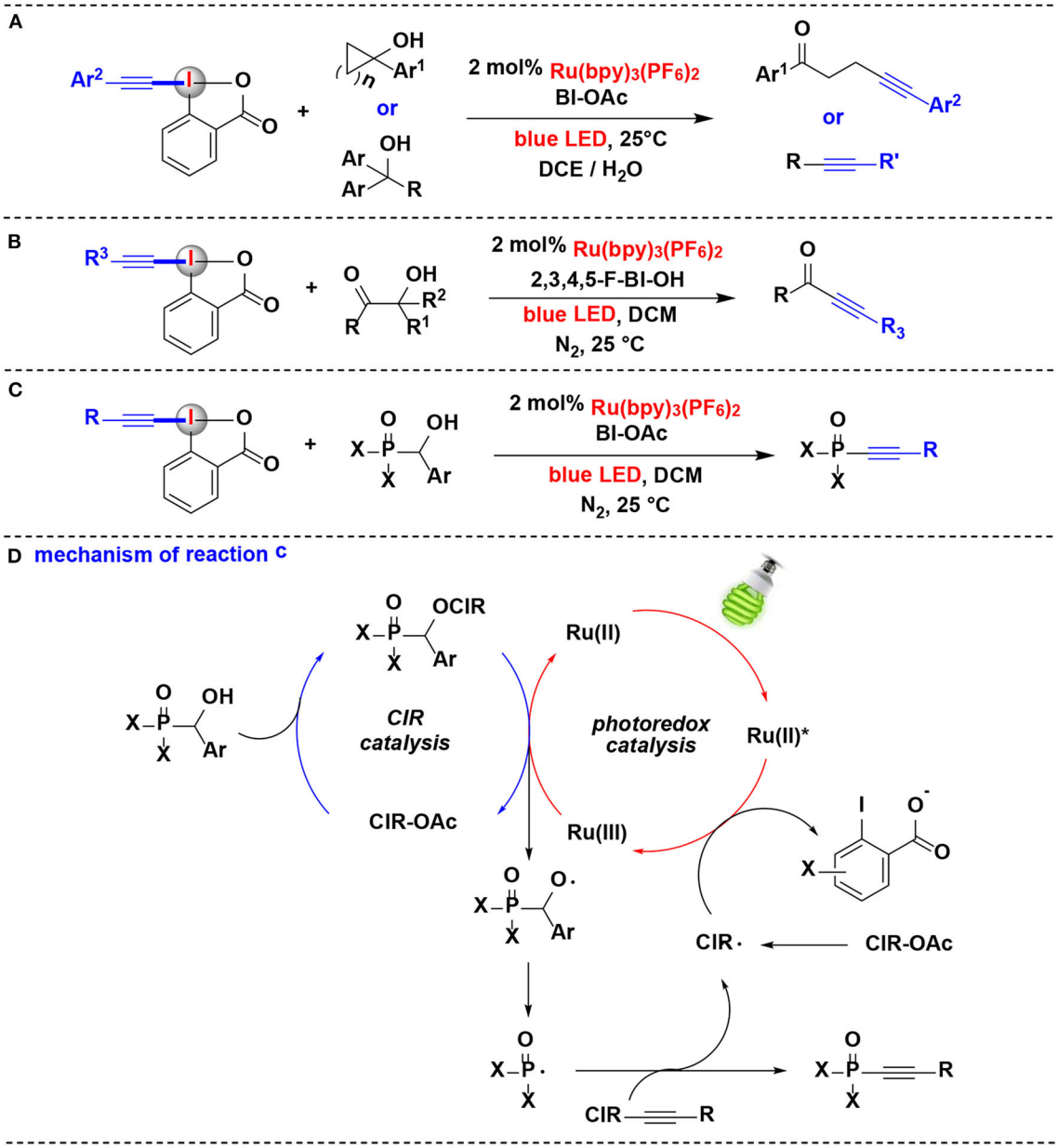

FIGURE 6 | Photoredox-catalyzed alkynylation of alcohols with EBXs. **(A)** Alkynylation of cycloalkanols and linear alcohols. **(B)** Alkynylation of β-amide/β-ester/β-ketone alcohols. **(C)** Alkynylation of α-phosphorus alcohols. **(D)** Mechanism of reaction **(C)**.

catalysis circle, in which HIR catalyzes the generation of alkoxyl radicals, is often combined with the photoredox catalysis circle in those methodologies.

Chen and co-workers have conducted a series of studies aiming at photoredox-catalyzed alkynylation of different types of alcohols. In 2016, this group exploited the combination of photoredox catalysis and CIR catalysis for alkynylation of alcohols using alkyl-EBX reagents (Jia et al., 2016) (**Figure 6A**). Under the dual CIR/photoredox catalytic system, both strained cycloalkanols and linear alcohols can react with alkyl-EBXs delivering the corresponding alkynylation adducts. Moreover, structurally complex steroidal cycloalkanols can also convert into χ-alkynyl ketones smoothly. Various aryl substituents appended to EBXs are suitable for this process. The key to success in this transformation was the visible-light-induced alcohol oxidation for generation alkoxyl radicals and the subsequent β-fragmentation of alkoxyl radicals into alkyl radicals. Compared with those that employ transition metal activation under strong oxidative conditions, visible-light-induced alkoxyl radical generation by CIR catalysis proceeds smoothly at room temperature.

In 2017, this group also developed another C-C bond cleavage/alkynylation reactions of β-amide, β-ester, and β-ketone alcohols with EBXs *via* similar dual CIR/photoredox catalysis, and ynamides, ynoates, and ynones were respectively constructed with excellent regio- and chemoselectivity (Jia et al., 2017) (**Figure 6B**).

Following the above successes, they further extended the dual CIR/photoredox catalytic methodology to α-phosphorus alcohols in 2018 (Jia et al., 2018) (**Figure 6C**). Various arylphosphinoyl-, alkylphosphinoyl-, phosphonate-, and phosphonic amide alcohols undergo P-C(sp^3) bond cleavage/radical alkynylation with EBXs to construct phosphonoalkynes for the first time. Different cyclic iodine(III) reagents, such as BIOAc, 3,4-F-BIOAc, 2,3,4,5-F-BIOH, and 3,4-OMe-BIOAc, were all effective to promote the reaction. A range of EBXs (BI-alkynes) including o*rtho*-, *meta*-, or *para*-aryl substituents were well tolerated in the reaction.

A plausible mechanism for this process is depicted in **Figure 6D**, the α-phosphorus alcohol first reacted with CIR to generate the benziodoxole/α-phosphorus alcohol complex *in situ*, which releases the alkoxyl radical and revives of CIR for the new catalytic cycle upon oxidation by $Ru(bpy)_3^{3+}$. The $Ru(bpy)_3^{3+}$ was originated from the oxidative quenching of the photoexcited $^*Ru(bpy)_3^{2+}$ by CIR. The resulting alkoxyl radical subsequent carries on P-C(sp^3) bond cleavage to generate the phosphorus radical, and further performs radical α-addition with the BI-alkyne to yield the desired phosphonoalkyne product.

Other Reactions

Cyanation

In 2017, Waser's group extensively investigated the photoredox mediated decarboxylative cyanation of aliphatic acids using HIRs as cyano-transfer reagents (Le Vaillant et al., 2017) (**Figure 7**). In their model reaction, the cyanation reactivities of six hypervalent iodine-based cyanation reagents were evaluated (**Figure 7A**). Under photoredox catalysis, CDBX and acyclic iodine reagent were almost inefficient while cyanobenziodoxolone (CBX) gave the product in excellent yield, these results showed the superiority of CBX as a cyanide source. The subsequent substrate scope investigation indicated that this methodology allowed efficient cyanation of α-amino and α-oxy acids into the corresponding nitriles (**Figures 7B,C**). Furthermore, the direct cyanation of dipeptides and drug precursors was also achieved.

Computational and experimental evidences suggested that the favored decarboxylative cyanation mechanism may probably different from the usually assumed decarboxylative alkynylation (Le Vaillant et al., 2015; Zhou et al., 2015). The proposed reaction mechanism (**Figure 7D**) consists of the irradiation of IrL_2^+ with blue LED gives the excited-state $^*IrL_2^+$, which subsequently carries on SET process with the *in situ* generated cesium carboxylate to regenerate the IrL_2 complex and together give the key nucleophilic radical intermediate. The reaction of the radical intermediate with CBX provides the desired nitrile and an iodine centered radical. Finally, this iodine centered radical undergoes another SET process with the IrL_2 complex to close the catalytic cycle.

Acetoxylation

In 2019, Santra, Hajra, Majee and coworkers developed a method for regioselective coupling of C(sp^3)-H of aryl-2*H*-azirine and (diacetoxy)-iodobenzene (PIDA) using visible light irradiation (De et al., 2019) (**Figure 8**). Aryl-2*H*-azirines with different functional groups were converted into the corresponding acetoxylated azirines under aerobic condition. Organophotocatalyst, rose Bengal (RB), was found to be more efficient in this reaction than transition-metal photoredox catalysts, such as $Ru(bpy)_3Cl_2{\cdot}6H_2O$ and $Ir(ppy)_3$. Notably, this protocol can be carried out in gram-scale.

The proposed mechanism of the acetoxylation reaction is shown in **Figure 8C**. Firstly, when irradiation with blue LED, rose bengal (RB) was excited into the excited state RB*, which performs an SET reduction with PIDA to generate the acetoxy radical ($CH_3COO\cdot$), accompanied by formation of the cation radical ($RB^{+\cdot}$), PhI, and CH_3COO^-. Abstraction of the hydrogen atom of aryl-2H-azirine by acetoxy radical provides the 2*H*-azirine radical. The 2*H*-azirine radical then undergoes a second SET oxidation with $RB^{+\cdot}$, leading to the formation of intermediate carbocation while completing the photocatalytic cycle. Finally, the intermediate carbocation couples with the acetate anion giving the corresponding acetoxylated azirine.

Diazomethylation

In 2018, Suero and co-workers developed an aromatic C-H bond diazomethylation reactions using the pseudocyclic hypervalent iodine (I) by ruthenium photoredox catalysis (Wang Z. et al., 2018) (**Figure 9**). The pseudocyclic hypervalent iodine (I) carrying a diazoacetate moiety served as a diazomethyl radical precursor through a SET process in photoredox-catalyzed protocol, and a wide range of aromatic hydrocarbons substituted with alkyl groups, halogens, amides and carbonyls undergo C-H diazomethylation to generate valuable diazo compounds.

The authors proposed the reaction mechanism depicted in **Figure 9C**. The photocatalytic system is initiated by the photoexcitation of $[Ru(bpy)_3]^{2+}$ to generate $^*[Ru(bpy)_3]^{2+}$. The photoexcited $^*[Ru(bpy)_3]^{2+}$ undergoes single-electron transfer with the pseudocyclic hypervalent iodine (I) to yield the diazomethyl radical as direct equivalent of carbyne specie, which is further intercepted an aromatic ring to facilitate the cyclohexadienyl radical formation. Finally, the resulting radical intermediate is oxidized by $[Ru(bpy)_3]^{3+}$ and eliminates the proton to obtain the expected diazo compound.

HIRS ACT AS OXIDANTS FOR SUBSTRATE ACTIVATION

Due to the excellent coordinating property of iodine atom, HIRs can easily experience ligand exchange reaction with organic acids to form the hypervalent iodine-coordinated carboxylates. When combination with the photoredox catalysis, those hypervalent iodine-coordinated carboxylates frequently undergo homolytic cleavage to access highly reactive hypervalent iodine radicals as well as the oxygen radicals, thus triggering the decarboxylative functionalization reactions or other

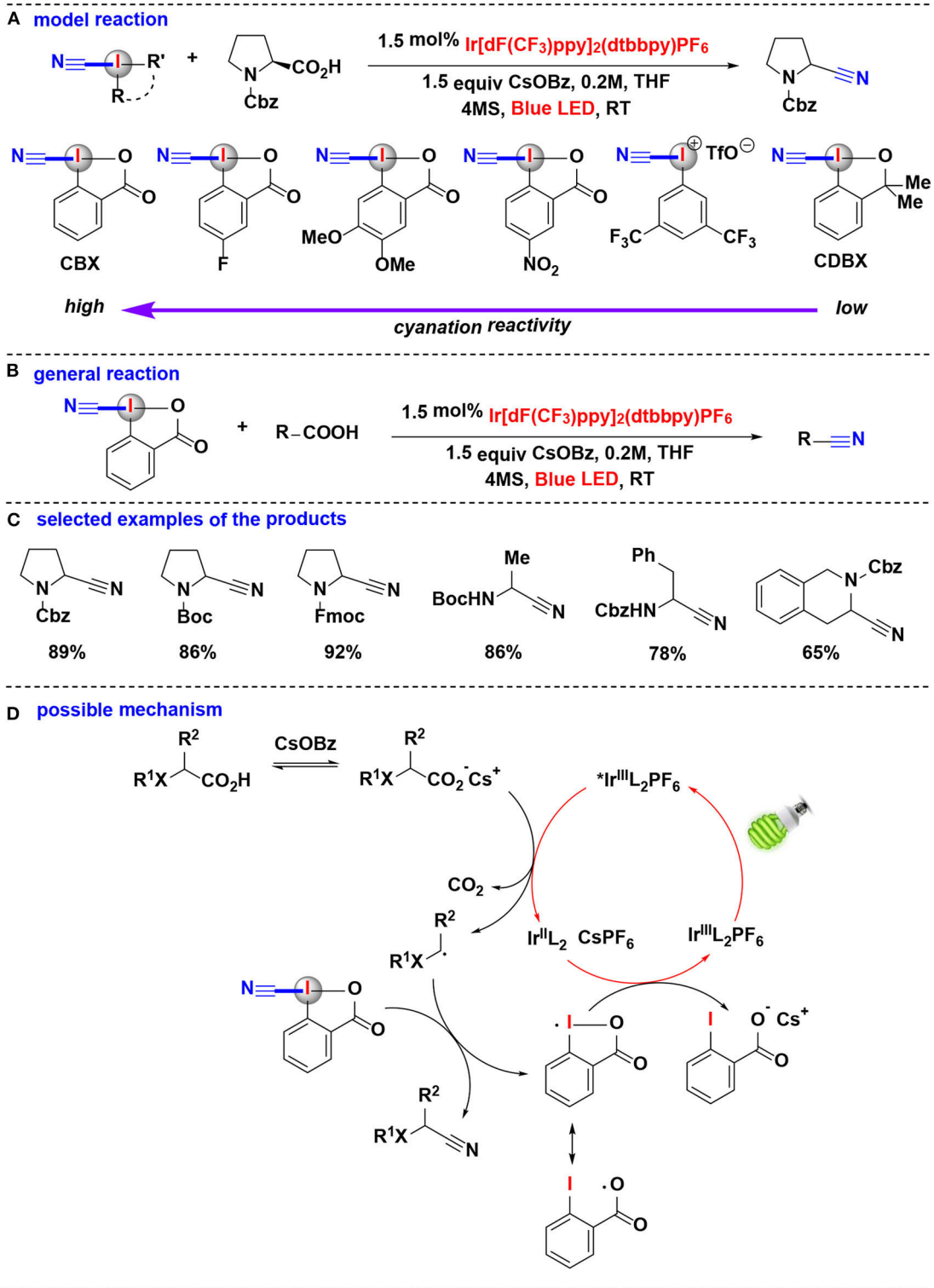

FIGURE 7 | Photoredox mediated decarboxylative cyanation of carboxylic acid with CBX. **(A)** Model reaction of decarboxylative cyanation. **(B)** General reaction of decarboxylative cyanation. **(C)** Selected examples of the cyanation products. **(D)** Possible mechanism.

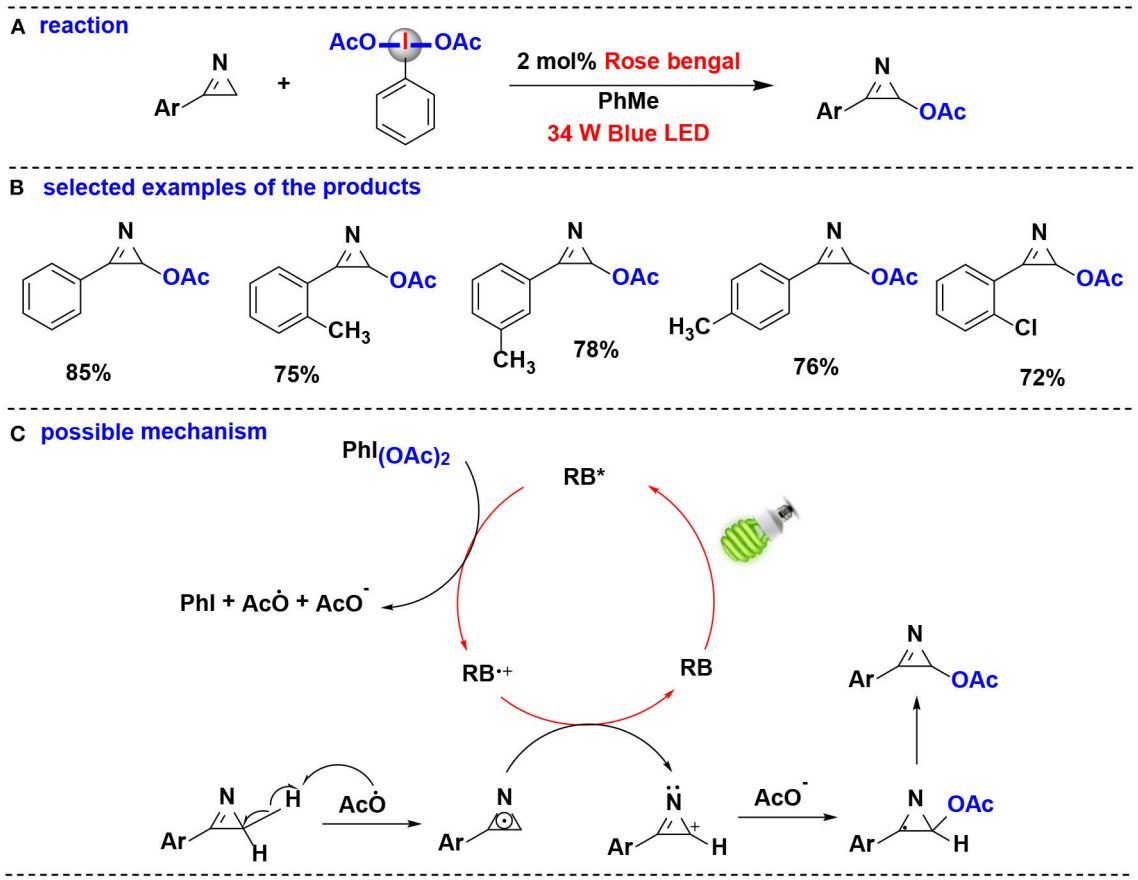

FIGURE 8 | Photoredox-catalyzed C(sp^3)-H acetoxylation of aryl-2*H*-azirines with PIDA. **(A)** General acetoxylation reaction of aryl-2H-azirines. **(B)** Selected examples of the products. **(C)** Possible mechanism.

transformations (Huang et al., 2016; Jia et al., 2018). Based on the above concept, Chen and co-workers have conducted a series of studies on novel dual CIR/photoredox catalytic system (Huang et al., 2015; Jia et al., 2016, 2017), and the research results proved that CIRs played a crucial role in activating the substrates of organic acids and alcohols toward photoredox catalysis.

HIR-Mediated Activation of Organic Acids

An example of CIR-enabled decarboxylative functionalization of α, α-difluoroarylacetic acids, mediated by dual CIR/photoredox catalysis, were developed by Qing and coworkers (Yang B. et al., 2016) (**Figure 10A**). A series of novel difluoroalkylated arenes were smoothly achieved through an HIR-promoted decarboxylation and radical hydroaryldifluoromethylation sequence. All of the tested HIRs including $PhI(OAc)_2$, $PhI(OCOCF_3)_2$, BIOAc and BIOMe give the desired transformation. Among them, BIOMe was the best choice. Further investigation revealed that BIOMe acts not only as an activating reagent but also as an oxidant in the process.

Feng, Xu, and coworkers disclosed a visible-light-enabled reaction in which α,β-unsaturated carboxylic acids are activated by BI-OH, thus leading to the decarboxylative mono- and difluoromethylation transformations (**Figure 10B**) (Tang et al., 2017). Four candidate HIRs, IBDA, IB, BI-OH, BI-OAc, were screened in the reaction. Among them, BI-OH turned out to be optimal. As explained in mechanistic pathway (**Figure 10D**), BI-OH can *in sute* generate a benziodoxole vinyl carboxylic acid complex (BI-OOCCH=CHR), thus activating of the vinyl carboxylic acid group.

Zhang, Luo, and coworker achieved enantioselective decarboxylative coupling of propiolic acid and β-ketocarbonyls by combination of chiral primary amine catalysis and visible-light photoredox catalysis (**Figure 10C**) (Wang et al., 2017). Various of alkynylation adducts were synthesized with excellent enantioselectivities under mild conditions. For HIRs tested in this process, PIFA, PIDA, BI-OAc, and BI-OMe performed almost no catalysis effect, and BI-OH were identified to give the optimal results in terms of both yield and enantioselectivity. Mechanistic studies revealed that BI-OH could *in situ* react with propiolic acid to generate the propiolate under the reaction conditions. This propiolate acted as a key intermediate both in photoredox catalytic circle and the aminocatalytic circle.

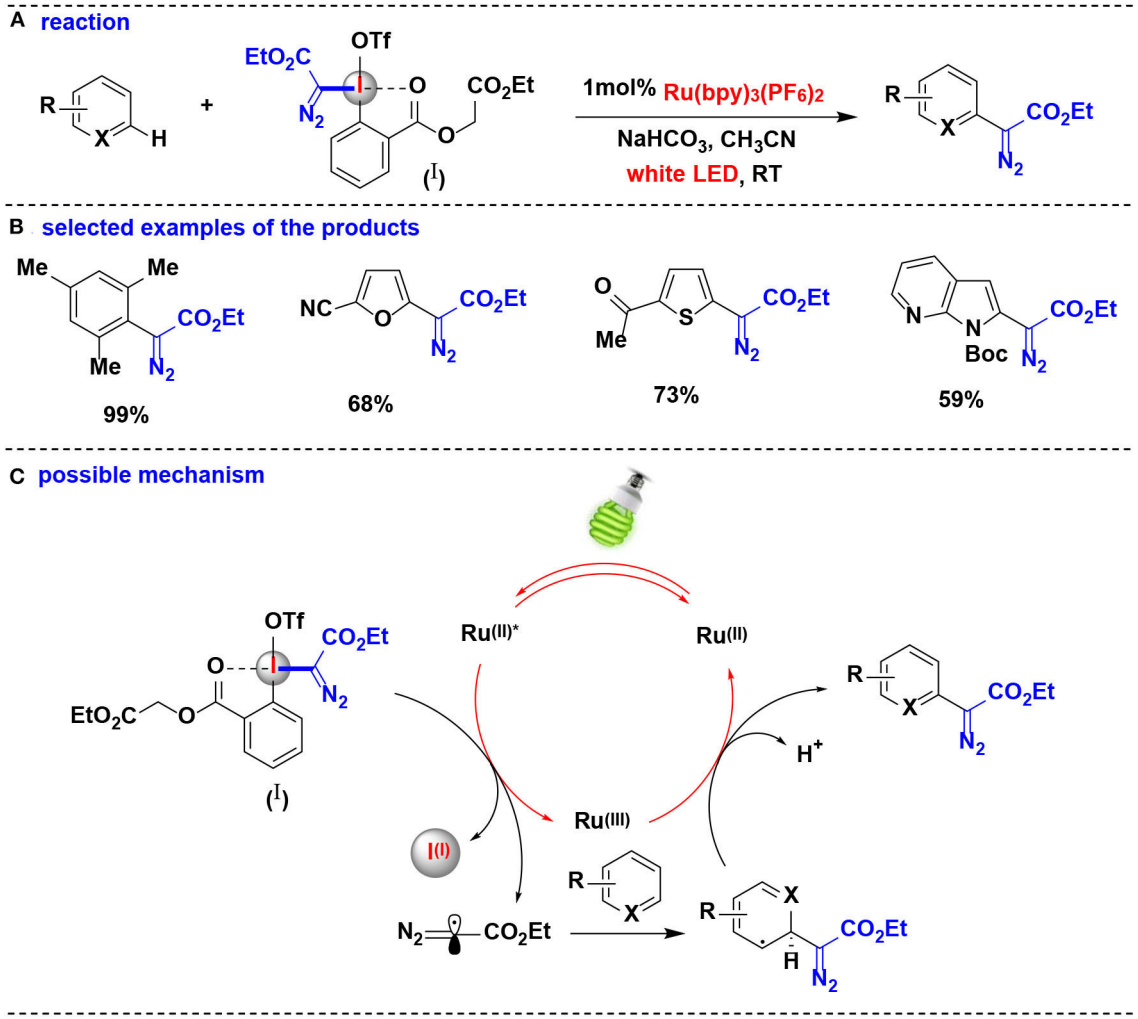

FIGURE 9 | Photoredox catalysis enabled C–H bond diazomethylation of arenes with pseudocyclic HIR. **(A)** General diazomethylation reaction of arenes. **(B)** Selected examples of the products. **(C)** Possible mechanism.

Itami and co-workers developed a mild method for the photoredox-catalyzed decarboxylation of arylacetic acids by HIR in air, thus leading to various aryl-aldehydes and ketones (Sakakibara et al., 2018a) (**Figure 11A**). Photoredox catalyst, HIR, blue light irradiation, and O_2 are all critically important for this transformation. CIR 1-butoxy 1-λ^3-benzo[*d*][1,2]iodaoxol-3(1*H*)-one (IBB) was proved more efficient in the procedure than non-cyclic iodine reagent PIDA. In contrast, Ph_2ICl was completely inefficient. In this process, IBB reacts with arylacetic acid to form intermediate *in situ*, thus activating of the arylacetic acid for decarboxylation.

The same group's subsequent study revealed that the same methodology can also be extended for construction of carbon–nitrogen and carbon–oxygen bonds (**Figure 11B**) (Sakakibara et al., 2018b). Under the activation of IBB, arylacetic acids were directly converted into nitrogen, oxygen, or chlorine functionalities. The reaction of IBB with arylacetic acid was confirmed by ^{1}H NMR, and the resulting complex was a key activated intermediate in the photoredox catalytic cycle of the mechanism pathway.

The authors raised a possible mechanism for the decarboxylative imidation (**Figure 11E**). Initially, arylacetic acid reacts *in situ* with IBB to form benziodoxole/arylacetic acid complex. Meanwhile, the photocatalyst ($[Ru(bpy)_3]^{2+}$) is excited under irradiation of blue light to generate its photoexcited state ($^*[Ru(bpy)_3]^{2+}$). Then the excited ruthenium photocatalyst reduces the benziodoxole/arylacetic acid complex to give $[Ru(bpy)_3]^{3+}$, arylacetic radical, and *o*-iodobenzoate. The arylacetic radical in turn suffers decarboxylation to produce benzyl radical. Parallel to this process, another substrate, imide, is oxidized by $[Ru(bpy)_3]^{3+}$ to provide imidyl radical. Finally, radical-radical coupling of the arylacetic radical and imidyl radical affords the imidation product.

In 2018, the Chen's group further expanded their protocol of photoredox-mediated Minisci alkylation of *N*-heteroarenes

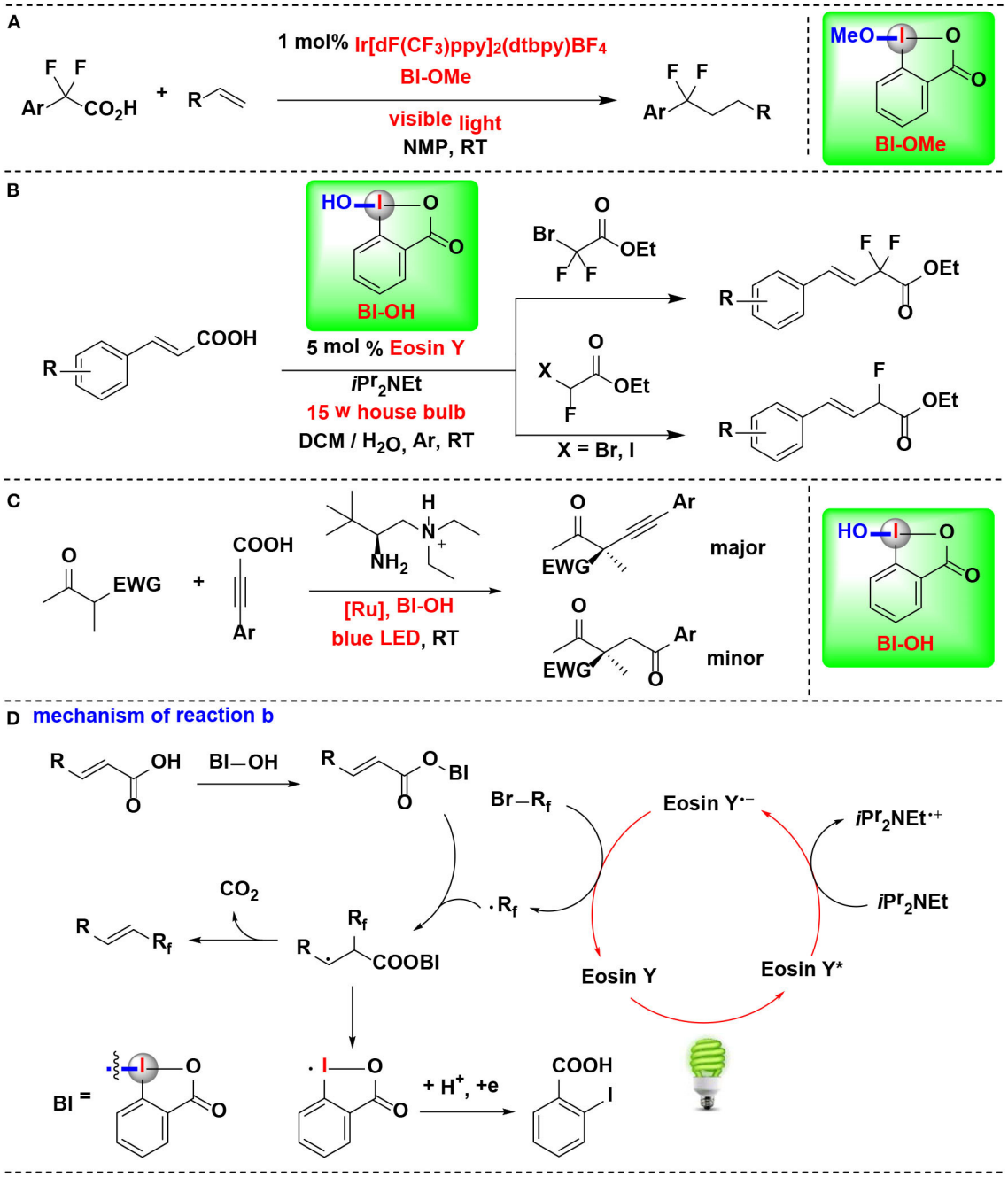

FIGURE 10 | HIR-mediated activation of α,α-difluoroarylacetic acids, α,β-unsaturated carboxylic acids and propiolic acid under photoredox catalysis. **(A)** Activation of α,α-difluoroarylacetic acids for hydroaryldifluoromethylation of alkenes. **(B)** Activation of α, β-unsaturated carboxylic acids for decarboxylative fluoromethylation. **(C)** Activation of propiolic acids for decarboxylative α-alkynylation. **(D)** Mechanism of reaction **(B)**.

reported in 2016 (Li G. X. et al., 2016). In the improved protocol (**Figure 11C**) (Wang J. et al., 2018), the alkylating agents were replaced by aliphatic carboxylic acids, which are more abundant, inexpensive, stable and structurally diverse than alkyl boronic acids. Although the same HIR was employed in both protocols, it actually demonstrated different roles under the photoredox catalysis conditions, and these two reactions proceed through different mechanisms. BI-OAc serves as a radical precursor in former, while in the improved protocol, it is used for substrate activation to facilitate decarboxylative functionalization of carboxylic acids.

Genovino, Frenette, and coworkers developed a C–H alkylation of heteroaromatics using an acridinium photocatalyst and HIRs (**Figure 11D**) (Genovino et al.,

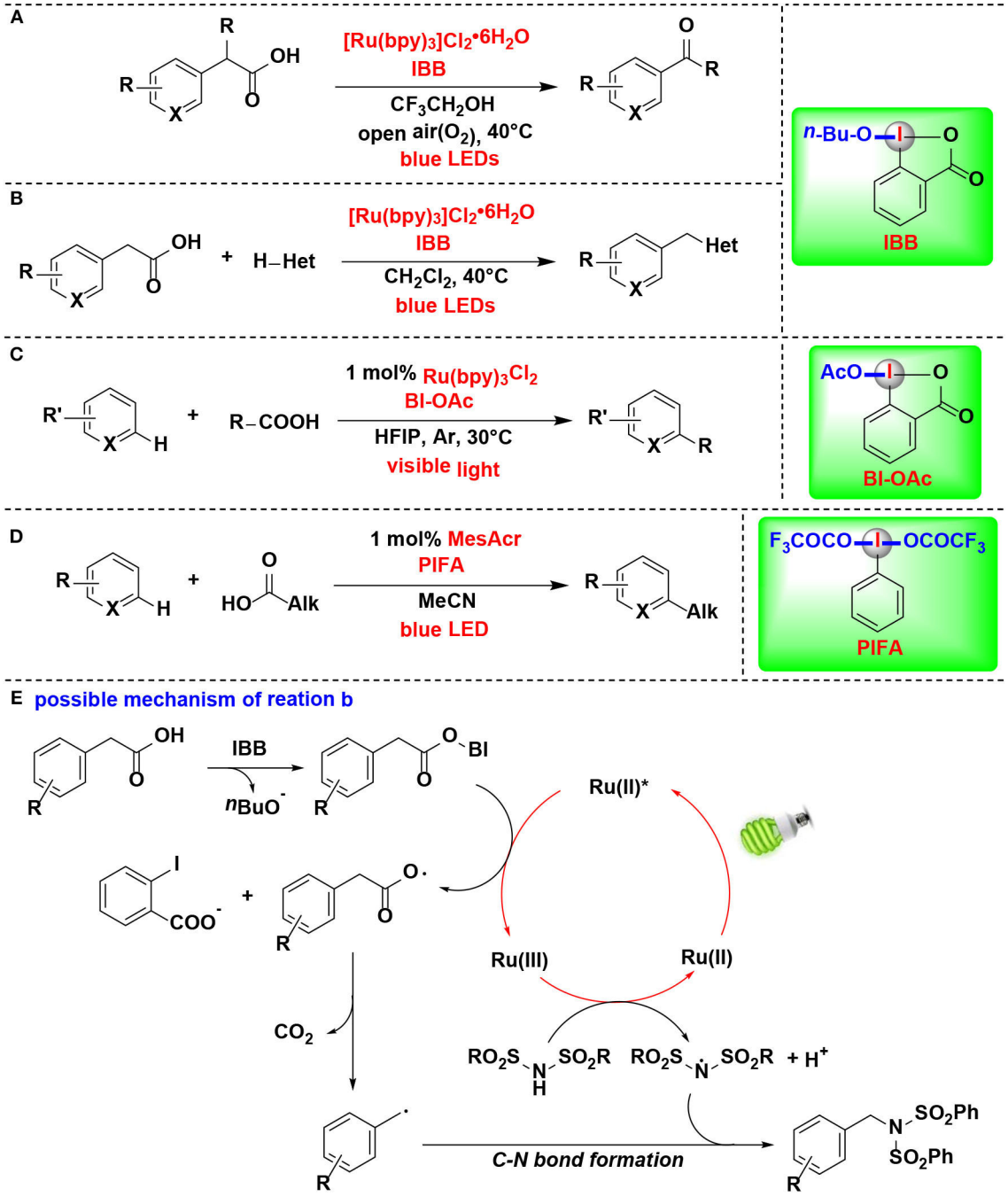

FIGURE 11 | HIR-mediated activation of carboxylic acids under photoredox catalysis. **(A)** Activation of arylacetic acids for decarboxylative oxidation. **(B)** Activation of arylacetic acids for decarboxylative C-X bond formation. **(C)** Activation of aliphatic carboxylic acids for Minisci alkylation. **(D)** Activation of carboxylic acids for C–H alkylation. **(E)** Possible mechanism of reaction **(B)**.

2018). Bis(trifluoroacetoxy)iodo benzene (PIFA), a more soluble and under-utilized HIR, was proved as attractive option. It is noteworthy that the more challenging linear carboxylic acids that form primary radicals are also suitable substrates. A mechanism pathway, which different from other photoredox Minisci reactions catalyzed by transation-metals, was proposed by the authors.

In 2019, Cheng reported a decarboxylative coupling of alkynyl carboxylic acids and aromatic diazonium salts using HIR under eosin Y photoredox catalysis (**Figure 12A**) (Yang

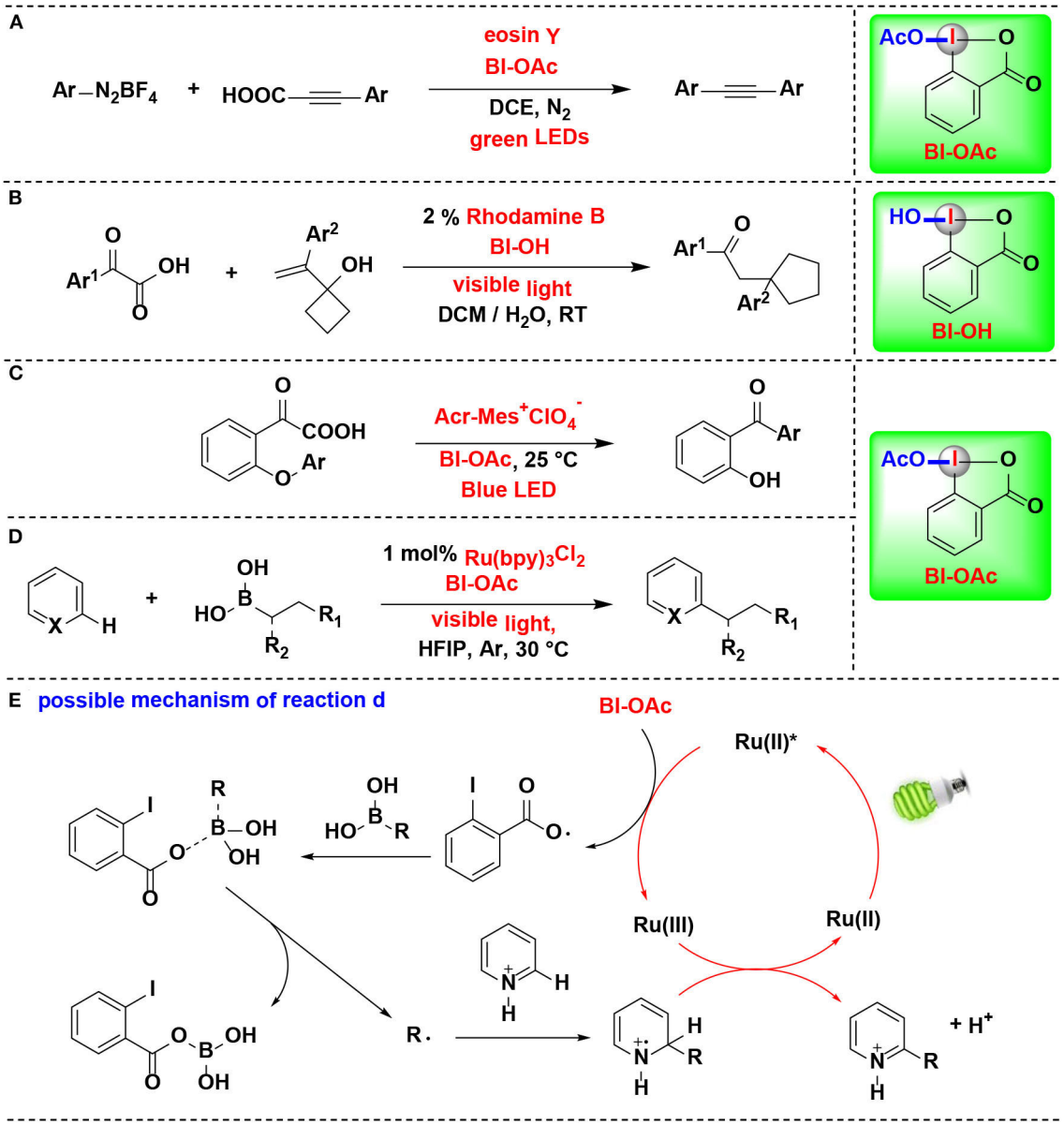

FIGURE 12 | HIR-mediated activation of arylpropiolic acids, α-keto acid and boronic acids under photoredox catalysis. **(A)** Activation of arylpropiolic acids for decarboxylative alkynylation. **(B)** Activation of α-keto acids for decarboxylative acylation/ring expansion. **(C)** Activation of α-keto acids for acyl Smiles rearrangement. **(D)** Activation of alkyl boronic acids for Minisci C–H alkylation. **(E)** Possible mechanism of reaction **(D)**.

et al., 2019). The results showed that BI-OAc superior to BI-OH and BIOMe as decarboxylation facilitated reagent for the reaction. BI-OAc and arylpropiolic acid generated a benziodoxole 3-phenylpropiolate complex *in situ*, which facilitated C–C triple bond conversion in the mechanical pathway proposed by the authors.

Duan and coworkers reported the decarboxylative acylation/ring expansion reactions between vinylcyclobutanols with α-keto acids to construct 1,4-dicarbonyl compounds (**Figure 12B**) (Zhang et al., 2017). This methodology takes advantage of organic photoredox catalysis and merges it with HIR. Both transition-metal and organic photoredox catalysts were examined in the reaction, among them, rhodamine B, an organic dye known for its low cost, less toxic and easy to handle, give the best results. BI-OH was proved to play an important role in facilitating decarboxylation of α-keto acids. Radical-trapping experiments confirmed that nucleophilic acyl radical, which originated from α-keto acid, was involved in this tandem radical process.

Chen and coworkers developed the first acyl radical Smiles rearrangement for transformation of biarylethers into hydroxybenzophenones (Li J. et al., 2019) (**Figure 12C**). Under dual hypervalent iodine(III)/photoredox catalysis, α-keto acids undergo ester exchange with BI-OAc to form BI-keto acid complexes *in situ*, which can readily afford acyl radicals and then suffer 1,5-ipso addition and eventually give hydroxybenzophenones. Two typical non-cyclic iodine(III) reagents, PIDA and PIFA, were proved both less effective than BI-OAc. Organic photocatalyst 9-mesityl-10-methylacridinium perchlorate ($Acr\text{-}Mes^{+}ClO_4^{-}$) superiors to $[Ru(bpy)_3](PF_6)_2$ and $[Ir(ppy)_2(dtbbby)]PF_6$ and gives optimal yields. Particularly, the reaction can be applied in gram-scale synthesis and performed in neutral aqueous conditions, implying its potential biomolecule applications in further.

In 2016, Chen and co-workers developed a new photoredox-mediated protocol for Minisci C–H alkylation of *N*-heteroarenes using alkyl boronic acids as alkylation regents, BI-OAc as oxidants, and $Ru(bpy)_3Cl_2$ as photocatalyst (Li G. X. et al., 2016) (**Figure 12D**). This protocol can be applicable to a range of easily accessible primary and secondary alkyl boronic acids for the preparation of various *N*-heteroarenes, and various functional groups, including alkyl bromide, aryl iodide, ester, amide, carbamate, terminal alkyne, and benzyl chloride, are well-tolerated. Mechanistic experiments suggested that BI-OAc serves as a facile precursor for an ortho-iodobenzoyloxy radical intermediate, which play a key role in the efficient transformation of usually less reactive alkyl boronic acids to form alkyl radicals (**Figure 12E**).

HIR-Mediated Activation of Alcohols

Chen and coworkers reported in 2018 that allylic alcohols can be activated by CIRs under photoredox catalysis conditions, and a series of cyclopentanones, cyclohexanones, and dihydrofuranones bearing α-quaternary centers were synthesized *via* alkyl boronate addition/semi-pinacol rearrangement (**Figure 13A**) (Liu et al., 2018). The interaction between tertiary allylic alcohol and BI-OAc was extensively investigated by crystallography, NMR spectroscopy and cyclic voltammetry experiments, and the results revealed that both the hydroxyl and olefin groups in allylic alcohols were greatly activated *via* coordination to the BI-OAc. The mechanistic investigations suggest that the CIRs employed in this reaction played at least triple roles in the whole pathway: (1) facilitating the formation of the alkyl radical and the cation intermediate, (2) activating the allylic alcohol, and (3) the *in situ* protecting of alcohols for avoiding the formation of the epoxide.

Mao, Zhu, and coworkers reported the synthesis of distal bromo-substituted alkyl ketones by visible light-promoted ring-opening functionalization of unstrained cycloalkanols (Wang D. et al., 2018) (**Figure 13B**). A set of medium- and large-sized rings, such as cyclopentanols, cyclohexanols, cycloheptanols, cyclododecanols, and cyclopentadecanols, are readily brominated through inert C–C bond scission with the assistance of HIR under visible-light irradiation. HIRs such as PIDA, BI-OH, IBX, and DMP were all effective for the reaction, and PIDA gave the best results. Two pathways were proposed for the formation of the key alkyloxy radical by authors. In one of them, PIDA was transesterificated with cycloalkanol *in situ*, thus facilitating generation of the challenging alkoxyl radical.

In 2019, Chen and coworkers discovered a method for δ C(sp^3)–H heteroarylation of free aliphatic alcohols with various *N*-heteroarenes using HIRs as oxidant under Ru photoredox catalysis (Li G. X. et al., 2019) (**Figure 13C**). Both cyclic I(III) reagents (BI-OAc, BI-OH, PFBI-OH and PFBI-OAc) and acyclic I(III) reagents (PIDA and PIFA) were examined and PFBI-OH achieved the highest efficiency. The high electrophilicity of the iodo center of PFBI-OH makes itself more electrophilic for alcoholysis and easily reducible in SET process. Notably, this method also possesses the advantage of avoiding the use of a large excess of alcohols.

The heteroarylation process (**Figure 13D**) starts with *in situ* alcoholysis of PFBI-OH with alcohol, and then an alkoxy radical intermediate is generated through the SET reduction. Subsequently, the alkoxyl radical intermediate undergoes 1,5-Hydrogen atom transfer (1,5-HAT) to generate C-radical, which is then engaged in Minisci-type C–C bond formation to give heteroaryl cation intermediate. Finally, the intermediate is converted into target heteroarene through SET oxidation process.

HIR-Mediated Activation of Alkyl C-H Bonds

Chen Gong and coworkers have conducted a series of studies using HIRs as oxidants to selective functionalization of alkyl C(sp^3)-H bonds under photoredox-catalysis. In these HIR-mediated methods, unactivated alkyl C(sp^3)-H bonds, such as tertiary, benzylic methylene, methylene, and methyl C-H bonds, can be selectively cleaved by benziodoxole radicals (BI·), thus offering straightforward methodologies to synthesis of complex alkyl-substituted compounds from a wide range of acyclic alkanes.

In 2017, this group demonstrated the use of HIRs in both hydroxylation and amidation of tertiary and benzylic C–H bonds, enabled by their corresponding benziodoxole radicals (Li et al., 2017) (**Figure 14**). H-abstraction reactivities of eight HIRs were investigated for C–H hydroxylation or amidation, and PFBI-OH and BI-OH were proved as the most effective oxidants respectively for tertiary C–H bonds and benzylic C–H bonds. Distinct from the typical radical chain mechanism, the authors proposed a new ionic pathway (**Figure 14C**) involving nucleophilic trapping of a carbocation intermediate with H_2O or nitrile cosolvent.

In an effort focused on extending this methodology, the same authors applied their PFBI-OH/photoredox system to functionalize the challenging methylene C-H bonds, and a range of alkyl-substituted *N*-heteroarenes were efficient and chemoselectively constructed through Minisci-type alkylation reaction of *N*-heteroarenes with alkanes (**Figures 15A,B**) (Li et al., 2018). The use of PFBI-OH was crucial to elicit both high reactivity and unique steric sensitivity for C-H abstraction of alkanes. The PFBI· radical, which generated by homolytic

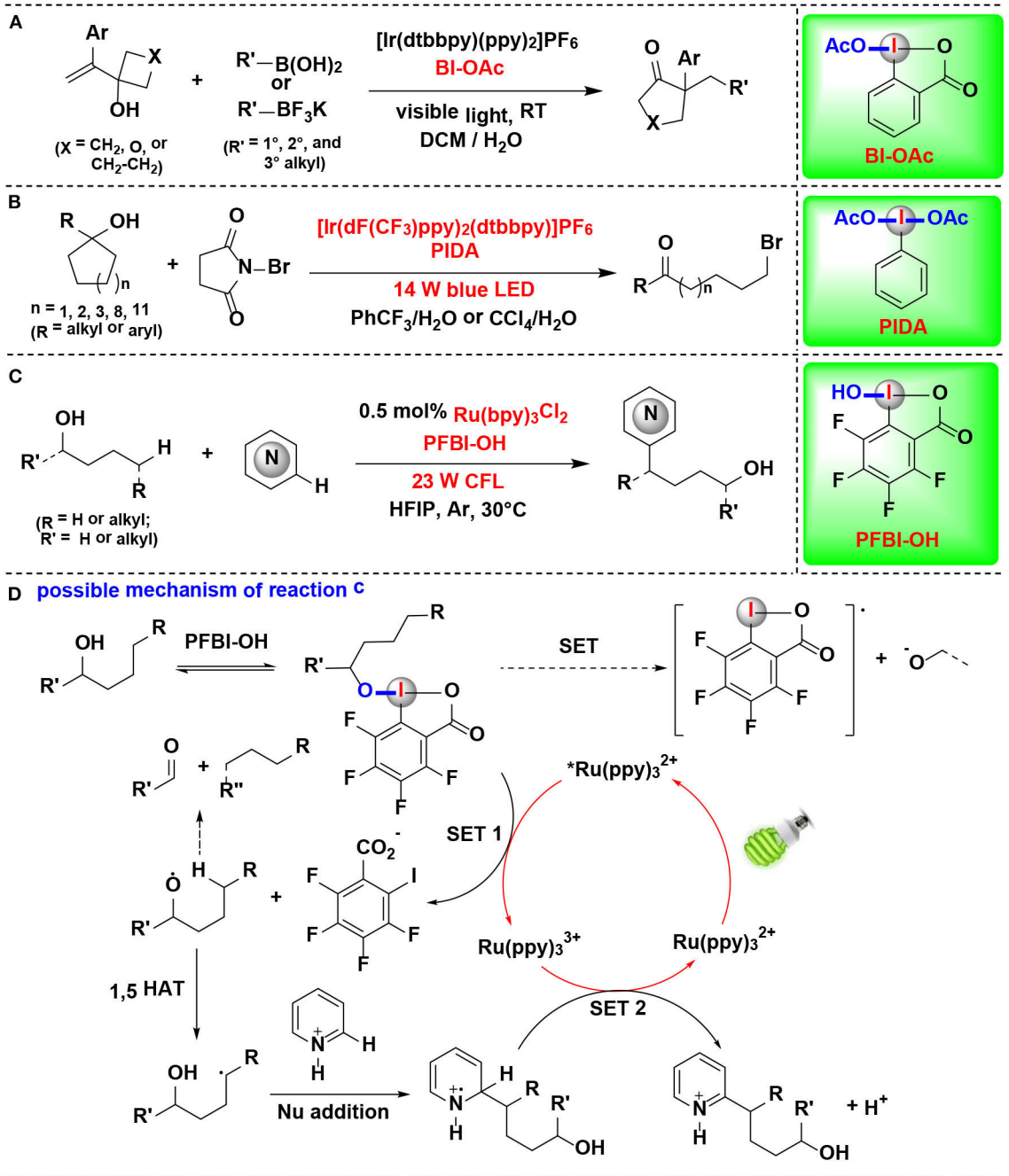

FIGURE 13 | HIR-mediated activation of alcohols under photoredox catalysis. **(A)** Activation of allylic alcohols for alkyl boronate addition/rearrangement. **(B)** Activation of unstrained cycloalkanols for ring-opening bromination. **(C)** Activation of aliphatic alcohols for remote C–H heteroarylation. **(D)** Possible mechanism of reaction **(C)**.

cleavage of I-OH bond under compact fluorescent lamp (CFL) irradiation, can smoothly cleave stronger 2°C-H bonds even in the presence of weaker 3°C-H bonds.

Cai and coworkers developed a visible-light-promoted C-H functionalization strategy to prepare α-aryl-γ-methylsulfinyl ketones (**Figures 15C,D**) (Lu et al., 2018). In this process, alkyl C(sp^3)–H bond of dimethyl sulfoxide (DMSO) can be cleaved by a new HIR to yield α-sulfinyl radical, which subsequent undergoes radical addition with allylic alcohol, followed by 1,2-aryl migration to give the desired sulfoxide derivatives. The new HIR was *in situ* generated from the reaction of PIFA and 1,3,5-trimethoxybenzene.

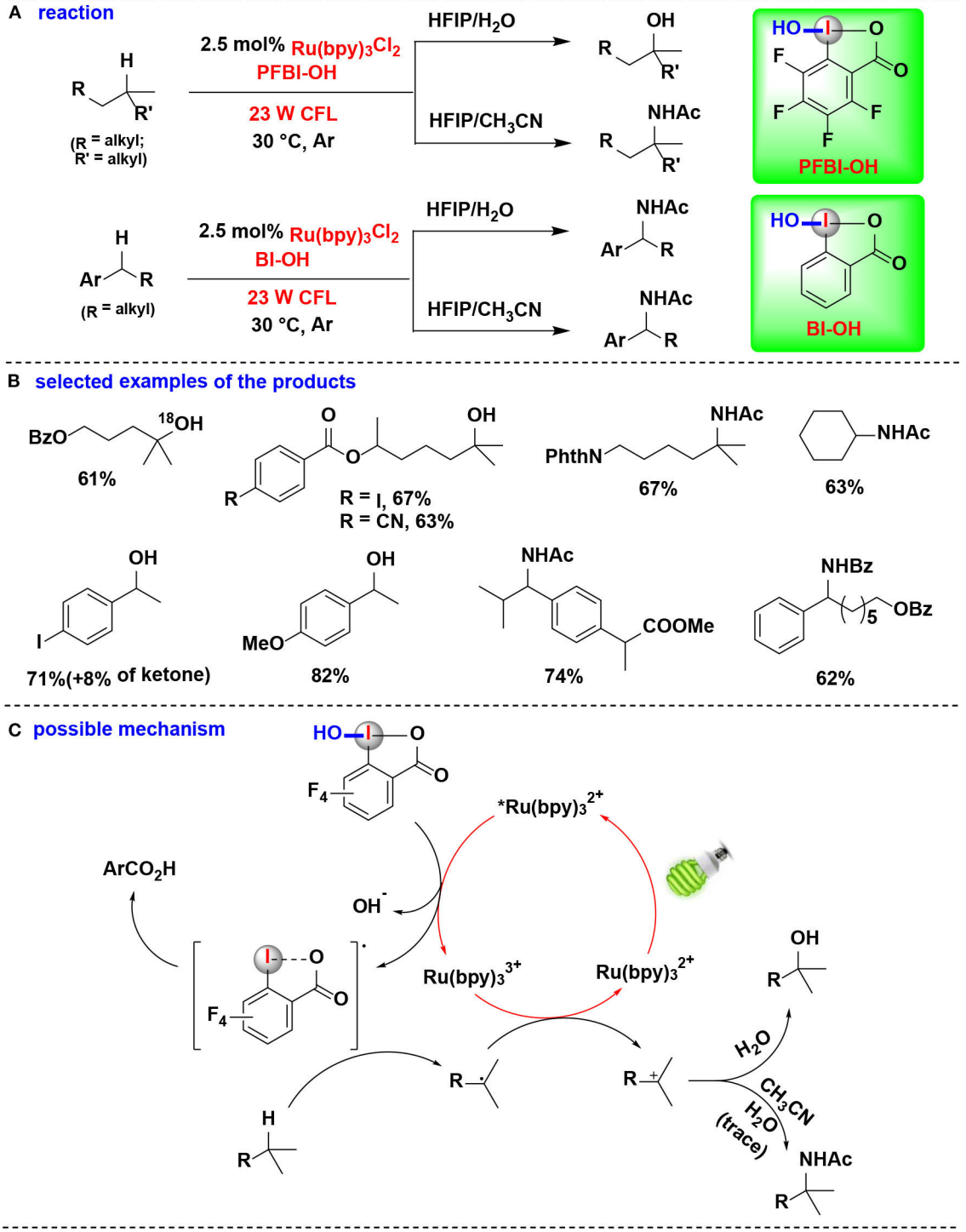

FIGURE 14 | Photoredox-catalyzed C(sp^3)–H hydroxylation and amidation. **(A)** Activation of tertiary and benzylic C–H bonds for hydroxylation and amidation. **(B)** Selected examples of the products. **(C)** Possible mechanism.

SUMMARY AND OUTLOOK

As shown herein, the synergistic combination of photoredox catalysis with HIRs has achieved numerous notable organic transformations. These reactions illustrated that hypervalent iodine chemistry can significantly benefit from the merger with photoredox catalysis systems. The ability to access highly reactive radical intermediates under very mild and

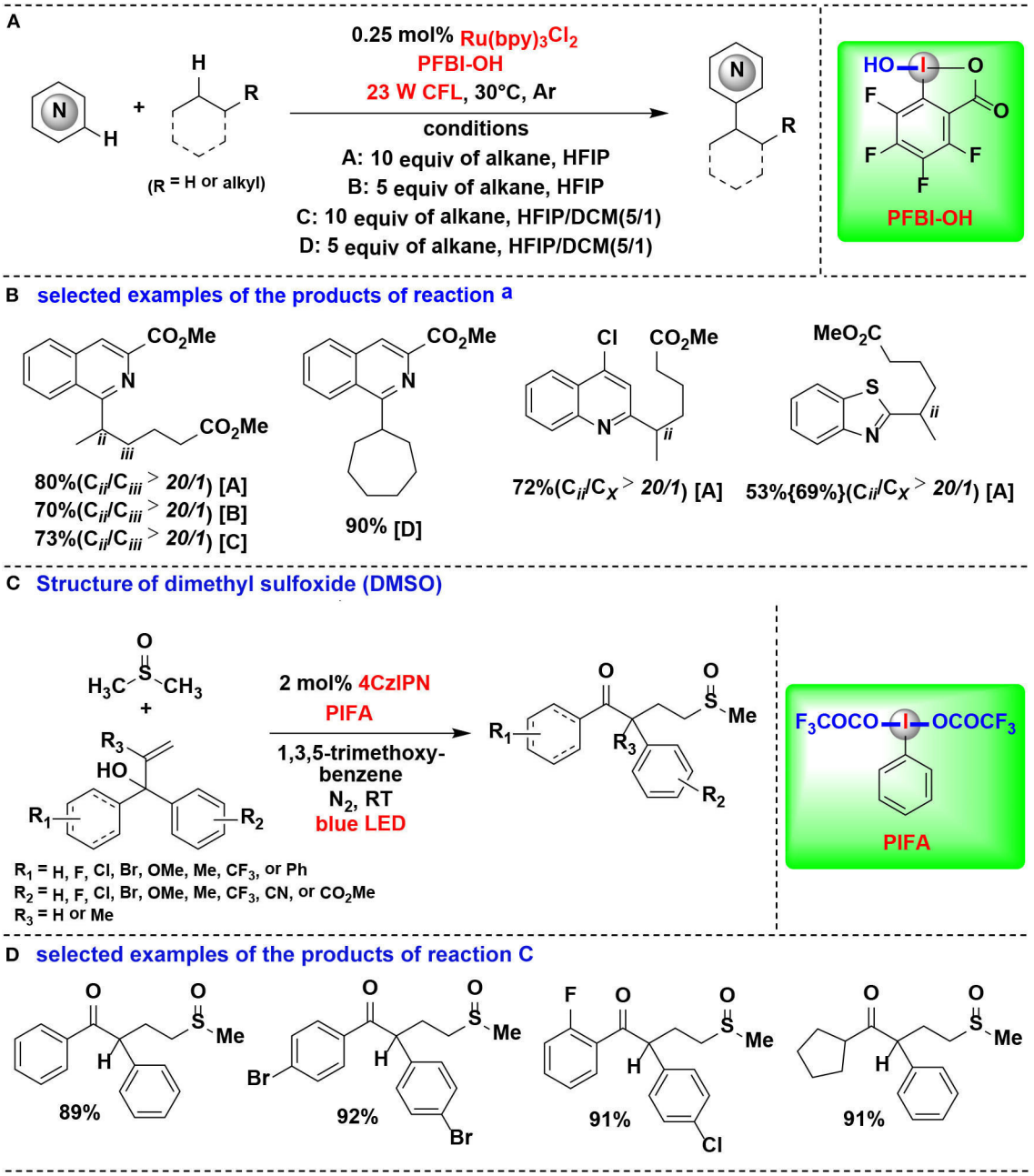

FIGURE 15 | HIR-mediated activation of alkyl C-H bonds under photoredox catalysis. **(A)** Activation of C–H bonds for Minisci-type alkylation of reaction **(A)**. **(B)** Selected examples of the products. **(C)** Activation of C–H bond in DMSO for 1,2-alkylarylation. **(D)** Selected examples of the products of reaction **(C)**.

environmentally benign conditions make these methodologies quite attractive.

Despite the significant progress made, there remain many opportunities for further exploration in the field of photoredox catalysis/HIR system. Firstly, there are a wide variety of HIRs yet to be engaged in photoredox-catalytic reactions. Moreover, from the perspective of green and sustainable chemistry, additional development of low-cost, non-toxic, and environmentally benign organic-dyes as a replacement of metal photoredox catalysts is highly desirable. Additionally, the discovery of stereoselective asymmetric reactions using chiral HIRs under photoredox-catalyzed conditions may potentially be a promising direction for future research. Finally, more in-depth mechanistic studies are highly warranted for fully understanding of the photoredox catalysis/HIR processes. It is highly anticipated that more and more HIRs as reagents or oxidants will

continue to be applied in the area of visible-light-induced photoredox catalysis.

AUTHOR CONTRIBUTIONS

TY designed this proposal, determined the contents, and revised the manuscript. CC collected the literature data related to this review and wrote the manuscript. XW drew the chemical structures and prepared the figures. All authors contributed to the final version of the manuscript.

FUNDING

This work was partially supported by the National Natural Science Foundation of China (grant number 51872140).

REFERENCES

Alazet, S., Le Vaillant, F., Nicolai, S., Courant, T., and Waser, J. (2017). Divergent access to (1,1) and (1,2)-azidolactones from alkenes using hypervalent iodine reagents. *Chem. Eur. J.* 23, 9501–9504. doi: 10.1002/chem.201702599

Alazet, S., Preindl, J., Simonet-Davin, R., Nicolai, S., Nanchen, A., Meyer, T., et al. (2018). Cyclic hypervalent iodine reagents for azidation: safer reagents and photoredox-catalyzed ring expansion. *J. Org. Chem.* 83, 12334–12356. doi: 10.1021/acs.joc.8b02068

Brand, J. P., González, D. F., Nicolai, S., and Waser, J. (2011). Benziodoxole-based hypervalent iodine reagents for atom-transfer reactions. *Chem. Commun.* 47, 102–115. doi: 10.1039/C0CC02265A

Charpentier, J., Fruh, N., and Togni, A. (2015). Electrophilic trifluoromethylation by use of hypervalent iodine reagents. *Chem. Rev.* 115, 650–682. doi: 10.1021/cr500223h

De, A., Santra, S., Hajra, A., Zyryanov, G. V., and Majee, A. (2019). Visible-light-induced regioselective C(sp3)-H acyloxylation of aryl-2h-azirines with (diacetoxy)iodobenzene. *J. Org. Chem.* 84, 11735–11740. doi: 10.1021/acs.joc.9b01625

Franck, L. V., Marion, G., Stefano, N., Ganna, G., Clemence, C., and Jerome, W. (2018). Fine-tuned organic photoredox catalysts for fragmentation-alkynylation cascades of cyclic oxime ethers. *Chem. Sci.* 9, 5883–5889. doi: 10.1039/c8sc01818a

Fumagalli, G., Rabet, P. T., Boyd, S., and Greaney, M. F. (2015). Three-component azidation of styrene-type double bonds: light-switchable behavior of a copper photoredox catalyst. *Angew. Chem. Int. Ed.* 54, 11481–11484. doi: 10.1002/anie.201502980

Garreau, M., Le Vaillant, F., and Waser, J. (2019). C-Terminal bioconjugation of peptides through photoredox catalyzed decarboxylative alkynylation. *Angew. Chem. Int. Ed.* 58, 8182–8186. doi: 10.1002/anie.201901922

Genovino, J., Lian, Y., Zhang, Y., Hope, T. O., Juneau, A., and Gagn,é, Y., et al. (2018). Metal-free-visible light C–H alkylation of heteroaromatics via hypervalent iodine-promoted decarboxylation. *Org. Lett.* 20, 3229–3232. doi: 10.1021/acs.orglett.8b01085

Han, J., Wang, G., Sun, J., Li, H., Duan, G., Li, F., et al. (2019). Photoredox-catalyzed perfluoroalkylation of aminoquinolines with hypervalent iodine(III) reagents that contain perfluoroalkanoate. *Catal. Commun.* 118, 81–85. doi: 10.1016/j.catcom.2018.10.001

Harayama, Y., Yoshida, M., Kamimura, D., Wada, Y., and Kita, Y. (2006). The efficient direct synthesis of N,O-acetal compounds as key intermediates of discorhabdin a: oxidative fragmentation reaction of α-amino acids or β-amino alcohols by using hypervalent iodine(III) reagents. *Chem. Eur. J.* 12, 4893–4899. doi: 10.1002/chem.200501635

Hari, D. P., Caramenti, P., and Waser, J. (2018). Cyclic hypervalent iodine reagents: enabling tools for bond disconnection via reactivity umpolung. *Acc. Chem. Res.* 51, 3212–3225, doi: 10.1021/acs.accounts.8b00468

Hu, C., and Chen, Y. (2015). Biomolecule-compatible chemical bond-formation and bond-cleavage reactions induced by visible light. *Tetrahedron Lett.* 56, 884–888. doi: 10.1016/j.tetlet.2014.12.034

Huang, H., Jia, K., and Chen, Y. (2016). Radical decarboxylative functionalizations enabled by dual photoredox catalysis. *ACS Catal.* 6, 4983–4988. doi: 10.1021/acscatal.6b01379

Huang, H. C., Zhang, G. J., Chen, Y. Y. (2015). Dual hypervalent iodine(III) reagents and photoredox catalysis enable decarboxylative ynonylation under mild conditions. *Angew. Chem. Int. Ed*. 54, 7872–7876. doi: 10.1002/anie.201502369

Huang, X., and Groves, J. T. (2016). Taming azide radicals for catalytic C–H azidation. *ACS Catal.* 6, 751–759. doi: 10.1021/acscatal.5b02474

Hyatt, I. F. D., Dave, L., David, N., Kaur, K., Medard, M., and Mowdawalla, C. (2019). Hypervalent iodine reactions utilized in carbon–carbon bond formations. *Org. Biomol. Chem.* 17, 7822–7848. doi: 10.1039/C9OB01267B

Jia, K., and Chen, Y. (2018). *PATAI's Chemistry of Functional Groups*: *Photochemistry of Hypervalent Iodine Compounds*. eds I. Marek, B. Olofsson, and Z. Rappoport. John Wiley & Sons.

Jia, K., Li, J., and Chen, Y. (2018). Selective P–C(sp^3) bond cleavage and radical alkynylation of α-phosphorus alcohols by photoredox catalysis. *Chem. Eur. J.* 24, 3174–3177. doi: 10.1002/chem.201800202

Jia, K., Pan, Y., and Chen, Y. (2017). Selective carbonyl-C(sp^3) bond cleavage to construct ynamides, ynoates, and ynones by photoredox catalysis. *Angew. Chem. Int. Ed.* 56, 2478–2481. doi: 10.1002/anie.201611897

Jia, K., Zhang, F., Huang, H., and Chen, Y. (2016). Visible-light-induced alkoxyl radical generation enables selective C(sp^3)–C(sp^3) bond cleavage and functionalizations. *J. Am. Chem. Soc.* 138, 1514–1517. doi: 10.1021/jacs.5b13066

Kaschel, J., and Werz, D. B. (2015). Ethynyl benziodoxolone (EBX): installing alkynes the reversed way, *Angew. Chem. Int. Ed.* 54, 8876–8878. doi: 10.1002/anie.201503405

Koike, T., and Akita, M. (2014). Visible-light radical reaction designed by Ru- and Ir-based photoredox catalysis. *Inorg. Chem. Front.* 1, 562–576, doi: 10.1039/C4QI00053F

Koike, T., and Akita, M. (2016). Fine design of photoredox systems for catalytic fluoromethylation of carbon–carbon multiple bonds. *Acc. Chem. Res.* 49, 1937–1945. doi: 10.1021/acs.accounts.6b00268

Le Vaillant, F., Courant, T., and Waser, J. (2015). Room-temperature decarboxylative alkynylation of carboxylic acids using photoredox catalysis and EBX reagents. *Angew. Chem. Int. Ed.* 54, 11200–11204. doi: 10.1002/anie.201505111

Le Vaillant, F., Wodrich, M. D., and and, J., Waser (2017). Room temperature decarboxylative cyanation of carboxylic acids using photoredox catalysis and cyanobenziodoxolones: a divergent mechanism compared to alkynylation. *Chem. Sci.* 8, 1790–1800. doi: 10.1039/c6sc04907a

Lemos, A., Lemaire, C., and Luxen, A. (2019). Progress in difluoroalkylation of organic substrates by visible light photoredox catalysis. *Adv. Synth. Catal.* 361, 1500–1537. doi: 10.1002/adsc.201801121

Li, G. X., Hu, X., He, G., and Chen, G. (2018). Photoredox-Mediated Minisci-type Alkylation of N-Heteroarenes with Alkanes with High Methylene Selectivity. *ACS Catal.* 8, 11847–11853. doi: 10.1021/acscatal.8b04079

Li, G. X., Hu, X., He, G., and Chen, G. (2019). Photoredox-mediated remote C(sp^3)–H heteroarylation of free alcohols. *Chem. Sci.* 10, 688–693. doi: 10.1039/c8sc04134b

Li, G. X., Morales-Rivera, C. A., Gao, F., Wang, Y., He, G., Liu, P., et al. (2017). A unified photoredox-catalysis strategy for C(sp^3)–H hydroxylation and amidation using hypervalent iodine. *Chem. Sci.* 8, 7180–7185. doi: 10.1039/c7sc02773g

Li, G. X., Morales-Rivera, C. A., Wang, Y., Gao, F., He, G., Liu, P., et al. (2016). Photoredox-mediated minisci C–H alkylation of N-heteroarenes using boronic acids and hypervalent iodine. *Chem. Sci.* 7, 6407–6412. doi: 10.1039/C6SC02653B

Li, J., Liu, Z., Wu, S., and Chen, Y. (2019). Acyl radical smiles rearrangement to construct hydroxybenzophenones by photoredox catalysis. *Org. Lett.* 21, 2077–2080. doi: 10.1021/acs.orglett.9b00353

Li, Y., Hari, D. P., Vita, M. V., and Waser, J. (2016). Cyclic hypervalent iodine reagents for atom-transfer reactions: beyond trifluoromethylation. *Angew. Chem. Int. Ed.* 55, 4436–4454. doi: 10.1002/anie.201509073

Liu, M., Huang, H., and Chen, Y. (2018). Cyclic Iodine Reagents Enable Allylic Alcohols for Alkyl Boronate Addition/Rearrangement by Photoredox Catalysis. *Chinese J. Chem.* 36, 1209–1212. doi: 10.1002/cjoc.201800461

Lu, M., Qin, H., Lin, Z., Huang, M., Weng, W., and Cai, S. (2018). Visible-Light-Enabled Oxidative Alkylation of Unactivated Alkenes with Dimethyl Sulfoxide through Concomitant 1,2-Aryl Migration. *Org. Lett.* 20, 7611–7615. doi: 10.1021/acs.orglett.8b03340

Neumeier, M., Sampedro, D., Májek, M., de la Pena O'Shea, V. A., Jacobi von Wangelin, A., and Pérez-Ruiz, R. (2018). Dichromatic photocatalytic substitutions of aryl halides with a small organic dye. *Chem. Eur. J.* 24, 105–108. doi: 10.1002/chem.201705326

Rabet, P. T., Fumagalli, G., Boyd, S., and Greaney, M. F. (2016). Benzylic C–H azidation using the Zhdankin reagent and a copper photoredox catalyst. *Org. let.* 18, 1646–1649. doi: 10.1021/acs.orglett.6b00512

Radzhabov, M. R., Sheremetev, A. B., and Pivina, T. S. (2020). Oxidative ability of organic iodine (iii) reagents: a theoretical assessment. *New J. Chem.* 44, 7051–7057. doi: 10.1039/d0nj00837k

Reckenthaler, M., and Griesbeck, A. G. (2013). Photoredox Catalysis for Organic Syntheses. *Adv. Synth. Catal.* 355, 2727–2744. doi: 10.1002/adsc.201300751

Romero, N. A., and Nicewicz, D. A. (2016). Organic photoredox catalysis. *Chem. Rev.* 116, 10075–10166, doi: 10.1021/acs.chemrev.6b00057

Roth, H. G., Romero, N. A., and Nicewicz, D. A. (2016). Experimental and calculated electrochemical potentials of common organic molecules for applications to single-electron redox chemistry. *Synlett* 27, 714–723. doi: 10.1055/s-0035-1561297

Sakakibara, Y., Cooper, P., Murakami, K., and Itami, K. (2018a). Photoredox-catalyzed decarboxylative oxidation of arylacetic acids. *Chem. Asian J.* 13, 2410–2413. doi: 10.1002/asia.201800529

Sakakibara, Y., Ito, E., Fukushima, T., Murakami, K., and Itami, K. (2018b). Late-stage functionalization of arylacetic acids by photoredox-catalyzed decarboxylative carbon–heteroatom bond formation. *Chem. Eur. J.* 24, 9254–9258. doi: 10.1002/chem.201802143

Shaw, M. H., Twilton, J., and MacMillan, D. W. C. (2016). Photoredox catalysis in organic chemistry. *J. Org. Chem.* 81, 6898–6926. doi: 10.1021/acs.joc.6b01449

Song, D., Wang, C. M., Ye, Z. P., Xia, P. J., and Yang, H. (2019). Visible-light-driven, photoredox-catalyzed cascade of ortho-hydroxycinnamic esters to access 3-fluoroalkylated coumarins. *J. Org. Chem.* 84, 7480–7487. doi: 10.1021/acs.joc.9b00715

Staveness, D., Bosque, I., and Stephenson, C. R. J. (2016). Free radical chemistry enabled by visible light-induced electron transfer. *Acc. Chem. Res.* 49, 2295–2306. doi: 10.1021/acs.accounts.6b00270

Tang, W. K., Feng, Y. S., Xu, Z. W., Cheng, Z. F., Xu, J., Dai, J. J., et al. (2017). Visible-light-enabled decarboxylative mono- and difluoromethylation of cinnamic acids under metal-free conditions. *Org. Lett.* 19, 5501–5504. doi: 10.1021/acs.orglett.7b02129

Twilton, J., Le, C., Zhang, P., Shaw, M. H., Evans, R. W., and Macmillan, D. W. C. (2017). The merger of transition metal and photocatalysis. *Nat. Rev. Chem.* 1, 0052. doi: 10.1038/s41570-017-0052

Vaillant, F. L., and Waser, J. (2017). Decarboxylative alkynylation and cyanation of carboxylic acids using photoredox catalysis and hypervalent iodine reagents. *Chimia* 71, 226–230. doi: 10.2533/chimia.2017.226

Wang, D., Mao, J., and Zhu, C. (2018). Visible light-promoted ring-opening functionalization of unstrained cycloalkanols via inert C–C bond scission. *Chem. Sci.* 9, 5805–5809. doi: 10.1039/c8sc01763h

Wang, D., Zhang, L., and Luo, S. (2017). Enantioselective decarboxylative α-alkynylation of β-ketocarbonyls via a catalytic α-imino radical intermediate. *Org. Lett.* 19, 4924–4927. doi: 10.1021/acs.orglett.7b02386

Wang, H., Zhang, J., Shi, J., Li, F., and Xu, K. (2019). Organic photoredox-catalyzed synthesis of δ-fluoromethylated alcohols and amines via 1,5-hydrogen-transfer radical relay. *Org. Lett.* 21, 5116–5120, doi: 10.1021/acs.orglett.9b01714

Wang, J., Li, G. X., He, G., and Chen, G. (2018). Photoredox-mediated minisci alkylation of N-heteroarenes using carboxylic acids and hypervalent iodine. *Asian J. Org. Chem.* 7, 1307–1310. doi: 10.1002/ajoc.201800197

Wang, L., and Liu, J. (2016). Synthetic applications of hypervalent iodine(III) reagents enabled by visible light photoredox catalysis. *Eur. J. Org. Chem.* 1813–1824. doi: 10.1002/ejoc.201501490

Wang, X., and Studer, A. (2017). Iodine(III) reagents in radical chemistry. *Acc. Chem. Res.* 50, 1712–1724. doi: 10.1021/acs.accounts.7b00148

Wang, Y., Li, G. X., Yang, G., He, G., and Chen, G. (2016). A visible-light-promoted radical reaction system for azidation and halogenation of tertiary aliphatic C–H bonds. *Chem. Sci.* 7, 2679–2683. doi: 10.1039/c5sc04169d

Wang, Z., Herraiz, A. G., del Hoyo, A. M., and Suero, M. G. (2018). Generating carbyne equivalents with photoredox catalysis. *Nature*, 554, 86–91. doi: 10.1038/nature25185

Waser, J. (2016). Benziodoxol(on)e reagents as tools in organic synthesis: the background behind the discovery at the laboratory of catalysis and organic synthesis. *Synlett*, 27, 2761–2773. doi: 10.1055/s-0036-1589409

Wu, D., Cui, S. S., Lin, Y., Li, L., and Yu, W. (2019). Visible light-driven azidation/difunctionalization of vinyl arenes with azidobenziodoxole under copper catalysis. *J. Org. Chem.* 84, 10978–10989. doi: 10.1021/acs.joc.9b01569

Xuan, J., and Xiao, W. J. (2012). Visible-light photoredox catalysis. *Angew. Chem. Int. Ed.*, 51, 2–13. doi: 10.1002/anie.201200223

Yang, B., Xu, X. H., and Qing, F. L. (2016). Synthesis of difluoroalkylated arenes by hydroaryldifluoromethylation of alkenes with α, α-difluoroarylacetic acids under photoredox catalysis. *Org. Lett.* 18, 5956–5959. doi: 10.1021/acs.orglett.6b03092

Yang, B., Yu, D., Xu, X. H., and Qing, F. L. (2018). Visible-light photoredox decarboxylation of perfluoroarene iodine(iii) trifluoroacetates for C–H trifluoromethylation of (hetero)arenes. *ACS Catal.* 8, 2839–2843. doi: 10.1021/acscatal.7b03990

Yang, C., Yang, J. D., Li, Y. H., Li, X., and Cheng, J. P. (2016). 9,10-Dicyanoanthracene catalyzed decarboxylative alkynylation of carboxylic acids under visible-light irradiation. *J. Org. Chem.* 81, 12357–12363. doi: 10.1021/acs.joc.6b02385

Yang, L., Li, H., Du, Y., Cheng, K., and Qi, C. (2019). Visible light-catalyzed decarboxylative alkynylation of arenediazonium salts with alkynyl carboxylic acids: direct access to aryl alkynes by organic photoredox catalysis. *Adv. Synth. Catal.* 361, 5030–5041. doi: 10.1002/adsc.201900603

Yoshimura, A., and Zhdankin, V. V. (2016). Advances in synthetic applications of hypervalent iodine compounds. *Chem. Rev.* 116, 3328–3435. doi: 10.1021/acs.chemrev.5b00547

Zagulyaeva, A. A., Yusubov, M. S., and Zhdankin, V. V. (2010). A general and convenient preparation of [bis(trifluoroacetoxy)iodo]perfluoroalkanes and [bis(trifluoroacetoxy)iodo]arenes by oxidation of organic iodides using oxone and trifluoroacetic acid. *J. Org. Chem.* 75, 2119–2122. doi: 10.1002/chin.201026055

Zhang, J. J., Cheng, Y. B., and Duan, X. H. (2017). Metal-free oxidative decarboxylative acylation/ring expansion of vinylcyclobutanols with α-keto acids by visible light photoredox catalysis. *Chinese J. Chem.* 35, 311–315. doi: 10.1002/cjoc.201600729

Zhdankin, V. V. (2009). Hypervalent iodine(III) reagents in organic synthesis. *ARKIVOC.* (i), 1–62. doi: 10.3998/ark.5550190.0010.101

Zhdankin, V. V. (2013). *Preparation, Structure and Properties of Polyvalent Iodine Compounds. Hypervalent Iodine Chemistry: Preparation, Structure and Synthetic Applications of Polyvalent Iodine Compounds*. 145–336. John Wiley & Sons.

Zhou, Q. Q., Guo,W., Ding, W., Wu, X., Chen, X., Lu, L. Q., et al. (2015). Decarboxylative alkynylation and carbonylative alkynylation of carboxylic acids enabled by visible-light photoredox catalysis. *Angew. Chem. Int. Ed.* 54, 11196–11199. doi: 10.1002/anie.201504559

Conflict of Interest: The authors declare that the research was conducted in the absence of any commercial or financial relationships that could be construed as a potential conflict of interest.

frontiers in Chemistry

REVIEW
published: 29 September 2020
doi: 10.3389/fchem.2020.00705

Hypervalent Iodine Reagents in Palladium-Catalyzed Oxidative Cross-Coupling Reactions

*Samata E. Shetgaonkar and Fateh V. Singh**

Chemistry Division, School of Advanced Science, Vellore Institute of Technology, Chennai, India

Hypervalent iodine compounds are valuable and versatile reagents in synthetic organic chemistry, generating a diverse array of useful organic molecules. Owing to their non-toxic and environmentally friendly features, these reagents find potential applications in various oxidative functionalization reactions. In recent years, the use of hypervalent iodine reagents in palladium-catalyzed transformations has been widely studied as they are strong electrophiles and powerful oxidizing agents. For instance, extensive work has been carried out in the field of C–H bond functionalization via Pd-catalysis using hypervalent iodine reagents as oxidants. In addition, nowadays, iodine(III) reagents have been frequently employed as arylating agents in Pd-catalyzed C–H arylation or Heck-type cross-coupling reactions. In this review, recent advancements in the area of palladium-catalyzed oxidative cross-coupling reactions using hypervalent iodine reagents are summarized in detail.

Keywords: hypervalent iodine reagents, palladium, oxidant, catalyst, bond formation

OPEN ACCESS

Edited by:
Ravi Kumar,
J.C. Bose University of Science and Technology, YMCA, India

Reviewed by:
Michal Szostak,
Rutgers University, Newark, United States
Egle Maria Beccalli,
University of Milan, Italy

****Correspondence:***
Fateh V. Singh
fatehveer.singh@vit.ac.in

Specialty section:
This article was submitted to Organic Chemistry, a section of the journal Frontiers in Chemistry

Received: *24 April 2020*
Accepted: *09 July 2020*
Published: *29 September 2020*

Citation:
Shetgaonkar SE and Singh FV (2020) Hypervalent Iodine Reagents in Palladium-Catalyzed Oxidative Cross-Coupling Reactions. Front. Chem. 8:705. doi: 10.3389/fchem.2020.00705

INTRODUCTION

Hypervalent iodine compounds are ubiquitous in organic synthesis since they have emerged as efficient and environmentally benign reagents for academic and industrial research (Zhdankin, 2014; Yoshimura and Zhdankin, 2016; Singh and Wirth, 2018). They are non-toxic, easily prepared, stable and alternative to metal-derived oxidants/catalysts in various oxidative transformations (Yusubov and Zhdankin, 2012; Singh and Wirth, 2014a,b, 2017; Mangaonkar et al., 2018; Singh et al., 2018a; Mangaonkar and Singh, 2019). Several research papers, book chapters and review articles have been published covering various aspects of hypervalent iodine compounds as reagents or as catalysts in α-functionalization of carbonyl compounds (Merritt and Olofsson, 2011; Dong et al., 2014), cyclizations (Singh and Wirth, 2011, 2012; Singh and Mangaonkar, 2018; Singh et al., 2018b), oxidative rearrangements (Singh et al., 2012; Singh and Wirth, 2013; Maertens and Canesi, 2015), alkene difunctionalizations (Li et al., 2018; Lee et al., 2019) and atom-transfer reactions (Li Y. et al., 2016). The inherent ability of hypervalent iodine reagents to act as oxidants as well as ligand transfer reagents is the key to the significant progress achieved in this area.

Representative examples of various hypervalent iodine(III)/(V) reagents commonly used as oxidants or atom transfer reagents are listed in **Figure 1**. Iodobenzenediacetate (PIDA) **1**, [bis(trifluoroacetoxy)iodo] benzenes (PIFA) **2** and iodosobenzene dipivalate **3** are routinely used iodine(III) oxidants (Wirth, 2005; Zhdankin, 2009). Apart from this, other oxidizing agents such as iodosobenzene **4**, Koser reagent **5**, 2-iodosobenzoic acid (IBA) **6** and l-hydroxy-1*H*-1,2,3-benziodoxathiole 3,3-dioxide **7** were used in various oxidative transformations (Singh and Wirth, 2014a). Dess–Martin periodinane (DMP) **8** and 2-iodoxybenzoic acid (IBX) **9** are extensively used

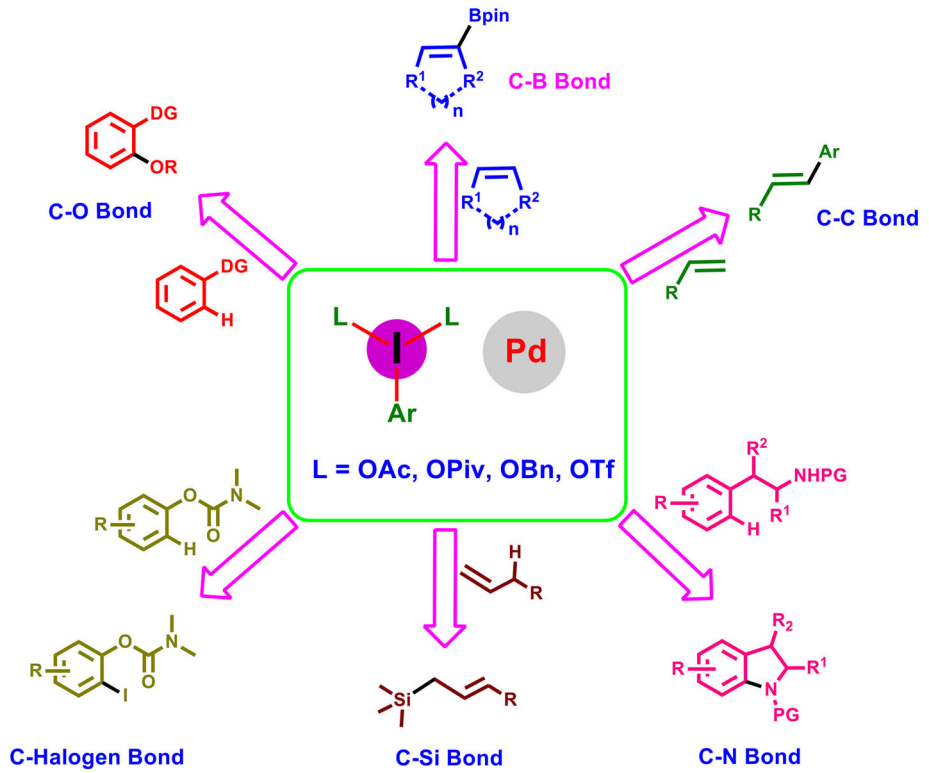

GRAPHICAL ABSTRACT | Representative palladium-catalyzed reactions using hypervalent iodine reagents.

cyclic iodine(V) reagents (Tohma and Kita, 2004; Uyanik and Ishihara, 2009). 2,3,4,5-tetrafluoro-6-iodoxybenzoic acid (FIBX) **10** having higher reactivity than IBX **9** was synthesized by Richardson et al. (2007). Zhdankin's group prepared 2-iodoxybenzenesulfonic acid (IBS) **11** via oxone-mediated oxidation of 2-iodobenzenesulfonic acid (Koposov et al., 2006). Another important aspect of iodine(III)/(V) reagents that has received considerable attention is to act as electrophilic synthons for functional-group transfer reactions. For example, benziodoxol(on)e reagents **12**–**15** have been employed as a source of nucleophilic groups such as acetate, trifluoromethyl, fluorides, and alkynes in various transformations (Li Y. et al., 2016). Diaryliodonium salts **16** being electrophilic and a naturally good leaving group, are widely used as arylating reagents (Merritt and Olofsson, 2009).

However, these reagents do have limitations such as stoichiometric generation of aryliodides as a byproduct, limited solubility in common organic solvents, and requirement of an excess amount of reagents thus lowering atom economy dramatically. For instance, IBA **6** is less explored due to its lower reactivity while DMP **8** is expensive and moisture sensitive. IBX **9** is associated with drawbacks such as an explosive nature, poor solubility in common organic solvents, and requirement of high reaction temperature which limits its synthetic applications to some extent (Singh and Wirth, 2014b). Also, IBS **11** is thermally unstable and highly reactive toward organic solvents, like acetonitrile, dimethyl sulfoxide, and methanol and readily decomposed into stable thia-analog of IBA **7** (Koposov et al., 2006). Although there are some drawbacks associated with these reagents, there is still great scope for these compounds as potential alternate candidates for toxic heavy-metal oxidants such as mercury, thallium, and lead based reagents (Silva L. F, 2002; Wirth et al., 2002).

On the other hand, palladium as a catalyst has become a fundamental part of various coupling reactions such as Suzuki-Miyaura, Heck, Buchwald–Hartwig, Sonagashira, and Negishi generating diverse array of useful molecules (Biffis et al., 2018). Hypervalent iodine reagents in palladium-catalyzed reactions constitute an interesting area of research in organic synthesis. Deprez and Sanford published the first review article explaining the unique reactivity of hypervalent iodine reagents in Pd-catalyzed reactions in 2007 (Deprez and Sanford, 2007). Later, the 2015 section of the review that describes the key role of polyvalent iodine reagents in high valent palladium chemistry was published by Wengryniuk's group (Silva et al., 2017). Owing to their excellent oxidizing and electrophilic nature, hypervalent iodine reagents reacts with palladium complexes and promotes reactions via Pd(0/II) or Pd(II/IV) redox cycles. For instance, iodine(III) reagents have been employed as a substitute for aryl halides in various Pd(0)/(II)-catalyzed cross-coupling reactions (Deprez and Sanford, 2007). Also, various Pd-catalyzed ligand transfer reactions employ few of these reagents as a source of aryl, alkynyl, and heteroatom ligands. Although substantial work has been carried out in Pd(0)/(II)-catalysis in the past, catalytic

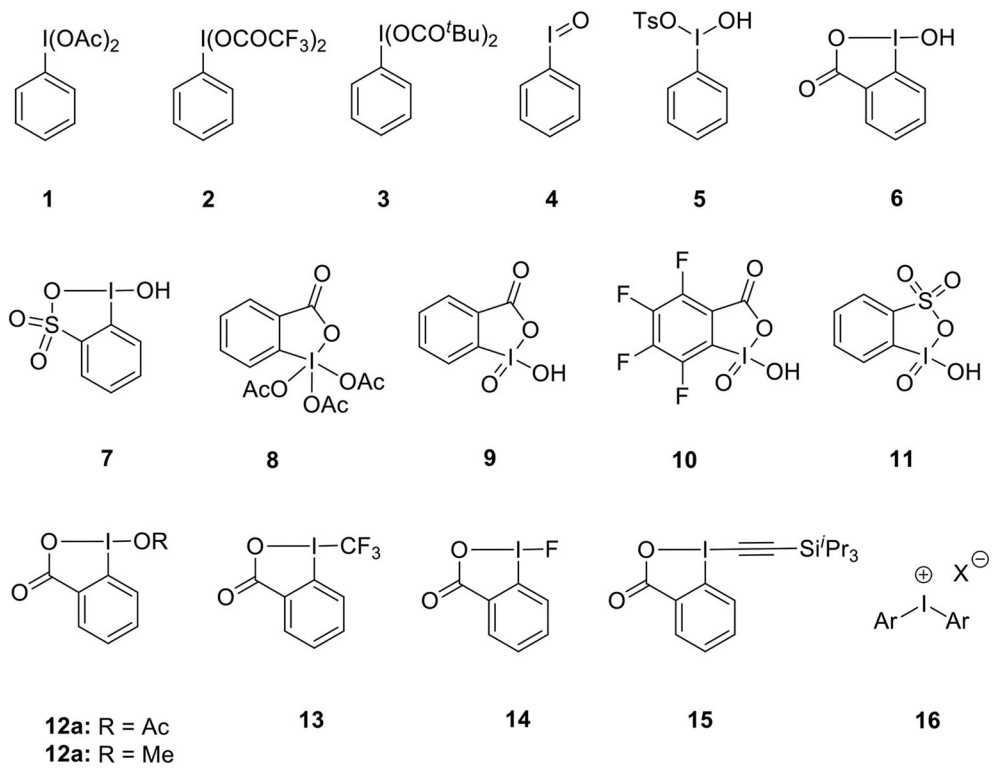

FIGURE 1 | Examples of hypervalent iodine(III)/(V) reagents **1–16**.

reactions via Pd(II)/(IV) pathway were less explored. However, with the aid of hypervalent iodine oxidants, Pd(II)/(IV)-catalysis have seen tremendous development in the last couple of decades enabling various synthetic transformations earlier inaccessible via traditional catalytic manifolds. For example, C–H functionalizations have become a powerful tool to construct new C–C and C–heteroatom bonds using Pd(II)/(IV)-catalysis.

Within this context, the present review focuses on the recent advancement accomplished in palladium-catalyzed transformations using hypervalent iodine reagents, highlighting its potential synthetic applications and mechanistic aspects. The article is classified on the basis of bonds formed such as C–O, C–N, C–C, C–Si, C–B, and C–halogen bonds and finally alkene difunctionalization reactions.

C–O BOND FORMATION

Palladium-catalyzed ligand assisted C–H functionalization has been proven to be one of the best, most atom economical, and effective tools in organic synthesis for the introduction of variable functional groups at the unactivated arene/alkane C–H bonds. Extensive research has been carried out by several groups in the field of C–O bond formation via palladium catalysis using hypervalent iodine reagents as oxidant or heteroatom ligand. Among them, Pd-catalyzed C–H oxidative cyclization, C–H acyloxylation, C–H alkoxylation and allylic oxidation constitutes important pathways in C–O bond formation reactions directed by directing functional groups such as oxime ether, oxazoline, amide, pyridine and pyrimidine, etc.

C–H Cyclization

Significant progress has been made in the field of Pd-catalyzed oxidative cyclization reactions using hypervalent iodine reagents, giving access to several oxygen-containing heterocycles. In 2010, Wang et al. developed a novel method for the construction of dihydrobenzofurans via $Pd(OAc)_2$-catalyzed hydroxyl group-directed C–H activation/C–O cyclization reaction in the presence of (diacetoxyiodo)benzene **1** as a terminal oxidant and promoted by base Li_2CO_3. Moreover, the scope of the reaction was extended to the preparation of important scaffolds such as spirocyclic dihydrobenzofurans (Wang X. et al., 2010).

Later, Gevorgyan's group demonstrated intramolecular silanol group-directed C–H oxygenation of phenoxy silanols **17** employing $Pd(OPiv)_2$ as catalyst and $PhI(OAc)_2$ **1** as an oxidant (Huang et al., 2011). This reaction involves the initial formation of cyclic silicon-protected catechols **18** which upon desilylation with TBAF/THF provides substituted catechols **19** (**Scheme 1A**). The plausible catalytic cycle involves initial coordination of Pd with silanols **17** to form palladacycle **20** accompanied by PIDA-mediated oxidation to forge Pd(IV)-intermediate **21**. Next, intermediate **21** is transformed into acetoxylated intermediate **23** via reductive acetoxylation and regenerates back palladium catalyst. Finally, acid-catalyzed transesterification of **24** gives **25** which subsequently loose acetic acid to form cyclic silyl

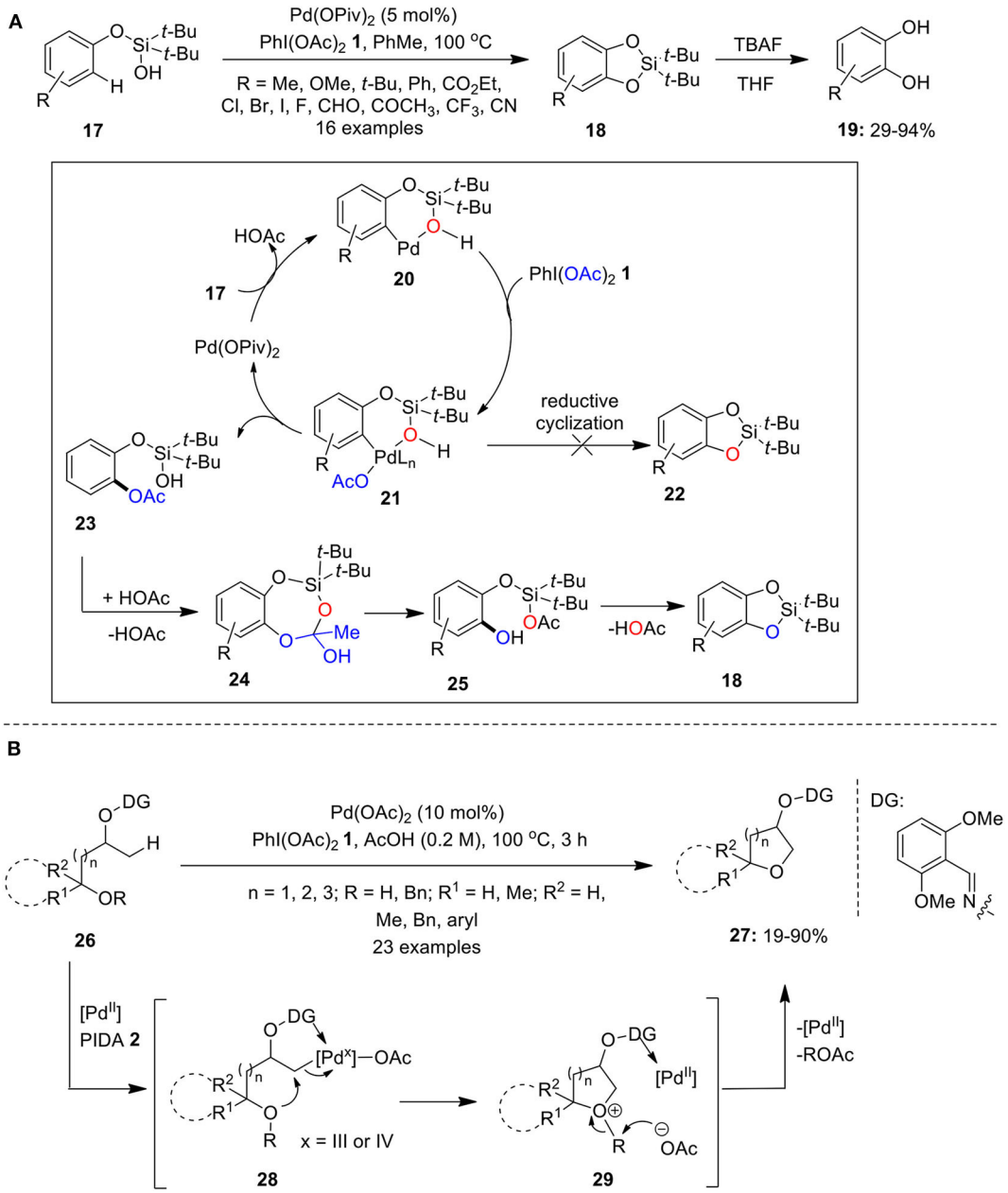

SCHEME 1 | (A) Pd(II)-catalyzed synthesis of substituted catechols **19** using $PhI(OAc)_2$ **1** as an oxidant and **(B)** Pd(II)-catalyzed synthesis of cyclic ethers **27** using $PhI(OAc)_2$ **1** as an oxidant.

protected catechols **18** followed by subsequent desilylation with TBAF furnishes catechols **19**. Further formation of products **22** through direct C–O reductive cyclization was eliminated based on ^{18}O-labeling studies. Further reactions featured excellent site selectivity and broad substrates scope, particularly, electron-rich substrates reacted much faster and provided high yields. Another interesting work published by Gevorgyan's research group employing C–H oxygenation strategy is the convenient synthesis of oxasilacycles from substituted benzyl-silanols using combination of $Pd(OAc)_2$ and $PhI(OAc)_2$ **1** in $PhCF_3$ at 100°C (Huang et al., 2012).

Furthermore, Thompson et al. reported the preparation of cyclic ethers **27** via Pd-catalyzed oxime masked-alcohol directed dehydrogenative annulation of sp^3 C–H bonds of substrates **26** using $PhI(OAc)_2$ **1** as an oxidant (Thompson et al., 2015). The reaction occurs selectively at the β-position and substrates **26** having primary, secondary, and tertiary hydroxyl group worked smoothly under the standard conditions (**Scheme 1B**). The reaction could proceed via C–H palladation, followed by oxidation of Pd to higher oxidation state species **28** and a subsequent intramolecular S_N2 reaction to form oxonium intermediate **29**. Finally, cyclic ethers **27**

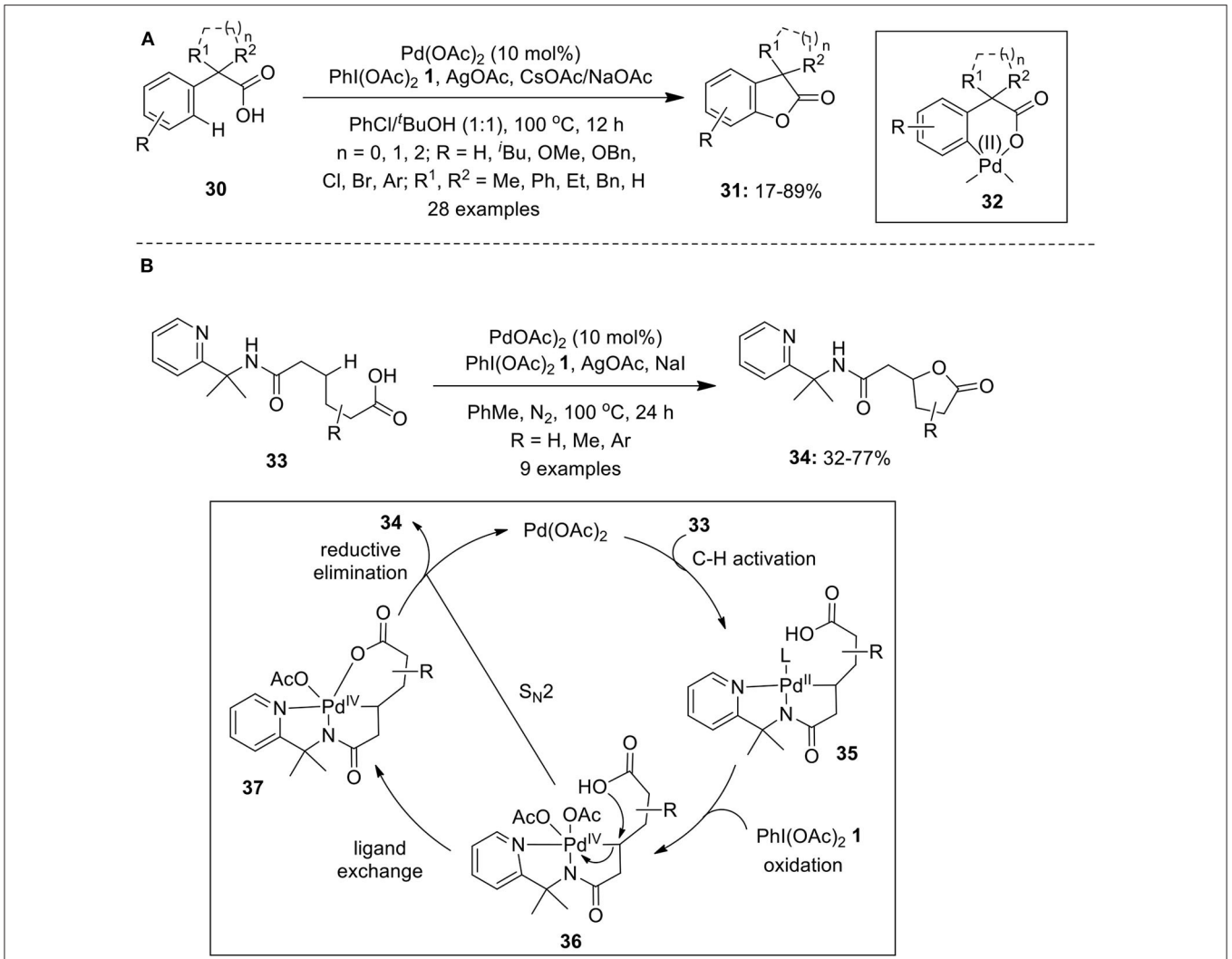

SCHEME 2 | (A) Pd(II)-catalyzed α,α-disubstituted benzofuran-2-ones **31** using $PhI(OAc)_2$ **1** and **(B)** Pd(II)-catalyzed synthesis of γ-lactones **34** using oxidant $PhI(OAc)_2$ **1**.

were obtained through deprotonation or debenzylation and regenerate Pd-catalyst.

Yang et al. reported Pd-catalyzed intramolecular lactonization of α, α-disubstituted arylacetic acids **30** in the presence of $PhI(OAc)_2$ **1** to furnish a series of α, α-disubstituted benzofuran-2-ones **31** in variable yields (Yang et al., 2013). The catalytic system composed of $Pd(OAc)_2$ and the combination of NaOAc and CsOAc along with AgOAc as most effective bases (**Scheme 2A**). The authors proposed that C–H cleavage occurs via concerted metalation deprotonation to form six-membered palladacycle **32** which further undergoes oxidation and subsequent reductive elimination to afford **31**. Similar catalytic C–H activation/C–O formation methods to construct functionalized benzofuranones (Cheng et al., 2013) and biaryl lactones (Li et al., 2013) were also developed employing acetyl-protected glycine (Ac-Gly-OH) as requisite ligand along with base KOAc in *t*-BuOH.

In 2016, Shi's group described a concise route to access γ-lactones **34** featuring Pd(II)-catalyzed PIP auxiliary-directed lactonization of unactivated methylene $C(sp^3)$–H bonds using oxidant PIDA **1** (Liu and Shi, 2016). The lactonization of aliphatic acids **33** bearing various substituents on the alkyl chain proceeded remarkably well to furnish anticipated γ-lactones **34** in 32–77% yields (**Scheme 2B**). The probable mechanism for the lactonization of aliphatic acids **32** involves formation of five-membered palladacycle **35** through Pd-catalyzed C–H activation assisted by bidentate auxiliary. In the presence of $PhI(OAc)_2$ **1**, palladacycle **35** underwent oxidation to give Pd(IV) intermediate **36** followed by ligand exchange to form **37** which finally undergoes reductive elimination to release target product **34** along with Pd(II) catalyst to complete the catalytic cycle (**Scheme 11**). Another path to generate lactone **34** is via direct S_N2-type attack by carboxylate group onto the Pd(IV)–C bond of **36** (**Scheme 2B**).

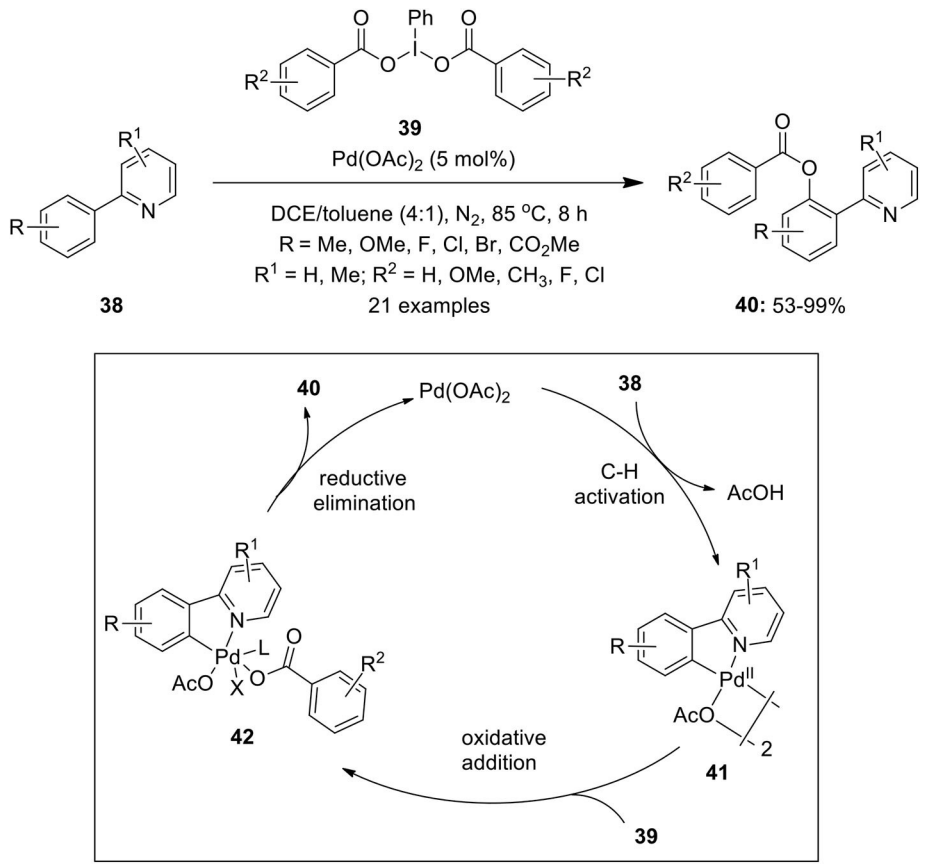

SCHEME 3 | Pd(II)-catalyzed *ortho* C–H benzoxylation of 2-arylpyridine**s 38** using substituted iodobenzene dibenzoates derivatives **39** as oxidant and source of benzoxyl group.

C(sp^2/sp^3)–H Acyloxylation

Over the years, C–H acyloxylation has made tremendous progress in transforming various unactivated sp^2 and sp^3 hybridized C–H bonds into valuable C–O bonds using palladium catalysts and iodine(III) reagents as oxidants. This method provides a concise route for the introduction of valuable ester functionality on to the aromatic or aliphatic substrates under mild conditions. Several C(sp^2)–H acyloxylation protocols have been developed employing $Pd(OAc)_2$/$PhI(OAc)_2$ **1** catalytic systems using a variety of directing groups such as pyrimidine (Gu et al., 2009), 8-aminoquinoline (Gou et al., 2009), oxime (Neufeldt and Sanford, 2010; Ren et al., 2015), pyridyldiisopropylsilyl (Chernyak et al., 2010; Gulevich et al., 2012), and 1,2,3-triazoles-pyridine (Ye et al., 2013).

Furthermore, a regioselective protocol featuring Pd(II)-catalyzed C–H benzoxylation of 2-arylpyridines **38** was performed by Zhang et al. affording mono-benzoxylation products **40** in moderate to excellent yields (Zhang et al., 2015). They employed easily accessible iodobenzene dibenzoate derivatives **39** as oxidants and sources of the benzoxyl group (**Scheme 3**). Furthermore, the present method was successfully applied for the benzoxylation of 2-thienyl pyridines to yield 3-benzoxylated thiophenes in high yields. The plausible mechanism proceeds via pyridyl-assisted C–H activation of substrates **38** with a palladium catalyst to form complex **41** which undergoes further oxidative addition with **39** to form high oxidation state complex **42**. Finally, the reductive elimination of **42** gives desired product **40** and regenerates the palladium catalyst to complete the catalytic cycle.

Although substantial development has been accomplished in the Pd-catalyzed ligand-directed C–H oxygenation reactions, the non-chelate assisted transformations are rarely explored. For instance, Pd-catalyzed C–H acetoxylation of arenes devoid of directing groups remains a challenge as it leads to the formation of mixtures of isomers. In this context, Emmert et al. developed non-chelate assisted palladium-catalyzed C–H acetoxylation of simple arenes using pyridine (Emmert et al., 2011) and acridine (Cook et al., 2013) as ancillary ligands in combination with hypervalent iodine reagents as oxidants.

Furthermore, the Pd-catalyzed allylic C–H acyloxylation represents one of the efficient methods in C–H functionalization reactions. Pilarski et al. have presented an excellent protocol for the preparation of allylic acetates or allylic benzoates via Pd-catalyzed allylic C–H acetoxylation/benzoyloxylation using $PhI(OAc)_2$ **1** or $PhI(OBz)_2$ as oxidant and source of acyloxy group (Pilarski et al., 2009). Later, the same group

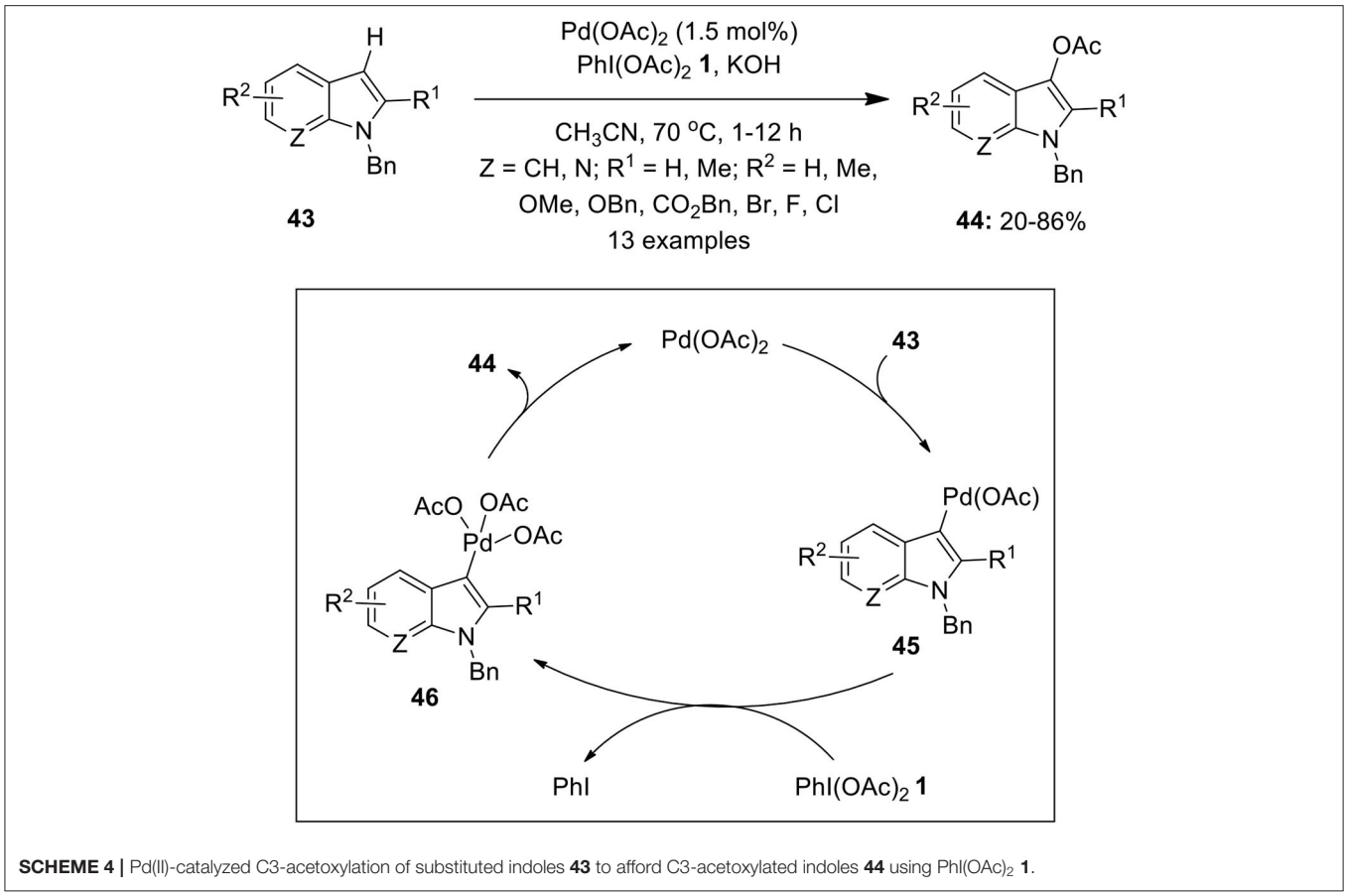

SCHEME 4 | Pd(II)-catalyzed C3-acetoxylation of substituted indoles **43** to afford C3-acetoxylated indoles **44** using $PhI(OAc)_2$ **1**.

described conversion of alkenes into allylic trifluoroacetates via Pd-catalyzed C–H trifluoroacetoxylation employing $PhI(OCOCF_3)_2$ **2** as an oxidant and trifluoroacetoxy source (Alam et al., 2012).

Regioselective C–H functionalization of indoles has been found to be a straight forward route to access biologically important 3-acetoxyindoles. In this regard, Suna's and Kwong's groups independently reported the synthesis of 3-acetoxyindoles via direct C3-oxidation of indole derivatives catalyzed by $Pd(OAc)_2$ (2–5 mol%) in the presence of terminal oxidant $PhI(OAc)_2$ **1** (Mutule et al., 2009; Choy et al., 2011). In continuation, Liu et al. developed a similar Pd-catalyzed approach for the selective C3-acetoxylation of substituted indoles **43** with reduced catalyst loading (1.5 mol%) using $PhI(OAc)_2$ **1** and KOH as a base (**Scheme 4**; Liu et al., 2011). Mechanistic insights revealed that the electrophilic palladation occurs at the C3 position of indole to generate Pd(II) species **45** which is oxidized to Pd(IV) intermediate **46** and subsequent reductive elimination affords corresponding C3-acetoxylated indoles **44**.

Acyloxylation of aliphatic sp^3 C–H bond is another important method for regioselective C–O bond formation. Elegant protocols have been developed employing various nitrogen-based directing groups for the selective oxygenation of unactivated $C(sp^3)$–H bond. In 2010, a novel chelation-assisted Pd-catalyzed $C(sp^3)$–H acyloxylation of 8-methylquinolines in the presence of a stoichiometric amount of oxidant $PhI(OAc)_2$ **1** was developed employing inexpensive arene carboxylic acids as acyloxy source (Zhang et al., 2010). A similar method for the catalytic acetoxylation of unactivated primary β-$C(sp^3)$–H bond of *S*-methyl-*S*-2-pyridylsulfoximine-*N*-amides at room temperature was described by Sahoo's group (Rit et al., 2012). This method employs *S*-methyl-*S*-2-pyridylsulfoximine (MPyS) as a bidentate directing group and β-C–H acetoxylated products were synthesized using different carboxylic acids as solvent and acetate sources.

Furthermore, a Pd-catalyzed oxime-directed β-$C(sp^3)$–H acetoxylation of substrates **47** was performed employing $PhI(OAc)_2$ **1** as a terminal oxidant (Ren et al., 2012). The catalytic reaction was expected to generate five-membered *exo*-palladacycle **49** which on oxidation gives masked 1,2-diols **48** (**Scheme 5A**). Also, the selective acetoxylation of β-methylene (CH_2) and β-methine (CH) groups in cyclopentanol and norbornyl-derived alcohols were also carried out under the same reaction conditions. Furthermore, the deprotection of DG and acetyl group was carried out by using Zn/AcOH & K_2CO_3/MeOH, respectively, to yield diols in excellent yield. Later, Zhang's group described an elegant work on Pd(II)-catalyzed benzylic $C(sp^3)$–H acetoxylation of picolinoyl- or quinoline-2-carbonyl-protected toluidine derivatives using $PhI(OAc)_2$ **1** as an oxidant and acetate source (Ju et al., 2013).

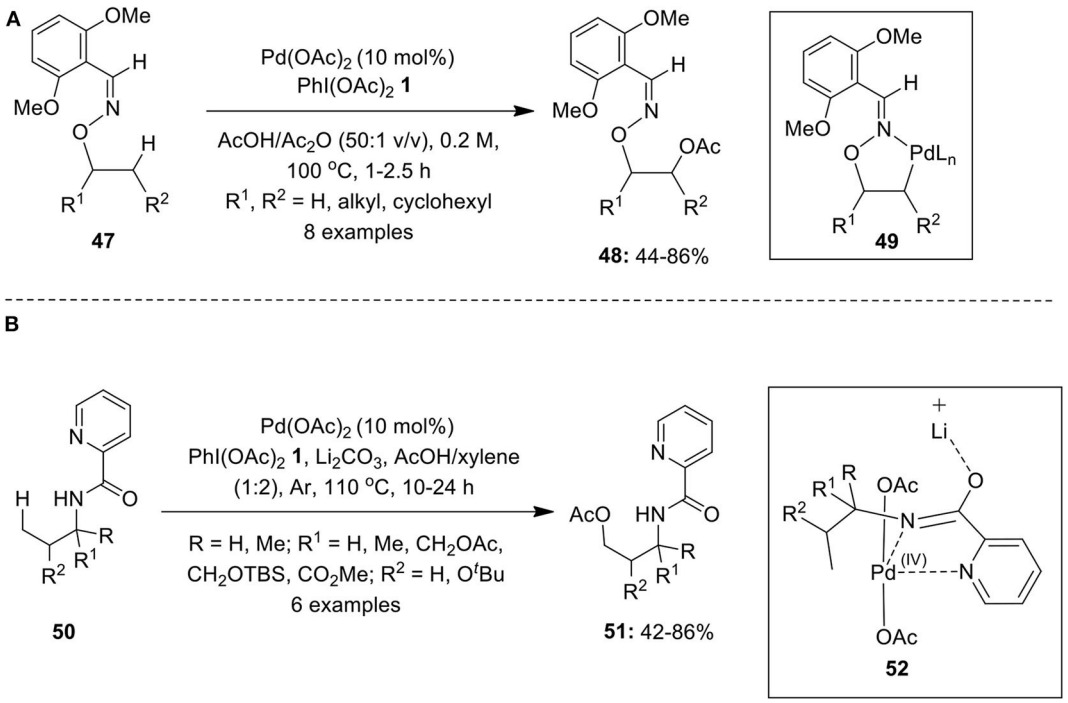

SCHEME 5 | (A) Pd-catalyzed PIDA-mediated C(sp^3)–H acetoxylation of substrates **47** and **(B)** Pd-catalyzed C(sp^3)–H acetoxylation of alkylamines **50** using oxidant PIDA **1**.

In 2014, Li et al. performed a $Pd(OAc)_2$-catalyzed acetoxylation of γ-C(sp^3)–H bond of simple alkylamines **50** directed by picolinamide (PA) using oxidant $PhI(OAc)_2$ **1** under an argon atmosphere (Li et al., 2014). The process provides an easy access to γ-acetoxylated product **51** in good yields (**Scheme 5B**). Additionally, C–H acetoxylation of γ-methyl group of arylamines proceeded smoothly under this condition. Authors speculated that reaction likely to procced via *C*, *N*, *N*-pincer type Pd(IV) intermediate **52**, in which Li_2CO_3 plays a crucial role as it interacts with *O*-imidate thereby suppressing the formation of cyclic azetidine through intramolecular C–H amination.

C(sp^2/sp^3)–H Alkoxylation

Another interesting Pd-catalyzed transformation enabling C–O bond formation is the C–H alkoxylation of sp^2 and sp^3 bonds using hypervalent iodine reagents as oxidant. Chen and Shi's group independently reported two methods for the palladium-catalyzed $PhI(OAc)_2$-mediated alkoxylation of methylene and methyl C(sp^3)–H bonds with a range of aliphatic alcohols as alkoxylation reagents, using picolinamide (Zhang et al., 2012) and pyridine (Chen et al., 2013) as easily removable directing groups. Later, azo group-directed selective C(sp^2)–H alkoxylation of azobenzene compounds with alcohols as the alkoxylation reagents was reported by Yin et al. using palladium catalysis in the presence of oxidant $PhI(OAc)_2$ **1** (Yin et al., 2013). Additionally, Zhang and Sun demonstrated the regioselective alkoxylation of *ortho*-C(sp^2)–H bond of 2-aryloxypyridines to provide *ortho*-alkoxylation products in the presence of catalytic amounts of $Pd(OAc)_2$ and oxidant $PhI(OAc)_2$ **1** (Zhang and Sun, 2014).

Shan et al. for the first time employed cyclic hypervalent iodine(III) reagent **12** as an efficient oxidant in the Pd-catalyzed C(sp^3)–H alkoxylation of unactivated methylene and methyl groups of 8-aminoquinoline-derived carboxylic acids **53** (Shan et al., 2013) (**Scheme 6**). The reaction worked perfectly well with DMP **8** (1.1 equivalents) at 110°C. Gratifyingly, C(sp^3)-H alkoxylation of cyclic substrates such as cyclopentyl, cyclohexyl, and cycloheptyl were also perfomed under identical conditions. Furthermore, the synthetic applicability of present method was demonstrated for the alkoxylation of various analogs of Ibuprofen such as, Naproxen, Ketoprofen, and Flurbiprofen to afford alkoxylated products in variable yields. Based on preliminary mechanistic studies, authors proposed that either DMP **8** or 1-acetoxy-1,2-benziodoxole-3(1*H*)-one **12a** serve as key precursors for the *in situ* generation of cyclic iodine(III) oxidant **56** which oxidizes cyclopalladium(II) intermediate **57** to Pd(IV) intermediate **58**. Next, $ArCO_2$ ligand of intermediate **58** could be easily displaced by alcohol **54** to give Pd(IV) intermediate **59** which finally undergoes C–O bond-forming reductive elimination to yield alkoxylated products **55** and regenerates palladium catalyst. Later, the same research group developed a similar method to prepare symmetrical and unsymmetric acetals via Pd-catalyzed regioselective double C(sp^3)–H bond alkoxylation of 8-aminoquinoline-derived substrates using cyclic iodine(III) reagent **12** as an oxidant (Zong and Rao, 2014).

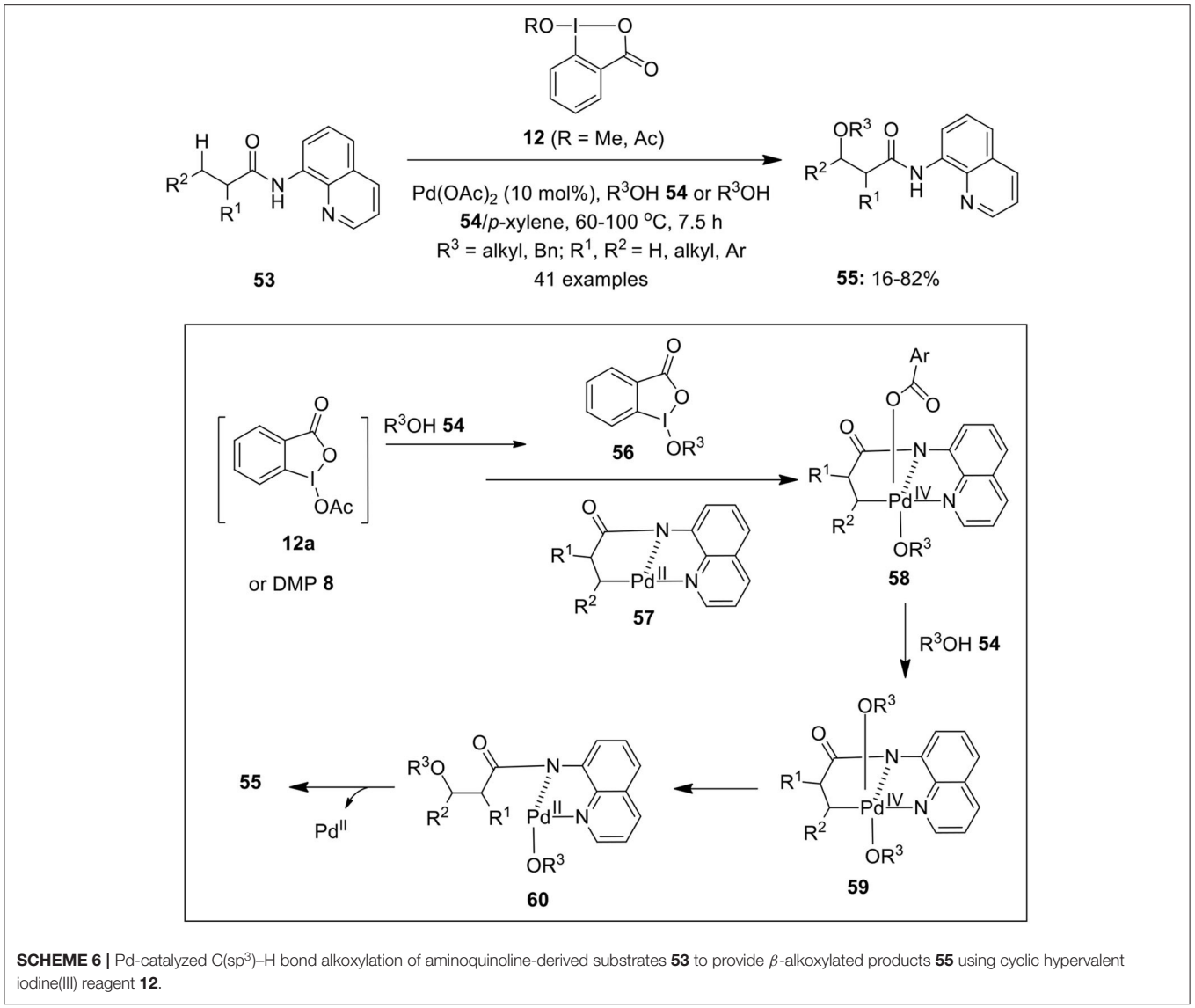

SCHEME 6 | Pd-catalyzed C(sp^3)–H bond alkoxylation of aminoquinoline-derived substrates **53** to provide β-alkoxylated products **55** using cyclic hypervalent iodine(III) reagent **12**.

C–H Oxidation and C–H Phosphorylation/Sulfonation

Chaudhari and Fernandes developed a Wacker–type oxidation protocol to convert various aliphatic and aromatic terminal alkenes **61** into functionally diversified methyl ketones 6**2** employing Dess-Martin Periodinane (DMP) **8** as an oxidant under nitrogen atmosphere (Chaudhari and Fernandes, 2016). Furthermore, the oxidation of a number of allylic or homoallylic compounds were also investigated under identical conditions to deliver methyl ketones in high yields. Excellent functional group compatibility, wide substrates scope and high isolated yields with complete Markovnikov selectivity are the key features associated with this methodology (**Scheme 7A**). A similar method for the conversion of terminal olefins into α,β-unsaturated ketones was developed by Bigi and White via a Wacker oxidation-dehydrogenation process employing $Pd(CH_3CN)_4(BF_4)_2$ (10 mol%) and $PhI(OAc)_2$ **1** (25 mol%) co-catalytic system in the presence of 1,4-benzoquinone as oxidant (Bigi and White, 2013). Interestingly, $PhI(OAc)_2$ **1** acts as a dehydrogenation catalyst and not as a terminal oxidant in this reaction.

Very recently, He et al. reported Pd(II)-catalyzed phosphorylation and sulfonation of unactivated benzyl C(sp^3)–H bond of 8-methylquinolines **63** employing organophosphorus or sulfonate hypervalent iodine(III) reagents **64** as an oxidant and as a functional group source (He et al., 2019). Using this protocol, desired products **65** or **66** were obtained in moderate to high yields with broad substrates scope (**Scheme 7B**). Additionally, the scope of reaction was extended for the C(sp^2)–H hydroxylation and arylation of 2-phenylpyridines.

Furthermore, limited protocols are available for the direct C–O bond formation without involving C–H bond functionalization. For instance, Kitamura and his research group disclosed efficient conversion of (trimethylsilyl)arenes into acetoxyarenes via $Pd(OAc)_2$-catalyzed desilylative acyloxylation

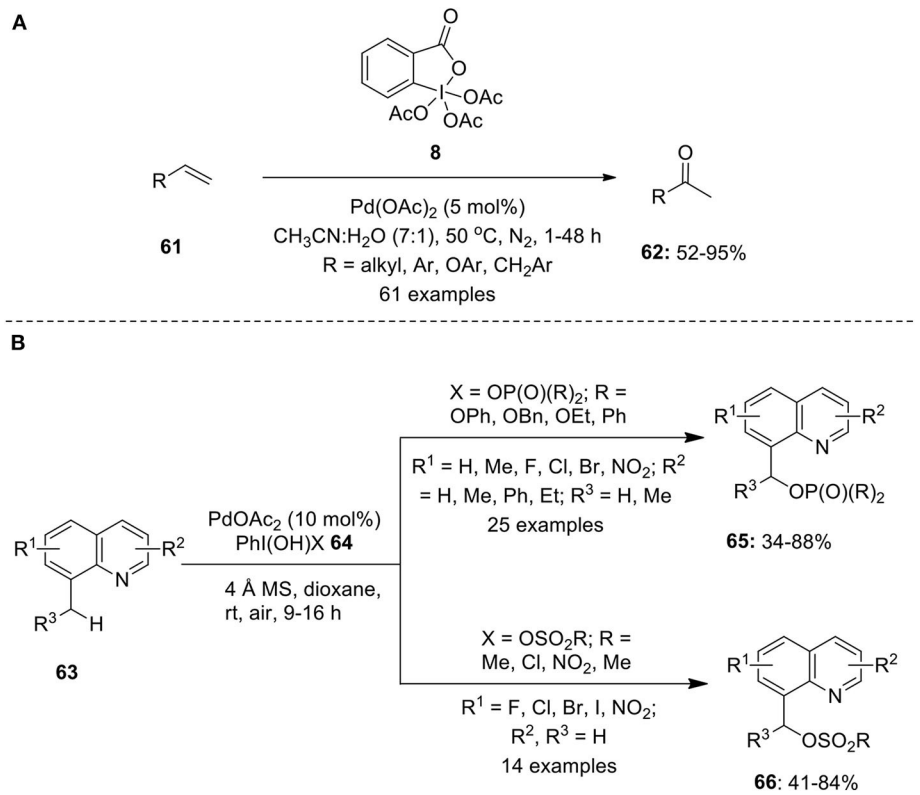

SCHEME 7 | (A) Pd(II)-catalyzed C–H oxidation of terminal alkenes **61** using DMP **8** as an oxidant and **(B)** Pd(II)-catalyzed C–H phosphorylation/sulfonation of methylquinolines **63** using hypervalent iodine reagent **64**.

strategy using $PhI(OCOCF_3)_2$ **2** as an oxidant in AcOH (Gondo et al., 2015). Meanwhile, Cheng et al. reported Pd-catalyzed acetoxylative, hydroxylative and alkoxylative cycloisomerization of polysubstituted homoallenyl amides enabling preparation of functionalized 2-aminofurans using hypervalent iodine(III)reagents as oxidant (Cheng C. et al., 2015). Another striking example to prepare α-acetoxylated enones from propargylic substituted alkynes through Pd-catalyzed oxidative acetoxylation in the presence of terminal oxidant $PhI(OAc)_2$ **1** and additive benzoquinone (10 mol%) in DMSO was developed (Jiang et al., 2016).

C–C BOND FORMATION

Palladium-catalyzed C–H functionalization constitutes an important method in C–C bond formation reactions. A number of catalytic transformations have been developed using hypervalent iodine(III) reagents as oxidant.

via Oxidative Cyclization

An interesting domino process highlighting Pd-catalyzed C–H functionalization of *N*-arylpropiolamides **67** using iodine(III) reagent **68** as an aryl source was demonstrated by Tang et al. (2008a). This elegant protocol leads to the synthesis of 3-(1-arylmethylene)oxindoles **69** in useful yields (**Scheme 8A**). The effect of various electron-rich and electron-deficient substituents on the aryl ring as well as on the triple bond was investigated. The catalytic cycle for this reaction starts with the coordination of Pd(II)-catalyst with alkyne and nitrogen to form intermediate **70** followed by cis-addition with Pd and $ArI(OAc)_2$ **68** to give Pd(II) intermediate **71**. Oxidation of intermediate **71** by $ArI(OAc)_2$ **68** forms Pd(IV) intermediate **72** which further gives intermediate **73** by activation of *ortho* C–H bond of **72**. Finally, intermediate **73** underwent reductive elimination to provide anticipated products **69** and releases active Pd(II) species. The same group also reported the synthesis of (*E*)-(2-oxindolin-3-ylidene)phthalimides and (*E*)-(2-oxoindolin-3-ylidene)methyl acetates via Pd-catalyzed C–H functionalization of *N*-arylpropiolamides using phthalimide and carboxylic acids as nucleophiles, respectively (Tang et al., 2008b,c). Later, synthesis of CF_3-substituted oxindoles was accomplished through palladium-catalyzed $PhI(OAc)_2$-mediated intramolecular trifluoromethylation of *N*-alkyl-*N*-arylacrylamide derivatives using $TMSCF_3$ as an efficient trifluoromethyl source in the presence of Lewis acid $Yb(OTf)_3$ (Mu et al., 2012).

Tong et al. coined the first Pd-catalyzed oxidative cyclization of 1,6-enynes into the corresponding bicyclo[3.1.0]hexane derivatives using oxidant PIDA **1** (Tong et al., 2007). Later, Sanford and Tong's research groups independently

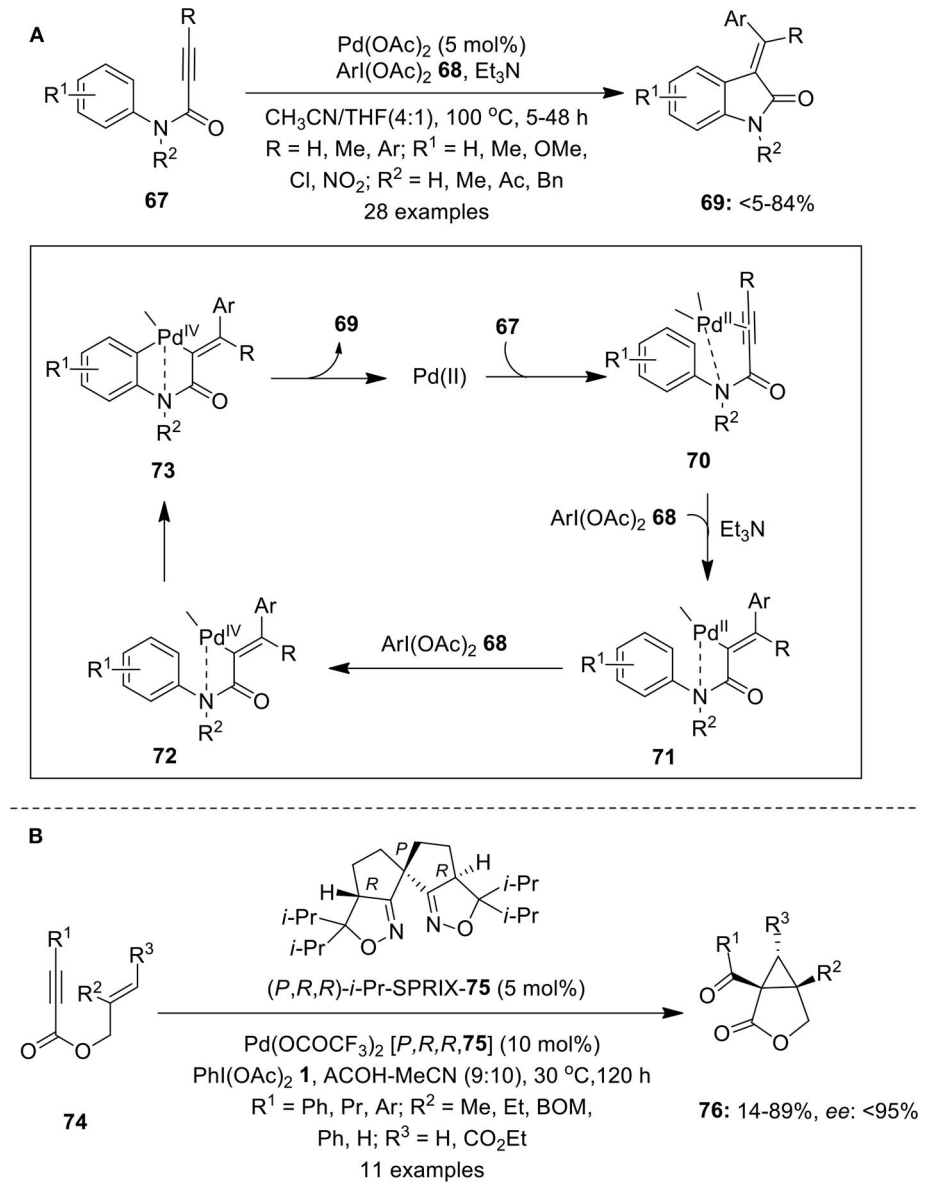

SCHEME 8 | (A) Pd(II)-catalyzed synthesis of 3-(1-arylmethylene)oxindoles **69** using iodine(III) reagent **68** and **(B)** Pd(II)-catalyzed enantioselective synthesis of bicyclic lactones **76** by employing terminal oxidant $PhI(OAc)_2$ **1**.

developed similar pathways toward the synthesis of multi-substituted bicyclo[3.1.0] ring systems using bipyridine as ligand (Welbes et al., 2007; Liu et al., 2008; Lyons and Sanford, 2009). Furthermore, Tsujihara et al. developed the first example featuring asymmetric Pd(II)/Pd(IV) catalysis for the enantioselective synthesis of bicyclic lactones **76** from 1,6-enynes **74** in variable yields with up to 95% enantiomeric excess (**Scheme 8B**) (Tsujihara et al., 2009). Reaction utilizes the spiro bis(isoxazoline) **75** (abbreviated as SPRIXs) as chiral ligand, Pd-SPRIX **75** complex as catalyst and $PhI(OAc)_2$ **1** as terminal oxidant.

Very recently, Xu et al. published an excellent example on the Pd(II/IV)-catalyzed intramolecular cycloaddition of the propargylic alcohol/amine and alkene of substrates **77** via acetoxylative (3 + 2) annulation strategy enabling the synthesis of bicyclic heterocycles **78** in significant yields (Xu et al., 2019) (**Scheme 9**). The possible catalytic cycle for this oxidative cycloaddition reaction initiates through the acetoxypalladation process generating alkenyl-Pd(II) intermediate **79** which is subsequently transform into alkyl-Pd(II) intermediate **81** via chair-like transition state (TS) **80**. Next, $PhI(OAc)_2$-mediated oxidation gives bicyclic Pd(IV) intermediate **82** which further gives **83** through loss of a molecule of AcOH. Finally, intermediate **83** undergoes direct C–O reductive elimination to deliver product **78** and regenerate palladium catalyst to continue the catalytic cycle (**Scheme 9**).

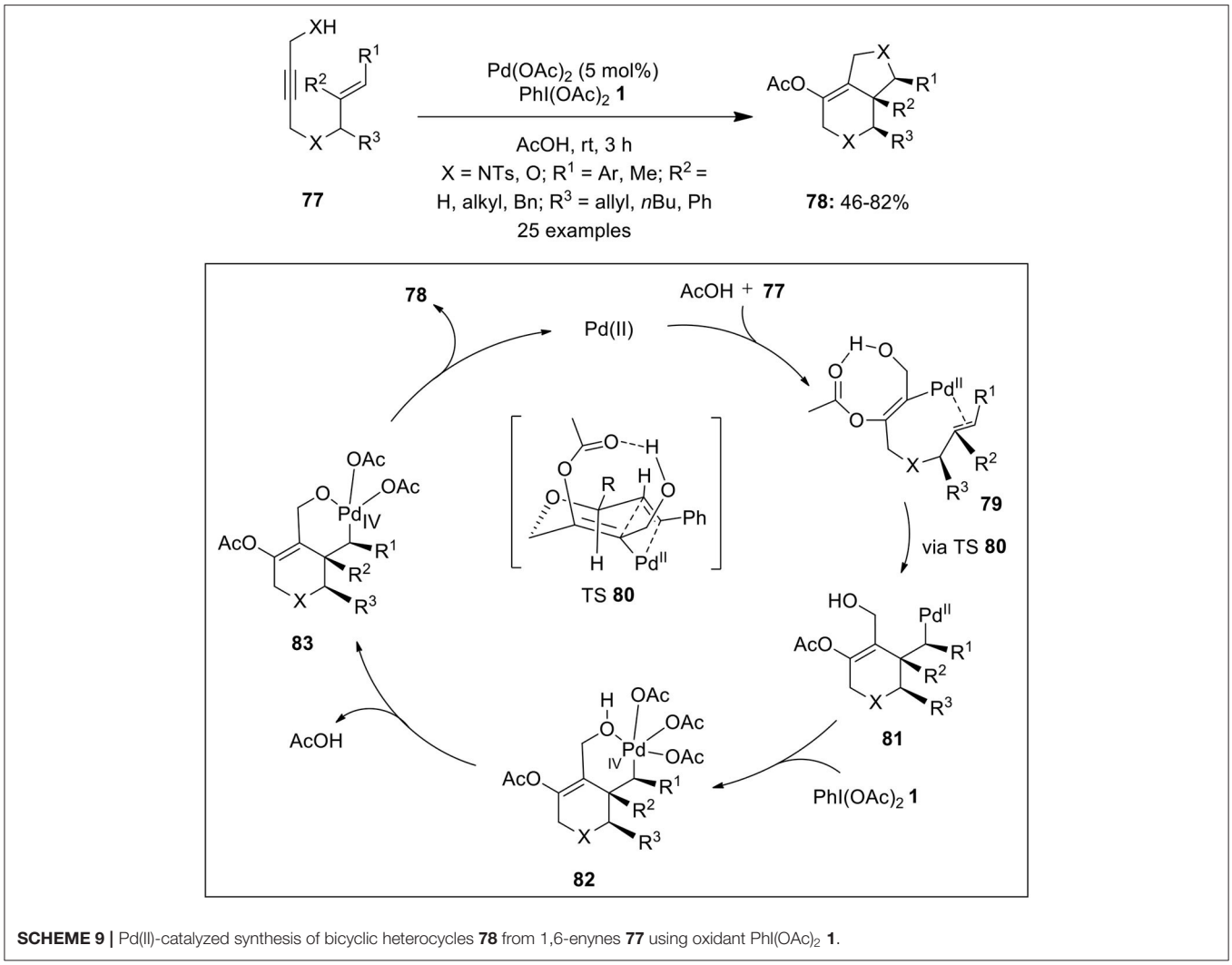

SCHEME 9 | Pd(II)-catalyzed synthesis of bicyclic heterocycles **78** from 1,6-enynes **77** using oxidant $PhI(OAc)_2$ **1**.

via C–H Bond Arylation

In 2011, Qu et al. demonstrated a Heck-type coupling reaction between olefins **61** and iodobenzene generated *in situ* from hypervalent iodine reagents **84** (Qu et al., 2011). The coupling reaction was performed using $Pd(OAc)_2$ (4 mol%), base K_2CO_3, and PEG-400 as solvent media under an open atmosphere at 40–60°C to afford coupling products **85** in 91–99% yields (**Scheme 10**). The catalytic system was free from any ligand or additive and possesses an excellent recyclability of catalyst (**Scheme 10**). A similar Pd-catalyzed Heck-type arylation of terminal alkenes with aryliodine(III) diacetates was developed by Evdokimov et al. (2011).

Later, Cheng's research group performed Pd(II)-catalyzed C–H functionalization of benzoxazoles **86** to furnish arylation products **88** using iodobenzene diacetates **84** as arylating reagent in the presence of ligand 1,10-phenanthroline **87** and base Cs_2CO_3 (Yu et al., 2012) (**Scheme 10**). Similarly, Fu et al. employed aryliodine(III) diacetates **84** as a coupling partner in the Pd-catalyzed C–H arylation of polyfluoroarenes **89** (Fu et al., 2015). Detailed mechanistic studies revealed *in situ* generation of aryliodides by the reduction of $ArI(OAc)_2$ **84** under basic conditions to furnish desired polyfluorobiaryls products **90** in moderate to good yields (**Scheme 10**).

Another interesting strategy to establish C–C bond formation is Pd-catalyzed oxidative coupling reactions of aromatic halides with different arylation reagents. Considering this, Xiong et al. illustrated the synthesis of useful symmetrical biaryls employing aryliodine(III) diacetates **68** as aryl precursor via Pd-catalyzed homocoupling reaction (Xiong et al., 2015). The reaction was carried out in DMF at 110°C in the presence of $Pd(OAc)_2$ (10 mol %), K_2CO_3 (4 equiv.) under an air atmosphere. In 2016, Wang et al. reported ligand-free arylation of pyridines and quinolines via direct coupling of bromo-substituted pyridines or quinolines with hypervalent iodine(III) compounds as efficient arylating reagents in the presence of catalyst $PdCl_2$ and base Cs_2CO_3 in DMF at 110°C (Wang et al., 2016).

via C–H Trifluoromethylation/Alkynylation

Mu et al. reported Pd-catalyzed C–H trifluoromethylation to prepare C2-trifluoromethylated indoles employing Ruppert–Prakash reagent, $TMSCF_3$ as CF_3 source in presence of oxidant $PhI(OAc)_2$ **1** and base CsF at room temperature (Mu

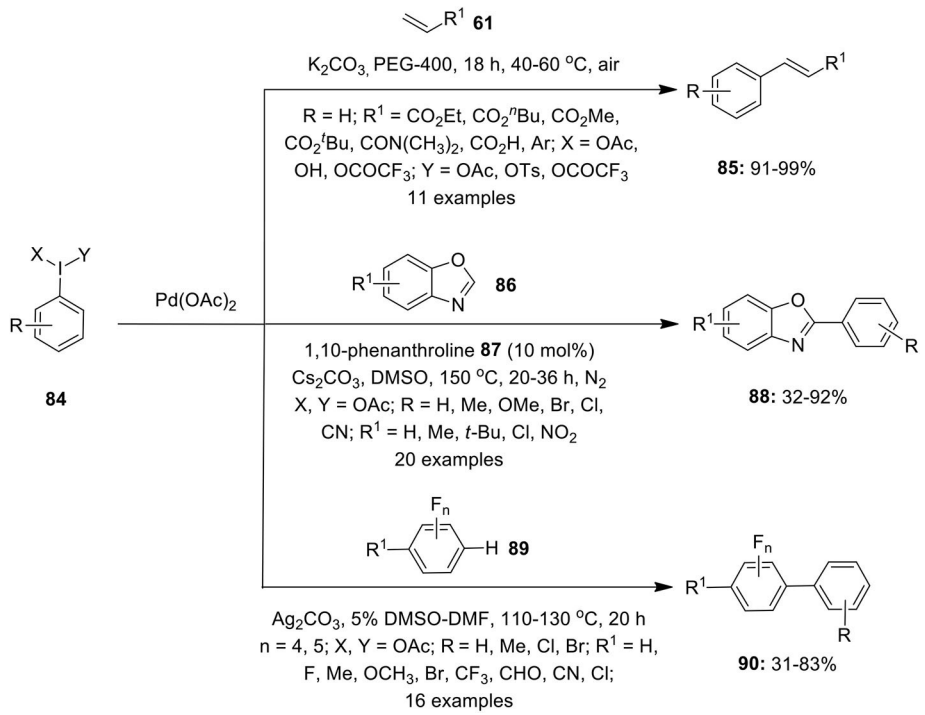

SCHEME 10 | Pd(II)-catalyzed Hseck-type coupling reactions using hypervalent iodine(III) reagents **84**.

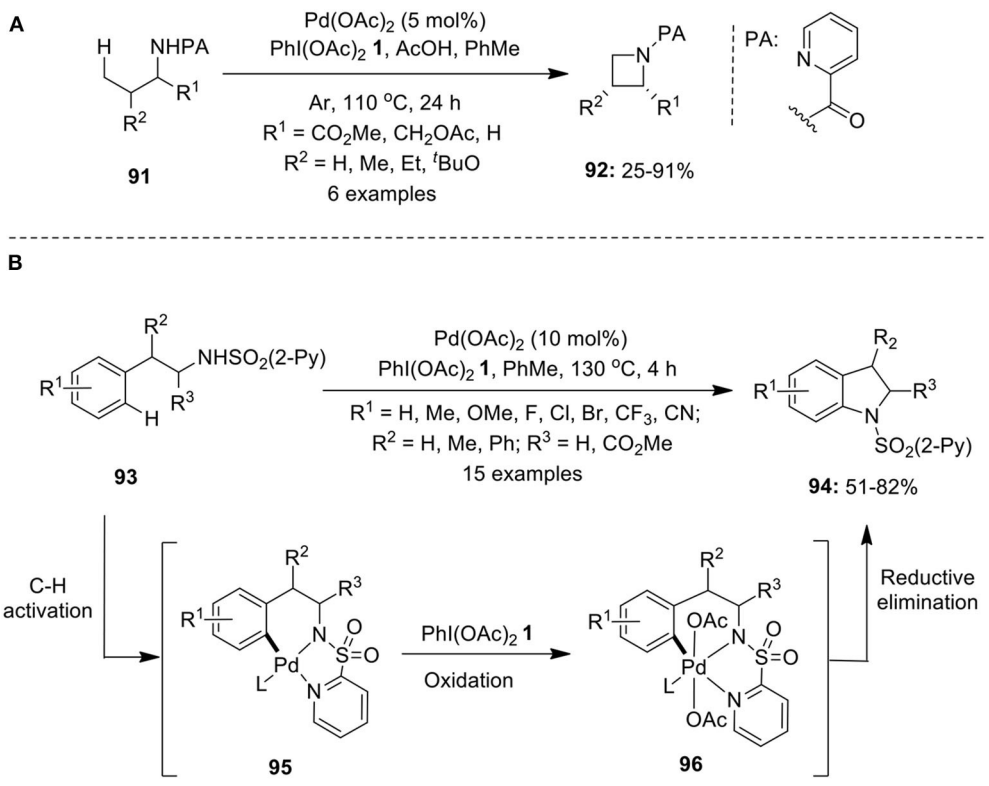

SCHEME 11 | (A) Pd(OAc)$_2$-catalyzed synthesis of azetidines **92** using oxidant PhI(OAc)$_2$ **1** and **(B)** Pd(OAc)$_2$-catalyzed synthesis of indolines **94** using oxidant PhI(OAc)$_2$ **1**.

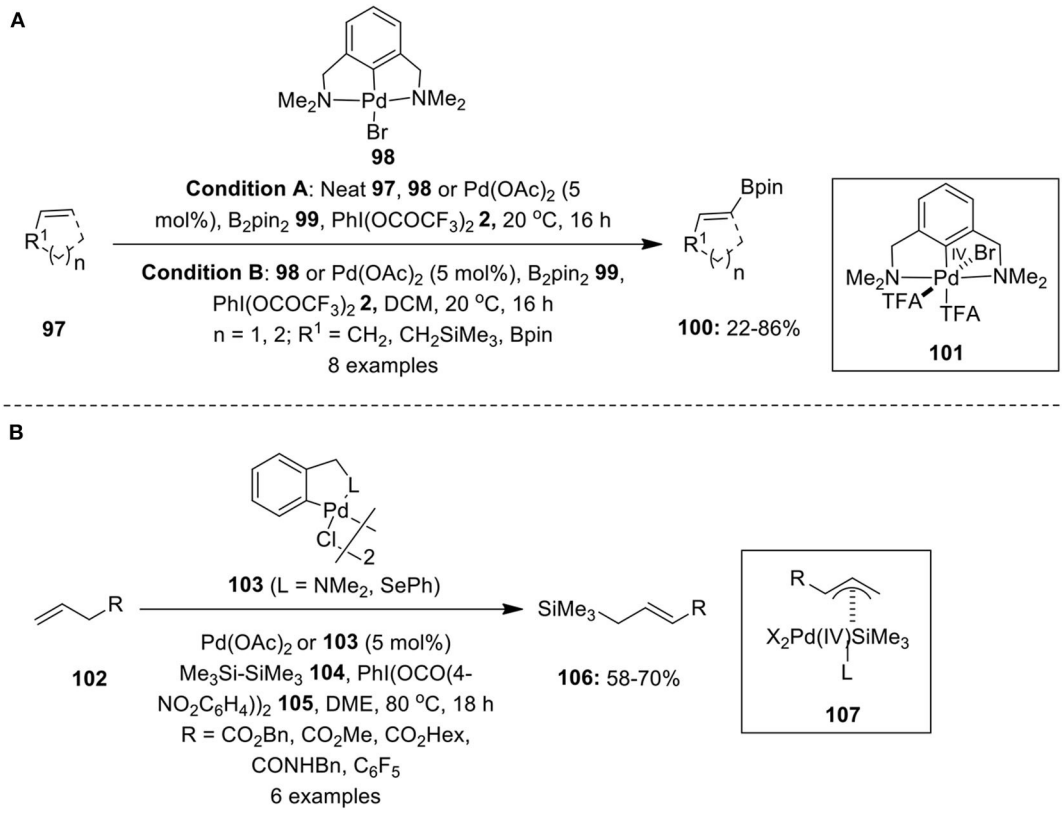

SCHEME 12 | (A) Palladium-catalyzed C–H borylation of olefins **97** mediated by $PhI(TFA)_2$ **2** and **(B)** Palladium-catalyzed C–H silylation of terminal olefins **102** using $PhI(OCO(4\text{-}NO_2C_6H_4))_2$ **105** as an oxidant.

et al., 2011). In 2013, Tolnai et al. employed 2 mol% of $Pd(MeCN)_4(BF_4)_2$ catalyst in the regioselective C2-alkynylation of *N*-alkylated indoles using 1-[(Triisopropyllsilyl)ethynyl]-1,2-benziodoxol-3(1*H*)-one (TIPS-EBX) as an alkynylating reagent (Tolnai et al., 2013). This reaction gave direct access to substituted 1-alkylated-2-[(triisopropylsilyl)ethynyl]-1*H*-indole at ambient temperature under air atmosphere in significant yields. A number of substituents including Cl, Br, F, & I remained intact in the final products which could be used for further synthetic modifications.

C–N BOND FORMATION

Catalytic C–H activation/C–N bond formation has gained considerable attention in recent times as it represents the versatile approach for the construction of *N*-containing aliphatic/aromatic heterocycles. Several intra- and intermolecular protocols for the palladium-catalyzed amination of sp^3 and sp^2 C–H bonds have been developed using hypervalent iodine reagents as oxidant. Gaunt has disclosed an elegant work on intramolecular C–H amination of *N*-substituted biphenyls for the synthesis of carbazoles at room temperature using catalyst $Pd(OAc)_2$ and oxidant $PhI(OAc)_2$ **1** in the presence of acetic acid in toluene (Jordan-Hore et al., 2008). Furthemore, Chen's research group synthesized azetidines **92** via intramolecular C–H amination of picolinamide-directed amine substrates **91** employing $Pd(OAc)_2$ and $PhI(OAc)_2$ **1** in toluene under argon atmosphere (**Scheme 11A**; He et al., 2012a). Additionally, the synthesis of pyrrolidines was also accomplished under identical reaction conditions.

Mei et al. demonstrated the synthesis of indolines **94** via $Pd(OAc)_2$-catalyzed intramolecular C–H activation/C–N cyclization of phenethylamine derivatives **93** using 2-pyridinesulfonyl as efficient directing group in the presence of oxidant $PhI(OAc)_2$ **1** (Mei et al., 2013). The intramolecular amination proposed to proceed via Pd-catalyzed C–H activation to generate organopalladium(II) complex **95**, followed by oxidation to form palladium(IV) intermediate **96** and final C–N reductive elimination to provide anticipated products **94**. Furthermore, the 2-pyridinesulfonyl moiety was easily removed under mild reaction conditions by treating with magnesium in MeOH at 0°C (**Scheme 11B**). Similar protocols to prepare indolines were independently reported by Daugulis, Chen, and Shi's research groups employing $Pd(OAc)_2/PhI(OAc)_2$ **1** catalytic system (He et al., 2012b; Nadres and Daugulis, 2012; Ye et al., 2013).

On the other hand, Yin et al. disclosed an intermolecular allylic C–H amination of alkyl olefins to furnish linear (*E*)-allylimides using *O*-alkyl *N*-sulfonylcarbamates as nitrogen nucleophile. The catalytic system comprises of catalyst

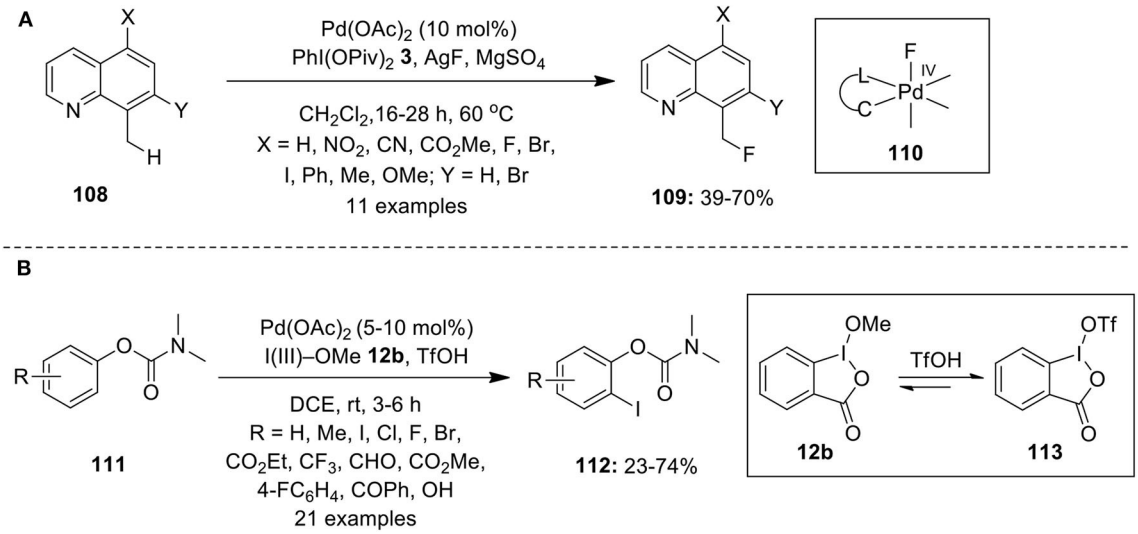

SCHEME 13 | (A) Pd(II)-catalyzed C–H fluorination of 8-methylquinoline analogs **108** using oxidant $PhI(OPiv)_2$ **3** and **(B)** Pd(II)-catalyzed C–H iodination of phenol carbamates **111** by employing Togni's reagent **12b**.

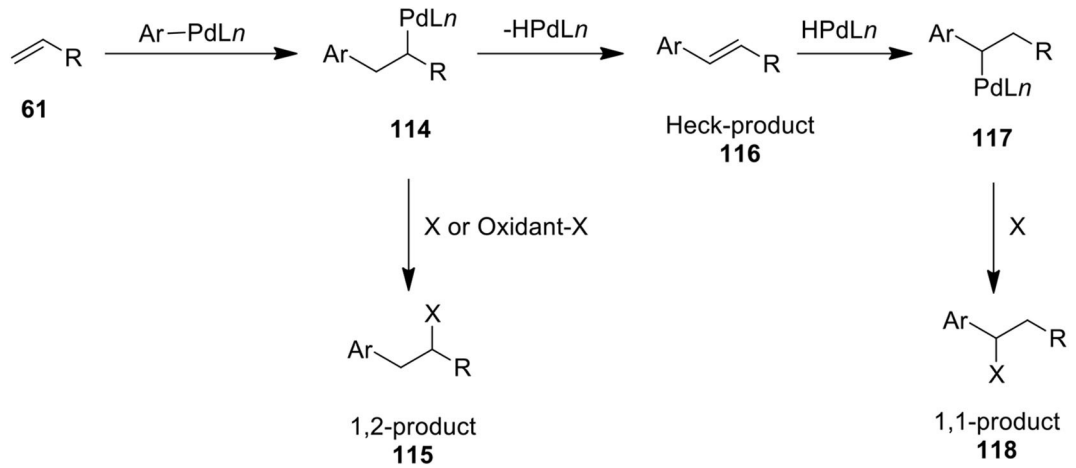

SCHEME 14 | Plausible mechanism for the Pd(II)-catalyzed difunctionalization of alkenes **61**.

$Pd(OAc)_2$ (5 mol%), terminal oxidant $PhI(OPiv)_2$, additive 1,4-naphthoquinone (20 mol%) and base Bu_4NOAc (Yin et al., 2010). Another interesting protocol featuring Pd-catalyzed regioselective intermolecular C–H amination of multi-substituted arenes using phthalimide as the nitrogen source was developed by Hartwig and co-workers (Shrestha et al., 2013).

C–B AND C–SI BOND FORMATION

Sazabo and his research group demonstrated the first example of selective C–H borylation of simple alkenes **97** employing a palladium pincer complex **98** as an effective catalyst and $PhI(TFA)_2$ **2** as an essential oxidant (Selander et al., 2010). Reaction was performed in neat alkenes (Condition A) or diluted alkenes (Condition B) at ambient temperature (**Scheme 12A**). Simple cycloalkenes **97** such as cyclopentene and cyclohexene (R^1: CH_2; $n = 1, 2$) were readily borylated with B_2pin_2 **99** to provide valuable organoboronates **100** with excellent vinylic selectivity. However, in the case that cycloheptane selectivity was reversed, the formation of allylic product was favored. Further borylation reaction of acyclic alkenes such as allylsilane and vinylboronate **98** (R^1: CH_2SiMe_3, Bpin; $n = 0$) were also carried out under similar reaction conditions. Additionally, the course of reaction was also studied with $Pd(OAc)_2$ as a catalyst, but products were obtained in albeit lower yields. The key step involves formation of Pd(IV) intermediate **101** via oxidation of catalyst using $PhI(TFA)_2$ **2**, which further undergoes transmetalation with B_2pin_2 and subsequent reaction with alkenes to deliver desired products **100**. Furthermore, the borylation reaction proceeded with excellent vinylic selectivity,

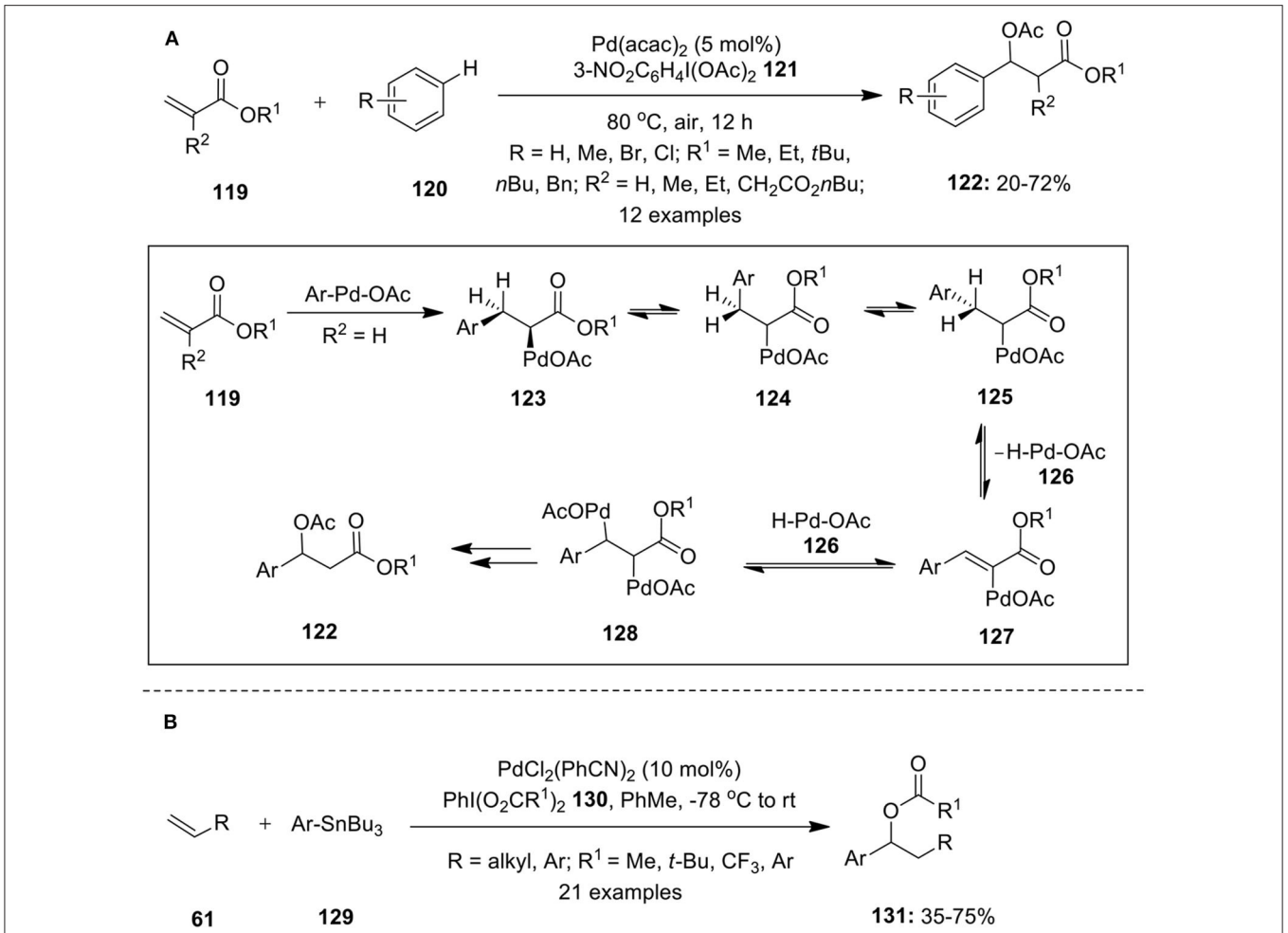

SCHEME 15 | (A) Pd(II)-catalyzed 1,1-difuntionalization of acrylate derivatives **119** using iodine(III) reagent **121** and **(B)** Pd(II)-catalyzed 1,1-difuntionalization of terminal olefins **61** using iodine(III) reagent **130** as oxidant.

except in the case of cycloheptane which yielded allylic products preferentially.

Later, the same research group developed the first Pd-catalyzed oxidative allylic C–H silylation of terminal olefins **102** using hexamethyldisilane **104** as the silyl source (Larsson et al., 2011). This catalytic process employs hypervalent iodine(III) reagent $PhI(OCO(4\text{-}NO_2C_6H_4))_2$ **105** as an oxidant and $Pd(OAc)_2$ or nitrogen and selenium-based palladium catalyst **103** (**Scheme 12B**). The reaction follows Pd(II)/Pd(IV) pathway involving formation of allylpalladium complex **107** which presumably undergoes reductive elimination to furnish allylsilanes **106**. Moreover, the functional groups such as ester, benzyl, and amide were well-tolerated under the oxidizing conditions and anticipated products **106** were obtained with high regio- and stereoselectivity.

C–HALOGEN BOND FORMATION

Palladium-catalyzed conversion of C–H bond into C–Halogen bond is an attractive method to access valuable aryl halides. However, in the past limited studies have been carried out in C–H halogenation reactions via high valent palladium catalysis. McMurtrey et al. published the first report on Pd-catalyzed C–H fluorination employing AgF as a fluoride source in combination with iodosobenzene dipivalate, $PhI(OPiv)_2$ **3** as oxidant (McMurtrey et al., 2012). Although the detailed mechanism is not given, high valent Pd-alkyl fluoride complex **110** was hypothesized as the key intermediate in this process that would further undergo C–F bond-forming reductive elimination to yield fluorination products **109** in moderate to good yields (**Scheme 13A**). Furthermore, the substrates **108** bearing electron-withdrawing groups produced better results than those with electron-donating groups.

In 2015, Rao's research group achieved *ortho* C–H iodination of phenol carbamates **111** through palladium catalysis employing Togni's reagent **12b** as an iodine source and as oxidant in DCE/TfOH at room temperature (Sun et al., 2015). Both electron-rich and -deficient substituents were well-tolerated, leading to the preparation of *o*-iodinated phenol derivatives in fair to good yields (**Scheme 13B**). NMR studies revealed that

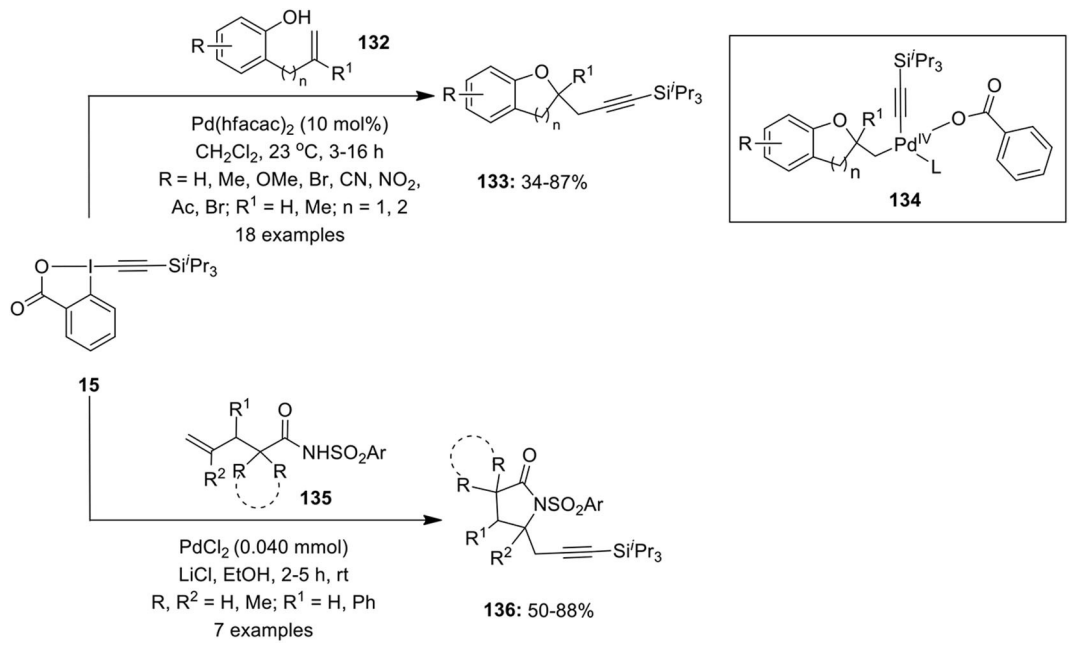

SCHEME 16 | Pd-catalyzed intramolecular oxyalkynylation of phenols **132** and aminoalkynylation of activated amides **135** by using TIPS-EBX **15** as acetylene transfer reagent.

some part of cyclic iodine(III)reagent on treatment with TfOH gets converted into **113** and probably both oxidants participates in this reaction.

ALKENE DIFUNCTIONALIZATION

Palladium-catalyzed difunctionalization of simple alkenes using hypervalent iodine reagents has emerged as a powerful method in organic synthesis. Various 1,1- and 1,2-difunctionalization protocols have been developed by several researchers for preparing a diverse array of useful molecules from alkenes. A general mechanism for the Pd-catalyzed oxidative functionalization of alkenes **61** is shown in **Scheme 14**. These transformations proposed to proceed through the formation of δ-alkyl Pd^{II} intermediate **114** obtained via olefin insertion into the aryl-Pd bond. Next, Heck intermediate **114** undergoes β-hydride elimination to form Heck product **116** and the resulting -HPdL*n*-species readds again to give benzylic Pd(II) intermediate **117** which can be intercepted with suitable nucleophile to furnish 1,1-difunctionalized product **118**. Furthermore, Heck intermediates **114** could be oxidatively functionalized into 1,2-difunctionalized product **115** in the presence of suitable nucleophile or oxidant.

Pd(II)-Catalyzed 1,1-Difunctionalization of Alkenes

Pd-catalyzed hypervalent iodine mediated 1,1-difunctionalization of alkenes are rare and only few examples are available in the literature. Moran and co-author published an article highlighting 1,1-difuntionalization of acrylate derivatives **119** using palladium catalysis (Rodriguez and Moran, 2009). This reaction involves three component coupling of activated alkenes **119,** substituted arenes **120** and hypervalent iodine(III) reagent **121** in acetic acid. Reaction possibly involves formation of Heck intermediate **123** via Heck-type addition of aryl-Pd complex to the alkene **119**, followed by β-hydride elimination and subsequent readdition of Pd-H species **126** at benzylic site to form intermediate **128**. Finally, oxidation of **128** to Pd(IV) intermediate using iodine(III) reagent **121** and subsequent functionalization with acetate ion lead to the formation of desired 1,1-aryloxygenated compounds **122** (**Scheme 15A**).

Later, Satterfield et al. disclosed 1,1-aryloxygenation protocol wherein arylstannanes **129** were successfully coupled with terminal olefins **61** in the presence of hypervalent iodine reagents ($PhI(O_2CR^1)_2$) **130** as an oxidant and palladium catalyst, $PdCl_2(PhCN)_2$ (Satterfield et al., 2011). This catalytic approach enabled simultaneous generation of C–C and C–O bond in a single step furnishing 1,1-arylacetoxylated products **131** in significant yields (**Scheme 15B**).

1,2-Difunctionalization of Alkenes

Over the years, great progress has been achieved in the field of Pd-catalyzed 1,2-difunctionalization of olefins using various hypervalent iodine reagents. Based on this strategy, a number intra- and intermolecular synthetic transformations such as diamination, dioxygenation, aminoacetoxylation, fluoroamination, and oxidative amination have been developed.

Intramolecular 1,2-Difunctionalization of Alkenes

Catalytic intramolecular difunctionalization of alkenes is one of the most powerful methods for the construction of heteroatom

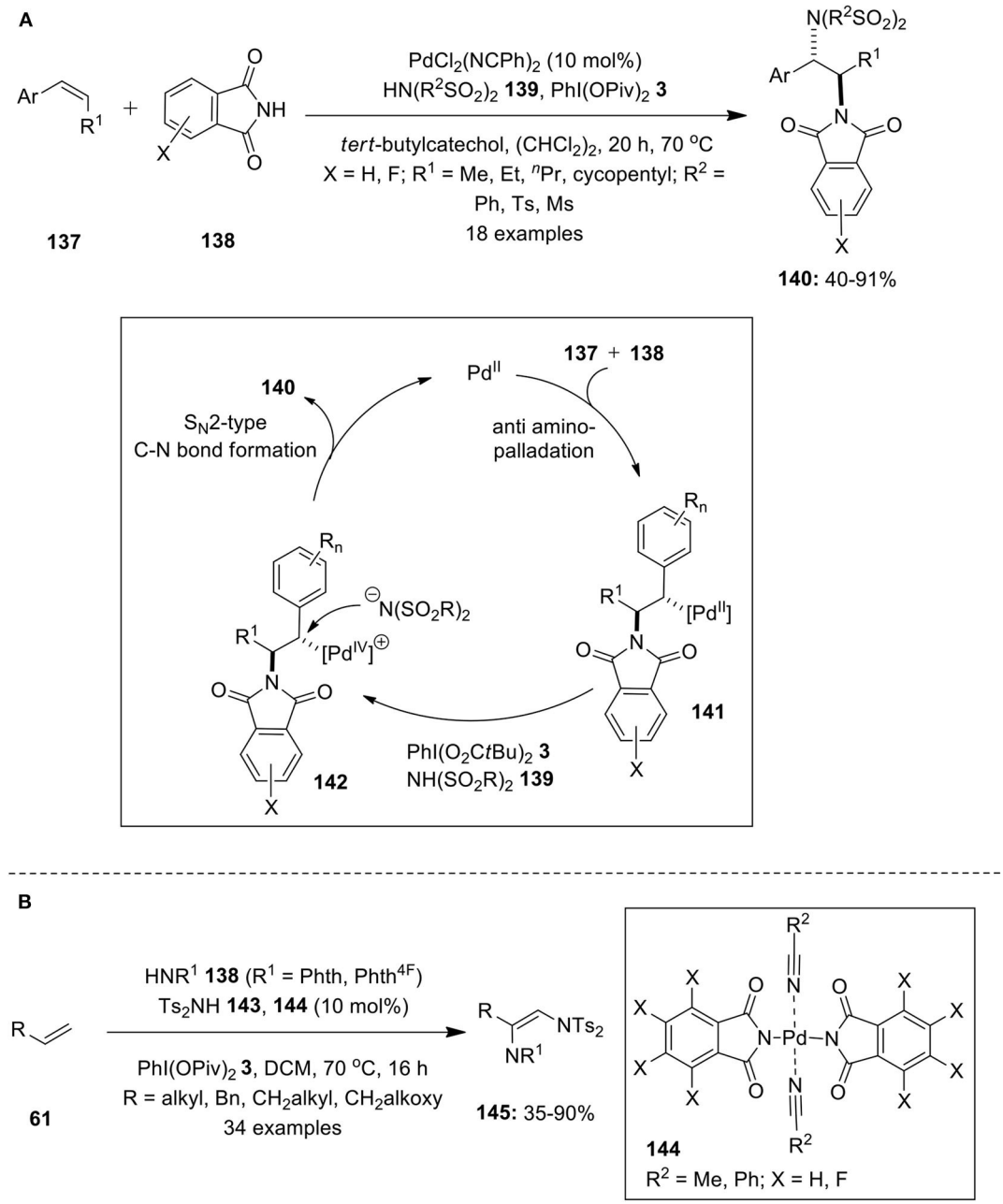

SCHEME 17 | (A) Intermolecular diamination of internal alkenes **137** using Pd/PhI(OPiv)$_2$-catalytic system and **(B)** Palladium-phthalimidato complex-catalyzed diamination of alkenes **61** using PhI(OPiv)$_2$ **3** as oxidant.

containing aromatic and aliphatic cyclic compounds. Sanford and co-workers reported Pd-catalyzed intramolecular oxidative amination strategy for the synthesis of tetrahydrofurans using oxidant PIDA **2** (Desai and Sanford, 2007). Subsequently, Muniz's research group developed an intramolecular alkene diamination protocol for the preparation of bisindoline and cyclic urea scaffolds using palladium catalysis (Streuff et al., 2005; Muniz, 2007; Muniz et al., 2008). Furthermore, Wu et al. performed Pd-catalyzed intramolecular aminofluorination of unactivated *N*-tosylamine alkenes with AgF as fluorinating reagent in the presence of PhI(OCO*t*Bu)$_2$ as terminal oxidant and $MgSO_4$ as additive in acetonitrile at room temperature (Wu et al., 2009).

Zhu's research group reported domino carboacetoxylation of *N*-aryl acrylamides to synthesize 3,3′-disubstituted oxindoles and spiropyrrolidinyloxindoles using catalytic amount of Pd(OAc)$_2$ or $PdCl_2$ and oxidant PhI(OAc)$_2$ **1** in AcOH at 100°C (Jaegli et al., 2010). Furthermore, another

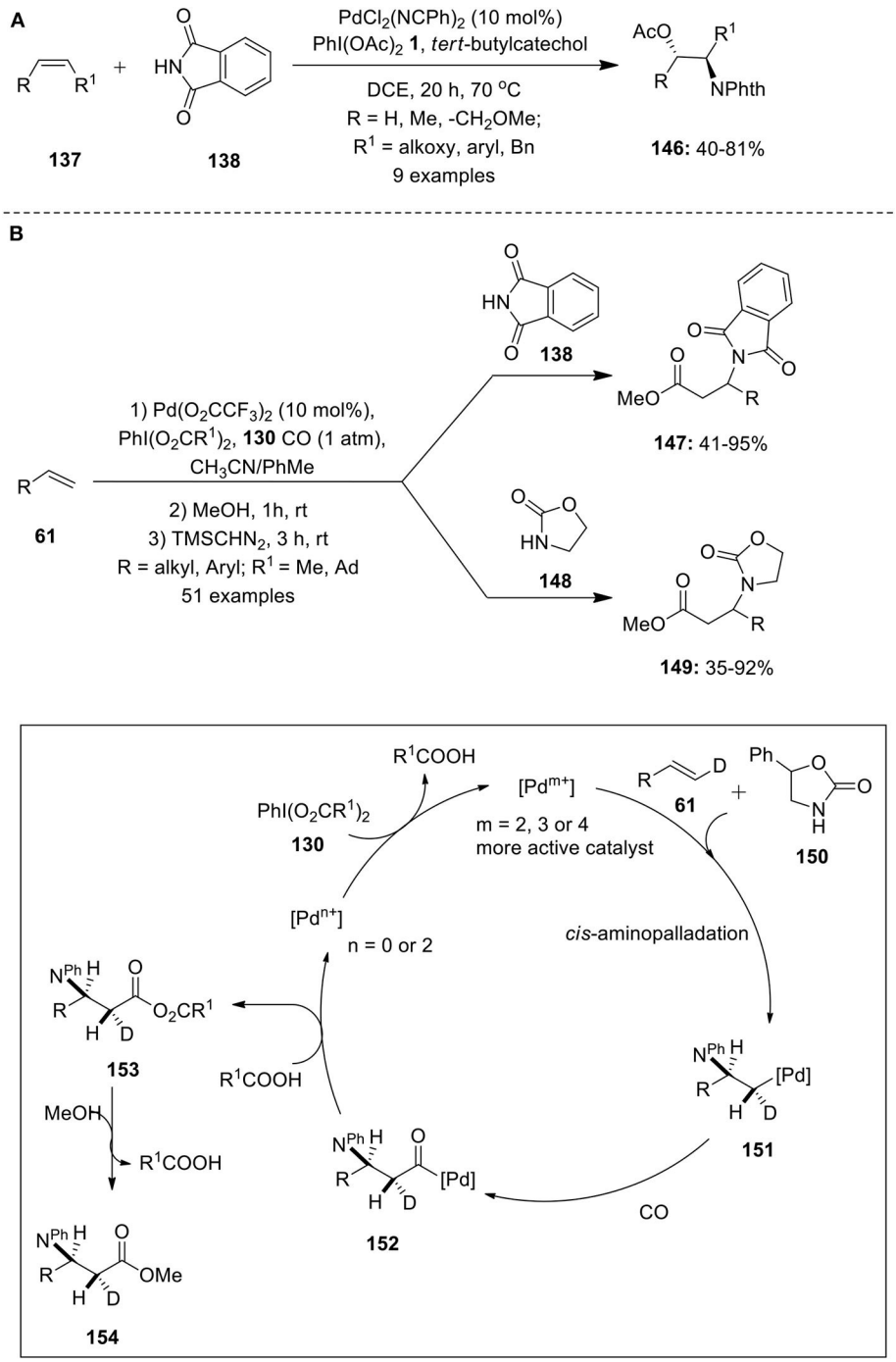

SCHEME 18 | (A) Pd(II)-catalyzed PIDA-mediated aminoacetoxylation of alkenes **137** and **(B)** Pd(II)-catalyzed aminocarbonylation of alkenes **61** induced by iodine(III) reagent **130**.

intramolecular carboacetoxylation protocol for the preparation of acetoxymethyl-substituted cyclopentane derivatives via oxidative cyclization of 4-pentenyl-substituted malonate esters employing bis(acetonitrile)dichloropalladium catalyst and oxidant $PhI(OAc)_2$ **1** was developed (Fujino et al., 2010). The reaction was performed in the presence of base titanium tetraisopropoxide in DCE/Ac_2O (1:1) solvent system at 50°C.

In 2010, Nicolai et al. reported the first intramolecular oxyalkynylation of non-activated terminal alkenes **132** using 1-[(triisopropylsilyl)ethynyl]-1,2-benziodoxol-3(1*H*)-one (TIPS-EBX) **15** as acetylene transfer reagent in DCM in

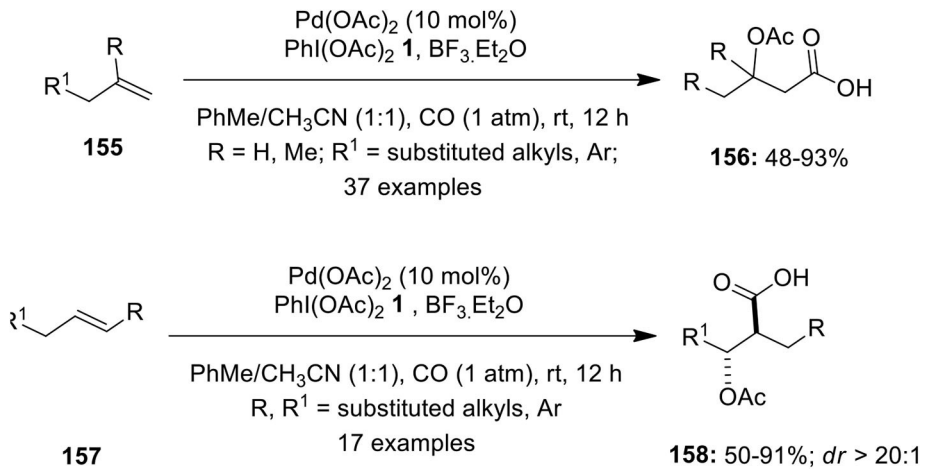

SCHEME 19 | Pd(II)-catalyzed oxycarbonylation of alkenes **154** and **156** using $PhI(OAc)_2$ **1** as an oxidant.

the presence of 10 mol% of $Pd(hfacac)_2$ as an efficient Pd species (Nicolai et al., 2010). The reaction was successful with different phenol substrates **132** giving cyclic ethers **133** via Pd(IV) intermediate **134** in variable yields (**Scheme 16**). Additionally, the scope of the reaction was examined with both aromatic and aliphatic carboxylic acids leading to the synthesis of γ-lactones under the same optimized reaction condition.

In continuation with the difunctionalization reaction, the Waser's group described an intramolecular aminoalkynylation of activated olefins **135** to afford 4-propargyl lactams **136** employing TIPS-EBX **15** as alkynylating agent (Nicolai et al., 2011). In the presence of $PdCl_2$ and LiCl, the active catalyst lithium palladate, $Li_2[PdCl_4]$ generates *in situ* which catalyzes the carboamination reaction (**Scheme 16**). Furthermore, the present protocol was successfully utilized for the synthesis of 4-propargyl oxazolidinone and imidazolidinones through the cyclization of allyl carbamates and allyl ureas, respectively. Additionally, the synthesized γ- and δ-lactams were employed as precursors for the synthesis of bicyclic heterocycles pyrrolizidine and indolizidine and also in the total synthesis of natural product (±)-trachelanthamidine (Nicolai et al., 2011).

Intermolecular 1,2-Difunctionalization of Alkenes

Iglesias et al. developed the first example of Pd-catalyzed intermolecular diamination of terminal alkenes employing saccharin and bissulfonimides as the nitrogen sources in the presence of $PhI(OPiv)_2$ **3** as an oxidant (Iglesias et al., 2010). Further allylic ethers were subjected to similar catalytic intermolecular 1,2-diamination reaction using nitrogen sources, phthalimide, and *N*-fluoro-bis(phenylsulfonyl)imide (Muniz et al., 2011). Later, Martinez and Muniz successfully employed $Pd/PhI(OPiv)_2$-catalytic system for the intermolecular vicinal diamination of internal alkenes **137** with phthalimide **138** and bissulfonimides **139** as the two nitrogen sources (Martinez and Muniz, 2012). This method employs alkene as the limiting reagent and desired diamination products **140** were isolated in moderate to high yields with complete regio- and diastereoselectivity (**Scheme 17A**). The mechanistic approach involves initial alkene **137** co-ordination with the Pd catalyst followed by subsequent aminopalladation involving nucleophilic addition of **138** via *trans* stereochemistry to form δ-alkylpalladium complex **141**. Rapid oxidation of complex **141** gives Pd(IV) intermediate **142** which is attacked by bissulfonimide **139** to provide desired product **140** with net inversion of configuration at benzylic position.

In continuation, Martinez and Muniz reported the synthesis of new palladium-phthalimidato complexes **144** and demonstrated its broad applicability as catalysts in the vicinal diamination of alkenes **61** with phthalimide **143** and bissulfonimides **144** as nitrogen sources (Martinez and Muniz, 2016). The treatment of phthalimide **143** with $Pd(OAc)_2$ in nitrile solution at room temperature resulted in the formation of palladium-phthalimidato complexes **144**. The air-stable preformed phthalimidato complexes proved to be versatile catalysts for the present diamination reaction providing desired products **145** in useful yields (**Scheme 17B**). Moreover, the same research group synthesized other bissaccharido palladium(II) complexes and investigated their application in catalytic regioselective diaminations and aminooxygenation of alkenes (Martinez et al., 2016).

Pd-catalyzed aminoacetoxylation of alkenes were independently reported by Sorensen and Stahl's groups employing 2 equivalence of olefin with respect to nitrogen nucleophiles (Alexanian et al., 2005; Liu and Stahl, 2006). Later, Muniz with his co-workers reported a modified method for an intermolecular aminoacetoxylation of internal/terminal alkenes **137** using alkene substrates as limiting reagent (Martinez et al., 2013). A series of alkenes such as allyl ethers, allyl benzenes, (Z)-β-methylstyrene, etc. were oxidized and converted into aminoacetoxylated product **146** using phthalimide **138** as a nitrogen source (**Scheme 18A**). Based on the experimental evidences, it was concluded that $PhI(OAc)_2$ **1** influences the

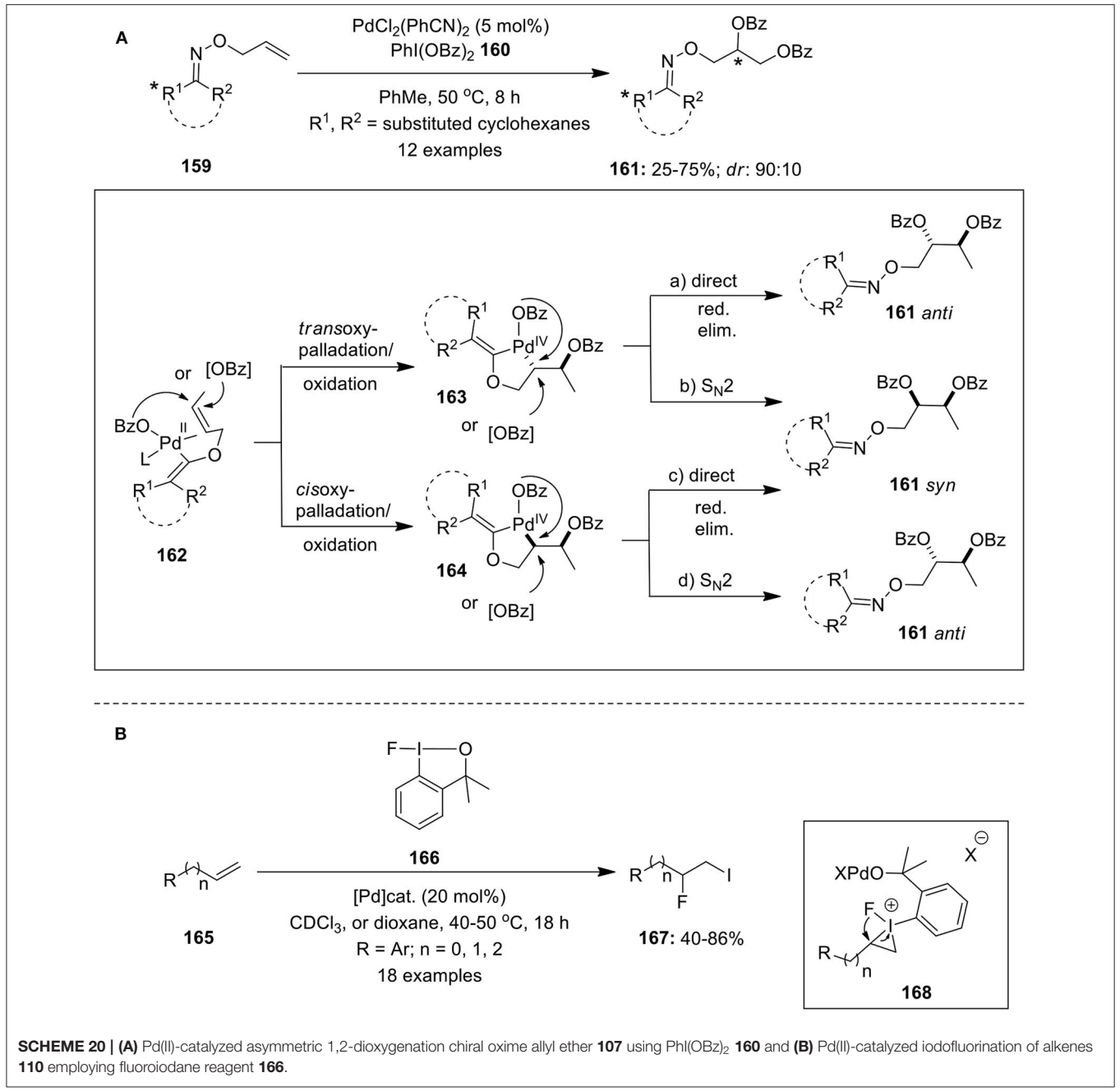

SCHEME 20 | (A) Pd(II)-catalyzed asymmetric 1,2-dioxygenation chiral oxime allyl ether **107** using $PhI(OBz)_2$ **160** and **(B)** Pd(II)-catalyzed iodofluorination of alkenes **110** employing fluoroiodane reagent **166**.

stereochemical aspect of the aminoacetoxylation reaction favoring *trans*-aminopalladation pathway.

In 2015, Cheng et al. have demonstrated an efficient and simple palladium-catalyzed protocol for the synthesis of β^{-} amino acid derivatives **147** and **149** from alkenes **61** via intermolecular aminocarbonylation reaction (Cheng J. et al., 2015). An array of aliphatic or aromatic terminal alkenes **61** were reacted with either phthalimide **138** or with 2-oxazolidone **148** under a carbon monoxide atmosphere in the presence of $PhI(O_2CR^1)_2$ **130** as an oxidant (**Scheme 18B**). The reaction possessed excellent regioselectivity, broad substrates scope, and remarkable functional group tolerance. Reaction mechanism and stereochemistry was studied by taking deuterium labeled alkene **61** and substituted 2-oxazolidone **149** as an example. The reaction initiates with *cis*-aminopalladation of alkene **61** to form alkyl-Pd complex **151** and subsequent CO insertion gives intermediate **152**. Next, nucleophilic attack of carboxylate on to the acyl-Pd species **152** afforded anhydride product **153** which upon alcoholysis yields carboxylic ester **154**. Further the experimental evindence revealed that the iodine(III) reagent plays a crucial role in accelerating the intermolecular aminopalladation process.

The same research group developed a novel Pd-catalyzed intermolecular oxycarbonylation of terminal **155** and

internal alkenes **157** under CO atmosphere using PIDA **1** as oxidant (Li M. et al., 2016). This difunctionalization reaction leads to the facile synthesis of various β-oxycarboxylic acids **156** and **158** in useful yields with excellent functional group compatibility, regioselectivity, and diastereoselectivity (**Scheme 19**). The potential scope of this method was extended toward the synthesis of natural product, (+)-honaucin C in 48% yield with *ee* up to 99% (Li M. et al., 2016).

Vicinal alkene dioxygenation is an important method for the preparation of valuble 1,2-dioxygenated scaffolds. In this regard, Dong and Shi's research groups independently reported Pd-catalyzed vicinal dioxygenation of olefins employing hypervalent iodine reagent as terminal oxidant following distinct $Pd^{(II)}/Pd^{(IV)}$ mechanism (Li et al., 2008; Wang W. et al., 2010). Subsequently, Sanford's group developed Pd(II)-catalyzed chiral oxime-directed asymmetric 1,2-dioxygenation of alkenes **159** using $PhI(OBz)_2$ **160** as an oxidant and benzoyloxy source (Neufeldt and Sanford, 2013). Various chiral allyl oxime ethers were screened and it was observed that menthone-derived substrates provided best reactivity and diastereoselectivity. This approach enabled efficient preparation of dibenzoylated products **161** with diasteriomeric ratio up to 9:1 (**Scheme 20A**). The proposed mechanism initiates with the coordination of oxime ether **159** with Pd catalyst to give intermediate **162** followed by subsequent oxypalladation and oxidation proceeding via either *trans* or *cis* geometry to deliver intermediate **163** or **164**. Final, reductive elimination could occur by direct (path "a" and "c") or by S_N2-type mechanisms (path b and d) that would lead to the formation of *syn* or *anti* products. Further, based on the experimental data authors suggested that reaction proceeds via *syn* addition and primary operative mechanism could be either "b" or "c".

Furthermore, the Pd-catalyzed iodofluorination of alkenes **165** was reported by Ilchenko et al. employing fluoroiodane reagent **166** as iodine and fluorine sources (Ilchenko et al., 2016). The reaction was carried out using either $Pd(BF_4)_2(MeCN)_4$ or $PdCl_2(MeCN)_2$ or $Pd(OAc)_2$ as palladium catalysts in $CDCl_3$ (**Scheme 20B**). The reaction proceeds via three-membered iodonium intermediate **168** which upon ring opening and subsequent $C(sp^2)$–I bond cleavage delivers the desired iodofluorinated products **167**. Simple cycloalkenes such as cyclohexene and cycloheptene also undergoes iodofluorination reaction to give iodofluorinated products in modest yields.

CONCLUSION

In conclusion, this review described various achievements made in palladium-catalyzed reactions mediated by hypervalent iodine compounds. Hypervalent iodine reagents are versatile, non-toxic, environment friendly, and easy to handle reagents in organic synthesis. In recent years, the use of hypervalent iodine reagents in palladium-catalyzed transformations has been widely studied as they are strong electrophiles and powerful oxidizing agents. Most of the reactions proceed via Pd(II/IV) redox cycles involving hypervalent iodine reagents-induced oxidation to generate Pd(IV) center as the key step. The inherent oxidizing nature and unique reactivity of these reagents with palladium catalysts enabled efficient preparation of synthetically useful molecules through C–O, C–N, C–C, C–Si, C–B, and C–halogen bond formation reactions. In addition, a number of Pd-catalyzed alkene difunctionalization reactions have been developed in recent times employing hypervalent iodine reagents. More importantly, oxidation of an unactivated $C(sp^3)$–H bond has been successfully accomplished using a palladium and hypervalent iodine catalytic system which is a challenging problem. From future perspectives, palladium catalysis is well-established with respect to achiral synthesis, however reactions concerning to asymmetric synthesis are limited. Thus, development of enantioselective Pd-catalyzed reaction with hypervalent iodine reagents would be a much-anticipated area of research in the near future. Apart from this, use of recyclable polymer-supported hypervalent iodine reagents in palladium catalyzed reactions would be another interesting field of research.

AUTHOR CONTRIBUTIONS

All authors listed have made a substantial, direct and intellectual contribution to the work, and approved it for publication.

ACKNOWLEDGMENTS

SS and FS are thankful to VIT Chennai for providing infrastructure for preparing the review article.

REFERENCES

Alam, R., Pilarski, L. T., Pershagen, E., and Szabo, K. J. (2012). Stereoselective intermolecular allylic C–H trifluoroacetoxylation of functionalized alkenes. *J. Am. Chem. Soc.* 134, 8778–8781. doi: 10.1021/ja302457p

Alexanian, E. J., Lee, C., and Sorensen, E. J. (2005). Palladium-catalyzed ring-forming aminoacetoxylation of alkenes. *J. Am. Chem. Soc.* 127, 7690–7691. doi: 10.1021/ja051406k

Biffis, A., Centomo, P., Zotto, A. D., and Zecca, M. (2018). Pd metal catalysts for cross-couplings and related reactions in the 21st Century: a critical review. *Chem. Rev.* 118, 2249–2295. doi: 10.1021/acs.chemrev.7b00443

Bigi, M. A., and White, M. C. (2013). Terminal olefins to linear α,β-unsaturated ketones: Pd(II)/ hypervalent iodine co-catalyzed Wacker oxidation–dehydrogenation. *J. Am. Chem. Soc.* 135, 7831–7834. doi: 10.1021/ja402651q

Chaudhari, D. A., and Fernandes, R. A. (2016). Hypervalent iodine as a terminal oxidant in wacker-type oxidation of terminal olefins to methyl ketones. *J. Org. Chem.* 81, 2113–2121. doi: 10.1021/acs.joc.6b00137

Chen, F.-J., Zhao, S., Hu, F., Chen, K., Zhang, Q., Zhang, S.-Q., et al. (2013). Pd(II)-catalyzed alkoxylation of unactivated $C(sp^3)$–H and $C(sp^2)$–H bonds using a removable directing group: efficient synthesis of alkyl ethers. *Chem. Sci.* 4, 4187–4192. doi: 10.1039/c3sc51993g

Cheng, C., Liu, S., and Zhu, G. (2015). Divergent synthesis of 2-aminofurans via palladium-catalyzed acetoxylative, alkoxylative, and hydroxylative

cycloisomerization of homoallenyl amides. *J. Org. Chem.* 80, 7604–7612. doi: 10.1021/acs.joc.5b01182

Cheng, J., Qi, X., Li, M., Chen, P., and Liu, G. (2015). Palladium-catalyzed intermolecular aminocarbonylation of alkenes: efficient access of β-amino acid derivatives. *J. Am. Chem. Soc.* 137, 2480–2483. doi: 10.1021/jacs.5b00719

Cheng, X.-F., Li, Y., Su, Y.-M., Yin, F., Wang, J.-Y., Sheng, J., et al. (2013). Pd(II)-catalyzed enantioselective C–H activation/C–O bond formation: synthesis of chiral benzofuranones. *J. Am. Chem. Soc.* 135, 1236–1239. doi: 10.1021/ja311259x

Chernyak, N., Dudnik, A. S., Huang, C., and Gevorgyan, V. (2010). PyDipSi: a general and easily modifiable/traceless Si-tethered directing group for C–H acyloxylation of arenes. *J. Am. Chem. Soc.* 132, 8270–8272. doi: 10.1021/ja1033167

Choy, P. Y., Lau, C. P., and Kwong, F. Y. (2011). Palladium-catalyzed direct and regioselective C–H bond functionalization/oxidative acetoxylation of indoles. *J. Org. Chem.* 76, 80–84. doi: 10.1021/jo101584k

Cook, A. K., Emmert, M. H., and Sanford, M. S. (2013). Steric control of site selectivity in the Pd-catalyzed C–H acetoxylation of simple arenes. *Org. Lett.* 15, 5428–5431. doi: 10.1021/ol4024248

Deprez, N. R., and Sanford, M. S. (2007). Reactions of hypervalent iodine reagents with palladium: Mechanisms and applications in organic synthesis. *Inorg. Chem.* 46, 1924–1935. doi: 10.1021/ic0620337

Desai, L. V., and Sanford, M. S. (2007). Construction of tetrahydrofurans by Pd^{II}/Pd^{IV}-catalyzed aminooxygenation of alkenes. *Angew. Chem. Int. Ed.* 46, 5737–5740. doi: 10.1002/anie.200701454

Dong, D.-Q., Hao, S.-H., Wang, Z.-L., and Chen, C. (2014). Hypervalent iodine: a powerful electrophile for asymmetric α-functionalization of carbonyl compounds. *Org. Biomol. Chem.* 12, 4278–4289. doi: 10.1039/c4ob00318g

Emmert, M. H., Cook, A. K., Xie, Y. J., and Sanford, M. S. (2011). Remarkably high reactivity of $Pd(OAc)_2$/pyridine catalysts: nondirected C–H oxygenation of arenes. *Angew. Chem. Int. Ed.* 50, 9409–9412. doi: 10.1002/anie.201103327

Evdokimov, N. M., Kornienko, A., and Magedov, I. V. (2011). Aryliodine(III) diacetates as substrates for Pd–Ag catalyzed arylation of alkenes. *Tetrahedron Lett.* 52, 4327–4329. doi: 10.1016/j.tetlet.2011.06.051

Fu, Z., Xiong, Q., Zhang, W., Li, Z., and Cai, H. (2015). Pd-catalyzed direct arylation of electron-deficient polyfluoroarenes with aryliodine(III) diacetates. *Tetrahedron Lett.* 56, 123–126. doi: 10.1016/j.tetlet.2014.11.033

Fujino, D., Yorimitsu, H., and Oshima, K. (2010). Palladium-catalyzed intramolecular carboacetoxylation of 4-pentenyl-substituted malonate esters with iodobenzene diacetate. *Chem. Asian J.* 5, 1758–1760. doi: 10.1002/asia.201000194

Gondo, K., Oyamada, J., and Kitamura, T. (2015). Palladium-catalyzed desilylative acyloxylation of silicon–carbon bonds on (trimethylsilyl)arenes: synthesis of phenol derivatives from trimethylsilylarenes. *Org. Lett.* 17, 4778–4781. doi: 10.1021/acs.orglett.5b02336

Gou, F.-R., Wang, X.-C., Huo, P.-F., Bi, H.-P., Guan, Z.-H., and Liang, Y.-M. (2009). Palladium-catalyzed aryl C–H bonds activation/acetoxylation utilizing a bidentate system. *Org. Lett.* 11, 5726–5729. doi: 10.1021/ol902497k

Gu, S., Chen, C., and Chen, W. (2009). Ortho-functionalization of 2-phenoxypyrimidines via palladium-catalyzed C–H bond activation. *J. Org. Chem.* 74, 7203–7206. doi: 10.1021/jo901316b

Gulevich, A. V., Melkonyan, F. S., Sarkar, D., and Gevorgyan, V. (2012). Double-Fold C–H oxygenation of arenes using PyrDipSi: a general and efficient traceless/modifiable silicon-tethered directing group. *J. Am. Chem. Soc.* 134, 5528–5531. doi: 10.1021/ja3010545

He, G., Lu, C., Zhao, Y., Nack, W. A., and Chen, G. (2012b). Improved protocol for indoline synthesis via palladium-catalyzed intramolecular $C(sp^2)$–H amination. *Org. Lett.* 14, 2944–2947. doi: 10.1021/ol301352v

He, G., Zhao, Y., Zhang, S., Lu, C., and Chen, G. (2012a). Highly efficient syntheses of azetidines, pyrrolidines, and indolines via palladium catalyzed intramolecular amination of $C(sp^3)$–H and $C(sp^2)$–H bonds at γ and δ positions. *J. Am. Chem. Soc.* 134, 3–6. doi: 10.1021/ja210660g

He, Y., Huang, L., Xie, L., Liu, P., Wei, Q., Mao, F., et al. (2019). Palladium-catalyzed C–H bond functionalization reactions using phosphate/sulfonate hypervalent iodine reagents. *J. Org. Chem.* 84, 10088–10101. doi: 10.1021/acs.joc.9b01278

Huang, C., Ghavtadze, N., Chattopadhyay, B., and Gevorgyan, V. (2011). Synthesis of catechols from phenols via Pd-catalyzed silanol-directed C–H oxygenation. *J. Am. Chem. Soc.* 133, 17630–17633. doi: 10.1021/ja208572v

Huang, C., Ghavtadze, N., Godoi, B., and Gevorgyan, V. (2012). Pd-catalyzed modifiable silanol-directed aromatic C–H oxygenation. *Chem. Eur. J.* 18, 9789–9792. doi: 10.1002/chem.201201616

Iglesias, A., Perez, E., and G., Muniz K (2010). An intermolecular palladium-catalyzed diamination of unactivated alkenes. *Angew. Chem. Int. Ed.* 49, 8109–8111. doi: 10.1002/anie.201003653

Ilchenko, N. O., Cortes, M. A., and Szabo, K. J. (2016). Palladium-catalyzed iodofluorination of alkenes using fluoro-iodoxole reagent. *ACS Catal.* 6, 447–450. doi: 10.1021/acscatal.5b02022

Jaegli, S., Dufour, J., Wei, H., Piou, T., Duan, X., Vors, J., et al. (2010). Palladium-catalyzed carbo-heterofunctionalization of alkenes for the synthesis of oxindoles and spirooxindoles. *Org. Lett.* 12, 4498–4501. doi: 10.1021/ol101778c

Jiang, T., Quan, X., Zhu, C., Andersson, P. G., and Backvall, J.-E. (2016). Palladium-catalyzed oxidative synthesis of α. Palladium-catnones from alkynes. *Angew. Chem. Int. Ed.* 55, 5824–5828. doi: 10.1002/anie.201600696

Jordan-Hore, J. A., Johansson, C. C. C., Gulias, M., Beck, E. M., and Gaunt, M. J. (2008). Oxidative Pd(II)-catalyzed C–H bond amination to carbazole at ambient temperature. *J. Am. Chem. Soc.* 130, 16184–16186. doi: 10.1021/ja806543s

Ju, L., Yao, J., Wu, Z., Liu, Z., and Zhang, Y. (2013). Palladium-catalyzed oxidative acetoxylation of benzylic C–H bond using bidentate auxiliary. *J. Org. Chem.* 78, 10821–10831. doi: 10.1021/jo401830k

Koposov, A. Y., Litvinov, D. N., Zhdankin, V. V., Ferguson, M. J., McDonald, R., Tykwinski, R. R., et al. (2006). Preparation and reductive decomposition of 2-iodoxybenzenesulfonic acid. X-ray crystal structure of 1-hydroxy-1H-1, 2, 3-benziodoxathiole 3, 3-dioxide. *Eur. J. Org. Chem.* 2006, 4791–4795. doi: 10.1002/ejoc.200600683

Larsson, J. M., Zhao, T. S. N., and Szabo, K. J. (2011). Palladium-catalyzed oxidative allylic C–H silylation. *Org. Lett.* 13, 1888–1891. doi: 10.1021/ol200445b

Lee, J. H., Choi, S., and Hong, K. B. (2019). Alkene difunctionalization using hypervalent iodine reagents: progress and developments in the past ten years. *Molecules* 24, 2634–2657. doi: 10.3390/molecules24142634

Li, M., Yu, F., Qi, X., Chen, P., and Liu, G. (2016). A cooperative strategy for the highly selective intermolecular oxycarbonylation reaction of alkenes using a palladium catalyst. *Angew. Chem. Int. Ed.* 55, 13843–13848. doi: 10.1002/anie.201607248

Li, Q., Zhang, S.-Y., He, G., Nack, W. A., and Chen, G. (2014). Palladium-catalyzed picolinamide-directed acetoxylation of unactivated γ. Pap^3)–H bonds of alkylamines. *Adv. Synth. Catal.* 356, 1544–1548. doi: 10.1002/adsc.201400121

Li, X., Chen, P., and Liu, G. (2018). Recent advances in hypervalent iodine(III)-catalyzed functionalization of alkenes. *Beilstein J. Org. Chem.* 14, 1813–1825. doi: 10.3762/bjoc.14.154

Li, Y., Ding, Y.-J., Wang, J.-Y., Su, Y.-M., and Wang, X.-S. (2013). Pd-catalyzed C–H lactonization for expedient synthesis of biaryl lactones and total synthesis of cannabinol. *Org. Lett.* 15, 2574–2577. doi: 10.1021/ol400877q

Li, Y., Hari, D. P., Vita, M. V., and Waser, J. (2016). Cyclic hypervalent iodine reagents for atom-transfer reactions: beyond trifluoromethylation. *Angew. Chem. Int. Ed.* 55, 4436–4454. doi: 10.1002/anie.201509073

Li, Y., Song, D., and Dong, V. M. (2008). Palladium-catalyzed olefin dioxygenation. *J. Am. Chem. Soc.* 130, 2962–2964. doi: 10.1021/ja711029u

Liu, B., and Shi, B.-F. (2016). γ-Lactone synthesis via palladium(II)-catalyzed lactonization of unactivated methylene $C(sp^3)$–H bonds. *Synlett* 27, 2396–2400. doi: 10.1055/s-0035-1562508

Liu, G., and Stahl, S. S. (2006). Highly regioselective Pd-catalyzed intermolecular aminoacetoxylation of alkenes and evidence for *cis*-aminopalladation and S_N2 C–O bond formation. *J. Am. Chem. Soc.* 128, 7179–7181. doi: 10.1002/chin.200641044

Liu, H., Yu, J., Wang, L., and Tong, X. (2008). Cyclization–oxidation of 1,6-enyne derivatived from baylis–hillman adducts via Pd(II)/Pd(IV)-catalyzed reactions: stereoselective synthesis of multi-substituted bicyclo[3.1.0] hexanes and insight into reaction pathways. *Tetrahedron Lett.* 49, 6924–6928. doi: 10.1016/j.tetlet.2008.09.108

Liu, Q., Li, G., Yi, H., Wu, P., Liu, J., and Lei, A. (2011). Pd-catalyzed direct and selective C–H functionalization: C3-acetoxylation of indoles. *Chem. Eur. J.* 17, 2353–2357. doi: 10.1002/chem.201002547

Lyons, T. W., and Sanford, M. S. (2009). Palladium (II/IV) catalyzed cyclopropanation reactions: scope and mechanism. *Tetrahedron* 65, 3211–3221. doi: 10.1016/j.tet.2008.10.107

Maertens, G., and Canesi, S. (2015). 'Rearrangements induced by hypervalent iodine. *Topics Curr. Chem.* 373, 223–241. doi: 10.1007/128_2015_657

Mangaonkar, S. R., Kole, P. B., and Singh, F. V. (2018). Oxidation of organosulfides to organosulfones with trifluoromethyl 3-Oxo-1λ3,2-benziodoxole-1(3H)-carboxylate as an oxidant. *Synlett* 18, 199–202. doi: 10.1055/s-0036-1588575

Mangaonkar, S. R., and Singh, F. V. (2019). Hypervalent iodine(III)-catalyzed epoxidation of β-cyanostyrenes. *Synthesis* 51, 4473–4486. doi: 10.1055/s-0039-1690621

Martinez, C., and Muniz, K. (2012). Palladium-catalyzed vicinal difunctionalization of internal alkenes: diastereoselective synthesis of diamines. *Angew. Chem. Int. Ed.* 51, 7031–7034. doi: 10.1002/anie.201201719

Martinez, C., and Muniz, K. (2016). Defined palladium–phthalimidato catalysts for improved oxidative amination. *Chem. Eur. J.* 22, 7367–7370. doi: 10.1002/chem.201601128

Martinez, C., Perez, E. G., Iglesias, A., Escudero-Adan, E. C., and Muniz,. K. (2016). Regioselective intermolecular diamination and aminooxygenation of alkenes with saccharin. *Org. Lett.* 18, 2998–3001. doi: 10.1021/acs.orglett.6b01368

Martinez, C., Wu, Y., Weinstein, A. B., Stahl, S. S., Liu, G., and Muniz, K. (2013). Palladium-catalyzed intermolecular aminoacetoxylation of alkenes and the influence of $PhI(OAc)_2$ on aminopalladation stereoselectivity. *J. Org. Chem.* 78, 6309–6315. doi: 10.1021/jo400671q

McMurtrey, K. B., Racowski, J. M., and Sanford, M. S. (2012). Pd-catalyzed C–H fluorination with nucleophilic fluoride. *Org. Lett.* 14, 4094–4097. doi: 10.1021/ol301739f

Mei, T., Leow, D., Xiao, H., Laforteza, B. N., and Yu, J. (2013). Synthesis of indolines via Pd(II)-catalyzed amination of C–H bonds using $PhI(OAc)_2$ as the bystanding oxidant. *Org. Lett.* 15, 3058–3061. doi: 10.1021/ol401246u

Merritt, E. A., and Olofsson, B. (2011). α-Functionalization of carbonyl compounds using hypervalent iodine reagents. *Synthesis* 4, 517–538. doi: 10.1055/s-0030-1258328

Merritt, E. A., Olofsson, B. O. (2009). Diaryliodonium salts: journey from obscurity to fame. *Angew. Chem. Int. Ed.* 48, 9052–9070. doi: 10.1002/anie.200904689

Mu, X., Chen, S., Zhen, X., and Liu, G. (2011). Palladium-catalyzed oxidative trifluoromethylation of indoles at room temperature. *Chem. Eur. J.* 17, 6039–6042. doi: 10.1002/chem.201100283

Mu, X., Wu, T., Wang, H., Guo, Y.-L., and Liu, G. (2012). Palladium-catalyzed oxidative aryltrifluoromethylation of activated alkenes at room temperature. *J. Am. Chem. Soc.* 134, 878–881. doi: 10.1021/ja210614y

Muniz, K. (2007). Advancing palladium-catalyzed C–N bond formation: bisindoline construction from successive amide transfer to internal alkenes. *J. Am. Chem. Soc.* 129, 14542–14543. doi: 10.1021/ja075655f

Muniz, K., Hovelmann, C. H., and Streuff, J. (2008). Oxidative diamination of alkenes with ureas as nitrogen sources: mechanistic pathways in the presence of a high oxidation state palladium catalyst. *J. Am. Chem. Soc.* 130, 763–773. doi: 10.1021/ja075041a

Muniz, K., Kirsch, J., and Chavez, P. (2011). Intermolecular regioselective 1,2-diamination of allylic ethers. *Adv. Synth. Catal.* 353, 689–694. doi: 10.1002/adsc.201000813

Mutule, I., Suna, E., Olofsson, K., and Pelcman, B. (2009). Catalytic direct acetoxylation of indoles. *J. Org. Chem.* 74, 7195–7198. doi: 10.1021/jo901321b

Nadres, E. T., and Daugulis, O. (2012). Heterocycle Synthesis via direct C–H/N–H coupling. *J. Am. Chem. Soc.* 134, 7–10. doi: 10.1021/ja210959p

Neufeldt, S. R., and Sanford, M. S. (2010). *O*-Acetyl oximes as transformable directing groups for Pd-catalyzed C–H bond functionalization. *Org. Lett.* 12, 532–535. doi: 10.1021/ol902720d

Neufeldt, S. R., and Sanford, M. S. (2013). Asymmetric chiral ligand-directed alkene dioxygenation. *Org. Lett.* 15, 46–49. doi: 10.1021/ol303003g

Nicolai, S., Erard, S., Gonzalez, D. F., and Waser, J. (2010). Pd-catalyzed intramolecular oxyalkynylation of alkenes with hypervalent iodine. *Org. Lett.* 12, 384–387. doi: 10.1021/ol9027286

Nicolai, S., Piemontesi, C., and Waser, J. (2011). A palladium-catalyzed aminoalkynylation strategy towards bicyclic heterocycles: synthesis of (±)-trachelanthamidine. *Angew. Chem. Int. Ed.* 50, 4680–4683. doi: 10.1002/anie.201100718

Pilarski, L. T., Selander, N., Bose, D., and Szabo, K. J. (2009). Catalytic allylic C–H acetoxylation and benzoyloxylation via suggested (η^3-allyl)palladium(IV) intermediates. *Org. Lett.* 11, 5518–5521. doi: 10.1021/ol9023369

Qu, X., Sun, P., Li, T., and Mao, J. (2011). Ligand-free reusable palladium-catalyzed Heck-type coupling reactions of hypervalent iodine reagents under mild conditions. *Adv. Synth. Catal.* 353, 1061–1066. doi: 10.1002/adsc.201100008

Ren, Z., Mo, F., and Dong, G. (2012). Catalytic functionalization of unactivated sp^3 C–H bonds via exo-directing groups: synthesis of chemically differentiated 1,2-diols. *J. Am. Chem. Soc.* 134, 16991–16994. doi: 10.1021/ja3082186

Ren, Z., Schulz, J. E., and Dong, G. (2015). Catalytic ortho-acetoxylation of masked benzyl alcohols via an *exo*-directing mode. *Org. Lett.* 17, 2696–2699. doi: 10.1021/acs.orglett.5b01098

Richardson, R. D., Zayed, J. M., Altermann, S., Smith, D., and Wirth, T. (2007). Tetrafluoro-IBA and-IBX: hypervalent iodine reagents. *Angew. Chem. Int. Ed.* 46, 6529–6532. doi: 10.1002/anie.200702313

Rit, R. K., Yadav, M. R., and Sahoo, A. K. (2012). Pd(II)-catalyzed primary-$C(sp^3)$–H acyloxylation at room temperature. *Org. Lett.* 14, 3724–3727. doi: 10.1021/ol301579q

Rodriguez, A., and Moran, W. J. (2009). Palladium-catalyzed three-component coupling reactions: 1,1-difunctionalization of activated alkenes. *Eur. J. Org. Chem.* 2009, 1313–1316. doi: 10.1002/ejoc.200801245

Satterfield, A. D., Kubota, A., and Sanford, M. S. (2011). Palladium-catalyzed 1,1-aryloxygenation of terminal olefins. *Org. Lett.* 13, 1076–1079. doi: 10.1021/ol103121r

Selander, N., Willy, B., and Szabo, K. J. (2010). Selective C–H borylation of alkenes by palladium pincer complex catalyzed oxidative functionalization. *Angew. Chem. Int. Ed.* 49, 4051–4053. doi: 10.1002/anie.201000690

Shan, G., Yang, X., Zong, Y., and Rao, Y. (2013). An efficient palladium-catalyzed C–H alkoxylation of unactivated methylene and methyl groups with cyclic hypervalent iodine (I^{3+}) oxidants. *Angew. Chem. Int. Ed.* 52, 13606–13610. doi: 10.1002/anie.201307090

Shrestha, R., Mukherjee, P., Tan, Y., Litman, Z. C., and Hartwig, J. F. (2013). Sterically controlled, palladium-catalyzed intermolecular amination of arenes. *J. Am. Chem. Soc.* 135, 8480–8483. doi: 10.1021/ja4032677

Silva L. F, Jr. (2002). Construction of cyclopentyl units by ring contraction reactions. *Tetrahedron* 58, 9137–9161. doi: 10.1016/S0040-4020(02)00990-0

Silva, F. C. S., Tierno, A. F., and Wengryniuk, S. E. (2017). Hypervalent iodine reagents in high valent transition metal chemistry. *Molecules* 22:780. doi: 10.3390/molecules22050780

Singh, F. V., Kole, P. B., Mangaonkar, S. R., and Shetgaonkar, S. E. (2018a). Synthesis of spirocyclic scaffolds using hypervalent iodine reagents. *Beilstein J. Org. Chem.* 14, 1778–1805. doi: 10.3762/bjoc.14.152

Singh, F. V., and Mangaonkar, S. R. (2018). Hypervalent iodine(III)-catalyzed synthesis of 2-arylbenzofurans. *Synthesis* 50, 4940–4948. doi: 10.1055/s-0037-1610650

Singh, F. V., Mangaonkar, S. R., and Kole, P. B. (2018b). Ultrasound-assisted rapid synthesis of β-cyanoepoxides using hypervalent iodine reagents. *Synth. Commun.* 48, 2169–2176. doi: 10.1080/00397911.2018.1479760

Singh, F. V., Rehbein, J., and Wirth, T. (2012). Facile oxidative rearrangements using hypervalent iodine reagents. *ChemistryOpen* 1, 245–250. doi: 10.1002/open.201200037

Singh, F. V., and Wirth, T. (2011). Selenium-catalyzed regioselective cyclization of unsaturated carboxylic acids using hypervalent iodine oxidants. *Org. Lett.* 13, 6504–6507. doi: 10.1021/ol202800k

Singh, F. V., and Wirth, T. (2012). Hypervalent iodine(III) mediated cyclization of ortho-stillbenes into benzofurans. *Synthesis* 44, 1171–1177. doi: 10.1055/s-0031-1290588

Singh, F. V., and Wirth, T. (2013). Oxidative rearrangements with hypervalent iodine reagents. *Synthesis* 45, 2499–2511. doi: 10.1055/s-0033-1339679

Singh, F. V., and Wirth, T. (2014a). "Oxidative functionalization with hypervalent halides," *in Comprehensive Organic Synthesis II*, eds G. A. Molander and P. Knochel (Oxford: Elsevier), 880–933.

Singh, F. V., and Wirth, T. (2014b). Hypervalent iodine-catalyzed oxidative functionalizations including stereoselective reactions. *Chem. Asian J.* 9, 950–971. doi: 10.1002/asia.201301582

Singh, F. V., and Wirth, T. (2017). Catalytic oxidation with hypervalent iodine. *Catal. Oxidat. Organic Synthes.* 1, 29–62.

Singh, F. V., and Wirth, T. (2018). "Stereoselective reactions," *in Patai's Chemistry of Functional Groups*, eds I. Marek, B. Olofsson, and Z. Rappoport (Chichester: John Wiley & Sons, Ltd).

Streuff, J., Hovelmann, C. H., Nieger, M., and Muniz, K. (2005). Palladium(II)-catalyzed intramolecular diamination of unfunctionalized alkenes. *J. Am. Chem. Soc.* 127, 14586. doi: 10.1021/ja055190y

Sun, X., Yao, X., Zhang, C., and Rao, Y. (2015). Pd(II) catalyzed *ortho* C–H iodination of phenylcarbamates at room temperature using cyclic hypervalent iodine reagents. *Chem. Commun.* 51, 10014–10017. doi: 10.1039/C5CC02533H

Tang, S., Peng, P., Pi, S., Liang, Y., Wang, N., and Li, J. (2008b). Sequential intermolecular aminopalladation/ortho-arene C-H activation reactions of *N*-phenylpropiolamides with phthalimide. *Org. Lett.* 10, 1179–1182. doi: 10.1021/ol800080w

Tang, S., Peng, P., Wang, Z., Tang, B., Deng, C., Li, J., et al. (2008c). Synthesis of (2-oxoindolin-3-ylidene)methyl acetates involving a C–H functionalization process. *Org. Lett.* 10, 1875–1878. doi: 10.1021/ol8006315

Tang, S., Peng, P., Zhong, P., and Li, J.-H. (2008a). Palladium-catalyzed C–H functionalization of *N*-arylpropiolamides with aryliodonium salts: selective synthesis of 3-(1-arylmethylene)oxindoles. *J. Org. Chem.* 73, 5476–5480. doi: 10.1021/jo8008808

Thompson, S. J., Thach, D. Q., and Dong, G. (2015). Cyclic ether synthesis via palladium-catalyzed directed dehydrogenative annulation at unactivated terminal positions. *J. Am. Chem. Soc.* 137, 11586–11589. doi: 10.1021/jacs.5b07384

Tohma, H., and Kita, Y. (2004). Hypervalent iodine reagents for the oxidation of alcohols and their application to complex molecule synthesis. *Adv. Synth. Catal.* 346, 111–124. doi: 10.1002/adsc.200303203

Tolnai, G. L., Ganss, S., Brand, J. P., and Waser, J. (2013). C2-selective direct alkynylation of indoles. *Org. Lett.* 15, 112–115. doi: 10.1021/ol3031389

Tong, X., Beller, M., and Tse, M. K. (2007). A Palladium-catalyzed cyclization-oxidation sequence: synthesis of bicyclo[3.1.0]hexanes and evidence for S_N2 C–O bond formation. *J. Am. Chem. Soc.* 129, 4906–4907. doi: 10.1021/ja070919j

Tsujihara, T., Takenaka, K., Onitsuka, K., Hatanaka, M., and Sasai, H. (2009). Pd^{II}/Pd^{IV} Catalytic enantioselective synthesis of bicyclo[3.1.0]hexanes via oxidative cyclization of enynes. *J. Am. Chem. Soc.* 131, 3452–3453. doi: 10.1021/ja809965e

Uyanik, M., and Ishihara, K. (2009). Hypervalent iodine-mediated oxidation of alcohols. *Chem. Commun.* 2009, 2086–2099. doi.org/10.1039/B823399C doi: 10.1039/b823399c

Wang, W., Wang, F., and Shi, M. (2010). Bis(NHC)-palladium(II) complex-catalyzed dioxygenation of alkenes. *Organometallics* 29, 928–933. doi: 10.1021/om900975a

Wang, X., He, Y., Ren, M., Liu, S., Liu, H., and Huang, G. (2016). Pd-Catalyzed ligand-free synthesis of arylated heteroaromatics by coupling of *N*-heteroaromatic bromides with iodobenzene diacetate, iodosobenzene, or diphenyliodonium salts. *J. Org. Chem.* 81, 7958–7962. doi: 10.1021/acs.joc.6b01103

Wang, X., Lu, Y., Dai, H.-X., and Yu, J.-Q. (2010). Pd(II)-catalyzed hydroxyl-directed C-H activation/C-O cyclization: expedient construction of dihydrobenzofurans. *J. Am. Chem. Soc.* 132, 12203–12205. doi: 10.1021/ja105366u

Welbes, L. L., Lyons, T. W., Cychosz, K. A., and Sanford, M. S. (2007). Synthesis of cyclopropanes via Pd(II/IV)-catalyzed reactions of enynes. *J. Am. Chem. Soc.* 129, 5836–5837. doi: 10.1021/ja071204j

Wirth, T. (2005). Hypervalent iodine chemistry in synthesis: scope and new directions. *Angew. Chem. Int. Ed.* 44, 3656–3665. doi: 10.1002/anie.200500115

Wirth, T., Ochiai, M., Zhdankin, V. V., Koser, G. F., Tohma, H., Kita, Y., et al. (2002). *Topics in Current Chemistry: Hypervalent Iodine Chemistry- Modern Developments in Organic Synthesis.* Berlin: Spinger-Verlag.

Wu, T., Yin, G., and Liu, G. (2009). Palladium-catalyzed intramolecular aminofluorination of unactivated alkenes. *J. Am. Chem. Soc.* 131, 16354–16355. doi: 10.1021/ja9076588

Xiong, Q., Fu, Z., Li, Z., and Cai, H. (2015). Synthesis of symmetrical biaryls through palladium-catalyzed ligand-free homocoupling of aryliodine(III) diacetates. *Synlett* 26, 975–979. doi: 10.1055/s-0034-1380320

Xu, T., Wang, D., and Tong, X. (2019). Pd(II)-catalyzed intramolecular acetoxylative (3 + 2) annulation of propargylic alcohol and alkene: Polycyclic oxa-heterocycle synthesis and mechanistic insight. *Org. Lett.* 21, 5368–5372. doi: 10.1021/acs.orglett.9b02096

Yang, M., Jiang, X., Shi, W.-J., Zhu, Q.-L., and Shi, Z.-J. (2013). Direct lactonization of 2-arylacetic acids through Pd(II)-catalyzed C–H activation/C–O formation. *Org. Lett.* 15, 690–693. doi: 10.1021/ol303569b

Ye, X., He, Z., Ahmed, T., Weise, K., Akhmedov, N. G., Petersen, J. L., et al. (2013). 1,2,3-triazoles as versatile directing group for selective sp^2 and sp^3 C–H activation: cyclization vs substitution. *Chem. Sci.* 4, 3712–3716. doi: 10.1039/c3sc51211h

Yin, G., Wu, Y., and Liu, G. (2010). Scope and mechanism of allylic C–H amination of terminal alkenes by the palladium/$PhI(OPiv)_2$ catalyst system: Insights into the effect of naphthoquinone. *J. Am. Chem. Soc.* 132, 11978–11987. doi: 10.1021/ja1030936

Yin, Z., Jiang, X., and Sun, P. (2013). Palladium-catalyzed direct ortho alkoxylation of aromatic azo compounds with alcohols. *J. Org. Chem.* 78, 10002–10007. doi: 10.1021/jo401623j

Yoshimura, A., and Zhdankin, V. V. (2016). Advances in synthetic applications of hypervalent iodine compounds. *Chem. Rev.* 116, 3328–3435. doi: 10.1021/acs.chemrev.5b00547

Yu, P., Zhang, G., Chen, F., and Cheng, J. (2012). Direct arylation of benzoxazole C–H bonds with iodobenzene diacetates. *Tetrahedron Lett.* 53 4588–4590. doi: 10.1016/j.tetlet.2012.06.076

Yusubov, M. S., and Zhdankin, V. V. (2012). Hypervalent iodine reagents and green chemistry. *Curr. Org. Synth.* 9, 247–272. doi: 10.2174/157017912799829021

Zhang, C., and Sun, P. (2014). Palladium-catalyzed direct C(sp^2)–H alkoxylation of 2-aryloxypyridines using 2-pyridyloxyl as the directing group. *J. Org. Chem.* 79, 8457–8461. doi: 10.1021/jo5014146

Zhang, Q., Wang, Y., Yang, T., Li, L., and Li, D. (2015). Palladium catalyzed *ortho*-C–H-benzoxylation of 2-arylpyridines using iodobenzene dibenzoates. *Tetrahedron Lett.* 56, 6136–6141. doi: 10.1016/j.tetlet.2015.09.097

Zhang, S., Luo, F., Wang, W., Jia, X., Hu, M., and Cheng, J. (2010). Chelation-assisted palladium-catalyzed acyloxylation of benzyl sp^3 C–H bonds using $PhI(OAc)_2$ as oxidant. *Tetrahedron Lett.* 51, 3317–3319. doi: 10.1016/j.tetlet.2010.04.075

Zhang, S.-Y., He, G., Zhao, Y., Wright, K., Nack, W. A., and Chen, G. (2012). Efficient alkyl ether synthesis via palladium-catalyzed, picolinamide-directed alkoxylation of unactivated C(sp^3)–H and C(sp^2)–H bonds at remote positions. *J. Am. Chem. Soc.* 134, 7313–7316. doi: 10.1021/ja3023972

Zhdankin, V. V. (2009). Hypervalent iodine(III) reagents in organic synthesis. *ARKIVOC* 2009, 1–62. doi: 10.3998/ark.5550190.0010.101

Zhdankin, V. V. (2014). *Hypervalent Iodine Chemistry: Preparation, Structure and Synthetic Application of Polyvalent Iodine Compounds.* Chichester: John Wiley & Sons Ltd. doi: 10.1002/9781118341155

Zong, Y., and Rao, Y. (2014). Developing Pd(II) catalyzed double sp^3 C–H alkoxylation for synthesis of symmetric and unsymmetric Acetal. *Org. Lett.* 16, 5278–5281. doi: 10.1021/ol502377x

Conflict of Interest: The authors declare that the research was conducted in the absence of any commercial or financial relationships that could be construed as a potential conflict of interest.

frontiers in Chemistry

ORIGINAL RESEARCH
published: 15 October 2020
doi: 10.3389/fchem.2020.563470

The Diaryliodonium(III) Salts Reaction With Free-Radicals Enables One-Pot Double Arylation of Naphthols

Yuvraj Satkar[1], *Kazimierz Wrobel*[1], *Daniel E. Trujillo-González*[1], *Rafael Ortiz-Alvarado*[2]*, *J. Oscar C. Jiménez-Halla*[1]* *and César R. Solorio-Alvarado*[1]*

[1] División de Ciencias Naturales y Exactas, Departamento de Química, Universidad de Guanajuato, Guanajuato, Mexico,
[2] Facultad de Químico Farmacobiología, Universidad Michoacana de San Nicolás de Hidalgo, Morelia, Mexico

OPEN ACCESS

Edited by:
Toshifumi Dohi,
Ritsumeikan University, Japan

Reviewed by:
Fengzhi Zhang,
Zhejiang University of Technology, China
Sami Lakhdar,
Université de Toulouse, France

***Correspondence:**
Rafael Ortiz-Alvarado
rafael.ortiz@umich.mx
J. Oscar C. Jiménez-Halla
jjimenez@ugto.mx
César R. Solorio-Alvarado
csolorio@ugto.mx

Specialty section:
This article was submitted to Organic Chemistry, a section of the journal Frontiers in Chemistry

Received: 18 May 2020
Accepted: 17 August 2020
Published: 15 October 2020

Citation:
Satkar Y, Wrobel K, Trujillo-González DE, Ortiz-Alvarado R, Jiménez-Halla JOC and Solorio-Alvarado CR (2020) The Diaryliodonium(III) Salts Reaction With Free-Radicals Enables One-Pot Double Arylation of Naphthols. Front. Chem. 8:563470. doi: 10.3389/fchem.2020.563470

The chemoselective reaction of the *C*- followed by the *O*-centered naphthyl radicals with the more electron-deficient hypervalent bond of the diaryliodonium(III) salts is described. This discovered reactivity constitutes a new activation mode of the diaryliodonium(III) salts which enabled a one-pot doubly arylation of naphthols through the sequential C^2_{sp}-C^2_{sp}/O-C^2_{sp} bond formation. The naphthyl radicals were generated in the reaction by the tetramethylpiperidinyl radical (TMP·) which resulted from the homolytic fragmentation of the precursor TMP_2O. Experimental and DFT calculations provided a complete panorama of the reaction mechanism.

Keywords: diaryliodonium(III) salts, reaction with free-radicals, double arylation, electron-deficient hypervalent bond, one-pot double arylation

INTRODUCTION

The chemistry of radicals is a powerful tool in organic synthesis allowing chemical transformations with high activation energy profiles via HAT (Capaldo and Ravelli, 2017), SET (Kita et al., 1994, 1996; Rosen and Percec, 2009) or SOMO (Beeson et al., 2007). Both *C*- and *O*-centered radical formation on the naphthol moiety are known processes carried out by metals such as Cu (Nakajima et al., 1999; Li et al., 2001), Ru (Irie et al., 2000), Fe (Egami and Katsuki, 2009; Narute et al., 2016), Cr (Nieves-Quinones et al., 2019), or V (Brodwel and Cheng, 1991; Hon et al., 2001; Lee et al., 2014; Kang et al., 2017). These radicals can also be generated electrochemically (Elsler et al., 2014) or through the radical anion sulfate ($SO_4^{\cdot -}$) (More and Jeganmohan, 2015).

On the other hand, diaryliodonium(III) salts (Ar_2IX) have emerged as an excellent source of aryl groups (Merrit and Olofsson, 2009) which successfully transfer one arene (Beringer and Mausner, 1958; Beringer and Chang, 1971; Wang et al., 2010; Malmgren et al., 2013; Stuart, 2017) with concomitant ArI release by reductive elimination at the iodine atom (III→I).

Both radical and Ar_2IX strategies (Moteki et al., 2013; Wang and Studer, 2017; Ye et al., 2018) have been used in the preparation of aryl phenols which are important synthetic targets due to their relevance as biologically active molecules (Zofou et al., 2013; Ramadoss et al., 2016, 2018a,b, 2019; Gutierrez-Cano et al., 2017), reagents (Grzybowski et al., 2013), building blocks (Dreher et al., 2000), and organocatalyst scaffolds (Parmar et al., 2014).

In this regard, the seminal work of Barton using Bi(V) (Barton et al., 1981, 1982, 1987) is the first precedent describing the arylation of phenols. More recently, the ionic *O*-arylation of phenols using Ar_2IOTf has been mainly documented by Olofsson (Jalalian et al., 2011a,b; Lindstedt et al., 2013, 2016; Nahide and Solorio-Alvarado, 2017; Reitti et al., 2018), while the also ionic path for the *C*-arylation has been much less explored. In this case, only few examples are known. Quideau (Ozanne-Beaudenon and Quideau, 2005), described *C*- and *O*-arylation mixtures and Kalek (Ghosh et al., 2019) reported on the selective *C*-arylation of naphthols using fluorinated Ar_2IOTf. In all these protocols, the stoichiometric use of a base is needed for the reaction giving rise to the monoarylation of naphthols by transferring one aryl group from Ar_2IX via an ionic pathway (Oh et al., 1999).

In this context, we present for the first time, the direct reaction of Ar_2IX at its more electron-deficient hypervalent bond (Lecroq et al., 2018) with naphthyl radicals (Np·) (Liu et al., 2012; Huang et al., 2014; Vaillant et al., 2015, 2016; Wang et al., 2015; Zhou et al., 2015) under base-free conditions. In this scenario, the Ar_2IX behaves as a donor synthon of aryl radicals in the reaction with the *C*- and *O*-centered naphthyl radicals. This reactivity constitutes a new activation mode of the diaryliodonium(III) salts (**Scheme 1**).

Considering the synthetic importance of aryl phenols, we focused on this target as a part of our research in the development of new iodine(III)-based reactions (Nahide et al., 2018; Satkar et al., 2018, 2019; Juárez-Ornelas et al., 2019; Segura-Quezada et al., 2019). Herein, we report the recent advances of our approach using Ar_2IX.

In the course of this work, we fortuitously discovered and later synthesized the new radical precursor TMP_2O [1,1′-oxybis(2,2,6,6-tetramethylpiperidine)] which, according to our DFT calculations, spontaneously undergoes homolytic fragmentation leading to the formation of the TEMPO and tetramethylpiperidinyl ($TMP^{\cdot}$) radicals. In orthogonal fashion, the $TMP^{\cdot}$ radical reacts with 2-naphthol derivatives to produce an *O*-centered radical via HAT. This is in resonance with its *C*-centered radical (**Scheme 1A**) which, in a new activation mode, consecutively reacts with two equivalents of Ar_2IX to generate a doubly arylated naphthol in a one-pot radical process (**Scheme 1B**).

MATERIALS AND METHODS

General Information

All moisture- and oxygen-sensitive reactions were carried out in flame-dried round-bottom flasks under an inert atmosphere of nitrogen. Unless otherwise specified, all commercial materials were used as received without further purification. Anhydrous solvents were purchased from Sigma-Aldrich in Sure Seal bottles. Column chromatography was performed using silica gel of sizes 100–200 and 230–400 mesh (Sigma-Aldrich). Thin layer chromatography was performed with TLC silica gel 60 F256 plates, and visualization was done with short wavelength UV light (254 nm). Compounds were characterized using ^1H and ^{13}C NMR. (^1H and ^{13}C NMR spectra are provided for all the compounds in the SI.) Data of known compounds were compared with existing literature characterization data, and the references are given. ^1H and ^{13}C NMR spectra were recorded with 500 MHz and Bruker advance 400 MHz instruments using deuterated solvents purchased from Sigma-Aldrich like $CDCl_3$. ^1H spectra were referenced with tetramethyl silane (TMS, 0.0 ppm) or chloroform ($CDCl_3$, 7.26 ppm) and are reported as follows: chemical shift, multiplicity (s = singlet, d = doublet, t = triplet, q = quartet, m = multiplet), coupling constant (Hz), and integration. Chemical shifts of the ^{13}C NMR spectra were measured relative to $CDCl_3$ (δ = 77.16 ppm). All the starting materials were synthesized according to reported procedures in the literature. High-resolution masses (HRMS) analyses were obtained under the following procedure: Samples were introduced by direct infusion at 3 μL min^{-1} to the electrospray ionization (ESI) source of a quadrupole time-of-flight mass spectrometer (Bruker Daltonics ESI-QTOF-MS maXis impact), equipped with Data Analysis 4.1. ESI was operated in positive mode with ion spray voltage 4 500 V, nitrogen dry gas 4 L min^{-1}, drying temperature 180°C, and gas pressure 0.4 bar. Mass calibration was accomplished based on sodium formate clusters. Chemical nomenclature was generated using Chemdraw. Infrared (IR) spectra were recorded using PerkinElmer system 2000 FT-IR spectrometer. Melting points of solids were measured using a Fisher-Johns melting point apparatus.

The following boronic acids were purchased from Sigma Aldrich and used without additional purification: *p*-tolylboronic acid, phenylboronic acid, naphtylboronic acid, 4-fluorophenylboronic acid, 4-chlorophenylbronic acid, and (3-choloro-4-fluorophenyl) boronic acid.

General Procedure for Suzuki-Miyaura Cross-Coupling

The starting materials of the examples **4, 6–10,** and **17–19** were synthesized by Suzuki-Miyaura cross-coupling according to the following procedure:

A 50 mL round bottom flask with a stir bar was fitted with a rubber septum and flame dried under high vacuum. The flask was purged with argon and charged with $Pd(PPh_3)_4$ (155.5 mg, 0.1 mmol), K_2CO_3 (580.46 mg, 4.2 mmol), 6-bromonaphthalen-2-ol (443.9 mg, 2.0 mmol), boronic acid (4.0 mmol), 10.0 mL 1,4-dioxane, and 2 mL of distilled water. The reaction mixture was then heated at 80°C for 8 h. After the reaction was cooled down to room temperature, the organic layer was separated, and the aqueous layer was extracted with ethyl acetate (3 × 10 mL), and the combined organic layer was dried over Na_2SO_4 and concentrated. The crude products were purified by flash chromatography on silica gel.

General Procedure for the Double Arylation Using the System TMP_2O/Ar_2IX

A 25 mL round bottom flask with a stir bar was fitted with a rubber septum and flame dried under high vacuum. The flask was purged with argon and charged with the corresponding

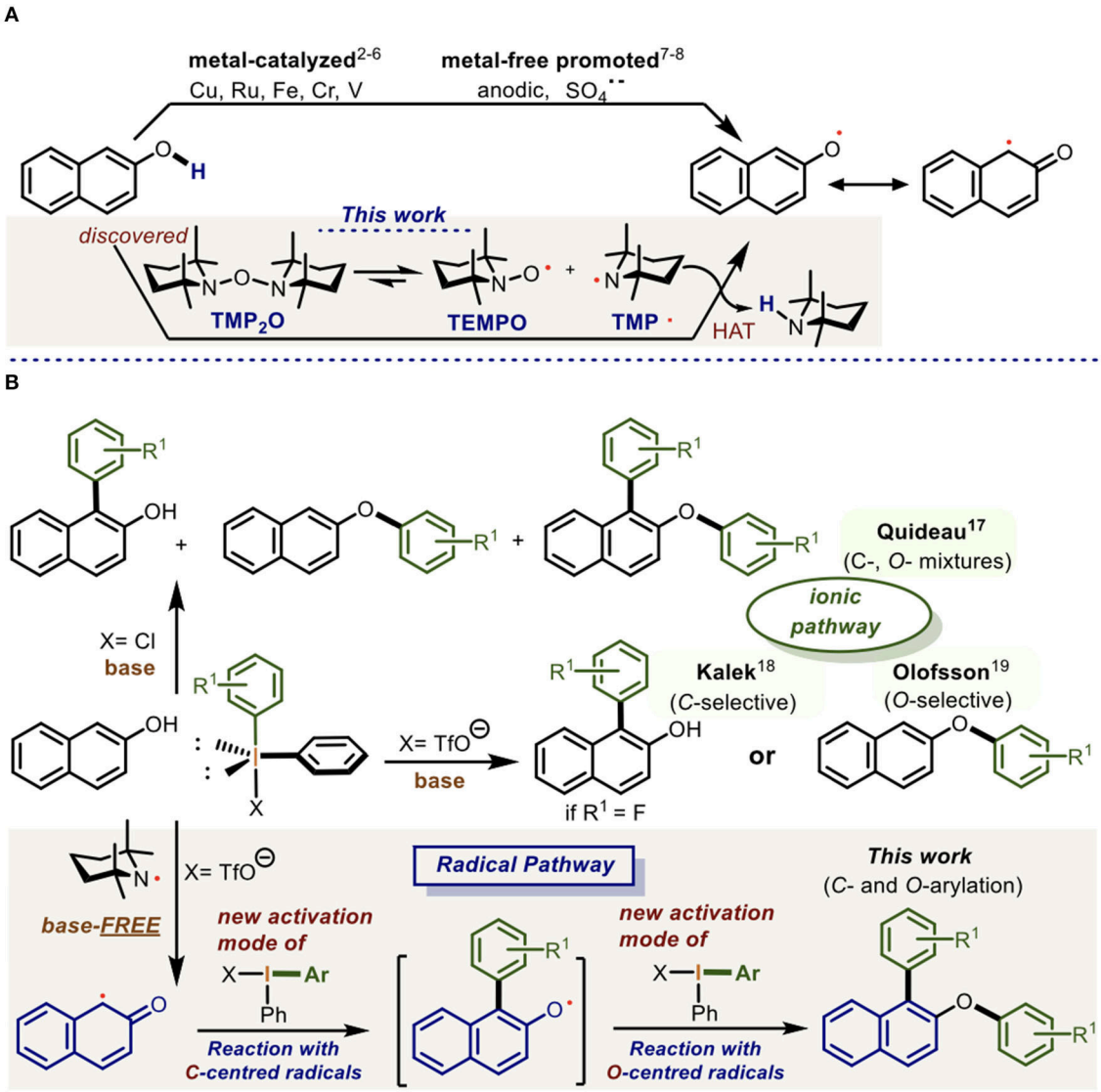

SCHEME 1 | Procedures for the *O*-/*C*-centered radical formation in the 2-naphthol and its arylation using diaryliodonium salts. **(A)** Procedures fot the O-/C-centred radical formation at 2-napthol. **(B)** Procedures for arylation of naphthols mediated by diaryliodonium(III) salts.

naphthols (0.25 mmol, 1 equiv), anhydrous diethyl ether and cyclohexane (1:1) (5 mL, 0.1 *M*) at 25°C. The corresponding amount of the solids mixture (1.575 g) containing TMP_2O (126 mg, 0.425 mmol, 1.7 equiv) was added and stirred for 15 min obtaining a homogeneous mixture. Then, the diaryliodonium salt (0.625 mmol, 2.5 equiv) was added and stirred at 25°C until fully consumption of the starting material (usually 3 h). The reaction was quenched with a saturated solution of ammonium chloride. The organic layer was separated, and the aqueous layer was extracted with ethyl acetate (3 × 10 mL), the combined organic layers were dried over Na_2SO_4 and concentrated. The crude products were purified by flash chromatography on silica gel (10% EtOAc/Hexane) to afford the corresponding double arylated naphthol.

Synthesis of the Radical Precursor TMP_2O

A 250 mL round bottom flask equipped with a stir bar was fitted with a rubber septum and flame dried under high vacuum. The flask was purged with argon and charged with TMP-H (5.57 mL, 33.0 mmol, 1 equiv). Anhydrous *n*-hexane (66 mL, 0.5 *M*) was added, and mixture was cooled to −78°C (dry ice-acetone) for 5 min. Then *n*-BuLi (2.5 *M* in hexanes, 14.4 mL, 36 mmol, 1.1 equiv) was added dropwise and reaction mixture was stirred for 30 min at −78°C, then warmed up to room temperature and stirred overnight. The reaction mixture was directly evaporated without inert atmosphere keeping the water bath does not raise more than 20°C. Then, the concentrated reaction mixture was dried at high pressure to afford 2.2 g "*a brown, not pyrophoric and air stable solid*" product which

corresponds to a 9:1 mixture of TMP-O-^{n}Bu (1-butoxy-2,2,6,6-tetramethylpiperidine) (27.3%) and TMP_2O [1,1′-oxybis(2,2,6,6-tetramethylpiperidine)] (3%) which was used without additional purification. m.p. = > 50°C dec.

IR (neat) ν/cm^{-1} = 3,137, 3,123, 3,068, 3,049, 1,330, 1,216, 1,198, 1,181, 1,127, 1,035.

Diarylphenols of Scheme 2

2-phenoxy-1-phenylnaphthalene (2a)

The following compound was obtained according to the general procedure by using 2-napthol and diphenyliodonium triflate as starting material. The crude material was purified by flash column chromatography over silica gel with the (2% EtOAc/Hexane) system to afford the product **2a** (72 mg, 74%) as a gel solid. R_f = 0.15 (4% EtOAc/Hexane). IR (neat) ν/cm^{-1} = 2,920, 1,585, 1,486, 1,232, 744. ^{1}H NMR (500 MHz, $CDCl_3$) δ 7.87 (dd, *J* = 11.8, 8.3 Hz, 2H), 7.63 (d, *J* = 8.4 Hz, 1H), 7.49–7.33 (m, 7H), 7.25–7.21 (m, 3H), 6.99 (t, *J* = 7.4 Hz, 1H), 6.87 (dd, *J* = 8.6, 0.9 Hz, 2H). ^{13}C NMR (126 MHz, $CDCl_3$) δ 158.6, 150.4, 135.5, 133.9, 131.1, 130.7, 130.3, 129.6, 129.4, 128.3, 128.4, 127.7, 126.6, 126.1, 125.5, 122.9, 120.7, 117.8. HRMS (EI): m/z calculated for $C_{22}H_{17}O$ $[M+H]^+$ = 297.1279, found 297.1299.

1-phenoxy-4-phenylnaphthalene (2b)

The following compound was obtained according to the general procedure A, by using naphthalen-1-ol and diphenyliodonium triflate as starting material. The crude material was purified by flash column chromatography over silica gel with the (2% EtOAc/Hexane) system to afford the product **2b** (48 mg, 47%) as a white solid. m.p. = 94–96°C. R_f = 0.15 (5% EtOAc/Hexane). IR (neat) ν/cm^{-1} = 2,910, 1,588, 1,486, 1,232, 748. ^{1}H NMR (500 MHz, $CDCl_3$) δ 7.90 (d, *J* = 8.4 Hz, 1H), 7.83 (d, *J* = 8.2 Hz, 1H), 7.75 (d, *J* = 8.5 Hz, 1H), 7.52 (d, *J* = 8.5 Hz, 1H), 7.50–7.47 (m, 2H), 7.44–7.40 (m, 1H), 7.36 (ddd, *J* = 8.1, 6.9, 1.2 Hz, 1H), 7.25 (dd, *J* = 10.4, 4.7 Hz, 2H), 7.19–7.15 (m, 1H), 7.06–7.01 (m, 2H), 6.63 (t, *J* = 8.2 Hz, 1H), 6.61(d, *J* = 8.5 Hz, 2H). ^{13}C NMR (126 MHz, $CDCl_3$) δ 159.6, 146.7, 137.8, 134.4, 131.0, 129.8, 129.3, 128.6, 128.3, 128.4, 127.8, 127.1, 126.7, 126.4, 125.9, 123.1, 121.3, 115.8. HRMS (EI): m/z calculated for $C_{22}H_{17}O$ $[M+H]^+$ = 297.1279, found 297.1312.

4-bromo-1-phenoxy-2-phenylnaphthalene (2c)

The following compound was obtained according to the general procedure A, by using 4-bromonaphthalen-1-ol and diphenyliodonium triflate as starting material. The crude material was purified by flash column chromatography over silica gel with the (3% EtOAc/Hexane) system to afford the product **2c** (47 mg, 56%) as a white solid. m.p. = 102–104°C. R_f = 0.45 (5% EtOAc/Hexane). IR (neat) ν/cm^{-1} = 3,010, 1,688, 1,566, 1,242, 758. ^{1}H NMR (500 MHz, $CDCl_3$) δ 8.27 (d, *J* = 8.5 Hz, 1H), 8.00 (d, *J* = 8.4 Hz, 1H), 7.93 (s, 1H), 7.62 (ddd, *J* = 8.3, 6.9, 1.2 Hz, 1H), 7.56–7.48 (m, 3H), 7.35–7.30 (m, 2H), 7.27 (t, *J* = 1.3 Hz, 1H), 7.14–7.08 (m, 2H), 6.87 (dd, *J* = 10.6, 4.1 Hz, 1H), 6.71–6.66 (m, 2H). ^{13}C NMR (126 MHz, $CDCl_3$) δ 158.8, 146.7, 136.7, 132.7, 132.8, 132.2, 129.8, 129.6, 129.4, 128.4, 127.9, 127.8, 127.55, 127.52, 123.8, 121.7, 119.8, 115.9. HRMS (EI): m/z calculated for $C_{22}H_{16}BrO$ $[M+H]^+$ = 375.0385, found 375.0376.

6-bromo-2-phenoxy-1-phenylnaphthalene (2d)

The following compound was obtained according to the general procedure A, by using 6-bromonaphthalen-2-ol and diphenyliodonium triflate as starting material. The crude material was purified by flash column chromatography over silica gel with the (3% EtOAc/Hexane) system to afford the product **2d** (62 mg, 74%) as a white solid. m.p. = 94–96°C. R_f = 0.55 (5% EtOAc/Hexane). IR (neat) ν/cm^{-1} = 3,034, 1,581, 1,484, 1,226, 825. ^{1}H NMR (500 MHz, $CDCl_3$) δ 8.02 (d, *J* = 1.9 Hz, 1 H), 7.75 (d, *J* = 8.9 Hz, 1H), 7.49 (d, *J* = 9.1 Hz, 1H), 7.46 (d, *J* = 2.0 Hz, 1H), 7.45–7.33 (m, 6H), 7.25–7.22 (m, 2H), 7.01 (t, *J* = 7.4 Hz, 1H), 6.86 (dd, *J* = 8.7, 0.9 Hz, 2H). ^{13}C NMR (126 MHz, $CDCl_3$) δ 158.3, 150.8, 134.9, 132.6, 132.3, 130.6, 130.9, 130.3, 129.8, 129.9, 128.4, 128.5, 127.9, 127.7, 122.9, 121.9, 119.7, 117.9. HRMS (EI): m/z calculated for $C_{22}H_{16}BrO$ $[M+H]^+$ = 375.0385, found 375.0377.

3-bromo-2-phenoxy-1-phenylnaphthalene (2e)

The following compound was obtained according to the general procedure A, by using 3-bromonaphthalen-2-ol and diphenyliodonium triflate as starting material. The crude material was purified by flash column chromatography over silica gel with the (2% EtOAc/Hexane) system to afford the product **2e** (61 mg, 72%) as a white solid. m.p. = 92–94°C. R_f = 0.45 (5% EtOAc/Hexane). IR (neat) ν/cm^{-1} = 3,035, 2,918, 1,582, 1,456, 1,201, 868. ^{1}H NMR (500 MHz, $CDCl_3$) δ 8.23 (s, 1H), 7.84 (d, *J* = 8.2 Hz, 1H), 7.50 (ddd, *J* = 9.1, 8.1, 4.8 Hz, 2H), 7.41 (ddd, *J* = 8.3, 6.9, 1.2 Hz, 1H), 7.36–7.29 (m, 3H), 7.25–7.20 (m, 2H), 7.16–7.08 (m, 2H), 6.90 (t, *J* = 7.4 Hz, 1H), 6.63 (dd, *J* = 8.7, 0.9 Hz, 2H).

^{13}C NMR (126 MHz, $CDCl_3$) δ 158.7, 146.8, 134.8, 134.4, 133.7, 132.5, 132.7, 130.9, 129.3, 128.1, 127.8, 127.2, 126.8, 126.9, 126.4, 121.8, 117.3, 115.6. HRMS (EI): m/z calculated for $C_{22}H_{16}BrO$ $[M+H]^+$ = 375.0385, found 375.0378.

2-phenoxy-1-phenyl-6-(p-tolyl)naphthalene (2f)

The following compound was obtained according to the general procedure A, by using 6-(*p*-tolyl)naphthalen-2-ol and diphenyliodonium triflate as starting material. The crude material was purified by flash column chromatography over silica gel with the (3% EtOAc/Hexane) system to afford the product **2f** (54 mg, 66%) as a white solid. m.p. = 122–124°C. R_f = 0.15 (5% EtOAc/Hexane). IR (neat) ν/cm^{-1} = 3,058, 1,510, 1,487, 1,230, 742. ^{1}H NMR (500 MHz, $CDCl_3$) δ 8.06 (d, *J* = 1.3 Hz, 1H), 7.90 (d, *J* = 8.9 Hz, 1H), 7.70–7.65 (m, 2H), 7.61 (d, *J* = 8.1 Hz, 2H), 7.45–7.36 (m, 5H), 7.32–7.27 (m, 3H), 7.26–7.21 (m, 2H), 7.00 (t, *J* = 7.4 Hz, 1H), 6.88 (d, *J* = 7.9 Hz, 2H), 2.42 (s, 3H). ^{13}C NMR (126 MHz, $CDCl_3$) δ 158.7, 150.4, 138.1, 137.8, 137.4, 135.5, 132.9, 131.3, 130.7, 130.0, 129.8, 129.64, 129.62, 128.3, 127.5, 127.3, 126.6, 126.3, 125.6, 122.4, 121.2, 117.8, 21.9. HRMS (EI): m/z calculated for $C_{29}H_{23}O$ $[M+H]^+$ = 387.1749, found 387.1760.

7-methoxy-2-phenoxy-1-phenylnaphthalene (2g)

The following compound was obtained according to the general procedure A, by using 7-methoxynaphthalen-2-ol and diphenyliodonium triflate as starting material. The crude

material was purified by flash column chromatography over silica gel with the (2% EtOAc/Hexane) system to afford the product **2g** (60 mg, 65%) as a white solid. m.p. = 122–124°C. R_f = 0.45 (4% EtOAc/Hexane). IR (neat) ν/cm^{-1} = 3,056, 1,934, 1,626, 1,459, 812. ^{1}H NMR (500 MHz, $CDCl_3$) δ 7.78 (d, *J* = 2.7 Hz, 1H), 7.76 (d, *J* = 2.6 Hz, 1H), 7.45–7.33 (m, 5H), 7.25–7.19 (m, 2H), 7.10 (ddd, *J* = 8.7, 8.3, 2.9 Hz, 2H), 7.01–6.96 (m, 1H), 6.92 (d, *J* = 2.5 Hz, 1H), 6.86 (dd, *J* = 8.6, 0.9 Hz, 2H), 3.71 (s, 3H). ^{13}C NMR (126 MHz, $CDCl_3$) δ 158.7, 158.8, 151.3, 135.6, 135.2, 130.7, 129.5, 129.4, 128.9, 128.8, 128.7, 127.9, 126.9, 122.2, 118.6, 117.7, 117.2, 104.7, 55.5. HRMS (EI): m/z calculated for $C_{23}H_{19}O_2$ $[M+H]^+$ = 327.1385, found 327.1391.

2-phenoxy-1,6-diphenylnaphthalene (2h)

The following compound was obtained according to the general procedure A, by using 6-phenylnaphthalen-2-ol and diphenyliodonium triflate as starting material. The crude material was purified by flash column chromatography over silica gel with the (6% EtOAc/Hexane) system to afford the product **2 h** (54 mg, 64%) as a white solid. m.p. = 132–134°C. R_f = 0.55 (8% EtOAc/Hexane). IR (neat) ν/cm^{-1} = 3,051, 1,621, 1,588, 1,204, 757. ^{1}H NMR (500 MHz, $CDCl_3$) δ 8.08 (d, *J* = 1.4 Hz, 1H), 7.91 (d, *J* = 8.9 Hz, 1H), 7.74–7.66 (m, 4H), 7.49 (t, *J* = 7.7 Hz, 2H), 7.46–7.36 (m, 6H), 7.28 (d, *J* = 8.9 Hz, 1H), 7.25–7.22 (m, 2H), 7.00 (t, *J* = 7.4 Hz, 1H), 6.88 (d, *J* = 7.8 Hz, 2H). ^{13}C NMR (126 MHz, $CDCl_3$) δ 158.6, 150.6, 140.9, 137.8, 135.7, 133.5, 131.7, 130.7, 129.9, 129.7, 129.6, 129.5, 128.9, 128.3, 127.5, 127.8, 126.6, 126.8, 126.1, 122.6, 121.2, 117.8. HRMS (EI): m/z calculated for $C_{28}H_{21}O$ $[M+H]^+$ = 373.1592, found 373.1595.

6-phenoxy-5-phenyl-2,2'-binaphthalene (2i)

The following compound was obtained according to the general procedure A, by using [2,2′-binaphthalen]-6-ol and diphenyliodonium triflate as starting material. The crude material was purified by flash column chromatography over silica gel with the (4% EtOAc/Hexane) system to afford the product **2i** (55 mg, 66%) as a white solid. m.p. = 126–128°C. R_f = 0.55 (6% EtOAc/Hexane). IR (neat) ν/cm^{-1} = 3,051, 1,621, 1,588, 1,204, 757. ^{1}H NMR (500 MHz, $CDCl_3$) δ 8.21 (d, *J* = 1.7 Hz, 1H), 8.16 (d, *J* = 0.7 Hz, 1H), 7.95 (dd, *J* = 15.2, 7.1 Hz, 3H), 7.90–7.86 (m, 2H), 7.81 (dd, *J* = 8.8, 1.8 Hz, 1H), 7.75 (d, *J* = 8.8 Hz, 1H), 7.55–7.37 (m, 7H), 7.29 (d, *J* = 8.9 Hz, 2H), 7.23 (t, *J* = 2.0 Hz, 1H), 7.01 (t, *J* = 7.4 Hz, 1H), 6.90 (d, *J* = 7.8 Hz, 2H). ^{13}C NMR (126 MHz, $CDCl_3$) δ 158.6, 150.8, 138.7, 137.9, 135.9, 133.9, 133.3, 132.8, 131.6, 130.7, 129.9, 129.7, 129.6, 128.7, 128.4, 128.3, 127.8, 127.7, 126.8, 126.6, 126.4, 126.3, 126.2, 126.1, 125.7, 122.5, 121.6, 117.8. HRMS (EI): m/z calculated for $C_{32}H_{23}O$ $[M+H]^+$ = 423.1749, found 423.1748.

6-(4-fluorophenyl)-2-phenoxy-1-phenylnaphthalene (2j)

The following compound was obtained according to the general procedure A, by using 6-(4-fluorophenyl)naphthalen-2-ol and diphenyliodonium triflate as starting material. The crude material was purified by flash column chromatography over silica gel with the (4% EtOAc/Hexane) system to afford the product **2j** (58 mg, 71%) as a white solid. m.p. = 134–136°C. R_f = 0.15 (8% EtOAc/Hexane). IR (neat) ν/cm^{-1} = 3,060, 1,734, 1,588, 1,487, 826. ^{1}H NMR (500 MHz, $CDCl_3$) δ 7.99 (d, *J* = 1.3 Hz, 1H), 7.87 (d, *J* = 8.9 Hz, 1H), 7.64 (ddd, *J* = 10.1, 8.6, 5.3 Hz, 3H), 7.58 (dd, *J* = 8.8, 1.8 Hz, 1H), 7.43–7.34 (m, 5H), 7.25–7.20 (m, 3H), 7.15 (t, *J* = 8.6 Hz, 2H), 6.98 (t, *J* = 7.4 Hz, 1H), 6.86 (d, *J* = 7.9 Hz, 2H). ^{13}C NMR (126 MHz, $CDCl_3$) δ 162.9 (d, *J* = 246.9 Hz), 158.7, 150.6, 137.8 (d, *J* = 2.9 Hz), 136.8, 135.4, 132.9, 131.2, 130.7, 129.9, 129.6 (d, *J* = 2.6 Hz), 129.0 (d, *J* = 8.1 Hz), 128.3, 127.6, 126.7, 126.1, 125.8, 122.5, 121.3, 117.8, 116.1, 115.8. HRMS (EI): m/z calculated for $C_{28}H_{20}FO$ $[M+H]^+$ = 391.1498, found 391.1508.

6-(4-chlorophenyl)-2-phenoxy-1-phenylnaphthalene (2k)

The following compound was obtained according to the general procedure A, by using 6-(4-chlorophenyl) naphthalen-2-ol as starting material. The crude material was purified by flash column chromatography over silica gel with the (4% EtOAc/Hexane) system to afford the product **2k** (55 mg, 68%) as a white solid. m.p. = 138–140°C. R_f = 0.15 (5% EtOAc/Hexane). IR (neat) ν/cm^{-1} = 3,045, 1,586, 1,485, 1,224, 703. ^{1}H NMR (500 MHz, $CDCl_3$) δ 8.04 (d, *J* = 1.8 Hz, 1H), 7.90 (d, *J* = 8.9 Hz, 1H), 7.70 (d, *J* = 8.8 Hz, 1H), 7.65–7.60 (m, 3H), 7.47–7.42 (m, 4H), 7.41–7.38 (m, 3H), 7.28 (d, *J* = 8.9 Hz, 1H), 7.24 (d, *J* = 1.1 Hz, 1H), 7.24–7.22 (m, 1H), 7.01 (t, *J* = 7.4 Hz, 1H), 6.88 (dd, *J* = 8.6, 0.8 Hz, 2H). ^{13}C NMR (126 MHz, $CDCl_3$) δ 158.5, 150.7, 139.4, 136.5, 135.3, 133.6, 133.2, 131.7, 130.7, 129.9, 129.8, 129.6, 129.2, 128.6, 128.3, 127.6, 126.8, 125.94, 125.89, 122.5, 121.3, 117.8. HRMS (EI): m/z calculated for $C_{28}H_{20}ClO$ $[M+H]^+$ = 407.1203, found 407.1210.

6-(3-chloro-4-fluorophenyl)-2-phenoxy-1-phenylnaphthalene (2l)

The following compound was obtained according to the general procedure A, by using 6-(4-chloro-3-fluorophenyl)naphthalen-2-ol and diphenyliodonium triflate as starting material. The crude material was purified by flash column chromatography over silica gel with the (4% EtOAc/Hexane) system to afford the product **2l** (53 mg, 68%) as a white solid. m.p. = 142–144°C. R_f = 0.55 (8% EtOAc/Hexane).

IR (neat) ν/cm^{-1} = 2,984, 1,560, 1,489, 1,309, 820. ^{1}H NMR (500 MHz, $CDCl_3$) δ 7.91 (d, *J* = 1.8 Hz, 1H), 7.80 (d, *J* = 8.9 Hz, 1H), 7.65–7.59 (m, 2H), 7.49–7.42 (m, 2H), 7.37–7.27 (m, 5H), 7.21–7.12 (m, 4H), 6.92 (t, *J* = 7.4 Hz, 1H), 6.80 (d, *J* = 7.8 Hz, 2H). ^{13}C NMR (126 MHz, $CDCl_3$) δ 158.8, 158.4, 156.8, 150.9, 138.2 (d, *J* = 15 Hz), 135.3 (d, *J* = 100 Hz), 133.2, 131.1, 130.7, 129.9, 129.7, 129.5, 128.3, 127.6, 127.1, 127.0, 126.94, 126.0, 125.7, 122.6, 121.6, 121.5, 117.9, 117.1 (d, *J* = 85 Hz). HRMS (EI): m/z calculated for $C_{28}H_{19}ClFO$ $[M+H]^+$ = 425.1108, found 425.1123.

Diarylphenols of Scheme 3

2-(4-chlorophenoxy)-1-(4-chlorophenyl)naphthalene (3a)

The following compound was obtained according to the general procedure A, by using 2-napthol and (4-chlorophenyl)(phenyl)-λ^3-iodanyl trifluoromethanesulfonate as starting material. The crude material was purified by flash column chromatography over silica gel with the (2% EtOAc/Hexane) system to afford the

product **3a** (92 mg, 73%) as a white solid. m.p. = 98–100°C. R_f = 0.56 (5% EtOAc/Hexane). IR (neat) ν/cm^{-1} = 2,919, 1,585, 1,485, 1,202, 821. ^{1}H NMR (500 MHz, $CDCl_3$) δ 7.81 (dd, J = 8.2, 3.7 Hz, 2H), 7.51 (d, J = 8.3 Hz, 1H), 7.42–7.30 (m, 4H), 7.22–7.17 (m, 2H), 7.16–7.09 (m, 3H), 6.69 (dd, J = 8.2, 3.7 Hz, 2H). ^{13}C NMR (126 MHz, $CDCl_3$) δ 157.1, 150.7, 133.7, 133.66, 133.64, 132.3, 131.8, 130.3, 129.6, 128.6, 128.3, 127.5, 127.0, 125.7, 125.4, 120.8, 118.7.

HRMS (EI): m/z calculated for $C_{22}H_{14}Cl_2O$ $[M]^+$ = 365.0500, found 365.0503.

2-(4-nitrophenoxy)-1-(4-nitrophenyl)naphthalene (3b)

The following compound was obtained according to the general procedure A, by using 2-napthol and (4-nitrophenyl)(phenyl)-λ^3-iodanyl trifluoromethanesulfonate as starting material. The crude material was purified by flash column chromatography over silica gel with the (8% EtOAc/Hexane) system to afford the product **3b** (99 mg, 76%) as a white solid. m.p. = 122–124°C. R_f = 0.36 (15% EtOAc/Hexane).

IR (neat) ν/cm^{-1} = 2,979, 1,484, 1,340, 1,235, 885. ^{1}H NMR (500 MHz, $CDCl_3$) δ 8.31–8.26 (m, 2H), 8.14–8.11 (m, 2H), 8.02 (d, J = 8.9 Hz, 1H), 7.97 (d, J = 8.2 Hz, 1H), 7.59–7.49 (m, 5H), 7.30 (d, J = 8.9 Hz, 1H), 6.90–6.84 (m, 2H). ^{13}C NMR (126 MHz, $CDCl_3$) δ 163.6, 148.5, 147.6, 142.8, 141.9, 133.0, 131.7, 131.6, 131.4, 128.7, 128.6, 127.8, 126.6, 126.1, 125.4, 123.7, 120.5, 116.6. HRMS (EI): m/z calculated for $C_{22}H_{14}N_2O_5$ $[M]^+$ = 386.0903, found 386.0910.

6-bromo-2-(4-chlorophenoxy)-1-(4-chlorophenyl) naphthalene (3c)

The following compound was obtained according to the general procedure A, by using 6-bromonaphthalen-2-ol and (4-chlorophenyl)(phenyl)-λ^3-iodanyl trifluoromethanesulfonate as starting material. The crude material was purified by flash column chromatography over silica gel with the (4% EtOAc/Hexane) system to afford the product **3c** (68 mg, 68%) as a white solid. m.p.=110–112°C. R_f = 0.55 (8% EtOAc/Hexane). IR (neat) ν/cm^{-1} = 2,979, 1,569, 1,459, 1,309, 840.^{1}H NMR (500 MHz, $CDCl_3$) δ 7.96 (d, J = 1.9 Hz, 1H), 7.69 (d, J = 8.9 Hz, 1H), 7.39 (dt, J = 19.1, 5.5 Hz, 2H), 7.34–7.31 (m, 2H), 7.20–7.10 (m, 5H), 6.70–6.66 (m, 2H). ^{13}C NMR (126 MHz, $CDCl_3$) δ 156.6, 150.3, 133.8, 133.4, 132.7, 132.5, 131.8, 130.16, 130.07, 129.6, 128.9, 128.8, 128.6, 127.7, 127.4, 121.3, 119.6, 118.7. HRMS (EI): m/z calculated for $C_{22}H_{13}BrCl_2O$ $[M]^+$ = 441.9527, found 441.9523.

3-bromo-2-(4-chlorophenoxy)-1-(4-chlorophenyl) naphthalene (3d)

The following compound was obtained according to the general procedure A, by using 3-bromonaphthalen-2-ol and (4-chlorophenyl)(phenyl)-λ^3-iodanyl trifluoromethanesulfonate as starting material. The crude material was purified by flash column chromatography over silica gel with the (3% EtOAc/Hexane) system to afford the product **3d** (64 mg, 64%) as a white solid. m.p. = 130–132°C. R_f = 0.15 (6% EtOAc/Hexane). IR (neat) ν/cm^{-1} = 2,984, 1,560, 1,489, 1,309, 820. ^{1}H NMR (500 MHz, $CDCl_3$) δ 8.23 (s, 1H), 7.84 (d, J = 8.2 Hz, 1H), 7.55–7.42 (m, 3H), 7.35–7.32 (m, 2H), 7.18–7.15 (m, 2H), 7.12–7.08 (m, 2H), 6.58–6.54 (m, 2H). ^{13}C NMR (126 MHz, $CDCl_3$) δ 156.7, 146.0, 133.9, 132.9, 132.8, 132.7, 132.6, 132.5, 132.3, 131.5, 129.8, 128.4, 127.2, 127.1, 126.8, 126.6, 126.0, 116.6.

HRMS (EI): m/z calculated for $C_{22}H_{13}BrCl_2O$ $[M]^+$ = 441.9527, found 441.9535.

2-(4-chlorophenoxy)-1-(4-chlorophenyl)-6-phenylnaphthalene (3e)

The following compound was obtained according to the general procedure A, by using 6-phenylnaphthalen-2-ol and (4-chlorophenyl)(phenyl)-λ^3-iodanyl trifluoromethanesulfonate as starting material. The crude material was purified by flash column chromatography over silica gel with the (3% EtOAc/Hexane) system to afford the product **3e** (85 mg, 72%) as a white solid. m.p. = 126–128°C. R_f = 0.38 (5% EtOAc/Hexane). IR (neat) ν/cm^{-1} = 2,922, 1,588, 1,465, 1,202, 828. ^{1}H NMR (500 MHz, $CDCl_3$) δ 8.01 (d, J = 1.5 Hz, 1H), 7.86 (d, J = 8.9 Hz, 1H), 7.65–7.61 (m, 3H), 7.58 (d, J = 8.8 Hz, 1H), 7.42 (t, J = 7.7 Hz, 2H), 7.36–7.30 (m, 3H), 7.25–7.22 (m, 2H), 7.19–7.16 (m, 1H), 7.14–7.10 (m, 2H), 6.72–6.68 (m, 2H). ^{13}C NMR (126 MHz, $CDCl_3$) δ 157.8, 150.5, 140.7, 138.2, 133.9, 133.7, 132.7, 132.3, 131.6, 130.7, 129.8, 129.1, 128.8, 128.6, 127.9, 127.8, 127.6, 126.7, 126.4, 126.1, 120.9, 118.7. HRMS (EI): m/z calculated for $C_{28}H_{18}Cl_2O$ $[M+H]^+$ = 441.0813, found 441.0820.

2-(4-chlorophenoxy)-1,6-bis(4-chlorophenyl) naphthalene (3f)

The following compound was obtained according to the general procedure A, by using 6-(4-chlorophenyl)naphthalen-2-ol and (4-chlorophenyl)(phenyl)-λ^3-iodanyl trifluoromethanesulfonate as starting material. The crude material was purified by flash column chromatography over silica gel with the (6% EtOAc/Hexane) system to afford the product **3f** (65 mg, 70%) as a white solid. m.p. = 134–136°C. R_f = 0.45 (10% EtOAc/Hexane). IR (neat) ν/cm^{-1} = IR (neat) ν/cm^{-1} = 3,015, 1,460, 1,389, 1,309, 720. ^{1}H NMR (500 MHz, $CDCl_3$) δ 8.06 (s, 1H), 7.94 (d, J = 8.9 Hz, 1H), 7.66 (dt, J = 10.0, 8.7 Hz, 4H), 7.48 (d, J = 8.5 Hz, 2H), 7.44 (d, J = 8.4 Hz, 2H), 7.32 (d, J = 8.4 Hz, 2H), 7.27–7.25 (m, 1H), 7.24–7.20 (m, 2H), 6.82–6.78 (m, 2H). ^{13}C NMR (126 MHz, $CDCl_3$) δ 156.9, 150.5, 139.7, 136.9, 133.9, 133.8, 133.7, 132.9, 132.1, 131.7, 130.5, 129.7, 129.6, 128.9, 128.8, 128.7, 127.7, 126.8, 126.5, 126.4, 121.5, 118.9. HRMS (EI): m/z calculated for $C_{28}H_{18}Cl_3O$ $[M+H]^+$ = 475.0423, found 475.0413.

6-(3-chloro-4-fluorophenyl)-2-(4-chlorophenoxy)-1-(4-chlorophenyl)naphthalene (3g)

The following compound was obtained according to the general procedure A, by using 2-napthol and (4-chlorophenyl)(phenyl)-λ^3-iodanyl trifluoromethanesulfonate as starting material. The crude material was purified by flash column chromatography over silica gel with the (6% EtOAc/Hexane) system to afford the product **3g** (59 mg, 66%) as a white solid. m.p.= 130–140°C.

R_f = 0.45 (15% EtOAc/Hexane). IR (neat) ν/cm^{-1} = 2,984, 1,560, 1,489, 1,309, 820. ^{1}H NMR (500 MHz, $CDCl_3$) δ 7.93 (d, J = 1.6 Hz, 1H), 7.84 (d, J = 8.9 Hz, 1H), 7.64 (dd, J = 7.0, 2.3 Hz, 1H), 7.58 (d, J = 8.8 Hz, 1H), 7.51 (dd, J = 8.8, 1.9 Hz, 1H),

7.46 (ddd, $J = 8.5, 4.5, 2.3$ Hz, 1H), 7.36–7.32 (m, 2H), 7.24–7.20 (m, 2H), 7.17 (dd, $J = 9.7, 5.9$ Hz, 2H), 7.15–7.10 (m, 2H), 6.72–6.68 (m, 2H). ^{13}C NMR (126 MHz, $CDCl_3$) δ 158.9, 156.9, 150.5, 138.0 (d, $J = 20$ Hz), 135.9, 133.8, 133.5, 133.0, 132.0, 131.3, 130.2, 129.7, 129.5, 128.8, 128.7, 127.7, 127.1, 127.0, 126.6, 126.1, 121.6 (d, $J = 70$ Hz), 121.1, 118.8, 117.1 (d, $J = 20$ Hz). HRMS (EI): m/z calculated for $C_{28}H_{16}Cl_3FO$ $[M]^+ = 492.0251$ found 492.0247.

4-bromo-1-(4-chlorophenoxy)-2-(4-chlorophenyl) naphthalene (3h)

The following compound was obtained according to the general procedure A, by using 4-bromonaphthalen-1-ol and (4-chlorophenyl)(phenyl)-λ^3-iodanyl trifluoromethanesulfonate as starting material. The crude material was purified by flash column chromatography over silica gel with the (3% EtOAc/Hexane) system to afford the product **3h** (62 mg, 62%) as a white solid. m.p. = 98–100°C. $R_f = 0.5$ (5% EtOAc/Hexane). IR (neat) $\nu/cm^{-1} = 2{,}984, 1{,}560, 1{,}489, 1{,}309, 820$. ^{1}H NMR (500 MHz, $CDCl_3$) δ 8.20 (d, $J = 7.5$ Hz, 1H), 7.87 (d, $J = 7.5$ Hz, 1H), 7.80 (s, 1H), 7.52 (t, $J = 7.5$ Hz, 1H), 7.40 (t, $J = 7.5$ Hz, 1H), 7.38 (d, $J = 8.5$ Hz, 2H), 7.24 (d, $J = 8.5$ Hz, 2H), 7.00(d, $J = 8.5$ Hz, 2H), 6.52 (d, $J = 8.5$ Hz, 2H). ^{13}C NMR (126 MHz, $CDCl_3$) δ 157.6, 146.8, 134.8, 134.2, 132.8, 131.6, 131.0, 130.6, 129.6, 129.3, 128.8, 128.3, 127.9, 127.7, 126.9, 123.7, 119.9, 116.8. HRMS (EI): m/z calculated for $C_{22}H_{13}BrCl_2O$ $[M]^+ = 441.9527$, found 441.9523.

Synthetic Utility of the Developed Procedure

Equation 1. 2-phenoxy-1,3-diphenylnaphthalene (4)

This compound was synthesized according to the general procedure for the Suzuki cross-coupling using **2c** as starting material and phenyl boronic acid. The purification was carried out using (3% EtOAc/Hexane) system to afford the product **4** in 62% of yield as a white solid. m.p. = 94–96°C. $R_f = 0.45$ (5% EtOAc/Hexane). IR (neat) $\nu/cm^{-1} = 3{,}046, 1{,}561, 1{,}474, 1{,}216, 925$. ^{1}H NMR (500 MHz, $CDCl_3$) δ 8.05 (d, $J = 1.3$ Hz, 1H), 7.89 (d, $J = 8.9$ Hz, 1H), 7.71–7.64 (m, 3H), 7.46 (t, $J = 7.7$ Hz, 2H), 7.43–7.34 (m, 6H), 7.25–7.19 (m, 4H), 6.98 (t, $J = 7.4$ Hz, 1H), 6.86 (d, $J = 7.8$ Hz, 2H). ^{13}C NMR (126 MHz, $CDCl_3$) δ 158.9, 150.4, 140.8, 137.9, 135.4, 132.9, 131.4, 130.9, 129.8, 129.5(x2), 129.3, 128.9, 128.4, 127.9, 127.3, 126.5, 126.4, 125.8, 122.3, 121.7, 117.8. HRMS (EI): m/z calculated for $C_{28}H_{21}O$ $[M+H]^+ = 373.1592$, found 373.1594.

RESULTS AND DISCUSSION

We first targeted the selective *C*-arylation of phenols considering the typical behavior of Ar_2IX.[12,13,22] In our strategy, we envisaged the deprotonation of the hydroxyl group in the naphthol to form a bidentate anion for reacting with the Ar_2IX. Then, the electron-poor aryl transfer from Ar_2IX to the naphthol would take place. This way, ionic conditions in basic media for proton abstraction of the hydroxyl group in naphthol using different bases, solvent and temperatures were assayed. 2-Naphthol and the inexpensive diphenyliodonium(III) nitrate were used as a model system (**Table 1**).

Initial attempts to induce the arylation of 2-naphthol were carried out using excess of diphenyliodonium nitrate and potassium carbonate in dimethylformamide since essentially no reaction was found with one equivalent.

The best reaction progress was found after 1 h at room temperature, obtaining 20% of *C*-arylation and 8% of the doubly arylated product (*C*-/*O*-arylation) (entry 1). A great amount of unreacted starting material was observed in this assay even after 12 h of reaction. When using THF as solvent, a considerable increase in the reaction yield was obtained with the same product ratio (entry 2). Also, large amounts of unreacted starting material were observed even by heating at 80°C; in this case a lower yield was obtained (entry 3). The change of base to bicarbonate did not improve the yields (entries 4 and 5). These attempts to get the single *C*-arylated product **1** resulted in a poor conversion of the starting material. Thus, we considered the use of a stronger base such as potassium *tert*-butoxide (entries 6–12). After an extensive experimentation with different solvents and temperatures, the complete consumption of the starting material was achieved. However, it resulted in a complex mixture of products. The single *C*-arylation product was identified and isolated from the crude when THF or DME were tested as solvents (entries 6, 11, and 12). Nevertheless, we were unable to get selectivity for any singly arylated product. We tried with cesium carbonate (entry 13) but, again, unreacted starting material and unselective mixtures of arylated products were observed. The base reactivity was scaled up and sodium hydride was assayed as a stronger reagent (entry 14). However, a lower conversion was obtained. Another experiment was performed using TMEDA as solvent and base, but no reaction was observed in this case (entry 15).

At this point, our hypothesis for the poor reactivity of the naphthyl anion formed after deprotonation was attributed mainly to the use of a not enough strong base, which may generate the proper chemical environment of reactivity, and the inappropriate choice of the reaction solvent. In consequence, we decided to use TMP-Li (lithium 2,2,6,6-tetramethylpiperidin-1-ide) as base and cyclohexane/diethyl ether (1:1) as reaction solvent, according to the related arylation procedure of Daugulis (Truong and Daugulis, 2012).

Therefore, the synthesis of the TMP-Li was started from the deprotonation of TMP-H with *n*-BuLi. During the work-up of this synthesis, *the direct evaporation of the crude reaction* lead to the formation of a brown, *non-pyrophoric* and *air stable* solid identified by HRMS as TMP_2O. This solid was tested in the following experiment. By using 1.2 equiv of TMP_2O and 2.5 equiv of diphenyliodonium nitrate at room temperature, the selective double arylated product (*C*-/*O*-arylation) was surprisingly obtained in 59% yield and 7% of starting material was recovered after 5 h (entry 16). Moreover, 1.5 equiv of TMP_2O produced the diarylated product in 65% yield and, again, 3% of starting material was recovered (entry 17). Finally, the use of 1.7 equiv of TMP_2O yielded the double arylated naphthol in 70% after 3 h. However, no remaining starting material was observed (entry 18). Remarkably, neither the single *O*- nor

TABLE 1 | Optimization of the *C*- and *O*-arylation of 2-naphthol using diphenyliodonium(III) nitrate[a].

Entry	$Ph_2I(X)$, equiv	Base (equiv)	Solvent	T (°C)	t (h)	yield (%)[b] 1 / 2 / 2a
1	(NO_3), 2.5	K_2CO_3, (1.5)	DMF	23	1.0	20/0/8
2	(NO_3), 2.5	K_2CO_3, (1.5)	THF	23	1.5	35/0/25
3	(NO_3), 2.5	K_2CO_3, (1.5)	THF	80	1.5	30/0/15
4	(NO_3), 2.5	$KHCO_3$, (1.5)	DMF	23	2.0	20/0/15
5	(NO_3), 2.5	$KHCO_3$, (1.5)	THF	23	1.0	12/0/18
6[c]	(NO_3), 3.5	^{t}BuOK, (2.5)	THF	23	0.5	35/10/28
7[c]	(NO_3), 3.5	^{t}BuOK, (2.5)	DCE	23	0.5	25/0/18
8[c]	(NO_3), 3.5	^{t}BuOK, (2.5)	MeCN	23	2.0	20/0/16
9[c]	(NO_3), 3.5	^{t}BuOK, (2.5)	Tol	23	2.0	20/0/14
10[c]	(NO_3), 3.5	^{t}BuOK, (2.5)	DMF	23	1.5	25/0/18
11[c,d]	(NO_3), 3.5	^{t}BuOK, (2.5)	THF	130	0.5	37/13/24
12[c,d]	(NO_3), 3.5	^{t}BuOK, (2.5)	DME	130	0.5	30/15/26
13	(NO_3), 3.5	Cs_2CO_3, (2.5)	THF	23	0.5	30/0/15
14	(NO_3), 3.5	NaH, (2.5)	THF	23	2.0	20/0/15
15	(NO_3), 2.5	–	TMEDA	23	0.5	n. r.
16[e,f]	(NO_3), 2.5	TMP_2O, (1.2)	Cy-H/Et_2O	23	5.0	0/0/59
17[e,f]	(NO_3), 2.5	TMP_2O, (1.5)	Cy-H/Et_2O	23	5.0	0/0/65
18[f]	(NO_3), 2.5	TMP_2O, (1.7)	Cy-H/Et_2O	23	3.0	0/0/70
19[f]	***(OTf), 2.5***	***TMP_2O, (1.7)***	***Cy-H/Et_2O***	***23***	***3.0***	***0/0/74***
20[f]	(OTs), 2.5	TMP_2O, (1.7)	Cy-H/Et_2O	23	3.0	0/0/65
21[f]	(PF_6), 2.5	TMP_2O, (1.7)	Cy-H/Et_2O	23	3.0	0/0/45
22[f]	(NO_3), 2.5	LiOH, (1.7)	Cy-H/Et_2O	23	3.0	18/0/54
23[f]	(NO_3), 2.5	NaOH, (1.7)	Cy-H/Et_2O	23	3.0	47/0/10
24[f,g]	(OTf), 2.5	–	Cy-H/Et_2O	23	12	5/0/10

[a]*Reaction conditions: 2-naphthol (0.25 mmol), solvent (0.1 M), open flask.* [b]*Isolated yields.* [c]*Complex reaction mixture obtained.* [d]*Microwave-assisted reaction in sealed tube at 1,500 W.* [e]*3–7% of remaining starting material was recovered.* [f]*A 1:1 mixture of solvents was used.* [g]*Yield is the average of three runs; 93% of starting material recovered. TMP_2O = [1,1′-oxybis(2,2,6,6-tetramethylpiperidine)]. TMEDA = N,N,N′,N′-tetramethyleth-ylenediamine. n.r. = no reaction observed.*

C-arylated naphthalenes were observed under these new base-free conditions.

We became interested in this doubly arylated product after considering that: (1) it was selectively formed as the sole arylation product, (2) new arylation reactivity was found by using TMP_2O and (3) this reaction proceeded under neutral and base-free conditions in contrast with the strongly basic conditions previously attempted. Thus, we considered this procedure as our first approach toward the selective *C*-arylation.

We continued the optimization to explore about the effect of the anion fragment within the Ar_2IX in the reaction. Triflate, tosylate and hexafluorophosphate gave exclusively the double arylated product in 74, 65, and 45% yield, respectively (entries 19–21). We identified the Ar_2IX with the triflate as anion as the best arylating reagent for this protocol. Next, lithium and sodium hydroxide were tested as bases, since they could have formed during the TMP_2O preparation and plausibly participated in the arylation. However, the typical mixture of *C*- and *C*-/*O*-arylation was obtained with those bases (entries 22 and 23). An inverse ratio in the product mixture was observed when Li^+ or Na^+ cations were present, highlighting their strong influence in the reaction.

For completing the optimization, a control experiment was carried out in absence of TMP_2O. Therefore, 5% of the *O*-arylation and 93% of starting 2-napthol was recovered after 12 h (entry 24). This essay confirmed the need of TMP_2O for the reaction to proceed.

With the optimized conditions identified in the entry 19, we continue to explore the scope of the protocol (**Scheme 2**).

Several substituted naphthols were assayed to determine the scope of the reaction when varying its electronic nature. Electron-neutral 2- and 1-naphthol underwent double phenylation in 74 and 47% yield (**2a** and **2b**). The lower yield for 1-napthol was attributed to the greater number of reactive centers, which allowed more side-reactions. On the other hand, 2-naphthol derivatives containing electron-attracting groups such as bromine at the positions 3 and 6, gave 72 and 74% yields, respectively (**2d** and **2e**). In contrast, with the 4-bromo-1-naphthol a lower yield (56%) was obtained (**2c**). The steric hindrance of bromine did not seem to affect the reaction. Additionally, the electron-donating groups 4-tolyl, methoxy, phenyl, and 2-naphthyl in the naphthol moiety were successfully tested. In these cases, slightly lower yields ranging from 64 to 66% were found (**2f** to **2i**). These results may indicate the formation of a less-stable intermediate species during the arylation which was reflected in decreasing yields. We also used 2-naphthol derivatives with electron-attracting groups, such as 4-fluorophenyl, 4-chlorophenyl, and 3-chloro-4-fluorophenyl,

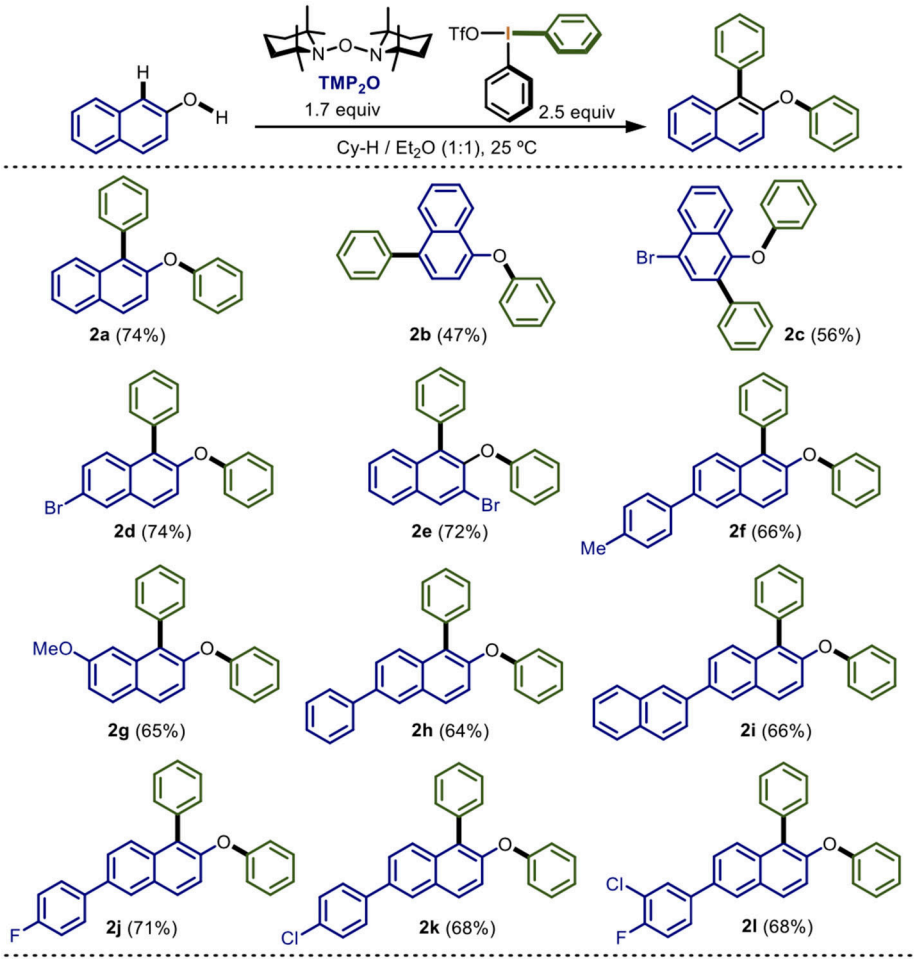

SCHEME 2 | Scope of electronic nature of naphthols in the double arylation mediated by TMP_2O/Ph_2IOTf[a,b].

leading to the formation of the doubly phenylated products in 71 and 68% yields, respectively (**2j** to **2l**). In general, very similar yields were obtained for various substrates in this one-pot double phenylation.

The previous set of experiments described the scope of the electronic nature of the 2-naphthol nucleus. The next step was to determine the functional-group tolerance of the reaction in the diaryliodonium(III) salt (**Scheme 3**).

Non-symmetrical diaryliodonium(III) salts containing electron-attracting groups were mainly tried. 2-Naphthol was subjected to our optimized reaction conditions using a diaryliodonium(III) salt which contains a chlorine atom in one of the aromatic rings. Gratifyingly, the double arylation product **3a** was isolated in 73% yield. Remarkably, only the electron-poor aryl was chemoselectively transferred following the Beringer and DiMagno observations (Beringer and Mausner, 1958; Beringer and Chang, 1971; Wang et al., 2010; Malmgren et al., 2013; Stuart, 2017). When nitro-containing diaryliodonium(III) salt was used, a 76% yield of **3b** was obtained, also by the selective transfer of the electron-poor aryl. Derivatives of 2-napthol having bromine atoms successfully reacted leading to the formation of **3c** and **3d** in 68 and 64% yields, respectively. Other derivatives substituted with phenyl, 4-chlorophenyl and 3-chloro-4-fluorophenyl groups proceeded in yields ranging from 68 to 72% (**3e** to **3g**). Additionally, by testing 4-bromo-1-naphthol with the chlorine-containing diaryliodonium(III) salt, the corresponding double arylation product was achieved in 62% yield (**3h**).

Finally, some mono-annular phenols assays did not display observable reaction, presumably due to their higher REDOX potential (2.1 eV) compared with naphthols (1.87 eV) (Brodwel and Cheng, 1991; Lee et al., 2014; Kang et al., 2017). In these cases, a stronger radical initiator different to TMP_2O or higher temperatures must be employed. On the other hand, the methyl or benzyl ethers as well as the acetyl and pivaloyl esters of the 2-napthol did not produce any reaction. This observation strongly suggested that *C*-arylation on the naphthol takes place prior to *O*-arylation. Other Ar_2IX containing electron-donating groups showed very low reactivity and were ruled out of the scope of this first report.

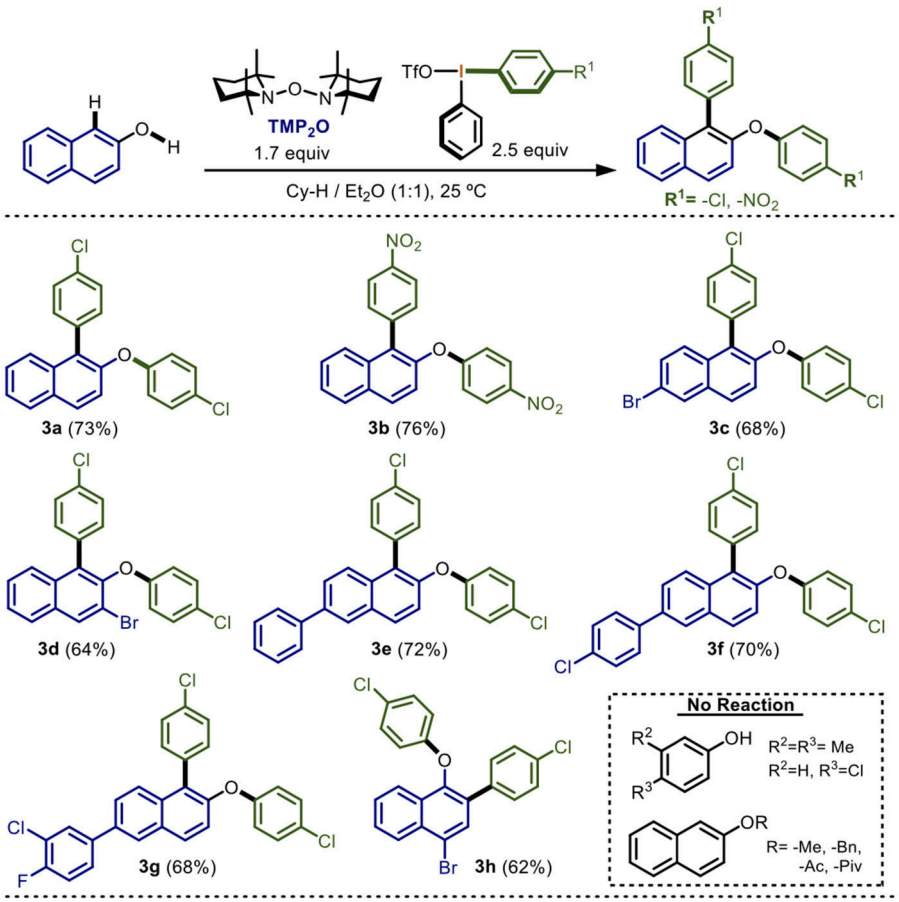

SCHEME 3 | Scope of the electronic nature of the diaryliodonium(III) salt in the one-pot double arylation[a,b].

The synthetic utility of our procedure was demonstrated by synthesizing a highly substituted 2-naphthol derivative **4** (Equation 1).

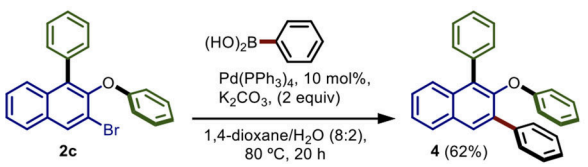

(1)

The Suzuki cross-coupling of **2c** with phenylboronic acid gave rise to the sterically hindered tris-arylated species **4** in 62% yield.

Intrigued by the observed new reactivity of this one-pot protocol of double arylation, we investigated a plausible reaction mechanism both theoretical and experimentally.

We first analyzed the brown, non-pyrophoric and air stable solid obtained from the reaction between TMP-H and *n*-BuLi which allowed the formation of TMP_2O. This solid was identified by HRMS as the mixture of two main compounds: the TMP-O-^{n}Bu $[M+H]^+ = 214.2171$ and TMP_2O $[M+H]^+ = 297.2906$ in 9:1 ratio. Therefore, DFT calculations at the (SMD:diethylether)ω-B97XD/6-311G(d) level were performed for measuring reaction energies and postulate a plausible reaction route (**Scheme 4**).

We suggest that four reaction pathways operate at the same time to produce both radicals in solution. TMP-H can either react with molecular oxygen or *n*-BuLi. In the case of O_2 (route A), this is inserted into the nitrogen to get intermediate **I** which readily tautomerizes to **II**. Transition states were located 8.67 and 21.13 kcal·mol^{-1} from reactants (see **Supporting Information**), for each reaction step. Then, peroxide **II** is in equilibrium with TEMPO and ·OH radicals, given the energy difference between both states ($\Delta G^0_R = -1.12$ kcal·mol^{-1}). On the other hand (route B), TMP-H combines with *n*-BuLi producing TMP-Li and *n*-butane ($\Delta G^0_R = -21.53$ kcal·mol^{-1}). The TMP-Li anion can transfer an electron to the ·OH radical leading to TMP· radical and OH^- spontaneously ($\Delta G^0_R = -12.89$ kcal·mol^{-1}). Both TEMPO and TMP· radicals do not combine in solution to derive TMP_2O according to the calculated energy ($\Delta G^0_R = +20.27$ kcal·mol^{-1}). However, because of the harsh conditions carried out during the HRMS technique, it is very possible that the TMP_2O can be detected as a single molecule. Also, an aside reaction (route C) comes from the possibility that ·OH radical absorbs one electron not only from TMP-Li anion but from the

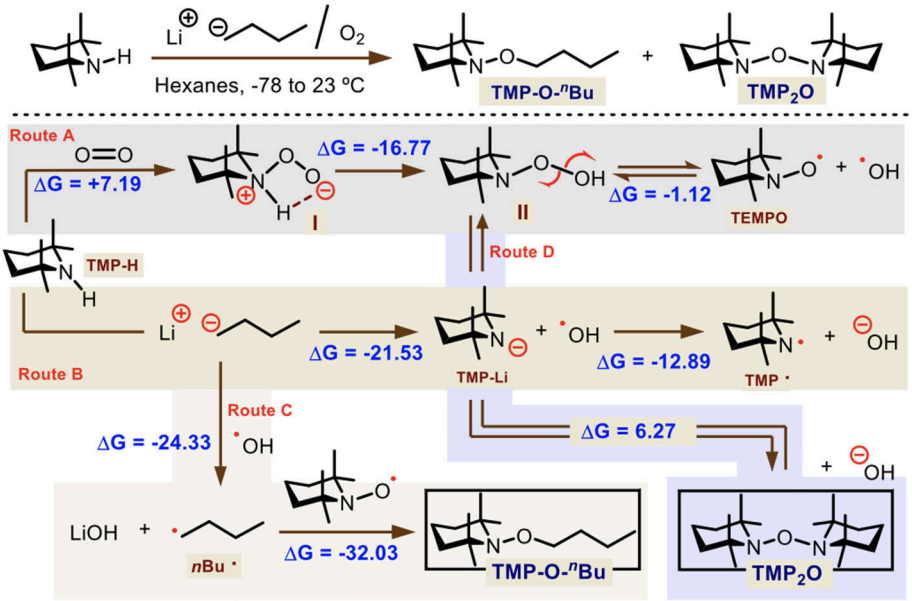

SCHEME 4 | Theoretical study of the mechanism for the TMP-O-^{n}Bu and TMP_2O formation. Gibbs free-energies are shown in kcal·mol^{-1}.

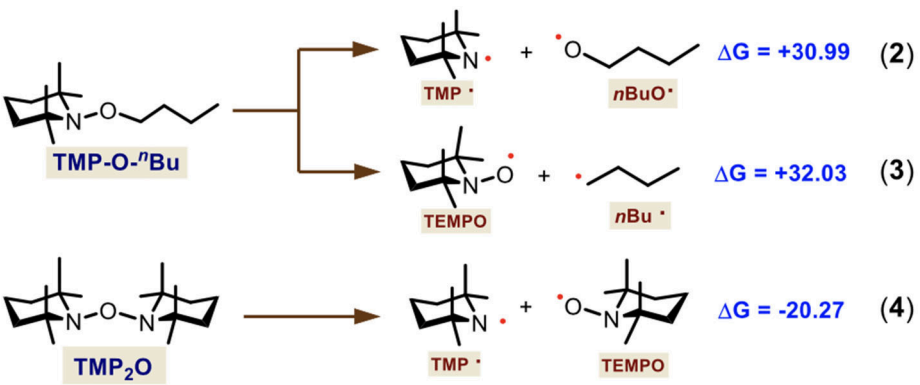

SCHEME 5 | Theoretical study of the TMP-O-^{n}Bu and TMP_2O homolytic fragmentation. Gibbs free-energies are shown in kcal·mol^{-1}.

initial Bu^- of *n*-BuLi. This reaction is more exergonic ($\Delta G^0_R = -24.33$ kcal·mol^{-1}) than the previous ones. And the reaction between TEMPO and Bu˙ radicals that gives TMP-O-^{n}Bu is also more favorable ($\Delta G^0_R = -32.03$ kcal·mol^{-1}). Thus, this product is mostly obtained than TEMPO and TMP· radicals, according to our calculations. Finally, one more possibility (route D) may come from the reaction among peroxide **II** and TMP-Li to form TMP_2O and OH^- in solid state. This is less exergonic than other pathways ($\Delta G^0_R = +6.27$ kcal·mol^{-1}), but not enough to keep the molecular TMP_2O in solution, which homolyze readily.

According to these results and considering that TMP-O-^{n}Bu and TMP_2O are the main species observed by HRMS, we hypothesized that a radical mechanism could be operating since several different ionic conditions previously tested just gave mixtures of non-selective arylation products (**Table 1**, entries 1–15, 22, and 23). Under this hypothesis, we also calculated two homolytic fragmentations for TMP-O-^{n}Bu as well as for TMP_2O. This way, we demonstrate that the radical source comes from TMP_2O and the other product is not involved in the subsequent reactions (**Scheme 5**).

We first calculated two possible fragmentations for TMP-O-^{n}Bu. These showed thermodinamically both nonfavorable processes which gave high-in-energy species, the TMP–O^{n}Bu ($\Delta G^0_R = +30.99$ kcal·mol^{-1}) (Equation 2) and the TMPO–^{n}Bu ($\Delta G^0_R = +32.03$ kcal·mol^{-1}) (Equation 3) homolysis. Thus, we identified that TMP_2O is the active initiator species, providing the TMP· and TEMPO radicals (Equation 4). For this calculated fragmentation, a very favorable process was found ($\Delta G^0_R = -20.27$ kcal·mol^{-1}). We also performed other theoretical calculations for reactions where these compounds act as bases

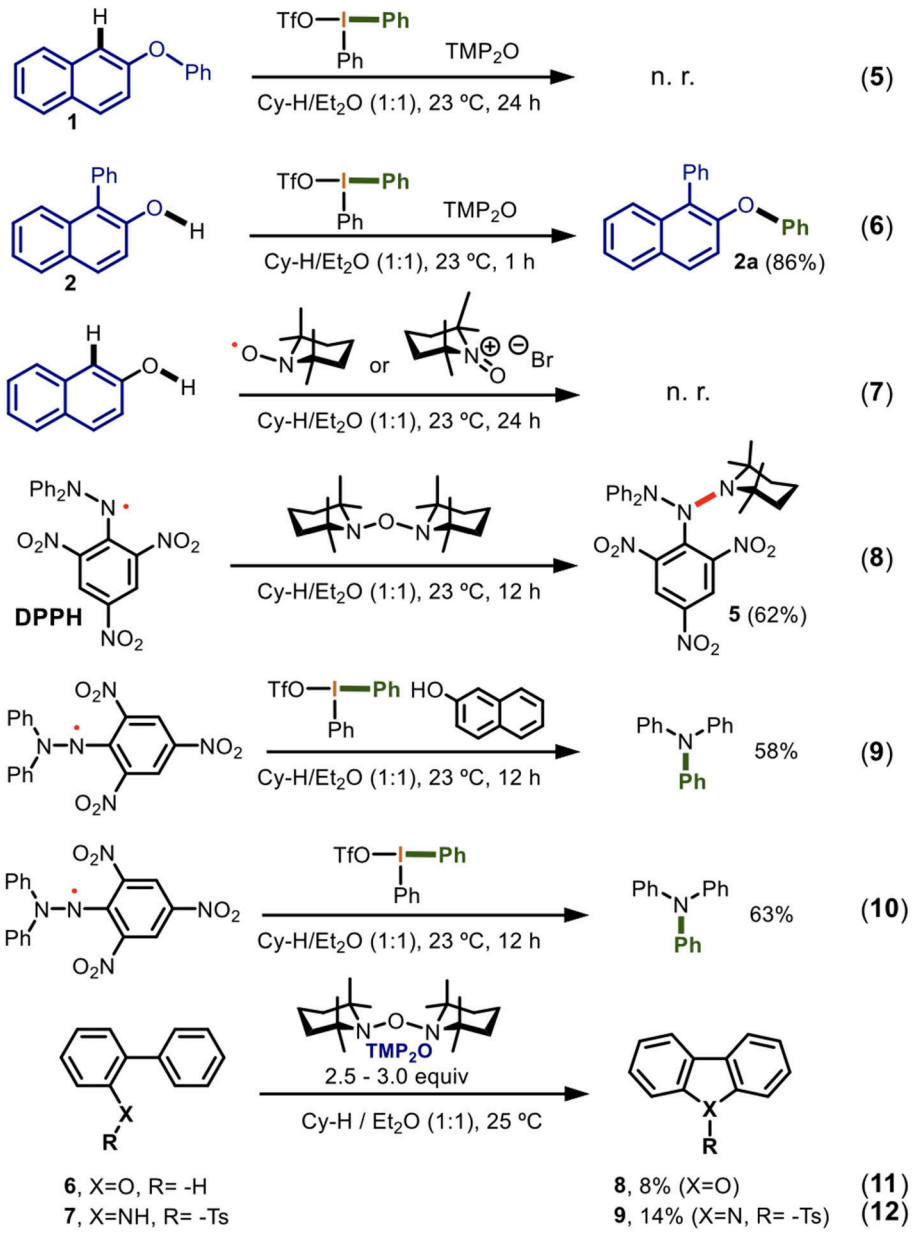

SCHEME 6 | Experimental mechanistic investigation of the one-pot double arylation of naphthols mediated by TMP_2O/DIS.

and deprotonate the 2-naphthol, which gave high exergonic free energies (see **Scheme S1** of Supporting Information). Thus, an ionic route was ruled out.

With these preliminary conclusions, we had enough information to experimentally elucidate a reaction mechanism for the observed double arylation. In consequence, a series of reactions were carried out (**Scheme 6**).

Different experiments were carried out to determine how the C-1 and the oxygen of the 2-naphthol derivatives were activated by TMP_2O. The mechanistic investigation started by the elucidation of the reaction center of the first arylation. Thus, when the optimized conditions (**Table 1**, entry 19) were applied to the 2-phenoxynaphthalene, no reaction was observed (Equation 5). However, 1-phenyl-2-naphthol led to the *O*-arylation product **2a** in 86% yield (Equation 6). These two experiments indicated that for this developed procedure in the 2-naphthol derivatives the first arylation occurred at the carbon followed by the arylation at the oxygen. The result is in line with the innate reactivity of 2-naphthol.

According to Equation 4, the homolytic fragmentation of TMP_2O is a very favored process and takes place spontaneously. Therefore, we experimentally confirmed the theoretical results

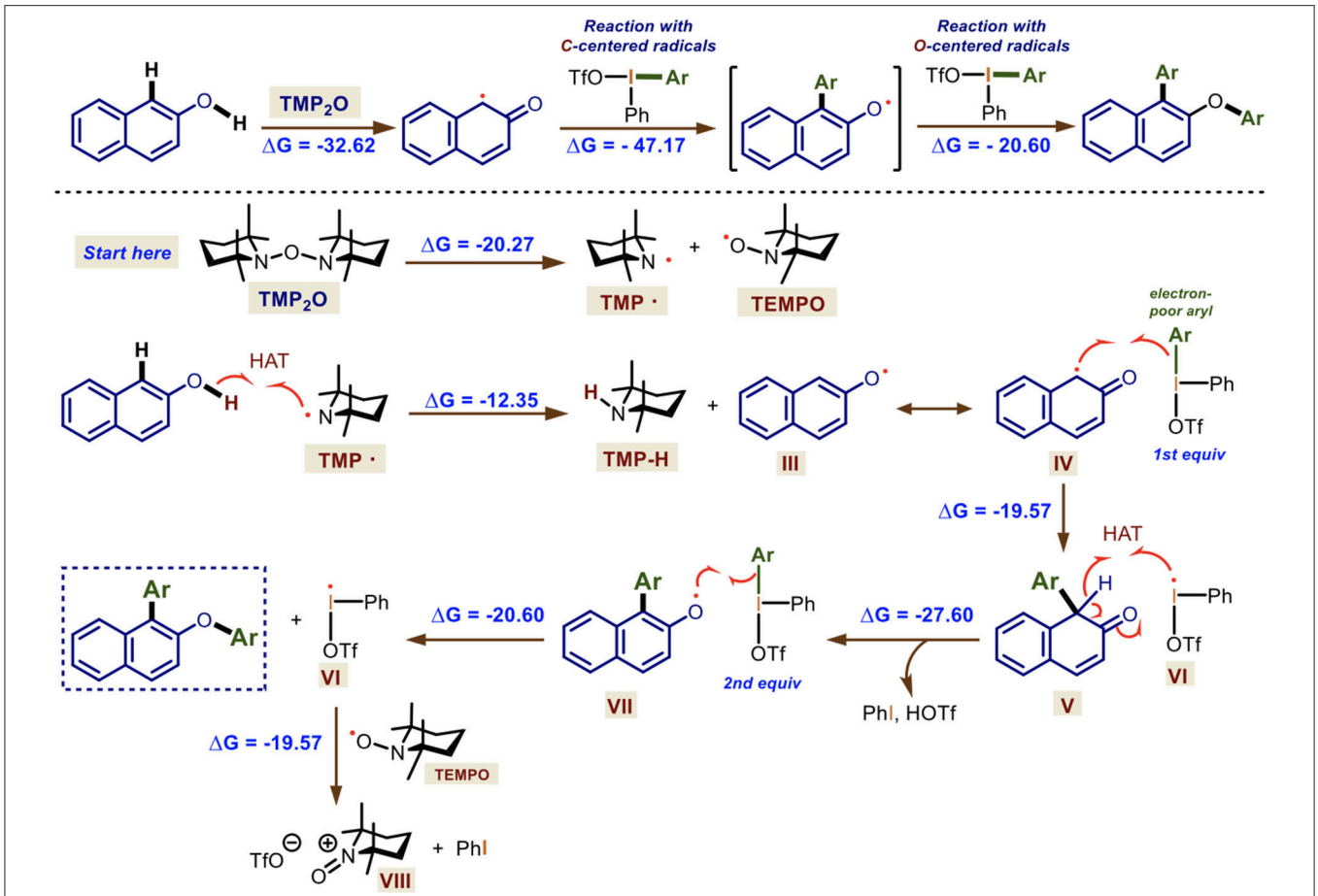

SCHEME 7 | Mechanistic rationale for the one-pot double arylation mediated by TMP_2O/DIS. Gibbs free-energies are shown in kcal·mol^{-1}.

on the generation of the TMP· and TEMPO radicals and its *N*-oxide with 2-naphthol as a model. No reaction was found for last two compounds (Equation 7). Also, to identify the TMP· radical, we designed a trapping experiment using the persistent radical DPPH (2,2-diphenyl-1-picrylhydrazyl). To our delight, we formed **5** in 62% yield (Equation 8). The result of this experiment can be explained exclusively via a radical pathway, thus unequivocally it demonstrated the homolytic fragmentation of TMP_2O and established it as a precursor of TMP· and TEMPO radicals. It also showed that the TMP· radical reacted faster than TEMPO, consistent with its greater reactivity.

We next sought to study the reaction of diaryliodonium(III) salts reaction with the *C*-centered radical of the 2-naphthol. We attempted to generate this naphthyl radical using DPPH instead of the TMP· under the optimized conditions. In this experiment, the *selective reaction* of the *N*-centered radical of DPPH with the hypervalent bond of the Ph_2IOTf instead of the *O*-centered radical formation in the 2-naphthol via HAT took place. This reaction produced triphenylamine in 58% by transferring one aryl group from Ph_2IOTf and fragmentating the picryl moiety (Equation 9). Thus, the DPPH· radical directly reacted with the Ph_2IOTf and not with 2-naphthol. To confirm this reactivity, the same reaction was carried out in absence 2-naphthol. Triphenylamine was again obtained in 63% yield (Equation 10). These two experiments (Equations 9 and 10) demonstrated that the diaryliodonium(III) salts reacted slowly at its hypervalent bond with persistent radicals such as DPPH. This observed reactivity represents a new activation mode of the Ph_2IOTf. Additional experiments are currently ongoing to determine if there is a pattern of chemo-selectivity in the reaction of transient and persistent radicals with naphthols or Ar_2IX.

Complementary studies to determine the radical precursor-nature of TMP_2O were conducted. Therefore, the radical cyclization of 2-phenylphenol **6** using 2.5 equiv of TMP_2O gave rise to the dibenzo[*b,d*]furan **8** in 8% of yield (Equation 11). Also, by using 3 equiv of TMP_2O, the radical cyclization of the *N*-tosyl-2-phenylaniline lead to the formation of 9-tosyl-9*H*-carbazole **9** in 14% of yield (Equation 12). The experiments are in line with a radical cyclization. However, the observed low yields are attributed in one side to the non-efficient radical formation in **6** and **8**. This low reactivity of TMP_2O for mono-annular phenols was previously observed (**Scheme 3**). On the other hand, there is a poor radical stabilization through the contiguous phenyl ring where the cyclization takes place, after the *O*- and *N*-centered radical formation occurs reacting with TMP_2O.

Finally, considering the overall spectroscopic, theoretical, and experimental mechanistic studies, additional DFT calculations at the same level of theory were carried out to support the plausible reaction mechanism of the double arylation of naphthols mediated by TMP_2O and Ar_2IOTf which is outlined in **Scheme 7**.

The reaction starts with the homolysis of TMP_2O generating the transient TMP· radical, which orthogonally reacts faster via HAT with the 2-naphthol derivatives ($\Delta G^0_R = -12.35$ kcal·mol^{-1}) forming an *O*-centered radical **III** in resonance with its *C*-centered radical **IV**. This reacts with the hypervalent bond of the first equivalent of the diaryliodonium(III) salt gave rise to the arylated, non-aromatic **V** and the iodanyl radical **VI** ($\Delta G^0_R = -19.57$ kcal·mol^{-1}). The following HAT reaction promoted by this *I*-centered radical leads to the formation of a new aromatic *O*-centered radical **VII**, releasing triflic acid and iodobenzene ($\Delta G^0_R = -27.60$ kcal·mol^{-1}). Then, **VII** reacts with a second equivalent of the diaryliodonium(III) salt at the hypervalent bond, yielding the doubly arylated naphthol and a second molecule of **VI** ($\Delta G^0_R = -20.60$ kcal·mol^{-1}). The final reaction of **VI** with the persistent radical TEMPO forms the *N*-oxide triflate **VIII** of TMP· and releases iodobenzene ($\Delta G^0_R = -19.57$ kcal·mol^{-1}).

Additional synthetic applications of this new radical precursor TMP_2O, as well as the new reactivity displayed by the Ar_2IOTf, are currently being explored and developed in our laboratory.

CONCLUSIONS

In summary, we demonstrated that the radical precursor TMP_2O spontaneously undergoes homolytic fragmentation in solution and generates the transient *N*-centered radical of tetramethylpiperidinyl (TMP·) as well as the persistent radical TEMPO. The TMP· radical reacts with 2-naphthol derivatives, giving rise to the formation of an *O*-centered radical via HAT, in resonance with its corresponding *C*-centered radical. These *C*- and *O*-centered naphthyl radicals sequentially react with diaryliodonium(III) salts at its more electron-deficient hypervalent bond, transferring chemoselectively the more electron-poor aryl group. This observed reactivity constitutes a new activation mode of the diaryliodonium salts, which was used for developing the first one-pot double arylation procedure of naphthols via the sequential C^2_{sp}-C $^2_{sp}$/O-C $^2_{sp}$ bond formation. Spectroscopic, theoretical and experimental mechanistic studies supported and revealed a complete panorama of the reaction pathway. Finally, this novel protocol was conducted under neutral and base-free, room temperature and operationally simple conditions.

DATA AVAILABILITY STATEMENT

All datasets generated for this study are included in the article/**Supplementary Material**.

AUTHOR CONTRIBUTIONS

YS: full experimental part. KW: TMP_2O and TMP-O-^{n}Bu analysis by HRMS and results discussion of this section. DT-G: radical calculations of **Schemes 4**, **5**. RO-A: first draft writing and initial discussion. JJ-H: writing of full theoretical calculations part. CS-A: full organization, supervision, writing of final version of manuscript, and submission. All authors contributed to the article and approved the submitted version.

FUNDING

This work was supported by The Office of Support to Research and Postgraduate of Guanajuato University (UG-DAIP) project number 296/2019.

ACKNOWLEDGMENTS

We acknowledge the facilities of the DCNyE, the Chemistry Department and the National Laboratory UG-CONACyT (LACAPFEM) at the University of Guanajuato. We also thank CONACyT for fellowship to YS. The authors thanks to David Vosburg for helpful comments on the manuscript.

SUPPLEMENTARY MATERIAL

The Supplementary Material for this article can be found online at: https://www.frontiersin.org/articles/10.3389/fchem.2020.563470/full#supplementary-material

REFERENCES

Barton, D. H. R., Blazejewski, J.-C., Charpiot, B., and Motherwell, W. B. (1981). Tetraphenylbismuth monotrifluoroacetate: a new reagent for regioselective aryl ether formation. *J. Chem. Soc. Chem. Commun*. 503–504.

Barton, D. H. R., Charpiot, B., and Motherwell, W. B. (1982). Regiospecific arylation by acid/base controlled reactions of tetraphenylbismuth esters. *Tetrahedron Lett.* 23, 3365–3368. doi: 10.1016/S0040-4039(00)87616-9

Barton, D. H. R., Finet, J.-P., Giannotti, C., and Halley, F. (1987). The chemistry of pentavalent organobismuth reagents. Part 7. the possible role of radical mechanisms in the phenylation process for bismuth(V), and related lead(IV), Iodine(III), and antimony(V) reagents. *J. Chem. Soc. Perk. Tans.* 1, 241–249. doi: 10.1016/S0040-4020(01)89960-9

Beesson, T. D., Mastracchio, A., Hong, J.-B., Ashton, K., and McMillan, D. W. (2007). Enantioselective organocatalysis using SOMO activation. *Science* 316, 582–585. doi: 10.1126/science.1142696

Beringer, F.-M., and Chang, L. L. (1971). Electrophilic and homolytic cleavage of 5-aryl-5*H*-dibenzio-doles. *J. Org. Chem.* 36, 4055–4060. doi: 10.1021/jo00825a011

Beringer, F. M., and Mausner, M. (1958). Diaryliodonium salts. VIII. decomposition of substituted diphenyliodonium halides in inert solvents. *J. Am. Chem. Soc.* 80, 4535–4536. doi: 10.1021/ja01550a027

Brodwel, F. G., and Cheng, J. (1991). Substituent effects on the stabilities of phenoxyl radicals and the acidities of phenoxyl radical cations. *J. Am. Chem. Soc.* 113, 1736–1743. doi: 10.1021/ja00005a042

Capaldo, L., and Ravelli, D. (2017). Hydrogen atom transfer (HAT): a versatile strategy for substrate activation in photocatalyzed organic synthesis. *Eur. J. Org. Chem.* 15, 2056–2017. doi: 10.1002/ejoc.201601485

Dreher, D. S., Katz, T. J., Lam, K.-C., and Rheingold, A. L. (2000). Application of the russig–laatsch reaction to synthesize a bis[5]helicene chiral pocket for asymmetric catalysis. *J. Org. Chem.* 65, 815–822. doi: 10.1021/jo991498u

Egami, H., and Katsuki, T. (2009). Iron-catalyzed asymmetric aerobic oxidation: oxidative coupling of 2-naphthols. *J. Am. Chem. Soc.* 131, 6082–6083. doi: 10.1021/ja901391u

Elsler, B., Schollmeyer, D., Dyballa, K. M., Franke, R., and Waldvogel, S. R. (2014). Metal and reagent-free, highly selective anodic cross-coupling of phenols. *Angew. Chem. Int. Ed.* 53, 1–5. doi: 10.1002/anie.201401136

Ghosh, M. K., Rzymkowski, J., and Kalek, M. (2019). Transition-metal-free aryl–aryl cross-coupling: C–H arylation of 2-naphthols with diaryliodonium salts. *Chem. Eur. J.* 25, 9619–9623. doi: 10.1002/chem.201902204

Grzybowski, M., Skonieczny, K., Butenschön, H., and Gryko, D. T. (2013). Comparison of oxidative aromatic coupling and the scholl reaction. *Angew. Chem. Int. Ed.* 52, 9900–9930. doi: 10.1002/anie.201210238

Gutierrez-Cano, J. R., Nahide, P. D., Ramadoss, V., Satkar, Y., Ortiz-Alvarado, R., Alba-Betancourt, C., et al. (2017). Synthesis and biological evaluation of new 3,4-diarylmaleimides as enhancers (modulators) of doxorubicin cytotoxic activity on cultured tumor cells from a real case of breast cancer. *J. Mex. Chem. Soc.* 61, 41–49. doi: 10.29356/jmcs.v61i1.126

Hon, S.-W., Li, C.-H., Kuo, J.-H., Barhate, N. B., Liu, Y.-H., Wang, Y., et al. (2001). Catalytic asymmetric coupling of 2-naphthols by chiral tridentate oxovanadium(IV) complexes. *Org. Lett.* 3, 869–872. doi: 10.1021/ol015505o

Huang, H., Zhang, G., Gong, L., Zhang, S., and Chen, Y. (2014). Visible-light-induced chemoselective deboronative alkynylation under biomolecule-compatible conditions. *J. Am. Chem. Soc.* 136, 2280–2283. doi: 10.1021/ja413208y

Irie, R., Masutani, K., and Katsuki, T. (2000). Asymmetric aerobic oxidative coupling of 2-naphthol derivatives catalyzed by photo-activated chiral (NO)Ru(II)-salen complex. *Synlett* 2000, 1433–1436. doi: 10.1055/s-2000-7654

Jalalian, N., Ishikawa, E. E., Silva, L. F. Jr, and Olofsson, B. (2011a). Room temperature, metal-free synthesis of diaryl ethers with use of diaryliodonium salts. *Org. Lett.* 13, 1552–1555. doi: 10.1021/ol200265t

Jalalian, N., Petersen, T. B., and Olofsson, B. (2011b). Metal-free arylation of oxygen nucleophiles with diaryliodonium salts. *Chem. Eur. J.* 18, 14140–14149. doi: 10.1002/chem.201201645

Juárez-Ornelas, K. A., Jiménez-Halla, J. O. C., Kato, T., Solorio-Alvarado, C. R., and Maruoka, K. (2019). Iodine(III)-catalyzed electrophilic nitration of phenols via non-brønsted acidic NO_2^+ generation. *Org. Lett.* 21, 1315–1319. doi: 10.1021/acs.orglett.8b04141

Kang, H., Lee, Y. E., Reddy, P. V. G., Dey, S., Allen, S. E., Niederer, K. A., et al. (2017). Asymmetric oxidative coupling of phenols and hydroxycarbazoles. *Org. Lett.* 19, 5505–5508. doi: 10.1021/acs.orglett.7b02552

Kita, Y., Takada, T., and Thoma, H. (1996). Hypervalent iodine reagents in organic synthesis: nucleophilic substitution of *p*-substituted phenol ethers. *Pure Appl. Chem.* 68, 627–630. doi: 10.1351/pac199668030627

Kita, Y., Thoma, H., Hatanaka, K., Takada, T., Fujita, S., Mitoh, S., et al. (1994). Hypervalent iodine-induced nucleophilic substitution of *para*-substituted phenol ethers. generation of cation radicals as reactive intermediates. *J. Am. Chem. Soc.* 116, 3684–3691. doi: 10.1021/ja00088a003

Lecroq, W., Bazille, P., Morlet-Savary, F., Breugst, M., Lalevée, J., Gaumont, A.-C., et al. (2018). Visible-light-mediated metal-free synthesis of aryl phosphonates: synthetic and mechanistic investigations. *Org. Lett.* 20, 4164–4167. doi: 10.1021/acs.orglett.8b01379

Lee, Y.-E., Cao, T., Torruellas, C., and Kozlowski, M. C. (2014). Selective oxidative homo- and cross-coupling of phenols with aerobic catalysts. *J. Am. Chem. Soc.* 136, 6782–6785. doi: 10.1021/ja500183z

Li, X., Yang, J., and Kozlowski, M. C. (2001). Enantioselective oxidative biaryl coupling reactions catalyzed by 1,5-diazadecalin metal complexes. *Org. Lett.* 3, 1137–1140. doi: 10.1021/ol015595x

Lindstedt, E., Ghosh, R., and Olofsson, B. (2013). Metal-free synthesis of aryl ethers in water. *Org. Lett.* 15, 6070–6073. doi: 10.1021/ol402960f

Lindstedt, E., Stridfeldt, E., and Olofsson, B. (2016). Mild synthesis of sterically congested alkyl aryl ethers. *Org. Lett.* 18, 4234–4237. doi: 10.1021/acs.orglett.6b01975

Liu, X., Wang, Z., Cheng, X., and Li, C. (2012). Silver-catalyzed decarboxylative alkynylation of aliphatic carboxylic acids in aqueous solution. *J. Am. Chem. Soc.* 134, 14330–14333. doi: 10.1021/ja306638s

Malmgren, J., Santoro, S., Jalalian, N., Himo, F., and Olofsson, B. (2013). Arylation with unsymmetrical diaryliodonium salts: a chemoselectivity study. *Chem. Eur. J.* 19, 10334–10342. doi: 10.1002/chem.201300860

Merrit, E. A., and Olofsson, B. (2009). Diaryliodonium salts: a journey from obscurity to fame. *Angew. Chem. Int. Ed.* 48, 9052–9070. doi: 10.1002/anie.200904689

More, N. Y., and Jeganmohan, M. (2015). Oxidative cross-coupling of two different phenols: an efficient route to unsymmetrical biphenols. *Org. Lett.* 17, 3042–3045. doi: 10.1021/acs.orglett.5b01324

Moteki, S. A., Usui, A., Zhang, T., Solorio-Alvarado, C. R., and Maruoka, K. (2013). Site-selective oxidation of unactivated Csp3-H bonds with hypervalent iodine(III) reagents. *Angew. Chem. Int. Ed.* 52, 13093–13096. doi: 10.1002/anie.201304359

Nahide, P. D., Ramadoss, V., Juárez-Ornelas, K. A., Satkar, Y., Ortiz-Alvarado, R., Cervera-Villanueva, J. M. J., et al. (2018). *In situ* formed I^{III}-based reagent for the electrophilic *ortho*-chlorination of phenols and phenol ethers: the use of PIFA-$AlCl_3$ system. *Eur. J. Org. Chem.* 2018, 485–493. doi: 10.1002/ejoc.201701399

Nahide, P. D., and Solorio-Alvarado, C. R. (2017). Mild, rapid and efficient metal-free synthesis of 2-aryl-4-aryloxyquinolines via direct Csp2-O bond formation by using diaryliodonium salts. *Tetrahedron Lett.* 58, 279–284. doi: 10.1016/j.tetlet.2016.11.093

Nakajima, M. M. I., Kanayama, K., Hasimoto, S. I., Noji, M., and Koga, K. (1999). Enantioselective synthesis of binaphthol derivatives by oxidative coupling of naphthol derivatives catalyzed by chiral diamine·copper complexes. *J. Org. Chem.* 64, 2264–2271. doi: 10.1021/jo981808t

Narute, S., Parnes, R., Toste, F. D., and Pappo, D. (2016). Enantioselective oxidative homocoupling and cross-coupling of 2-naphthols catalyzed by chiral iron phosphate complexes. *J. Am. Chem. Soc.* 138, 16553–16560. doi: 10.1021/jacs.6b11198

Nieves-Quinones, Y., Paniak, T. J., Lee, Y. E., Kim, S. M., Tcyrulnikov, S., and Kozlowski, M. C. (2019). Chromium-salen catalyzed cross-coupling of phenols: mechanism and origin of the selectivity. *J. Am. Chem. Soc.* 141, 10016–10032. doi: 10.1021/jacs.9b03890

Oh, C. H., Kim, J. S., and Hung, H. H. (1999). Highly efficient arylation of malonates with diaryliodonium salts. *J. Org. Chem.* 64, 1338–1340. doi: 10.1021/jo981065b

Ozanne-Beaudenon, A., and Quideau, S. (2005). Regioselective hypervalent-iodine(III)-mediated dearomatizing phenylation of phenols through direct ligand coupling. *Angew. Chem. Int. Ed.* 44, 7065–7069. doi: 10.1002/anie.200501638

Parmar, D., Sugiono, E., Raja, S., and Rueping, M. (2014). Complete field guide to asymmetric BINOL-phosphate derived brønsted acid and metal catalysis: history and classification by mode of activation; brønsted acidity, hydrogen bonding, ion pairing, and metal phosphates. *Chem. Rev.* 114, 9047–9153. doi: 10.1021/cr5001496

Ramadoss, V., Alonso-Castro, A. J., Campos-Xolalpa, N., Ortiz-Alvarado, R., Yahuaca-Juárez, B., and Solorio-Alvarado, C. R. (2018b). Total synthesis of kealiiquinone: the regio-controlled strategy for accessing to its 1-methyl-4-arylbenzimidazolone core. *RSC. Adv.* 8, 30761–30776. doi: 10.1039/C8RA06676K

Ramadoss, V., Alonso-Castro, A. J., Campos-Xolalpa, N., and Solorio-Alvarado, C. R. (2018a). Protecting-group-free total synthesis and biological evaluation of 3-methylkealiiquinone and structural analogues. *J. Org. Chem.* 83, 10627–10635. doi: 10.1021/acs.joc.8b01436

Ramadoss, V., Gámez-Montaño, R., Zapata-Morales, J. R., Alonso-Castro, A. J., and Solorio-Alvarado, C. R. (2019). Total synthesis of the linear and angular 3-methylated regioisomers of the marine natural product kealiiquinone and biological evaluation of related *leucetta sp* alkaloids on human breast cancer. *Med. Chem. Res.* 28, 473–484. doi: 10.1007/s00044-019-02290-z

Ramadoss, V., Nahide, P., Juárez-Ornelas, K. A., Rentería-Gómez, M., Ortíz-Alvarado, R., and Solorio-Alvarado, C. R. (2016). A four-step scalable formal synthesis of ningalin C. *ARKIVOC. iv*, 385–394. doi: 10.3998/ark.5550190.p009.631

Reitti, M., Gurubrahamam, R., Walther, M., Lindstedt, E., and Olofsson, B. (2018). Synthesis of phenols and aryl silyl ethers via arylation of complementary hydroxide surrogates. *Org. Lett.* 20, 1785–1788. doi: 10.1021/acs.orglett.8b00287

Rosen, B. M., and Percec, V. (2009). Single-electron transfer and single-electron transfer degenerative chain transfer living radical polymerization. *Chem. Rev.* 109, 5069–5119. doi: 10.1021/cr900024j

Satkar, Y., Ramadoss, V., Nahide, P. D., García-Medina, E., Juárez-Ornelas, K. A., Alonso-Castro, A. J., et al. (2018). Practical, mild and efficient electrophilic bromination of phenols by a new I(III)-based reagent: the PIDA–$AlBr_3$ system. *RSC. Adv*. 8, 17806–17812. doi: 10.1039/C8RA02982B

Satkar, Y., Yera-Ledesma, L. F., Mali, N., Patil, D., Navarro-Santos, P., Segura-Quezada, L. A., et al. (2019). Iodine(III)-mediated, controlled di- or monoiodination of phenols. *J. Org. Chem.* 84, 4149–4164. doi: 10.1021/acs.joc.9b00161

Segura-Quezada, L. A., Satkar, Y., Patil, D., Mali, N., Wröbel, K., Gónzalez, G., et al. (2019). Iodine(III)/AlX_3-mediated electrophilic chlorination and bromination of arenes. Dual role of AlX_3 (X = Cl, Br) for (PhIO)n depolymerization and as the halogen source. *Tetrahedron Lett.* 60, 1551–1555. doi: 10.1016/j.tetlet.2019.05.019

Stuart, D. R. (2017). Aryl transfer selectivity in metal-free reactions of unsymmetrical diaryliodonium salts. *Chem. Eur. J.* 23, 15852–15863. doi: 10.1002/chem.201702732

Truong, T., and Daugulis, O. (2012). Direct intermolecular aniline *ortho*-arylation via benzyne intermediates. *Org. Lett.* 14, 5964–5967. doi: 10.1021/ol302875x

Vaillant, F. L., Courant, T., and Waser, J. (2015). Room-temperature decarboxylative alkynylation of carboxylic acids using photoredox catalysis and EBX reagents. *Angew. Chem. Int. Ed.* 54, 11200–11204. doi: 10.1002/anie.201505111

Vaillant, F. L., Wodrich, M. D., and Waser, J. (2016). Room temperature decarboxylative cyanation of carboxylic acids using photoredox catalysis and cyanobenziodoxolones: a divergent mechanism compared to alkynylation. *Chem. Sci.* 8, 1790–1800. doi: 10.1039/C6SC04907A

Wang, B., Graskemper, J. W., Qin, L., and DiMagno, S. G. (2010). Regiospecific reductive elimination from diaryliodonium salts. *Angew. Chem. Int. Ed.* 49, 4079–4083. doi: 10.1002/anie.201000695

Wang, H., Guo, L.-N., Wang, S., and Duan, X.-H. (2015). Decarboxylative alkynylation of α-keto acids and oxamic acids in aqueous media. *Org. Lett.* 17, 3054–3057. doi: 10.1021/acs.orglett.5b01336

Wang, X., and Studer, A. (2017). Iodine(III) reagents in radical chemistry. *Acc. Chem. Res.* 50, 1712–1724. doi: 10.1021/acs.accounts.7b00148

Ye, B., Zhao, J., Zhao, K., McKenna, J. M., and Toste, F. D. (2018). Chiral diaryliodonium phosphate enables light driven diastereoselective α-C(sp3)–H acetalization. *J. Am. Chem. Soc.* 140, 8350–8356. doi: 10.1021/jacs.8b05962

Zhou, Q.-Q., Guo, W., Ding, W., Wu, X., Chen, X., Lu, X., et al. (2015). Decarboxylative alkynylation and carbonylative alkynylation of carboxylic acids enabled by visible-light photoredox catalysis. *Angew. Chem. Int. Ed.* 54, 11196–11199. doi: 10.1002/anie.201504559

Zofou, D., Ntie-Kang, F., Sippl, W., and Efange, S. M. N. (2013). Bioactive natural products derived from the central African flora against neglected tropical diseases and HIV. *Nat. Prod. Rep.* 30, 1098–1120. doi: 10.1039/c3n70030e

Conflict of Interest: The authors declare that the research was conducted in the absence of any commercial or financial relationships that could be construed as a potential conflict of interest.

frontiers in Chemistry

MINI REVIEW
published: 20 November 2020
doi: 10.3389/fchem.2020.599026

Heteroaryliodonium(III) Salts as Highly Reactive Electrophiles

Naoko Takenaga[1]*, *Ravi Kumar*[2] and *Toshifumi Dohi*[3]*

[1] Faculty of Pharmacy, Meijo University, Nagoya, Japan, [2] J.C. Bose University of Science & Technology, YMCA, Faridabad, India, [3] College of Pharmaceutical Sciences, Ritsumeikan University, Kusatsu, Japan

In recent years, the chemistry of heteroaryliodonium(III) salts has undergone significant developments. Heteroaryliodonium(III) salts have been found to be useful synthetic tools for the transfer of heteroaryl groups under metal-catalyzed and metal-free conditions for the preparation of functionalized heteroarene-containing compounds. Synthetic transformations mediated by these heteroaryliodonium(III) salts are classified into two categories: (1) reactions utilizing the high reactivity of the hypervalent iodine(III) species, and (2) reactions based on unique and new reactivities not observed in other types of conventional diaryliodonium salts. The latter feature is of particular interest and so has been intensively investigated in recent decades. This mini-review therefore aims to summarize the recent synthetic applications of heteroaryliodonium(III) salts as highly reactive electrophiles.

Keywords: iodine, hypervalent compound, diaryliodonium(III) salt, aromatic substitution, arylation, heteroaromatic compound

OPEN ACCESS

Edited by:
Gwilherm Evano,
Université Libre de Bruxelles, Belgium

Reviewed by:
Martín Fañanás-Mastral,
Universidad de Santiago de Compostela, Spain
Boris Nachtsheim,
University of Bremen, Germany

***Correspondence:**
Naoko Takenaga
ntakenag@meijo-u.ac.jp
Toshifumi Dohi
td1203@ph.ritsumei.ac.jp

Specialty section:
This article was submitted to Organic Chemistry, a section of the journal Frontiers in Chemistry

Received: *26 August 2020*
Accepted: *16 October 2020*
Published: *20 November 2020*

Citation:
Takenaga N, Kumar R and Dohi T (2020) Heteroaryliodonium(III) Salts as Highly Reactive Electrophiles. Front. Chem. 8:599026. doi: 10.3389/fchem.2020.599026

INTRODUCTION

Over the past few decades, the hypervalent iodine(III) reagent has been widely recognized as a versatile oxidant for performing environmentally friendly oxidation reactions. It has gained great importance as a promising alternative to toxic heavy metal oxidants, such as Pb(IV), Tl(III), and Hg(II) because of its low toxicity, high stability, and easy handling (Stang and Zhdankin, 1996; Zhdankin and Stang, 2002, 2008; Zheng et al., 2014; Yoshimura and Zhdankin, 2016). Diaryliodonium salts ($Ar^1Ar^2I^+X^-$), which have two aryl groups and one counter-anion on the trivalent iodine atom, represent one of the most useful classes of hypervalent iodine(III) compounds (Merritt and Olofsson, 2009; Yusubov et al., 2011; Aradi et al., 2016; Fañanás-Mastral, 2017; Stuart, 2017). Due to the highly electron-deficient nature of the iodine(III) center in diaryliodonium salts and the excellent leaving-group ability of the iodobenzene group, they serve as highly reactive arylating agents toward a wide range of nucleophiles, even under metal-free conditions. Although the chemistry of conventional diaryliodonium salts is well developed and widely applied, synthetic transformations using heteroaryliodonium salts have received little attention to date.

In early studies, symmetric diaryliodonium salts ($Ar^1Ar^2I^+X^-$; $Ar^1 = Ar^2$) were preferred over unsymmetric salts ($Ar^1Ar^2I^+X^-$; $Ar^1 \neq Ar^2$) to avoid selectivity issues during the aryl-transfer processes. Meanwhile, the introduction of a "dummy aryl" into asymmetric salts to act as a nontransferable group has been favored in recent studies to modulate and control the reactivities of the diaryliodonioum salts. On the other hand, the reactions of heteroaryliodonium salts have some limitations in the past; for example, the heteroaryl group present in phenyl(heteroaryl)iodonium salts tends to serve as a "dummy aryl," and it was not possible to transfer the heteroaryl group

during the reactions (Martín-Santamaría et al., 2000). However, during the last decade or so, quite interesting and highly valuable transformations utilizing aryl(heteroaryl)iodonium salts have been reported. Thus, this mini-review highlights the representative examples in both metal-catalyzed and metal-free reactions based on the currently available literature.

HETEROARYLIODONIUM(III) SALTS: PREPARATION

The conventional synthetic routes to heteroaryliodonium salts rely on stepwise processes using a series of organometallic nucleophiles instead of heteroarenes themselves, as outlined in **Figures 1A–D**. One general method for the preparation of heteroaryliodonium salts is based on the iodonium(III)-atom transfer of iodine(III) cyanides to heteroarylstannanes (**Figure 1A**). More specifically, (dicyano)iodonium(III) triflate [$(NC)_2I^{+-}OTf$] **1**, generated *in situ* from iodosyl triflate and trimethylsilyl cyanide (TMSCN), reacts with tributyltin precursors **2** derived from furans, thiophenes, and pyrazoles, to afford the corresponding symmetrical bis(heteroaryl)iodonium triflates **3a–3d** (**Figure 1A**; Stang et al., 1992a,b). Aryl(cyano)iodonium(III) triflates (ArI^+CN^-OTf) **4** could also be used as an iodine transfer agent, reacting with stannylated derivatives **5** and **6** to afford a variety of mixed thienyl(aryl)iodonium salts **7** and **8**, respectively (**Figure 1A**; Gallop et al., 1993; Zhdankin et al., 1993; Bykowski et al., 2002).

The iodonium(III)-transfer procedure using *trans*-(chlorovinyl)iodonium dichloride **9** (Beringer and Nathan, 1969) was reported to access the bis(heteroaryl)iodonium chlorides **11** by the reaction of lithiated nitrogen-containing heteroarenes **10** (**Figure 1B**; Stang and Chen, 1995; Stang et al., 1995). Thus, the prepared bis(heteroaryl)iodonium chlorides **11** could be converted to the corresponding triflates **12** by treatment with trimethylsilyl triflate (TMSOTf). For the preparation of unsymmetrical heteroaryl(phenyl)iodonium triflate **15**, the ligand-transfer reaction between vinyliodonium salt **13** with heteroaryllithium **14** was developed by Kitamura et al. (**Figure 1B**; Kitamura et al., 1996).

Another approach to unsymmetrical heteroaryl(phenyl)iodonium salts is the combination of readily available heteroarylboronic acids **16** with hydroxy(tosyloxy)iodobenzene (PhI(OH)OTs; Koser's reagent), which is useful for the mild and regioselective preparation of tosylate salts **17** (**Figure 1C**; Carroll et al., 2000).

Silylated heteroarenes can also be utilized for the preparation of heteroaryliodonium salts; phenyliodonium triflate **19** was prepared from bis(trimethylsilyl)thiophene **18** by the reaction with phenyliodine diacetate [$PhI(OAc)_2$; PIDA] and triflic acid (Ye et al., 1996), while pyrrolyliodonium triflate **21** was obtained by the reaction of bis(trimethylsilyl)pyrroles **20** with iodosobenzene (PhIO) in the presence of $BF_3{\bullet}Et_2O$ (**Figure 1D**; Liu et al., 1999).

Straightforward approaches for the direct/one-pot preparation of heteroaryliodonium salts from heteroarenes have been elaborated as shown in **Figures 1E,F**, which allow expansion of the substrate scope to provide diverse types of heteroaryliodonium salts. In contrast to the aforementioned iodonium(III) salts containing fundamental heteroarene units, such as thiophene, pyridine, and furan, iodonium(III) salts bearing nucleobase and nucleoside moieties did not appear in the literature until 1998. Kim et al. reported the preparation of phenyliodonium(III)-substituted uracil nucleosides **23** by the reaction of uracil nucleosides **22** with PIDA in the presence of triflic acid, and its subsequent application in palladium-catalyzed alkenylation reaction (**Figure 1E**; Roh et al., 1998, 1999). Utilizing the unique character of the fluoroalcohol medium as a solvent, Kita et al. developed a facile synthesis of heteroaryliodonium salts **24** and **25** through the condensation of thiophenes and pyrroles with an iodine(III) reagent, whereby trifluoroethanol (TFE) enhanced the efficiency of this type of condensation, significantly extending the product scope (Dohi et al., 2007, 2010; Ito et al., 2010). Furthermore, this procedure could also be applied to the preparation of uracil-aryliodonium salts **26** possessing different types of aryl moieties and various counterions (Takenaga et al., 2018, 2019a).

Moreover, Olofsson et al. developed an efficient one-pot synthesis to heteroaryliodonium triflates **27** and **28** from arenes and aryl iodides using *m*-chloroperbenzoic acid (*m*CPBA) as a stoichiometric oxidant in the presence of triflic acid. In a seminal report, heteroaryliodonium tosylates could be prepared using *p*-toluenesulfonic acid instead of triflic acid as an additive (**Figure 1F**; Bielawski and Olofsson, 2007; Bielawski et al., 2007, 2014). Symmetrical di(heteroaryl)iodonium salt **29** was synthesized *via* a modified one-pot procedure employing elemental iodine, arenes, *m*CPBA, and toluenesulfonic acid under similar conditions (**Figure 1F**; Zhu et al., 2008). The one-pot procedure was also applied to the preparation of uracil-aryliodonium salts **30** bearing various aryl moieties (Toh et al., 2013; Modha and Greaney, 2015). As a result, recent progress in the efficient synthesis of diaryliodonium(III) salts has enabled the facile preparation of diverse types of heteroaryliodonium salts.

SYNTHETIC APPLICATIONS

Various organic synthetic transformations utilizing diaryliodonium salts have emerged over the past few decades, and this research field includes diverse metal-catalyzed and metal-free arylations for a wide range of nucleophiles, in addition to benzyne generation and the dearomatization of phenols. In addition to these reactions, new synthetic applications of heteroaryliodonium salts have been investigated in recent years. Herein, we outline the strategies based on the use of heteroaryliodonium(III) salts as electrophilic aryl transfer reagents for the C-O, C-N, and C-C bond formations. The synthetic transformations of heteroaryliodonium salts are classified into the following two categories: (1) reactions utilizing the high reactivities of iodonium(III) salts, and (2) reactions based on the unique and new reactivities of heteroaryliodonium salts. The former category of transformation has been applied to C-O and C-N bond formation reactions (**Figures 2A,B**), while the latter has been employed in C-C bond formation processes (**Figure 2C**).

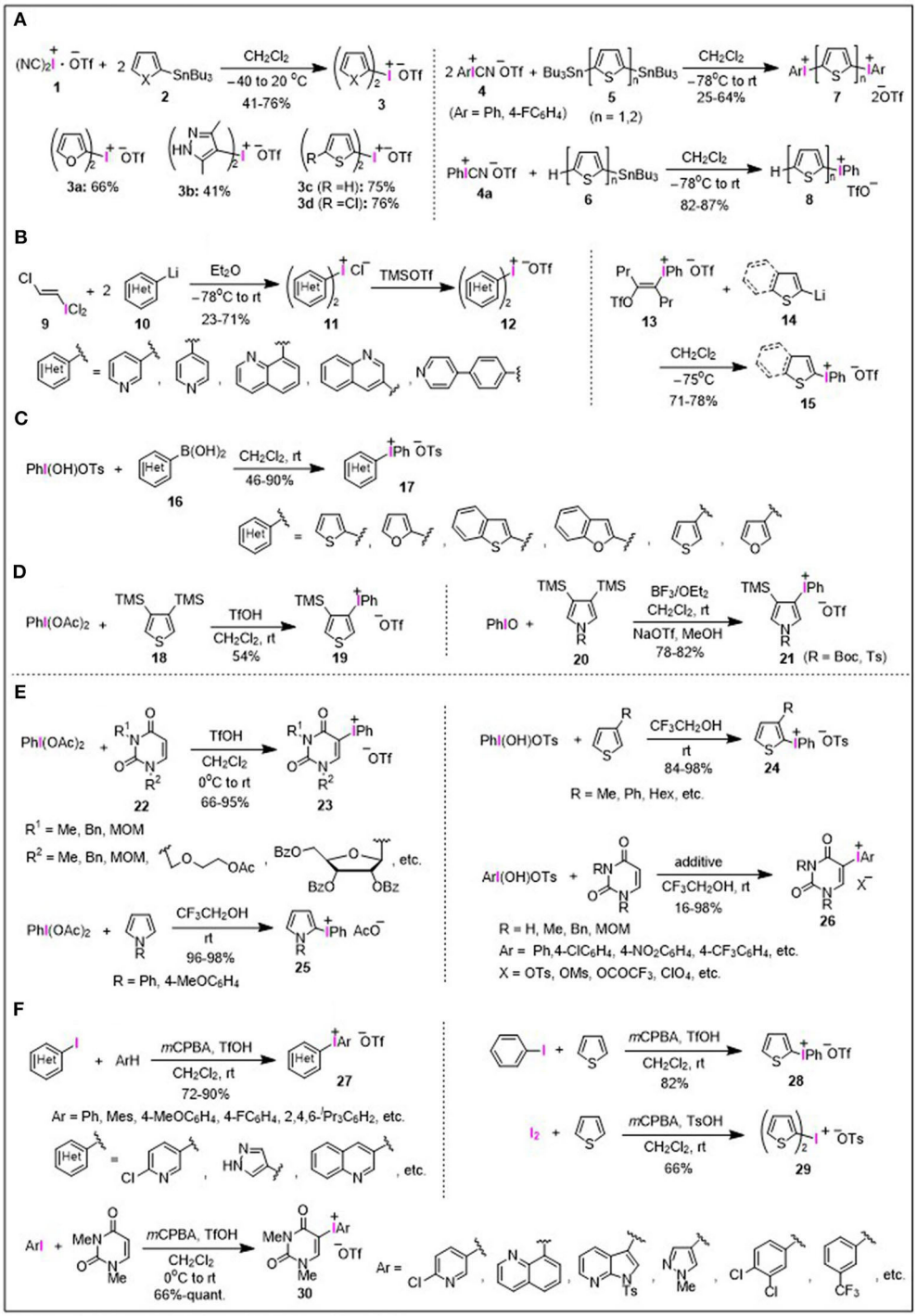

FIGURE 1 | Synthesis of heteroaryliodonium salts. **(A)** Stannyl heteroarenes. **(B)** Lithio heteroarenes. **(C)** Boryl heteroarenes. **(D)** Silyl heteroarenes. **(E)** Direct synthesis. **(F)** One-pot synthesis from iodoarenes.

Dummy Groups for Selective Aryl Transfer From Diaryliodonium Salts

Over the past few decades, symmetrical heteroaryliodonium salts ($Ar^1Ar^2I^+X^-$; $Ar^1 = Ar^2$) have found numerous applications as electrophilic arylating agents for nucleophiles. In contrast, unsymmetrical salts ($Ar^1Ar^2I^+X^-$; $Ar^1 \neq Ar^2$) have been less frequently employed since the presence of two different aromatic moieties in the salts could potentially give mixtures

of two arylated products (i.e., Ar^1-Nu and Ar^2-Nu). Recently however, by the introduction of a nontransferable dummy group, unsymmetrical iodonium salts participate in a wide range of transformations. The representative examples of dummy groups are *p*-anisyl (Ma et al., 2015; Xiong et al., 2015), mesityl (Matsuzaki et al., 2015; Sundalam and Stuart, 2015), and 2,4,6-trimethoxyphenyl (TMP) (Malmgren et al., 2013; Seidl et al., 2016) groups, and these dummy groups were utilized in reactions of the conventional diaryliodonium salts.

Heteroaryliodonium Salts as Highly Reactive Pseudo-Halides

Selected examples of C-O bond formation reactions by the electrophilic arylation of phenols using heteroaryliodonium salts are shown in **Figure 2A**, Equation a–c. In such cases, phenols were efficiently arylated to afford industrially important aryl(heteroaryl) ether compounds. In 2012, Olofsson et al. studied the metal-free arylation of phenols under basic conditions. They confirmed the chemoselective reactivity pattern of unsymmetrical diaryliodonium salts (Jalalian et al., 2012; Bielawski et al., 2014) (**Figure 2A**, Equation a). It was revealed that the electronic effect of the aryl rings was dominant during the reaction of *p*-anisyl (pyridyl) triflate **31** with phenols **32**; the phenol nucleophiles selectively coupled to the electron-deficient pyridyl group to yield pyridyl ether **33** in 65–88% yield. This chemoselectivity trend has been further applied by other researchers to transfer the electron-poor aryl group of unsymmetrical iodonium salts, and it was noted that the TMP group serves as an improved dummy ligand for aryl transfer processes from heteroaryl(TMP)iodonium salts (Seidl et al., 2016; Dohi et al., 2017). In 2020, Stuart et al. reported a convenient method for phenol arylation using the *in-situ*-generated aryl(TMP)iodonium salts **34** (Gallagher et al., 2020) (**Figure 2A**, Equation b). Thus, in metal-free reactions, nucleophiles would preferentially react with the more electron-deficient aromatic ring out of the two aryl moieties in unsymmetrical diaryliodonium salts. The results are however different in case of metal-catalyzed reactions. Suna et al. demonstrated that the presence of a Cu(I) catalyst directed the selectivity of the arylation to the more electron-rich heteroarene moiety during the reaction between heteroaryliodonium salts **35** and phenols (Sokolovs and Suna, 2016) (**Figure 2A**, Equation c). This Cu(I)-catalyzed synthesis of diaryl ethers using diaryliodonium salts is a complementary strategy to the previously mentioned metal-free arylation of phenols. The arylation of oxygen nucleophiles using heteroaryliodonium salts was not limited to the preparation of aryl(heteroaryl) ethers; as in the cases of other oxygen nucleophiles, it was demonstrated that benzoic acid was also arylated to produce quinolin-3-yl benzoate *via* the *in-situ*-generated iodonium salt bearing a 3-quinolyl group (Dohi et al., 2017). Further, the chemistry of cyclic iodonium salts has recently experienced growing development (Chatterjee and Goswami, 2017). As for just an emerging interesting compound, Nachtsheim et al. investigated that the direct oxidative cyclization of 3-(2-iodophenyl)-1*H*-pyrazole to novel iodolopyrazolium salt **36** *via in-situ* formed *N*-heterocyclic stabilized hydroxy- λ^3-iodane (Boelke et al., 2020) (**Figure 2A**, Equation d). They also demonstrated that the copper-catalyzed ring opening of **36** with acetate followed by hydrolysis produced functionalized heteroaromatic biaryl **37** in 70% yield.

Various heteroaryliodonium salt-mediated C-N bond formation processes are summarized in **Figure 2B**; these reactions include the azidation, amination, and nitration of heteroarenes. In 2012, Suna et al. reported the Cu(I)-catalyzed transformation of C–H to C–N in electron-rich heteroaromatics (i.e., pyrroles, pyrrolopyridines, thienopyrroles, pyrrolopyrimidines, and uracil), which involves the reaction of *in-situ* prepared heteroaryl(phenyl)iodonium tosylates **38** with sodium azide, whereby complete regiocontrol is accomplished (Lubriks et al., 2012) (**Figure 2B**, Equation e). Based on this study, they further demonstrated the C–H amination of electron-rich heteroarenes, comprising the *in-situ* formation of heteroaryliodonium salts **39** bearing sterically hindered mesityl (Mes) or triisopropylphenyl (TIPP) group (Sokolovs et al., 2014; Berzina et al., 2015) (**Figure 2B**, Equation f). The electronic effects observed for the aryl transfer are consistent with those mentioned earlier for *O*-nucleophiles. Thus, the electron-rich heteroarene moieties of these salts were transferred in Cu(I)-catalyzed arylations, while *N*-nucleophiles were preferentially coupled with the electron-deficient heteroaromatic ring under metal-free conditions. Sodium nitrite was recently used as a nucleophile for diaryliodonium salts as a convenient approach to access synthetically useful nitroarenes. In 2016, Olofsson et al. reported the metal-free nitration of *p*-anisyl(pyridyl) salt **40** to afford nitropyridine **41** (Reitti et al., 2016) (**Figure 2B**, Equation g). Other metal-free reactions with *N*-nucleophiles include application of the TMP group as an extremely electron-rich aryl dummy ligand to transfer electron-deficient pyridyl groups to alicyclic amines or the azide ion (Sandtorv and Stuart, 2016; Seidl and Stuart, 2017).

Unique Reactions Based on the Use of Heteroaryliodonium Salts

Figure 2C lists the versatile C-C bond forming reaction based on the use of heteroaryliodonium salts as aryl sources and reaction intermediates. For example, in 2009, Kita et al. demonstrated the metal-free oxidative cross-coupling of heteroarenes with electron-rich arenes by direct C–H transformations. The reaction proceeded through the *in-situ* formation of thienyliodonium salt **42** from an electron-rich thiopene and Koser's reagent in hexafluoroisopropanol (HFIP). It was proposed that the intermediate thienyliodonium species was activated by the addition of trimethylsilyl bromide, followed by its coupling with electron-rich arenes to provide a wide range of useful mixed biaryl products **43** (Kita et al., 2009, 2011; Morimoto et al., 2010, 2011; Dohi et al., 2013) (**Figure 2C**, Equation h). In 2013, Gaunt et al. developed a new acyl coupling reaction that merges the aryl transfer ability of diaryliodonium salts with carbonyl umpolung using an *N*-heterocyclic carbene (NHC) catalyst **44**. They also established the transfer of a pyridyl group from several pyridyliodonium salts to provide

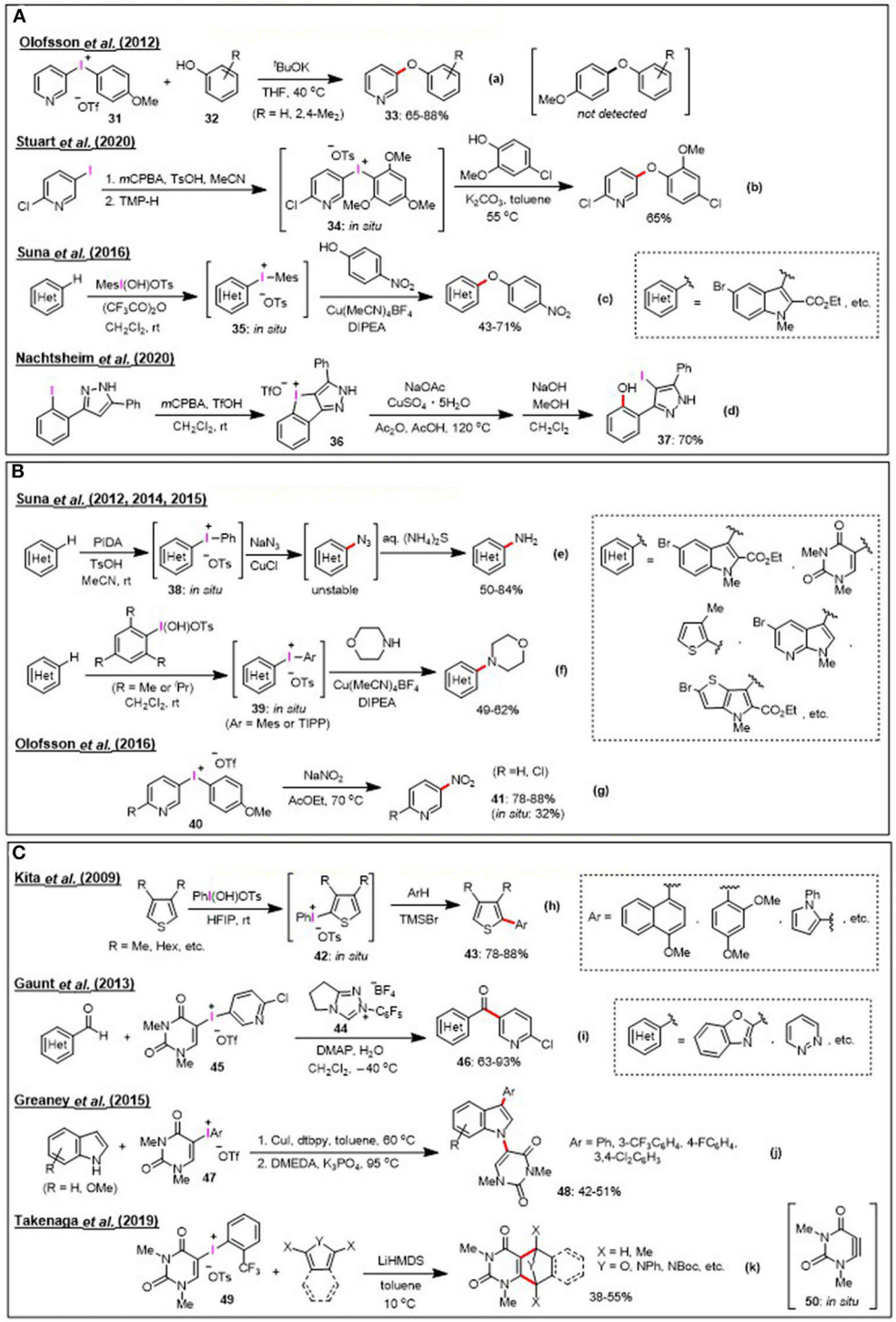

FIGURE 2 | New synthetic application of heteroaryliodonium salts. **(A)** C-O bond formation [metal-free: (a,b), metal-catalyzed: (c,d)]. **(B)** C-N bond formation [metal-catalyzed: (e,f), metal-free: (g)]. **(C)** C-C bond formation [metal-free: (h,i), metal-catalyzed: (j), aryne analog precursor: (k)].

di(hetero)aryl ketones **46**, and exclusive pyridyl transfer was observed when a uracil-derived salt **45** was used. This is an interesting example of utilization of the uracil moiety as a nontransferable dummy group for the organocatalytic reactions of diaryliodoniuim(III) salts, with more frequently used dummy groups for arylations being the Mes, TMP, and TIPP groups

(Toh et al., 2013) (**Figure 2C**, Equation i). In general, arylation using diaryiodonium salts produces one equivalent of iodoarene as a waste byproduct, which is problematic in the context of atom economy. Thus, Greaney et al. reported the very atom-economical transformation of heteroaryliodonium salts (Modha and Greaney, 2015) (**Figure 2C**, Equation j). They showed that uracil-iodonium salts **47** could undergo Cu-catalyzed tandem C-H/N-H arylation reactions to produce double-arylated indoles **48** by incorporation of both the uracil and aryl groups. As another copper-catalyzed tandem reaction, Fañanás-Mastral et al. described an interesting example, carboarylation/cyclization of alkynyl phosphonate with a mesityl thienyl iodonium salt (Pérez-Saavedra et al., 2017). The recent report by Takenaga et al. highlighted the synthesis of bicyclic uracil systems and the vicinal functionalization of uracils with the basic activation of salts **49** being stabilized by the *o*-trifluorophenyl group. The reactive intermediate of this reaction is believed to involve the generation of a highly strained heterocyclic alkyne species, uracilyne **50**, a non-reported heteroaryne analog (Takenaga et al., 2019a,b) (**Figure 2C**, Equation k).

CONCLUSION AND OUTLOOK (FUTURE PERSPECTIVES)

In the twentieth century, the synthetic scope of heteroaryliodonium(III) salts was limited, and thus only relatively simple heteroaryliodonium salts, such as symmetrical bis(heteroaryl)iodonium salts and unsymmetrical phenyl(heteroaryl)iodonium salts, were previously reported. With recent advances in efficient synthetic procedures, heteroaryliodonium salts bearing sterically hindered mesityl, trimethoxyphenyl, and triisopropylphenyl groups were efficiently synthesized. These designer heteroaryliodonium salts have been found to control the chemoselectivity of aryl transfer in a wide range of reactions. The metal-free and metal-catalyzed reactions show significant selectivity toward aryl/heteroaryl group transfer and unearth an important synthetic methodology for selective synthetic purposes. The synthetic utilities of heteroaryliodonium salts highlighted in this mini-review, such as NHC-catalyzed C-H bond arylation, Cu-catalyzed tandem arylation of indoles, and vicinal functionalization, undoubtedly pave a useful pathway in this direction, and developments of new synthetic transformations in this area are highly demanded in future.

AUTHOR CONTRIBUTIONS

NT and TD conceived and wrote the manuscript. All authors provided comments, discussed the manuscript, and approved it for publication.

FUNDING

This work was supported by JSPS KAKENHI Grant Number JP20K06980. TD acknowledges support from JSPS KAKENHI Grant Number JP19K05466 and the Ritsumeikan Global Innovation Research Organization (R-GIRO) project.

REFERENCES

Aradi, K., Tóth, B., Tolnai, G., and Novák, Z. (2016). Diaryliodonium salts in organic syntheses: a useful compound class for novel arylation strategies. *Synlett* 27, 1456–1485. doi: 10.1055/s-0035-1561369

Beringer, F. M., and Nathan, R. A. (1969). Diaryliodonium salts from aryllithium reagents with trans-chlorovinyliodoso dichloride. *J. Org. Chem.* 34, 685–689. doi: 10.1021/jo01255a044

Berzina, B., Sokolovs, I., and Suna, E. (2015). Copper-catalyzed para-selective C–H amination of electron-rich arenes. *ACS Catal.* 5, 7008–7014. doi: 10.1021/acscatal.5b01992

Bielawski, M., Malmgren, J., Pardo, L. M., Wikmark, Y., and Olofsson, B. (2014). One-pot synthesis and applications of N-heteroaryl iodonium salts. *Chem. Open*. 3, 19–22. doi: 10.1002/open.201300042

Bielawski, M., and Olofsson, B. (2007). High-yielding one-pot synthesis of diaryliodonium triflates from arenes and iodine or aryl iodides. *Chem. Commun.* 2521–2523. doi: 10.1039/b701864a

Bielawski, M., Zhu, M., and Olofsson, B. (2007). Efficient and general one-pot synthesis of diaryliodonium triflates: optimization, scope and limitations. *Adv. Synth. Catal.* 349, 2610–2618. doi: 10.1002/adsc.200700373

Boelke, A., Kuczmera, T. J., Caspers, L. D., Lork, E., and Nachtsheim, B. J. (2020). Iodolopyrazolium salts: synthesis, derivatizations, and applications. *Org. Lett.* 22, 7261–7266. doi: 10.1021/acs.orglett.0c02593

Bykowski, D., McDonald, R., Hinkle, R. J., and Tykwinski, R. R. (2002). Structural and electronic characteristics of thienyl(aryl)iodonium triflates. *J. Org. Chem.* 67, 2798–2804. doi: 10.1021/jo015910t

Carroll, M. A., Pike, V. W., and Widdowson, D. A. (2000). New synthesis of diaryliodonium sulfonates from arylboronic acids. *Tetrahedron Lett.* 41, 5393–5396. doi: 10.1016/S0040-4039(00)00861-3

Chatterjee, N., and Goswami, A. (2017). Synthesis and application of cyclic diaryliodonium salts: a platform for bifunctionalization in a single step. *Eur. J. Org. Chem.* 2017, 3023–3032. doi: 10.1002/ejoc.201601651

Dohi, T., Ito, M., Morimoto, K., Minamitsuji, Y., Takenaga, N., and Kita, Y. (2007). Versatile direct dehydrative approach for diaryliodonium(III) salts in fluoroalcohol media. *Chem. Commun.* 4152–4154. doi: 10.1039/b708802g

Dohi, T., Koseki, D., Sumida, K., Okada, K., Mizuno, S., Kato, A., et al. (2017). Metal-free *O*-arylation of carboxylic acid by active diaryliodonium(III) intermediates generated *in situ* from iodosoarenes. *Adv. Synth. Catal.* 359, 3503–3508. doi: 10.1002/adsc.201700843

Dohi, T., Yamaoka, N., and Kita, Y. (2010). Fluoroalcohols: versatile solvents in hypervalent iodine chemistry and syntheses of diaryliodonium(III) salts. *Tetrahedron* 66, 5775–5785. doi: 10.1016/j.tet.2010.04.116

Dohi, T., Yamaoka, N., Nakamura, S., Sumida, K., Morimoto, K., and Kita, Y. (2013). Efficient synthesis of a regioregular oligothiophene photovoltaic dye molecule, MK-2, and related compounds: a cooperative hypervalent iodine and metal-catalyzed synthetic route. *Chem. Eur. J.* 19, 2067–2075. doi: 10.1002/chem.201203503

Fañanás-Mastral, M. (2017). Copper-catalyzed arylation with diaryliodonium salts. *Synthesis* 49, 1905–1930. doi: 10.1055/s-0036-1589483

Gallagher, R. T., Basu, S., and Stuart, D. R. (2020). Trimethoxyphenyl (TMP) as a useful auxiliary for *in situ* formation and reaction of aryl(TMP)iodonium salts: synthesis of diaryl ethers. *Adv. Synth. Catal.* 362, 320–325. doi: 10.1002/adsc.201901187

Gallop, P. M., Paz, M. A., Fluckiger, R., Stang, P. J., Zhdankin, V. V., and Tykwinski, R. R. (1993). Highly effective PQQ inhibition by alkynyl and aryl mono- and diiodonium salts. *J. Am. Chem. Soc.* 115, 11702–11704. doi: 10.1021/ja00078a007

Ito, M., Ogawa, C., Yamaoka, N., Fujioka, H., Dohi, T., and Kita, Y. (2010). Enhanced reactivity of [hydroxy(tosyloxy)iodo]benzene in fluoroalcohol

media. Efficient direct synthesis of thienyl(aryl)iodonium salts. *Molecules* 15, 1918–1931. doi: 10.3390/molecules15031918

Jalalian, N., Petersen, T. B., and Olofsson, B. (2012). Metal-free arylation of oxygen nucleophiles with diaryliodonium salts. *Chem. Eur. J.* 18, 14140–14149. doi: 10.1002/chem.201201645

Kita, Y., Dohi, T., and Morimoto, K. (2011). Hypervalent iodine induced metal-free C-H cross couplings to biaryls. *J. Synth. Org. Chem. Jpn.* 69, 1241–1250. doi: 10.5059/yukigoseikyokaishi.69.1241

Kita, Y., Morimoto, K., Ito, M., Ogawa, C., Goto, A., and Dohi, T. (2009). Metal-free oxidative cross-coupling of unfunctionalized aromatic compounds. *J. Am. Chem. Soc.* 131, 1668–1669. doi: 10.1021/ja808940n

Kitamura, T., Kotani, M., and Fujiwara, Y. (1996). An efficient ligand exchange reaction of β-(trifyloxy)vinyliodonium triflates with aryllithium reagents leading to diaryliodonium triflates. *Tetrahedron Lett.* 37, 3721–3722. doi: 10.1016/0040-4039(96)00668-5

Liu, J. H., Chan, H. W., Xue, F., Wang, Q. G., Mak, T. C., and Wong, H. N. (1999). Generation and Trapping reactions of 1-tert-butoxycarbonyl-3,4-didehydro-1H-pyrrole. *J. Org. Chem.* 64, 1630–1634. doi: 10.1021/jo982129l

Lubriks, D., Sokolovs, I., and Suna, E. (2012). Indirect C-H azidation of heterocycles via copper-catalyzed regioselective fragmentation of unsymmetrical λ^3-iodanes. *J. Am. Chem. Soc.* 134, 15436–15442. doi: 10.1021/ja305574k

Ma, X. P., Shi, W. M., Mo, X. L., Li, X. H., Li, L. G., Pan, C. X., et al. (2015). Synthesis of alpha,beta-unsaturated N-aryl ketonitrones from oximes and diaryliodonium salts: observation of a metal-free N-arylation process. *J. Org. Chem.* 80, 10098–10107. doi: 10.1021/acs.joc.5b01716

Malmgren, J., Santoro, S., Jalalian, N., Himo, F., and Olofsson, B. (2013). Arylation with unsymmetrical diaryliodonium salts: a chemoselectivity study. *Chem. Eur. J.* 19, 10334–10342. doi: 10.1002/chem.201300860

Martín-Santamaría, S., Carroll, M. A., Carroll, C. M., Carter, C. D., Pike, V. W., Rzepa, H. S., et al. (2000). Fluoridation of heteroaromatic iodonium salts—experimental evidence supporting theoretical prediction of the selectivity of the process. *Chem. Commun.* 649–650. doi: 10.1039/b000868k

Matsuzaki, K., Okuyama, K., Tokunaga, E., Saito, N., Shiro, M., and Shibata, N. (2015). Synthesis of diaryliodonium salts having pentafluorosulfanylarenes and their application to electrophilic pentafluorosulfanylarylation of C-, O-, N-, and S-nucleophiles. *Org. Lett.* 17, 3038–3041. doi: 10.1021/acs.orglett.5b01323

Merritt, E. A., and Olofsson, B. (2009). Diaryliodonium salts: a journey from obscurity to fame. *Angew. Chem. Int. Ed.* 48, 9052–9070. doi: 10.1002/anie.200904689

Modha, S.G., and Greaney, M.F. (2015). Atom-economical transformation of diaryliodonium salts: tandem C-H and N-H arylation of indoles. *J. Am. Chem. Soc.* 137, 1416–1419. doi: 10.1021/ja5124754

Morimoto, K., Nakae, T., Yamaoka, N., Dohi, T., and Kita, Y. (2011). Metal-free oxidative coupling reactions via σ-iodonium intermediates: the efficient synthesis of bithiophenes using hypervalent iodine reagents. *Eur. J. Org. Chem.* 2011, 6326–6334. doi: 10.1002/ejoc.201100969

Morimoto, K., Yamaoka, N., Ogawa, C., Nakae, T., Fujioka, H., Dohi, T., et al. (2010). Metal-free regioselective oxidative biaryl coupling leading to head-to-tail bithiophenes: reactivity switching, a concept based on the iodonium(III) intermediate. *Org. Lett.* 12, 3804–3807. doi: 10.1021/ol101498r

Pérez-Saavedra, B., Vázquez-Galiñanes, N., Saá, C., and Fañanás-Mastral, M. (2017). Copper(I)-catalyzed tandem carboarylation/cyclization of alkynyl phosphonates with diaryliodonium salts. *ACS Catal.* 7, 6104–6109. doi: 10.1021/acscatal.7b02434

Reitti, M., Villo, P., and Olofsson, B. (2016). One-pot C-H functionalization of arenes by diaryliodonium salts. *Angew. Chem. Int. Ed.* 55, 8928–8932. doi: 10.1002/anie.201603175

Roh, K.R., Kim, J.Y., and Kim, Y.H. (1998). Novel synthesis of 5-phenyliodonium triflate substituted uracil nucleosides. *Chem. Lett.* 27, 1095–1096. doi: 10.1246/cl.1998.1095

Roh, K.R., Kim, J.Y., and Kim, Y.H. (1999). Palladium catalyzed alkenylation or alkynylation at C-5 of uracil nucleosides using novel phenyliodonium triflate. *Tetrahedron Lett.* 40, 1903–1906. doi: 10.1016/S0040-4039(98)02491-5

Sandtorv, A. H., and Stuart, D. R. (2016). Metal-free synthesis of aryl amines: beyond nucleophilic aromatic substitution. *Angew. Chem. Int. Ed.* 55, 15812–15815. doi: 10.1002/anie.201610086

Seidl, T. L., and Stuart, D. R. (2017). An admix approach to determine counter anion effects on metal-free arylation reactions with diaryliodonium salts. *J. Org. Chem.* 82, 11765–11771. doi: 10.1021/acs.joc.7b01599

Seidl, T. L., Sundalam, S. K., MiCullough, B., and Sruart, D. R. (2016). Unsymmetrical aryl(2,4,6-trimethoxyphenyl)iodonium salts: one-pot synthesis, scope, stability, and synthetic studies. *J. Org. Chem.* 81, 1998–2009. doi: 10.1021/acs.joc.5b02833

Sokolovs, I., Lubriks, D., and Suna, E. (2014). Copper-catalyzed intermolecular C-H amination of (hetero)arenes via transient unsymmetrical λ^3-iodanes. *J. Am. Chem. Soc.* 136, 6920–6928. doi: 10.1021/ja502174d

Sokolovs, I., and Suna, E. (2016). *Para*-selective Cu-catalyzed C-H aryloxylation of electron-rich arenes and heteroarenes. *J. Org. Chem.* 81, 371–379. doi: 10.1021/acs.joc.5b02728

Stang, P. J., and Chen, K. (1995). Hybrid, iodonium-transition metal, cationic tetranuclear macrocyclic squares. *J. Am. Chem. Soc.* 117, 1667–1668. doi: 10.1021/ja00110a035

Stang, P. J., Olenyuk, B., and Chen, K. (1995). Preparation of nitrogen-containing bis(heteroaryl)iodonium salts. *Synthesis* 937–938. doi: 10.1055/s-1995-4023

Stang, P. J., Tykwinski, R., and Zhdankin, V. V. (1992a). Preparation of bis(heteroaryl)iodonium saltsviaan iodonium transfer reaction between di(cyano)iodonium triflate and organostannes. *J. Heterocycl. Chem.* 29, 815–818. doi: 10.1002/jhet.5570290424

Stang, P. J., and Zhdankin, V. V. (1996). Organic polyvalent iodine compounds. *Chem. Rev.* 96, 1123–1178. doi: 10.1021/cr940424+

Stang, P. J., Zhdankin, V. V., Tykwinski, R., and Zefirov, N. S. (1992b). (Dicyano)iodonium triflate- novel iodonium species and a versatile reagent for the preparation of iodonium salts via an iodonium transfer reaction with organostannanes. *Tetrahedron Lett.* 33, 1419–1422. doi: 10.1016/S0040-4039(00)91636-8

Stuart, D. R. (2017). Aryl transfer selectivity in metal-free reactions of unsymmetrical diaryliodonium salts. *Chem. Eur. J.* 23, 15852–15863. doi: 10.1002/chem.201702732

Sundalam, S. K., and Stuart, D. R. (2015). Base mediated synthesis of alkyl-aryl ethers from the reaction of aliphatic alcohols and unsymmetric diaryliodonium salts. *J. Org. Chem.* 80, 6456–6466. doi: 10.1021/acs.joc.5b00907

Takenaga, N., Hayashi, T., Ueda, S., Satake, H., Yamada, Y., Kodama, T., et al. (2019a). Synthesis of uracil-iodonium(III) salts for practical utilization as nucleobase synthetic modules. *Molecules* 24, 3034–3046. doi: 10.3390/molecules24173034

Takenaga, N., Ueda, S., Hayashi, T., Dohi, T., and Kitagaki, S. (2018). Facile synthesis of stable uracil-iodonium(III) salts with various counterions *Heterocycles* 97, 1248–1256. doi: 10.3987/COM-18-S(T)80

Takenaga, N., Ueda, S., Hayashi, T., Dohi, T., and Kitagaki, S. (2019b). Vicinal functionalization of uracil heterocycles with base activation of iodonium(III) salts. *Heterocycles* 99, 865–874. doi: 10.3987/COM-18-S(F)93

Toh, Q.Y., McNally, A., Vera, S., Erdmann, N., and Gaunt, M.J. (2013). Organocatalytic C-H bond arylation of aldehydes to bis-heteroaryl ketones. *J. Am. Chem. Soc.* 135, 3772–3775. doi: 10.1021/ja400051d

Xiong, W., Qi, C., Peng, Y., Guo, T., Zhang, M., and Jiang, H. (2015). Base-promoted coupling of carbon dioxide, amines, and diaryliodonium salts: a phosgene- and metal-free route to *O*-aryl carbamates. *Chem. Eur. J.* 21, 14314–14318. doi: 10.1002/chem.201502689

Ye, X.-S., Li, W.-K., and Wong, H. N. C. (1996). 3,4-Didehydrothiophene: generation, trappingreactions, andab initiostudy. *J. Am. Chem. Soc.* 118, 2511–2512. doi: 10.1021/ja953747b

Yoshimura, A., and Zhdankin, V. V. (2016). Advances in synthetic applications of hypervalent iodine compounds. *Chem. Rev.* 116, 3328–3435. doi: 10.1021/acs.chemrev.5b00547

Yusubov, M. S., Maskaev, A. V., and Zhdankin, V. V. (2011). Iodonium salts in organic synthesis. *Arkivoc.* 2011, 370–409. doi: 10.3998/ark.5550190.0012.107

Zhdankin, V. V., Scheuller, M. C., and Stang, P. J. (1993). A general approach to aryl(cyano)iodonium triflates - versatile iodonium transfer reagents. *Tetrahedron. Lett.* 34, 6853–6856. doi: 10.1016/S0040-4039(00)91812-4

Zhdankin, V. V., and Stang, P. J. (2002). Recent developments in the chemistry of polyvalent iodine compounds. *Chem. Rev.* 102, 2523–2584. doi: 10.1021/cr010003+

Zhdankin, V. V., and Stang, P. J. (2008). Chemistry of polyvalent iodine. *Chem. Rev.* 108, 5299–5358. doi: 10.1021/cr800332c

Zheng, Z., Zhang-Negrerie, D., Du, Y. F., and Zhao, K. (2014). The applications of hypervalent iodine(III) reagents in the construction of heterocyclic compounds through oxidative coupling reactions. *Sci. China: Chem.* 57, 189–214. doi: 10.1007/s11426-013-5043-1

Zhu, M., Jalalian, N., and Olofsson, B. (2008). One-pot synthesis of diaryliodonium salts using toluenesulfonic acid: a fast entry to electron-rich diaryliodonium tosylates and triflates. *Synlett* 592–596. doi: 10.1055/s-2008-1032050

Conflict of Interest: The authors declare that the research was conducted in the absence of any commercial or financial relationships that could be construed as a potential conflict of interest.

Advantages of publishing in Frontiers

OPEN ACCESS
Articles are free to read for greatest visibility and readership

FAST PUBLICATION
Around 90 days from submission to decision

HIGH QUALITY PEER-REVIEW
Rigorous, collaborative, and constructive peer-review

TRANSPARENT PEER-REVIEW
Editors and reviewers acknowledged by name on published articles

Frontiers
Avenue du Tribunal-Fédéral 34
1005 Lausanne | Switzerland

Visit us: www.frontiersin.org
Contact us: frontiersin.org/about/contact

REPRODUCIBILITY OF RESEARCH
Support open data and methods to enhance research reproducibility

DIGITAL PUBLISHING
Articles designed for optimal readership across devices

FOLLOW US
@frontiersin

IMPACT METRICS
Advanced article metrics track visibility across digital media

EXTENSIVE PROMOTION
Marketing and promotion of impactful research

LOOP RESEARCH NETWORK
Our network increases your article's readership